EFFECTS OF SELECTED ADDITIVES ON A LUMINOUS DIFFUSION FLAME

by

Mohamed A.H. Serag-El-Din, M.Sc(Eng)

August 1976

A thesis submitted for the degree of Doctor of Philosophy of the University of London and for the Diploma of Imperial College.

Department of Chemical Engineering
and Chemical Technology,
Imperial College,
London, S.W.7.

ERRATA

p. 1	line	1	for "parameter" read "parameters"
	"	21	for "temperature" read "temperatures"
p. 2	"	1	for "miscrostructure" read "microstructure"
p. 9	"	7	for "gas-weighing" read "gas-weighting"
p. 10	"	8	for "$E_{b,\lambda}$" read "E_b"
			for "$ET^{-1}\ell^{-3}$" read "$ET^{-1}\ell^{-2}$"
p. 13	"	2	for "KW" read "kW"
	"	8	for Net dimension of "Ω" is "-"
p. 18	"	1	for "may" read "many"
	"	2	for "smelting" read "melting"
p. 21	"	6	for "turbostatic" read "turbostratic"
p. 22	"	6*	for "represenation" read "representation"
p. 24	"	4	for "$0 \rightarrow \infty$ " read "$\lambda = 0 \rightarrow \infty$"
	"	5	for "blackbody" read "black body per unit solid angle"
	"	9	for "of" effective read "or" effective
p. 25	"	3*	for "represent" read "represents"
p. 27	"	8	for "$\|m\|/\lambda$" read "$\lambda/\|m-1\|$"
p. 31	"	5	for "(23-25d) read "(23-25a)"
	"	6*	for "$(1 - B\bar{C}LT/c_2)^{-4}$" read "$(1 + B\bar{C}LT/c_2)^{-4}$"
	"	6	for "inner" read "increase in "
	"	10 &1*	for "$\bar{m}K$" read "m K"
	"	5*	for "$T < 0.\beta \times 10^{-2}$ mK" read "$\lambda T < 0.3 \times 10^{-2}$mK"
p. 34	"	7	for "structual" read "structural"
p. 36	"	17	for "step" "steep"
p. 42	"	9	for "$g = 1.39$" read $g_m = 1.39$
p. 43	"	6*	for "g read " g_λ"
p. 45	"	1*	for "1.46" read "1.39'
p. 47	"	1	for "have been" read "have"

*Counted from bottom of page

p. 48	line	9	for "5 per cent m" read "50 per cent"
	"	16	for "not" read "no"
p. 49	"	7	for "prelimainary" read "preliminary"
p. 50	"	18	for "heat flow" read "shear flow"
p. 51	"	9	for "ratio" read "mass ratio"
p. 51	"	3*	for "constantcy" read "constancy"
p. 52	"	5*	for "distribution" read "size distribution"
p. 55	"	4*	for "0.473" read "0.500"
p. 56	"	12	for "Hoster" read "Foster"
p. 61	"	9*	for "experiments" read "Experiments"
	"	10*	for "Place and Weinberg [99]" read "Lawton and Weinberg [92]"
p. 62	"	1	for "coreflow" read "coreflow,"
	"	12	for "polyacetylens" read "polyacetylenes"
p. 63	"	7	for "Butadienne" read "Butadiene"
	"	9*	for "compounds" read compounds over the other"
p. 64	"	6*	for "ehtylene" read "ethylene"
p. 65	"	12*	for "Ch_4" read "CH_4"
p. 66	"	12	In reaction mechanism for "$\longrightarrow \overset{\uparrow}{C_3H_3}(+H_2)$" read "$\xrightarrow{+C_2H_2} \overset{\uparrow}{C_8H_3}(+H_2)$"
p. 67	"	6	for "naphtalene" read "naphthalene"
	"	10*	for "leis" read "lies"
p. 69	"	9	for "Jessen and Gäydon" read "Jessen and Gaydon [102]"
p. 74	"	19	for "atomospheric" read "atmospheric"
p. 75	"	9*	for CO_2 "and" N_2 read CO_2 "than" N_2
p. 78	"	14	for "Ibirrious" read "Ibiricu"
p. 79	"	13	for "and halogen acid" read "and an increase in halogen acid"

* Counted from bottom of page

p. 82	line	14	for "escpaes" read "escapes"
	"	15	for "hydorgen" read "hydrogen"
	"	18	for "halogen" read "halogen and fuel"
	"	22	for "strenth (163)" read "strength (138)"
p. 83	"	3	for "amount of soot" read "amount of soot and an increase in the amount of soot respectively"
p. 86	"	5*	"equilibrium concentrations" read "the total concentration"
	"	4*	$M^+ \geq H_3O^+ + R^+$ read $M > H_3O^+ + R^+$
p. 87	"	1	for "following reaction" read "following slow reaction
	"	2	for "The level" read "the level"
	"	3*	for "sublimation" read "directly from gaseous"
	"	8	for "weight number" read "weight and number of particles"
p. 89	"	11*	for "metal (141),(142)" read "metal (131),(141),(142)"
p. 90	"	12	for "which is" read "The former group increased the radiant efficiency by a factor of 2 which is"
p. 92	"	3*	for "extentent to fuel" read "extent of fuel"
	"	8*	for "in tube" read "in a tube"
p. 93	"	1	for "In may" read "In many"
p. 97	"	5	for "srpings" read "springs"
p. 99	"	3*	for "10,500" read "X10,500"
p. 104	"	16	for "the" read "them"
	"	1*	for "apperance" read "appearance"
p. 106	"	12*	for "introducing the" read "introducing a"
p. 110	"	3	for "Friston" read "Fristrom"
	"	4	for "designd" read "designed"
p. 111	"	4	for "perfomred" read "performed"
p. 112	"	11*	for "conetration" read "concentration"
p. 113	"	4	for "acpillaries" read "capillaries"
	"	12*	for "in the soot" read "on the soot"

*Counted from bottom of page

p. 116	line	9	for "surface with" read "surface and with"
	"	13*	for "or plane" read "on plane"
	"	2*	for "for polutted" read "polluted"
	"	1	for "weighted" read "weighed"
p. 119	"	8*	for "protecture" read "protecting"
p. 120	"	15	for "$0.95^{(25f)}$" read "$0.95^{(17)}$"
p. 122	"	2*	for "position cited" read "positions sighted"
p. 127	"	2	for "A_rS_3" read "ArS_3"
p. 131	"	14	for "galss" read "glass"
	"	17	for "chlorine" read "chlorine $^{(134)}$"
p. 135	"	1*	for "page (18)" read "page (35)"
p. 136	"	8	for "page (25)" read "page (42)"
	"	13	for "procedure" read "procedures"
p. 137	"	10*	equation should read $g_\lambda \neq - \partial \ell n k_\lambda / \partial \ell n \lambda$
	"	12	"refracture" read "refractive"
p. 138	"	11	for "the mean factor" read "the main factor"
	"	3*	for "methene" read "methane"
p. 139	"	8*	for "was 90%" read "was $\sim$90%"
p. 140	"	3	for "planimetre" read "planimeter"
p. 142	"	8	for "resove" read "resolve"
p. 143	"	14	for "are weighted" read "were weighed"
	"	16	for "weighted" read "weighed"
	"	21	for "reweighted read "reweighed"
p. 144	"	11*	for "$\bar{T}_t$ (Appendix II)" read "$\bar{T}_t$"
	"	4*	for "range of T" read "range of"
p. 146	"	3*	for "analysed" read "is analysed"
p. 148	"	10	for "realting" read "relating"
p. 149	"	8	for "case. In the" read "case as the"
p. 152	"	11	for "of fuel" read "of more rapid fuel"
p. 155	"	4	for "bluee" read "blue"

* Counted from bottom of page

p. 155	line	17	for "example" read "for example"
	"	20	for "polimeric" read "polymeric"
	"	24	for "$\bar{T}_t + T_{max}/2$ " read $(\bar{T}_t + T_{max})/2$
p. 156	"	4	for "oxidant" read "oxidation"
p. 157	"	1	"in not" read "is not"
p. 161	"	3	for "Fig. 27a" read "Figs. 27a and b"
	"	10	for "Fig. 27b" read "Figs. 27c and d"
p. 164	"	10	for "small" read "small when the radiation exit was closed"
p. 163	"	7*	for "exists" read "exits"
p. 167	"	21	for "is small" read is not small"
			for "one value" read "more than one value"
	"	22	for "could" read "should"
p. 171	"	6	for "constant A'" read "constant B"
	"	8	for "$A'_n \simeq A'_1$" read "$B_n \simeq B_1$"
	"	7*	for "intermeidate" read "intermediate"
p. 173	"	5*	for "of flame" read "of inner tube"
	"	4*	for "A_f" read "A_i"
	"	3*	Eqn. should read $Q_c = wc_p\Delta T - \sigma T_b^4 A_i$
p. 174	"	17	for "is therefore" read "of therefore"
p. 178	"	1	for "in particular" read "on particle"
p. 180			π is missing in the numerator of 1st equation
			z is " " " " " 3rd equation
			R should read T in denominator of 3rd equation
p. 182			Denominator in equation (2) should read 1.80 x 72
p. 184	"	10	for "Arimthmetic man" read "Arithmetic mean"
	"	13	for "the inlet" read "the effective inlet"
p. 185			should read p. 186

* Counted from bottom of page

p. 185	line 1	Eqn. should read $\frac{1}{\bar{h}_o} = \frac{1}{n} \sum_{1}^{n} \frac{1}{\bar{h}_n}$
	" 11	for "equation (b)" read "equation (2)"
p. 186		should read p. 185
	" 5*	for "the error is" read "the error in"
p. 187	title	for "Wein read "Wien"
p. 209		for "BRIVAD" read "BRIAUD"
p. 216		Ref. 120 last column: for "of hydrocarbon" read "of feed hydrocarbon"
p. 220		Ref. 137, H_2 and CO dropped under type of fuel
		Ref. 134 comma missing between H_2 and SO_3
p. 228		Units on Y axis should read $KWm^{-2}\ \mu m^{-1} \times 10^{-1}$

N.B. Pages 168 to 170 attached.

*Counted from bottom of page

ABSTRACT

The purpose of this work is to investigate certain parameter influencing the emission of thermal radiation from flames produced by burning a gaseous hydro-carbon fuel. The flame is contained in a vertical water-cooled space. The following experimental conditions are examined:

a) Effect of adding oxygen to the fuel.

b) Effect of adding oxygen to the air.

c) Effect of air preheat.

d) Effect of halogenated hydrocarbons.

The effect of these conditions on temperature distribution, heat transfer to the cooling water, flame width and a number of other factors are analysed.

The general effect of additives was to increase the total heat flux, with the exception of the addition of small amounts of oxygen or carbon tetrachloride to the fuel. Addition of oxygen increased radiation in the lower part of the flame. It also brought about a decrease in flame width. The effectiveness of oxygen in reducing the flame width was greater when it was added to the fuel side. A somewhat smaller increase was produced when the air was preheated.

Additions of oxygen increased the maximum temperature but reduced the mean temperature ($\overline{T}$). Preheating the air generally increased both temperature, while addition of CCl_4 produced the opposite effect. It was possible, using a simplified model, to predict within limits the radiation produced from such a flame by considering only the flame temperature and the total amount of flame material. The mass of soot plus polymeric material collected under different experimental conditions showed a linear dependence on the mean temperature in the region where the blue reaction zone was observed, and practically no dependence where it ceased to exist.

A possible factor affecting flame emissivity is the C/H ratio of the soot. This was studied in some detail and it would appear that for C/H ratios

> 7, it is the change in miscrostructure that is important, rather than in composition, although the limit may in fact be lower. There is, however, evidence that the concentration of heavy hydrocarbons in the flame is important and determines the extent of dependence on composition.

Finally the shape of soot particles may modify the radiation and an attempt was therefore made to analyse this factor. It was found that the size and number of chain-like agglomerates of soot collected on an electron microscope grid could be greatly reduced by altering the speed by which the grid was introduced into the flames. This, together with the aforementioned dependence of radiation on temperature distribution and soot weight found in this study, suggests that individual soot particles agglomerate in chains during sampling, or if they do so in situ their shape is such that it does not have an important effect on the flame emissivity.

To SAMIA and KAREEM

ACKNOWLEDGEMENTS

I wish to thank Dr. A.R. Jones for his encouragement and valuable guidance throughout all aspects of this work - and the National Research Centre, Cairo for a generous leave of absence.

I am grateful to my parents who in the course of my academic career have given me all the necessary moral and material support, and to my wife for her invaluable encouragement and patience.

Thanks are also due to the glass blowing workshop and the main workshop for their help and for the construction of the apparatus. The cooperation of Miss S.M. Bell and Miss V.A. Milne in their capacity as librarians is greatly appreciated as well as the help provided by Mrs. Pat Brown in the translation of a number of papers.

Lastly, credit is attributed to Mrs. B. Robinson and Mr. L. Moulder for carrying out the electron microscopy and the photography respectively.

CONTENTS

NOMENCLATURE

NOTE: Seven dimensions Energy,E; Force,F;mass,m;length,ℓ; temperature,θ; time, T; and solid angle,Ω- are used to define the net dimensions. These are in terms of S.I. units unless specified otherwise.

Symbol		Net Dimensions
α	Absorptivity (or absorptance) of a body	-
$\alpha_\lambda(T)$	Monochromatic absorptivity (or absorpance)	-
$a_{g,i}$	Grey gas-weighing coefficient for a gas mixture	-
A	Area	ℓ^2
B	Is a constant (equations 2.10 and 2.15 to 2.17) dimensions depends on that of $\bar{c}$, usually (Note: In Ch. 7, dimensions = $m^{-1}T$)	$m^{-1}\ell^3$
B_o	Is an overall constant, its dimension depends on that of $\bar{c}$, usually (Note:In Ch.7, dimensions= $m^{-1}\ell^{-1}T\theta^{-1}$)	$m^{-1}\ell^2\theta^{-1}$
$\bar{c}$	Mass concentration of particles per unit volume of cloud. (Note: In Chap. 7, dimension = mT^{-1})	$m\ell^{-3}$
c_1	First constant in Planck's function, equation 2.1, = 3.74×10^{-19} KW m^2	$ET^{-1}\ell^2$
c_2	Second constant in Planck's function, equation 2.1, = 1.439×10^{-2} mK	$\ell\theta$

Symbol		Net Dimensions
C $C_{ab,\lambda}$ $C_{sc,\lambda}$ $C_{ex,\lambda}$	Particle cross-section (Subscripts refer to absorption, scattering and total extinction respectively at one wavelength	ℓ^{-2}
c_p	Specific heat at constant pressure	$Em^{-1}\theta^{-1}$
d_p	Soot particle diameter	ℓ
D	Inside diameter of combustor	ℓ
$E_{b,\lambda}$	Hemispherical black body emissive power or hemispherical black body flux density emitted from a surface unit area	$ET^{-1}\ell^{-3}$
$E_{b,\lambda}$	Monochromatic emissive power of a black body or surface	$ET^{-1}\ell^{-3}$
ε_T	Total emissivity (or emittance)	-
ε_λ	Monochromatic emissivity (or emittance)	-
F_c	Number of free conduction electrons	-
h	Convective heat transfer coefficient	$ET^{-1}\ell^{-2}\theta^{-1}$
$\bar{h}$	Average heat transfer coefficient based on the hot side	$ET^{-1}\ell^{-2}\theta^{-1}$
I	Intensity defined as the energy per unit area normal to the direction of emission per unit solid angle	$ET^{-1}\ell^{-2}\Omega^{-1}$
I_λ	Monochromatic intensity from a real body	$ET^{-1}\ell^{-3}\Omega^{-1}$
I_o	Intensity incident on a system of interest	$ET^{-1}\ell^{-2}\Omega^{-1}$
I_L	Intensity after a distance L	$ET^{-1}\ell^{-2}\Omega^{-1}$
$I_{b,\lambda}$	Monochromatic intensity from a black body	$ET^{-1}\ell^{-3}\Omega^{-1}$
Im	Imaginary part of	-

Symbols		Net Dimensions
K ab,λ sc,λ ex,λ	Monochromatic extinction or attenuation coefficients (Subscripts refer to absorpition, scattering and total extinction respectively)	ℓ^{-1}
$K_{p,\lambda}$ $K_{g,\lambda}$	Subscripts refer to soot particles and gas respectively, at one wavelength	ℓ^{-1}
K_m	Mean absorption coefficient	ℓ^{-1}
KL	Absorption strength (or optical thickness)	-
k_m	Mean specific (mass) absorption coefficient, i.e. $K_m/\bar{c}$ (Note: In Ch. 7, dimension = $\ell^{-1}{}_m{}^{-1}{}_T$)	$m^{-1}\ell^2$
k_p	Specific absorption coefficient on a pressure basis	$F^{-1}\ell^{-1}$
k_c	Specific absorption coefficient on a concentration basis	$m^{-1}\ell^2$
k_i	Specific absorption coefficient of the i^{th} component	$F^{-1}\ell^{-1}$
k_o	Constant of proportionality = $B\bar{c}L$ in equation 2.11	ℓ
L	Path length	ℓ
$\dot{m}$	Mass flow rate	mT^{-1}
m	Complex refractive index $\equiv n(1 - iK)$	-
n	Real part of refractive index	-
p_c	Partial pressure of carbon dioxide	$F\ell^{-2}$
p_w	Partial pressure of water vapour	$F\ell^{-2}$
p_i	Partial pressure of i^{th} component	$F\ell^{-2}$
p	Total pressure	$F\ell^{-2}$
q	Flux density	$ET^{-1}\ell^{-2}$

Symbols		Net Dimensions
$Q(Q_r, Q_c)$	Flux energy per unit time (where subscripts r and c stand for radiation and convection respectively)	ET^{-1}
R	Spectral reflectivity	-
r	radius	ℓ
r	correlation coefficient	-
t	Time	T
T_s, T_e	Absolute temperature for wall surface on the flame side and flue gas exit respectively	θ
T_z	Absolute temperature at position z	θ
T_{sz}	Local wall temperature at position z	θ
T_i, T_o	Absolute temperature (suffixes denote inlet and outlet temperatures respectively)	θ
$\overline{T}$	Mean temperature across reactor	θ
T_t	Mean temperature across the flame	θ
T_{max}	Maximum temperature (absolute)	θ
ΔT	Driving force	Θ
$V(V_p)$	Volume of one particle of projected area $\pi d_p^2/4$	ℓ^3
w	Flow rate of water	mT^{-1}
x	Size parameter ($\pi d_p/\lambda$)	-
z	height measured from lowest calorimeter	ℓ
κ	Absorption index	-
λ	Wavelength	ℓ
λ_{ph}	Photon mean free path	ℓ
ρ	Density	$m\ell^{-3}$

Symbol		Net Dimensions
σ	Stefan-Boltzmann constant: 56.7×10^{-12} KW/m^{2}K^4	$ET^{-1}\ell^{-2}\theta^{-4}$
g_λ	Spectral dispersion exponent (or index) relating $K_{ab,\lambda}$ and λ - see equation 2.10	-
g_m	Mean dispersion exponent (or index) calculated for a specified wave band - see equations 2.18 and 2.19	-
Ω	Solid angle	Ω
γ	A constant in equation 7.12	$ET^{-1}\ell^{3-5}\theta$
ν	Frequency ($\equiv c\lambda^{-1}$)	T^{-1}

Key to Selected Subscripts:

Symbol	
c	Stands for convection unless stated otherwise.
g	Non-luminous gases (e.g. CO_2 and H_2O)
p	Particles of soot
T	Total
f_λ	Monochromatic value of a function, where f stands for any function
$f_\lambda(T)$	Function depends on wavelength and temperature
f(T)	Function depends on temperature only.
-	A dash on top of any symbol signifies a mean value.

LIST OF FIGURES

LIST OF TABLES

CHAPTER ONE

INTRODUCTION

Radiative transfer is of great importance in may applications, e.g. in glass smelting operations, steam boilers, combustors, etc. The radiant flux from a unit volume of a luminous flame is a function of the composition, particle size and shape, temperature, etc. A review of recent work related to flames indicates that there is yet insufficient information on the physical and chemical properties of the solid particles formed in these flames and on the optical properties at flame temperatures.

The effect of the carbon to hydrogen ratio of the solids on the mean specific absorption coefficient k_m is still inconclusive and is difficult to estimate in the wavelength region of interest (0.5-7 μm), as direct measurements on the refractive index m have not yet been made. The existence of agglomerates, irregular particles and particle size and refractive index distributions are believed to be further complicating factors[1]. The effect of agglomeration was studied theoretically and indicated that a considerable error could be introduced in the values of the emissivity if the agglomeration into chains was not allowed for [2],[3]. Lastly, information concerning the formation of flame particles is still insufficient and is needed to assist in the prediction of soot distribution in luminous flames[4].

In this work, we are interested in the luminosity of flames containing soot, rather than larger particles, such as those formed by carbonisation of oil droplets. Such flames may be represented as a system composed of very fine soot particles dispersed into a medium of partly-emitting hot gases. The concentration and temperature throughout the medium are variable with respect to both time and position.

It is now well established that the radiation from any luminous flame is made up of two main components: the yellow continuum caused by the

hot solid bodies formed in the flame as a result of incomplete combustion, and gaseous species such as H_2O, CO_2 and CO, which possess band spectra of appreciable strength in the spectral region (0.5 - 7 μm). It has been suggested that molecular species may emit in the visible [5-9] and infrared[10], and that absorption of radiation in the infrared by unburnt fuel in the central part close to the burner, where a low temperature exists, may be important[11]. Emission from CO or absorption by unburnt fuel is, however, relatively unimportant in practical flames, since they are not in general present in significant concentrations at such high temperatures[12].

The process of combustion can be influenced either by varying external parameters, such as nozzle and furnace shapes, flow rate and so on, which will have a direct effect on the aerodynamics, or by the use of additives (as in this work). The second method is used to study some of the parameters which may influence radiation from the flame. This study will provide information on the rate of formation of soot in this flame as well as an indication of the relative level of emission at the exhaust, which is a function of the rate of burn-up of the solids in the hot combustion gases. It would be ideal if the radiation could be increased without increasing the level of particulate emission, or even better, by reducing its level.

The literature on radiation is reviewed in Chapter 2. The importance of various emitters is discussed and a number of laws of black body radiation are presented. The attenuation of light from particles and gases is treated theoretically in a following Section, which defines the conditions when scattering from small particles is negligible and when $K_\lambda \propto \lambda^{-g_\lambda}$ The various representations of the total emissivity are discussed. The exponential form of the total emissivity is com-

pared with a recent representation obtained by integration using Wien's function rather than Planck's function. The error in using Wien's function is small for soot, as may be inferred from Appendix V.

The last thing to be compared in this section is the absorption coefficient, which was calculated for a number of soots, using different models. The range of application of the various representations of the emissivity is also tentatively defined. In Section 2.3, the condition under which self-absorption is not important is presented. Its relevance will become apparent in Chapter 7, where a simple model is discussed.

A detailed review of the factors which affect soot emissivity, such as mass concentration, soot composition and so on, is given in Section 2.4. The abundant literature cited made possible a comparision of the usefulness of optical techniques, as against sampling techniques, for determining particle size distribution and mass concentration. The literature related to the soot refractive index (m) is grouped under three different headings, namely m, g_λ and C/H ratio, which simplified the comparision of the numerous works on this subject. The effect of temperature on the refractive index, and hence on the absorption coefficient, is presented in some detail. The absorption coefficient is treated in a separate section, in which earlier findings are partly summarised and in which work scattered in a number of references is brought together, probably for the first time.

Chapter 3 is a general review of soot in flames. Several points of interest are combined here. An attempt is made to reach a better understanding of the chemical and physical processes involved in the formation of soot, as well as the intermediate stages, such as nucleation, coagulation and surface growth. The microstructure is presented in some detail to serve a number of purposes. It provides a clearer understanding of the internal

morphology of soot particles, and shows that the "crystallite" theory put forward a few decades ago by Warren[13] is no longer valid, in compliance with recent models of particle growth[14,15] and of microstructural arrangement[16]. A knowledge of the microstructure brings home the difference between thermal and flame soots and indicates that the structure of soot is "turbostatic" rather than "amorphous".[16]

A discussion of the mechanisms is presented, in which thermal and flame soots are not given separate treatment. This seems justifiable, considering the nature and morphology of soot produced in these systems The different works related to the chemical mechanism are reviewed under three main groups, namely: acetylene and polyacetylenes; polycyclic aromatic hydrocarbons and reactive polycyclic hydrocarbons. The idea originated from an early review by Homann and Wagner[7] on soot.

The physical mechanism of formation is discussed separately and provides, together with the discussion of the chemical mechanisms, a good background for understanding the effect of additives, discussed later in this chapter. Throughout the various stages of the presentation, tentative explanations are tendered in order to align various conflicting observations. The existence of a number of definitions for a soot nucleus earned it separate treatment.

The effect of additives is also treated extensively and is summarised in a number of tables. It includes a wide range of compounds, which are sub-divided into five groups. Various observations are analysed and tentatively explained. The lack of sufficient information and the diversity of experimental conditions, position, etc., are complicating factors. This section of the study on soot pointed to the possible usefulness of a number of groups of additives. This chapter, together with Chapter 2, provided the necessary background for the analysis of the results in Chapters 6 and 7 and influenced the choice of the equation used to estimate

the gas emissivity and mean specific absorption coefficient.

Chapter 4 presents the results of experiments made by the author on sampling and particle size distribution of soot particles. Two different techniques are compared, both using a free-flowing and an enclosed diffusion flame, so that the extent of agglomeration in these types of flames is shown. The various problems faced while using these instruments are presented. The importance of isokinetic sampling and the usefulness of a number of filters under the present experimental conditions are discussed in context. The problems involved when thermocouples are used to measure flame temperature under conditions where soot may deposit on it are also discussed in this chapter.

The description of the main apparatus as well as the auxiliary apparatus is covered in the first section of Chapter 5. The rest of the chapter deals with the planning of experiments which involved exploratory studies using the apparatus and influenced the choice of the most appropriate additives for the purpose of studying their effect on radiation, as well as the levels of the additives used.

The effect of the additives used on the components of radiation is discussed in Chapter 6. The first factor presented is the soot composition. This is treated somewhat exhaustively and includes a number of correlations obtained by fitting least-square equations to the data of a number of investigators.The dependence of g_λ on the concentration of heavy hydrocarbon species is stressed.

In Chapter 7 mean gas emissivities and mean absorption coefficients are determined using the more recent represenation of the total emissivity and the exponential form are presented for comparison. The oxidation of soot in diffusion flames is discussed to test the validity of a number of assumptions made concerning the formation of soot and the role played by O_2 or its products of decomposition. A model is presented which describes the flame emission in terms of mass concentration and temperature. It is

compared with experimental data. The effect of these additives on the convective and total heat transfer are also examined. Finally, the findings are summarised and recommendations are made.

CHAPTER TWO

REVIEW OF LITERATURE ON RADIATION

2.1 Thermal Radiation

The fundamental law for black body radiation, i.e. Planck's Law, may be represented, since $E_{b,\lambda}(T) = \pi I_{b,\lambda}(T)$, as follows[17a]:-

$$I_{b,\lambda}(T) = \frac{1}{\pi} \cdot \frac{c_1 \lambda^{-5}}{\exp(c_2/\lambda T - 1)} \quad . \tag{2.1}$$

Integration of this equation from $0 \rightarrow \infty$ gives the intensity emitted per unit area of a black body and is known as the Stefan-Boltzmann Law:

$$I_b(T) = \frac{\sigma}{\pi} T^4. \tag{2.2}$$

Real sources radiate less energy than a black body at the same temperature and the Planck function is reduced by a fraction $\varepsilon_\lambda(T)$, which is the emissivity of the medium. This is an average of effective emissivity, since the temperature distribution across the flame is generally variable.

Flame emission is mainly due to the banded radiation from CO_2 and H_2O vapour superimposed on the continous radiation of soot particles, as previously mentioned, and the emissivity takes the form

$$\varepsilon_\lambda(T) = 1 - \exp(- K_{p,\lambda} + K_{g,\lambda})L. \tag{2.3}$$

where $K_{p,\lambda}$ and $K_{g,\lambda}$ are the attenuation coefficients for soot particles and gases respectively. This expression may be derived in a similar way to that in Section 2.2 considering $\varepsilon_\lambda(T) = \alpha_\lambda(T)$.

It is relevant at this stage to point out that it is assumed that we are dealing with diffuse emitters, i.e. there is no important variation of emissivity with angle of emission. The emissivity or absorptivity will therefore not be defined as a function of angle of emission or reception. In order to simplify the equations, the emissivity and intensity will

henceforth be presented without indicating their dependence on temperature, as was done above.

2.2 Theoretical Treatment of the Attenuation of Light

2.2.1 By a suspension of small particles

If a plane parallel monochromatic beam of intensity I and wavelength λ is incident on a cloud of absorbing/scattering particles in a slab of thickness dL, the incident beam will be attenuated, in the absence of multiple scattering, by an amount

$$-\frac{dI}{I} = K_{ex,\lambda} dL. \tag{2.4}$$

where $K_{ex,\lambda}$ is the constant of proportionality due to both scattering and absorption. It is called the extinction coefficient and is equal to the sum of the coefficients of absorption, $K_{ab,\lambda}$ and scattering, $K_{sc,\lambda}$. If $K_{ex,\lambda}$ is independent of position, then equation (2.4), when integrated, becomes

$$I_{L,\lambda} = I_{o,\lambda} \exp(- K_{ex,\lambda} L). \tag{2.5}$$

and the intensity extinguished by the cloud may therefore be given as

$$I_{ex,\lambda} = I_{o,\lambda} \left[1 - \exp(- K_{ex,\lambda} L) \right]. \tag{2.6}$$

The monochromatic extinction coefficient for a cloud of spherical particles of the same composition is represented as

$$K_{ex,\lambda} = \int N(r)\ C_{ex,\lambda}(r)\ dr. \tag{2.7}$$

where the total number of particles per unit volume, $N = \int N(r)\ dr$ and $N(r)\ dr$, represent the number of particles in the unit volume falling within the size range r to r + dr.

If the particles are very small in comparison to the wavelength,

to the extent that the applied field may be considered homogeneous, and if the field inside the particle is in phase with that outside, then the Rayleigh approximations may be used to calculate the scattering and the extinction cross-section, as follows[17b]:

$$C_{ab,\lambda} = - \frac{6\pi V_p}{\lambda} \mathrm{Im}\left(\frac{m^2-1}{m^2+2}\right) \tag{2.8a}$$

$$C_{sc,\lambda} = \frac{24\pi^3 V_p^2}{\lambda^4} \left| \frac{m^2-1}{m^2+2} \right|^2 . \tag{2.8b}$$

In the case of soot particles, their size is small with respect to the wavelength of thermal emission, and therefore $K_{ex,\lambda} \rightarrow K_{ab,\lambda}$, since $C_{ab,\lambda} >> C_{sc,\lambda}$. Thus from equation (2.7), $K_{ab,\lambda}$ may be written as

$$K_{ab,\lambda} = - \frac{6\pi \bar{c}}{\lambda \rho} \mathrm{Im}\left(\frac{m^2-1}{m^2+2}\right). \tag{2.9}$$

if $\frac{\bar{c}}{\rho} = NV_p = \int N(r)\ V(r)\ dr.$

Equation (2.9) implies that the absorption coefficient per unit mass of the particle cloud is independent of particle size or size distribution.

The value of the refractive index of soot at flame temperatures has not yet been determined experimentally in the infrared. Room temperature measurements exist and have been theoretically extrapolated to flame temperatures[18]. In order to avoid the problem of determining the refractive index, empirical relations are resorted to.

It is possible to write equation (2.9) as

$$K_{ab,\lambda} \propto \lambda^{-1} .$$

if m = constant. The refractive index, however, varies with wavelength and the modified equation is usually employed, where B and g_λ are constants

and $g_\lambda \sim 1$ in the infrared, as follows:

$$K_{ab,\lambda} = B \bar{c} \lambda^{-g_\lambda} \tag{2.10}$$

The monochromatic emissivity of the soot cloud may be represented, through substitution of equation (2.10) in equation (2.3), with $K_{g\,\lambda} = 0$, giving

$$\varepsilon_{p,\lambda} = 1 - \exp(- B \bar{c} \lambda^{-g_\lambda} L). \tag{2.11}$$

The previous calculations are based on the assumption that the particles in the cloud concerned are spherical and very small compared to λ and $|m|/\lambda$ (where m is the complex refractive index)[17b]. If the same number of particles agglomerate into larger spherical particles (maximum size governed by previous restrictions), there will be no change in the absorptivity, since $N V_p$ is constant. If, however, agglomerates are slightly elongated, as soot particles often appear in electron micrographs, the absorptivity will increase. The effect of elongation has been treated in several reports[2,3].

2.2.2 By a solid-free gas volume

The attenuation of a monochromatic beam of intensity I by an isothermal slab of absorbing gas of thickness dL may be represented as

$$- dI = K_{g,\lambda} I \, dL.$$

The intensity absorbed after passing through a path of length L of gas is

$$I_{ab,\lambda} = I_{O,\lambda} \left[1 - \exp(- K_{g,\lambda} L)\right]. \tag{2.12}$$

The above equation is correct provided that $K_{g,\lambda}$ is independent of position. Suffixes ab, and O stand for absorbed gas and value of the intensity at

L = 0 respectively. $K_{g,\lambda}$ is represented for engineering calculations as a function of partial pressure of the gas component ($\equiv k_p\, p$) rather than molar concentration ($\equiv k_c\, c$), where k_p and k_c are the specific absorption coefficients.

The quantities inside the brackets on the right-hand side of equation (2.12) represent the monochromatic absorptivity of the gas, which is also equal to the monochromatic emissivity. The latter may be represented as

$$\varepsilon_{g,\lambda} = 1 - \exp(-K_{g,\lambda}L). \qquad (2.13)$$

If the gas mixture is grey, i.e. $K_{g,\lambda}$ does not vary with wavelength, then within the gases in question its total emissivity may be written in the form of Bouguer's Law, equation (2.13). Real gases, for example CO_2 and H_2O, emit in discrete bands in the infrared, and the contribution to the emissivity varies with λ. If, however, the gas in question is visualised as a mixture of grey gases, it is still possible to represent the emissivity in an exponential series form as follows[17c]:-

$$\varepsilon_{g,\lambda} = \sum_{i=1}^{n} a_{g,i}\left[1 - \exp(-k_i p_i L)\right],$$

on condition that (i): $\sum_{i=1}^{n} a_{g,i} = 1$

and (ii): all values of a are positive,

where $a_{g,i}$ is the fractional amount of the i^{th} component or the weighting factor and $k_i p_i$ is the absorption coefficient.

Both these restrictions imply that $\varepsilon_{g,\lambda} \leq 1$. The $k = 0$ term corresponds to the "windows" in the spectrum between the strong emission bands. The accuracy in the value of $\varepsilon_{g,\lambda}$ increases with the number of terms presented for fitting. For example, at 1371 K a mixture of three grey terms and one clear term adequately represents the emissivity of an equimolar mixture of CO_2 and H_2O[17c].

Taylor[19] produced a number of curves by which the total gas emissivity ε_g, may be obtained from values of $(p_w + p_c)L$ at various temperatures. The method followed was fitting points evaluated from General Dynamics data[20] into a four-term model in which k is assumed to be independent of temperature and the weighting factor alone bears the effect of temperature. The methods of fitting the above exponential series to emissivities of CO_2 and H_2O and to gas/soot mixtures will not be discussed here, since it is not of immediate interest and has already been discussed in detail elsewhere (17c), (19), (21).

2.3 A General Discussion concerning Flame Emissivities

In the last two sections, the attenuation of a monochromatic beam of light was discussed for the case of a solid-free gas and a suspension of soot particles in a non-absorbing medium. In hydrocarbon flames there are a number of possible effects, such as:-

(i) Absorption of solid-particle radiation by flame gases;

(ii) Self-absorption of gas radiation;

(iii) Self-absorption of particle radiation;

(iv) Absorption of gas radiation by solid particles.

The above factors will influence the measured effective radiant temperature (spectral and total) of a flame, provided that the optical thickness of the medium is not very much less than one. If, for example, the flame temperature is cooler on the outside than on the inside, then the temperature measured by a radiometer will be low, since the effective flame emissivity is derived from the total absorptivity. This effective temperature will therefore depend on the extent of self-absorption in the cold boundary of the flame and will decrease for a given flame with size of the colder surrounding absorbing fluid outside the flame core.

It should be noted that the extent of absorption of the solid particles and of the gaseous species CO_2 and H_2O vapour will be different. This is because the absorptivity of soot particles increases with a decrease in the wavelength of radiation (i.e. with an increase in temperature), while on the otherhand the total absorptivities of CO_2 and H_2O, or of other possible absorbers, such as unburnt fuel close to the burner, decrease with temperature [11].

If the optical thickness of the flame is very much less than one, which is sometimes referred to as the optically thin limit, the flame would be expected not to absorb any of its emitted radiation [22]. Any photon emitted inside the flame is expected to reach the bounding walls, as the photon mean-free path is much larger than the characteristic dimension of the flame (i.e. the diameter, in the case of a cylindrical flame).

$$\tau_{f,\lambda} = \frac{L}{\lambda_{ph}} \ll 1,$$

where $\tau_{f,\lambda}$ is the optical thickness (KL) and λ_{ph} the photon mean-free path. In most industrial applications, self-absorption of flame radiation by the various fluid elements is important to various extents.

The second and last point to be discussed under this heading is the various representations of the total emissivity and displacement constants.

The total emissivity of an isothermal volume of a soot-laden gas is, by definition:

$$\varepsilon_T = \frac{1}{\sigma T^4} \int_0^\infty \varepsilon_\lambda E_{b,\lambda} d\lambda, \qquad (2.14)$$

where $E_{b,\lambda}$ is the Planck function. In predicting ε_T, a problem arises due to lack of detailed information of the spectral properties of flames. The integral equation (2.14) may, however, be evaluated graphically, from

the values of absorptivity and spectral temperature of the flame obtained experimentally at various wavelengths over the range of interest. This can be done by a number of established procedures, e.g. the Schmidt method, using a number of filters . Information concerning this method may be found in references (11) and (23-25d).

If integration is to be avoided, total emissivity can be obtained with little error by substituting in equation (2.11) the value of λ which divides the black body energy spectrum (obtained from Planck's Law) into two equal parts. The emission mean wavelength is determined at the cloud temperature, where $\lambda_{0.5}T = 0.4107 \times 10^{-2}$ mK, so that equation (2.11) for the infrared becomes

$$\varepsilon_T = 1 - \exp(-\ 3.501\ \bar{B}cLT/c_2) \qquad (2.15)$$

where the above exponential index divided by L is the absorption coefficient $K_{ab,\lambda_{0.5}}$.

If, however, Wien's function,

$$E_{b,\lambda} = c_1\lambda^{-5} \exp(-c_2/\lambda T),$$

is substituted for Planck's function in equation (2.4), the total emissivity may be represented as

$$\varepsilon_T = 1 - (1 - \bar{B}c\, LT/c_2)^{-4} \qquad (2.16)$$

Although Wien's function is valid in the region $T < 0.3 \times 10^{-2}$ mK, the error is expected to be small for soot particles (see Appendix V).

Hottel and Sarofim[17a] provided a new displacement law (or constant), which was obtained algebraically:-

$$\lambda T = 0.3670 \times 10^{-2}\ \text{mK}.$$

λT is the spectrum which contains maximum energy per unit fractional change in the interval λT. When this value is substituted in equation (2.11), it becomes

$$\varepsilon_T = 1 - \exp(-3.9207\ B\bar{c}LT/c_2). \qquad (2.17)$$

Equations (2.15) and (2.17) will compare well with equation (2.16) when the emissivity is in the vicinity of 0.65 and 0.15 respectively[26]. These values are obtained from Table 1, which was compiled by determining the constant B in equation (2.16) for different emissivities. By forcing the aforementioned equation in the exponential form, the corresponding constant, say B', was evaluated for the same emissivities.

Heap and Lowes[12] compared methods of evaluating attenuation coefficient for a number of soots using the same properties, namely mass concentration, density, temperature and characteristic dimensions. The results are shown in Fig. (1). The first coefficient, K_1, was evaluated from ε_T calculated from the Mie series[17e]. The second, K_2, was calculated using Hawksley's[27] approximate expression for the extinction coefficient and assuming a rectangular hyperbolic relationship existing between K and λ. The third, K_3, was evaluated using the displacement constant, = 0.4110×10^{-2} mK.

Comparing K_1 to K_4 (where $K_4 = 3.9207\ B\bar{c}T/c_2$) in Fig. (1), it is possible to conclude that no fixed relationship exists with the soots reported. Generally speaking, it is difficult to say which method will give values closest to K_1 because the variation of optical properties of the soots with λ is unpredictable. A reasonable guide[26] is that K_3 will give a more correct estimate of the absorption coefficient if the total emissivity is in the vicinity of $\varepsilon_T = 0.65$, whereas K_4 will give the more correct value if it is in the vicinity of $\varepsilon_T = 0.15$. The agreement of K_3 with increase in emissivity can be inferred from Fig. (2), i.e. an

imaginary line which divides the black-body spectrum into two halves will nearly coincide as L tends to 1.0 m. The same effect on emissivity is produced with an increase in particle mass concentration.

The above values of the emissivity represent the result of evaluating the ratio of the overall constant in an equation of the form of (2.15) and in equation (2.16) for various values of the emissivity[26]. It may be observed from Fig. (1) that the values of K_4 are generally in agreement with those of K_2 than in K_3.

To conclude this section, it should be pointed out that emissivities and absorption coefficients obtained experimentally for the entire flame, though useful, are subject to various forms of bias, since the concentration of emitting species and the temperature profile vary along, as well as across, the flame. A better representation of total flame emissivity could be calculated if the total radiation, temperature and soot concentration were known at various points across the flame Details of the methods available for measuring the local radiation inside a flame may be found elsewhere[23,24].

2.4 Factors Which Influence Soot Emissivity

The properties of soot which affect emission from a flame are:-

1) mass concentration;
2) refractive index (C/H ratio, complex refractive index and dispersion exponent);
3) particle size and shape;
4) particle density.

In this section, these factors will be examined, the work of many authors and their contribution will be reviewed and the relative importance of the individual factors will be discussed.

2.4.1 Mass concentration

It may be inferred from equations (2.15) to (2.17), in which $K = B_{\sigma}\bar{C}T$, that the concentration of soot in a flame is amongst the factors which have a significant influence on its attenuation capacity.

2.4.2 Refractive index:

a) Carbon/Hydrogen Atomic Ratio (C/H):

The C/H ratio has been used for some time to measure the inner rank, as well as the structual change, in coal. Coals with a C/H ratio of less than 1.4 are classified as low-rank coals[28]. There is some concensus that the chemical composition of soot may have an important effect on the emission coefficient, i.e. the radiant emission from a flame. The atomic ratio of carbon to hydrogen of soot in flames is generally believed to be about 8:1[25b].

Sato and Kunitomo[29] studied the variation of the C/H ratio with distance from the burner for a number of liquid and gaseous fuels The ratio for the various flames generally increased, approaching a constant value which varied between 2.78 and 8.33 at the far end of the furnace. Their next step was to study the effect of chemical composition on the specific absorption coefficient k_m determined experimentally. They observed that in most cases the value of k_m, calculated using an exponential form of the emissivity, corresponded inversely with the C/H ratio of the solid particles, though on the whole the effect of chemical composition was small. This was a useful conclusion, as the scatter observed in the points representing particle emissivity and effective emission thickness of a number of fuels could then be mainly explained by the effect of particle size distribution. The particle size in some cases ranged up to 100 μm.

Lowes and Heap[30], however, found no correlation between the calculated mean specific emission coefficient k_m and chemical composition. The data used to calculate k_m were based on room temperature values of the complex refractive index for a cloud having a mean particle diameter of 0.03 μm and a density of 1.65×10^3 kg/m^3. Interesting features of the plot were the wavy appearance of the k_m vs. carbon content curve and the fact that soot with different origins but equal carbon conten- had different emission coefficients. For example, for a composition of 99.5 per cent carbon in the 1-5 μm range computed values of k_m for acetylene and sterling soot were 1.4×10^3 and 1.15×10^3 m^2/kg respectively.

Results obtained on small laboratory-scale flames were somewhat different. Millikan[31] showed that the mean dispersion exponent g_m of soot is approximately proportional to the inverse of the C/H atomic ratio in the spectral range (0.33 - 1.0 μm) for a number of premixed flames of ethylene/oxidant and one acetylene/oxygen flame. The soot composition from the plots appeared to vary between $C_{1.8}H$ and $C_{10}H$, and within this range the mean dispersion exponent varied between 1.9 and 0.9. Their data can be represented approximately as:

$$g_m = \frac{2.45}{C/H} + 0.66. \qquad (2.18)$$

Another relevant study was presented by Siddall and McGrath[32]. They investigated the dependence of the mean dispersion exponent g_m (in the infrared) on the C/H ratio from soot produced by burning a number of gaseous and liquid flames, and suggested that the plot showed a linear correlation. These data were plotted by Jones and Schwar[1]. While determining equation (2.18) above, however, g_m showed a higher linear correlation with the inverse of the C/H ratio, resulting in the following equation:-

$$g_m = \frac{.7368}{C/H} + .7956 \qquad (2.19)$$

There is no direct correspondence between equations (2.18) and (2.19), as would be expected, since they do not refer to the same region of the spectrum. Other aspects of equation (2.18).will be presented in Chapter 6.

The effect of temperature on the composition of soot samples has been noted by Bonne and Wagner[9]. When they re-inserted a sample collected at a height of 27 mm into the flat flame used in the experiment for a short while, the C/H atomic ratio was increased by approximately a factor of 5. They believed that the reduction in the amount of hydrogen resulted from evaporation of the more volatile hydrocarbons absorbed on the soot. The formation of these hydrocarbons with low C/H atomic ratio has been discussed in a number of publications, e.g. by Long et al.[33-38] and others[39,40,6].

A few years later, Homann and Wagner[7] studied the variation of C/H ratio with height in a flat acetylene oxygen flame. There was a step rise up to a value of about 20 mm, corresponding to a soot molecular formula of C_6H. This corresponds to the region in which young soot was growing from "adding" polyacetylenes. The second stage of growth was less steep and approximately linear. The first soot particles collected here had a molecular formula of approximately C_4H at about a height of 14 mm and increase to about $C_{14}H$ at 40 mm.

A similar trend was recently observed by D'Alessio et al[6], who studied the variation of C/H ratio of soot produced in a flat pre-mixed methane/oxygen flame according to distance from the burner. The first soot collected had a molecular formula $C_{2.4}H$, which shows a high hydrogen content. Although the latter decreased with distance, it was still present in considerable amounts at a height of 30 mm ($C/H \sim 5.6$). They also determined that polycyclic aromatic hydro-

carbons may account for up to 30% of the hydrogen in the collected soot.

Although heights have been mentioned during the discussion above, this was only to indicate the speed at which the change in temperature occurred and the stages of particle development.

b) Refractive Index:

The complex refractive index of a medium may be written in the form $m = n(1 - i\kappa)$, where n and κ are the indices of dispersion (real refractive index) and absorption respectively. It is usually measured at room temperature, as it is not yet possible to determine its value by measuring directly inside the flame, with the possible exception of light scattering methods for particles of narrow size distribution[30]. Foster and Howarth[41] determined the refractive indices of soot collected from a number of oil flames in the wavelength range (1.0 - 5.0 μm) by measuring the reflectivity of each sample. A similar study was made by Dalzell and Sarofim[42] on soots from acetylene and propane flames. The spectral range of interest was extended to include the visible and near infrared up to 10.0 μm. Values of n reported in the visible appear to be nearly constant, unlike those reported by Senftleben and Benedict (see ref. 43) for carbon, where it increases slightly with an increase in λ.

Lowes and Newal[44] commented on the optical constants of soot obtained by the authors mentioned above by suggestingthat there was tendency for the dispersion indices of soots to increase with C/H, but that there was no obvious correlation that could explain the variation of absorption indices. This is interesting, since previous findings by McCartney and and Ergun[28] in the green (0.5 - 0.57 μm) indicated that the absorption indices of coal appeared to be a much more sensitive measure of the structural variation of composition of graphite and coal than the dispersion indices. They gained this impression from plotting their results, as

well as those of others, for maximum dispersion and absorption indices in the form of a logarithm against the inverse of the C/H ratio. Only in the case of the absorption indices did the increase tend to follow a logarithmic straight line relationship, within the range of $1.70 \leq C/H \leq 5$. A similar plot of the variation of reflectivity with C/H suggested the following approximate relationship:-

$$R_\lambda = R_{g,\lambda} \exp(-3.6\ H/C),$$

where $R_{g,\lambda}$ is the reflectivity of graphite. The authors[28] were, however, unable to explain what this constant stood for theoretically.

It is worth noting that the logarithm of the resistivity of a number of coal samples was found by Waters[45] to be inversely proportional to the C/H ratio (i.e. between 1.75 and 5). Since the reflectivity is inversely proportional to the resistivity, this corroborates the above relationship. Above a C/H ratio of 5, the resistivity of the coals tended to a constant value, though their hydrogen content was still high. This is interesting, considering that the dispersion exponent g_λ of a soot (measured in the visible) tended to a constant vlaue when the soot's composition was $> C_{4,3}H$[6]. It is by no means implied that g_λ is synonymous with the resistivity, but that their similar behaviour is deserving of comment.

The magnitude of the error which would be introduced if room temperature values of m were used to calculate the emission of soot at high temperatures could present a real problem. Theoretical computations using a typical room temperature refractive index of (2.10 - 0.7 i) showed[30], however, that, for a change of temperature between 1250 and 1750 K, the mean specific emission coefficient $k_m (m^2/kg)$ was reasonably affected only when the particle diameters were given values $< 1\ \mu m$. The range studied was up to

3 μm. At $d_p < 1$ μm, however, the maximum value of the specific emission coefficient was shifted to smaller diameters, as the value of the temperature was increased: this effect is sometimes termed 'black-body shift'[30].

The above authors illustrated in a number of curves the effect of varying only the absorption index of the above room temperature refractive index on the value of k_m. It was possible to deduce from these curves that, for a soot cloud of average particle size ~0.05 μm and at 1500 K, an increase in the absorption index κ from 0.33 to 0.40 is at lease one- and a-half times as effective in increasing the value of k_m as a temperature increase of 250°C.

Howarth, Foster and Thring[18] had, some time ago, calculated the values of n and κ at various temperatures for the case of a perfect graphite crystal, using a dispersion equation derived from classical electron theory. These were used to calculate the "normal" reflectivity of a plane surface. In order to test the validity of their theory, they plotted experimental values obtained by Grenis and Levitt[46] for pyrographite, using $R_\lambda = \varepsilon_\lambda - 1$, where R_λ is the reflectivity at a wavelength λ. There was good agreement with the values of R_λ obtained theoretically down to a wavelength of about 0.5 μm. At this value, the predicted reflectivity did not vary with temperature. They were aware that, as a result of certain assumptions, the model may over-estimate the effect of temperature. Judging from their results and the difference between soot and graphite, they believed that the effect of temperature on k_m for soots is negligible.

Dalzell and Sarofim[42] stressed that the optical properties of soot cannot be equated with those of amorphous or graphitic carbon, mainly due to the differences in chemical composition, i.e. C/H ratio, and partily as a result of the differences in structure. They admitted some reservation about the procedure by which Stull and Plass[47] and Howarth et al[18] extrapolated their room temperature measurements of n and κ to flame temperatures. Their reservation was based on the fact that the values as well as

the temperature dependence of the constants in the dispersion equations were not definitely known.

From their own conclusion, as well as the existence of other relevant works which also point to the "near zero" dependence of m on temperature e.g. Bennett and Porteus[48] for carbon at 0.65 μm and Ditchburn[49] for graphite in the infrared - Dalzell and Sarofim suggested room temperature values of the optical constants of soot were valid at normal flame temperatures.

An interesting study was undertaken by Boynton et al.[50], in an attempt to evaluate the spectral and temperature dependence of a cloud of small 'carbon' particles. They extended the calculations of Stull and Plass[47] for carbon in bulk form from 2500 K down to 1000 K. The range of wavelengths studied was between 1 and 4 μm. At temperatures below 1700 K, there was good agreement between theoretical predictions of spectral change of k with their experimental data, as well as the value of k obtained from data on transmission compiled by Hottel and Broughton[51]. Above 1700 K, the theoretical and experimental values diverged. The disagreement between the experimental and computed values of k decreased with a decrease in wavelenth, so that at λ = 1 μm there was good agreement to about 2000 K. In the temperature region T > 1700 K, k appears to depend only on temperature and very little on wavelength.

It is interesting that the complex refractive index of coal is also insignificantly changed with temperature up to 1700 K[52].

Beér and Howarth[53] reported discrepancies between the calculated and measured absorption coefficients for soot from a plug-flow type oil flame at 2000 K. An electron micrograph presented by the authors showed that the particles had a hexagonal appearance. This is important, as it indicates that graphitisation could occur at temperatures much lower than 2730 K in flames without stabilisation near the burner, which explains the high values of k_m, e.g. 0.032, λ=2.79 μm, obtained under such conditions.

This value is close to the theoretical limits of k_m for small particles[53], i.e. m = 1 - i 1.6. Data of n and K obtained by a number of investigators for a cloud of small particles (soot, carbon) are plotted, together with calculated absorption coefficients in the above reference.

It is not possible to be conclusive at this stage, however attractive this explanation may be, as to the cause of the disagreement between theory and experiment above 1700 K in the paper of Boynton et al. This is because it is not possible to observe the structure of the particles from stereographic photomicrographs in the paper, and because the authors have not mentioned the presence of graphitised particles, although they were able to distinguish individual particles at oxygen/fuel ratios > 1.6.

c) Dispersion Exponent (g):

It is clear from the previous sub-section that the spectral variation of the optical constants of soot in the wavelength range important to thermal radiation, i.e. 0.5 - 7 μm, has not yet been determined in flames in situ. Fortunately, the monochromatic absorption coefficient obtained experimentally can be represented as

$$K_\lambda \propto \frac{1}{\lambda^{g_\lambda}} ,$$

where g_λ is the monochromatic dispersion exponent and includes the effect of soot composition, structure, temperature and wavelength (see equation (2.10) . The dispersion exponent has already been discussed in connection with C/H ratio or refractive index. The concern of this sub-section is to describe the experimental as well as present some of the most important work involved in obtaining the constant.

Rossler[54] determined the monochromatic absorption coefficient by measuring the monochromatic transmissivity τ_λ of soot deposited on an uncooled glass plate, using an equation of the form

$$\tau_\lambda = \frac{I_{L,\lambda}}{I_{O,\lambda}} = \exp(-K_\lambda L),$$

where $I_{L,\lambda}$ is the intensity leaving a plate of thickness L. The value of g_m was obtained from the slope of a plot of

$$\ln \ln \frac{I_{O,\lambda}}{I_{L,\lambda}} = \ln k_O - g_m \ln\lambda .$$

The mean dispersion exponent g_m varied between 0.75 and 1.43. It was found to depend solely on the type of fuel used and showed no dependence on the thickness of the deposited layer of soot which is contained in k_O. The wavelength range studied was $0.35 < \lambda < 10.0$ μm.

Hottel and Broughton[51] obtained a mean value of g = 1.39 for soot in an amyl acetate flame from two temperature measurements using a red and green filter. This value was in excellent agreement with the value of 1.4 obtained from Becker's[55] transmissivity data for the same fuel. This also tested the validity of the two-colour method developed by the authors. As a result of plotting the transmissivity data obtained on flames and soot deposits by previous authors, they suggested that a value of $g_m = 1.39$ should be used to measure ε_λ from the green to the red, and that a value of $g_m = 0.95$ was more suitable in the range $0.8 < \lambda < 10.0$ μm.

Since the value of g_m for different fuels was obviously not the same, Hottel and Broughton's next step was to evaluate the magnitide of the deviation. The results indicated that the error in the value of the true temperature introduced by an error in the value of g_m is relatively small and may be reduced with an increase in optical depth of luminous flames. Conversely, it can also be inferred from these results that the temperature is more or less independent of the value of g_m within this range. There was also close agreement between measurements of g_m on an uncooled glass plate and in flames in situ. A similar conclusion concerning this agreement was later reached by Millikan[31], using an extinction technique

only. Agreement between flame and plate measurements was, however, obtained only in the case when the plate used to collect soot was water cooled.

A related study was undertaken by D'Alessio et al.[6], who plotted the dispersion exponent of a flat, pre-mixed flame in the visible from light-scattering and extinction measurements on a flame and on a cooled quartz plate. The results obtained from both methods also matched well. Their analytical results indicated that extinction up to a distance of 8 mm from the burner mouth is representative of absorption by a fluid phase of boiling point > 673 K. At and beyond this distance, soot particles were deposited on the cooled quartz plate. The contribution due to solid particles becomes important with distance. The dependence of g_λ on the amount of polycyclic hydrocarbon was important up to about 17.5 mm, after which it tended to a constant value of about 1.42; this is close to the approximate value of 1.50 obtained by Bonne and Wagner[9] using a flat acetylene flame. In this region, although the amount of hydrogen present is still considerable, g_λ tends to be independent of the C/H ratio. The authors believed that g_λ in this region is only dependent on particle size. It is interesting to observe that the maximum value of g_λ measured for the early soot formation region very close to the burner is greater in both the studies in question than the theoretically calculated limit of 2, which has been suggested by Rossler[54] and by Siddall and McGrath[32].

The dependence of the dispersion exponent g on wavelenght was studied in some detail by Siddall and McGrath[32]. A number of liquid and gaseous fuels were chosen to produce a distribution of mean soot particle diameters. Their general conclusions were as follows:-

i) A parabolic representation is required to describe the overall variation of g_λ with λ;

ii) In some cases the dispersion exponent can be represented as

$g_\lambda = a + b\ell n\ \lambda$,

where a and b are constants for a particular type of soot at a given temperature. An equation in this form may also be used to represent the variation of λ over a short wavelength range, i.e. from 1 to 2 μm with reasonable accuracy.

iii) A constant value of g_λ is satisfactory in the visible. Although it may be possible to represent the range (1 - 8 μm) by one value of g_λ, this may produce misleading results in the region where g_λ varies greatly with λ. The mean values of g_λ corresponding to the various soot samples varied between 0.77 and 1.25 in Siddall and McGrath's case. However, most of the values of g_m were reasonably close to one.

Dalzell and Sarofim[42] derived a procedure to calculate the real and imaginary components of the refractive index of soot. This was achieved by fitting a dispersion model to data of optical constants of propane soot. By means of this model, they predicted that an increase in the number of free (or conduction) electrons per unit volume F_c, would result in an increase in the value of k_λ and a decrease in the value of the dispersion exponent g_λ ($\equiv \partial \ln k_\lambda / \partial \ln \lambda$). The study covered the following spectral range: 0.4 μm < λ < 10 μm.

The experimental values of g_λ and g_m reported by various workers[6,51,54] range between 0.65 and 2.4. This is very close to the theoretical range of $0.7 < g_\lambda < 2.1$, which represents the minimum and maximum of values of g_λ computed for a ten-fold increase in F_c using two different models[42]. On the basis of this evidence the difference in the value of the refractive index m and dispersion exponent reported by various investigators could be due mainly to the difference in C/H ratio of soot and partly to its molecular structure as had been suggested by Dalzell and Sarofim[42].

Conclusion:

The carbon/hydrogen atomic ratio varies along the flame height and with fuel type. A linear correlation between C/H ratio and the dispersion exponent of a number of fuels has been suggested by Millikan[31]. Others do not believe that variation in this parameter had an important effect on spectral emissivity or was correlated to the emission coefficient.

The determination of the complex refractive index of soot still poses serious problems. Values at room temperature have been obtained by measuring the reflectivity of soot samples. The effect of temperature on the complex refractive index is still inconclusive. The evidence compiled here suggests in general that flame temperature values will not differ to any great extent from those obtained at room temperature. The different values of the refractive index (m) the difference in C/H ratio of the soot and partly due to its molecular structure.

Attempts to determine the effect of temperature (or composition) using dispersion equations are liable to be somewhat misleading, since many of the constants required have only been evaluated for carbon or graphite. There is some doubt about the values of the constants and their temperature dependence. However the information they provide is needed in cases where experimental results are not available. The effect of an increase in C/H ratio could theoretically be accounted for in terms of a change in the value of the free electron concentration F_c. The different values of dispersion exponent in the visible and in the infrared, reported in literature, can also be accounted for by an increase in the value of the F_c corresponding to an increase in C/H ratio. These conclusions were reached regardless of the effect of temperature on the concentration of free electrons.

The dispersion exponent g_λ may be related theoretically to m using equations (2.9) and (2.10). It is a useful criterion for determining the effect of λ on the absorption coefficient. Mean values of g_m of 1.46 and

1.0 represent the visible and infrared respectively. Although the latter value of g_m is representative of the whole spectrum in the infrared, the mean value may give incorrect results within a given spectral range (see section 2.4.2 and 2.4.5). Finally, g_λ does not appear to be dependent on particle size of soot in the infrared region[32] of the spectrum, unlike in the visible[6] where a dependence on d_p is indicated.

2.4.3 Particle Size and Shape:

The mean particle diameter of solids formed in a flame is a function of of the fuel used and the aerodynamic conditions since the formation and subsequent growth or destruction of the soot particle will depend on the oxygen/carbon ratio and temperature in its vicinity. Due to the diversity of sources of soot, average diameters vary between .025 and 0.1 μm, when measured from electron micrographs. However, larger particle sizes 0.2 μm may be formed in flames burning liquid fuels.

A distribution of particle size exists in flames and any one position in both the horizontal and vertical directions. Therefore it is essential to know the type of distribution or the effective mean diameter for any particular application. There are numerous techniques for particle size determination. The most useful, considering the size range discussed above are:

i) electron microscopy.

ii) optical techniques, namely by light scattering and extinction.

a) Electron Microscopy:

Particles collected on an electron micrograph usually appear in the form of agglomerates. The distribution of their positions is random which suggests that there is a possibility of their being formed in the flame.[56]

The agglomerates are composed of primary particles, which may have been a spherical appearance. The force which binds the primary particles to form the agglomerate is relatively weak, unlike that which keeps the primary particles together. In fact each primary particle is itself made of very small particles permanently fused together[14,15].

A method for characterising the shape of soot agglomerates was presented in two parts by Medalia[57] and Medalia and Heckman[15].

Experimental evidence from both pyrolysis and flame studies indicates that particles may exist in other forms than as cross-linked chains; A detailed electron-microscope study of carbon formation during pyrolysis of hydrocarbons was undertaken by Johnson and Anderson[58]. They illustrated that it was possible by manipulating the pyrolysis temperature ($823 < T < 1273$), the concentration of acetylene ($< 20\%$ by volume), and the contact time (> 9 seconds), to obtain a range of particle types from poylmers to chain-structured particles.

The above-mentioned conditions cannot be compared directly with conditions under which soot is formed in flames, since the residence time in the pyrolysis region of , for example, a diffusion flame, is $\sim 10^{-3}$ seconds. Residence times in premixed flames are much shorter. A relevant point, discussed in the paper by Johnson and Anderson[58] is the effect of the pyrolysis temperature on the size of the primary particles in an agglomerate. Above 1273K the size of the primary particle decreased with temperature; the opposite trend was established for temperature increase > 823K, i.e. the size of the solid sphere increased. In general the size of primary soot particles is smaller the higher the linear velocity of the gas and the smaller the diameter of the pyrolysis tube. It is independent of the chemical mechanism by which soot nuclei are formed or that by which they subsequently grow[59].

Tesner[59] studied the pyrolysis of methane and acetylene under tem-

perature and residence times comparable to flame conditions. He concluded that agglomeration of soot cannot occur in the region of "intensive" formation and growth of primary particles, due to the outward flow of hydrogen from each particle. Hydrogen results from chemical condensation reactions and from the decomposition of hydrocarbon molecules on the soot surface.

In another study of Tesner[60] presented a curve relating the rate of particle formation to height along a diffusion flame. The fuel was 99.4 per cent methane by volume and 240 m in height. The rate of particle formation rose very slowly up to about 5 per cent m of the flame height and few particles seemed to have been formed. In the region between 54 and 67 per cent of the flame height, on the other hand, the curve rose sharply. This was the region where the greater part of the soot mass was formed. Below the halfway mark of the flame height the particle size distribution varied from .015 to .045 μm and was comparable to the distribution in Tesner's pyrolysis experiments, discussed above. One would therefore expect that in this region at least, little or not agglomeration takes place. This suggests that the position of sampling or observation is an important factor.

The work of Parker and Wolfhard[61] concerns this study insofar as it is related to the dispersion exponent and particle size distribution. They reported that in a non-smoky Hefner candle the size of primary particles in chains collected on a microscope grid were ~ .01 μm. When the flame was made to smoke, larger particles, d_p = 0.05 μm, were collected. However sampling positions were not varied.

Wersborg et al[5] collected soot along the height of a flat premixed acetylene-oxygen flame by a molecular beam system. The soot particles were roughly spherical up to about a height of 50 mm above the burner. At 60 mm agglomerates began to form. Ball and Howard[14] in a related study reported that the equivalent diameter of agglomerates, down-

stream of the reaction zone of a flat premixed flame of propane-oxygen, ranged from 0.12 to 0.48 μm, the average size being about 0.28 μm. Under these conditions the average particle size within the different agglomerates varied between .017 and .035 μm, which is equivalent to about 10^2 to 10^4 particles per agglomerate.

b) Optical Techniques:

Techniques which involve the prelimainary removal of the particles from the flame, distort the flow to some extent and this may affect the chemical reaction and therefore the size of the particles sampled. There is always the possibility that agglomerates may break up or grow in the process of transferring the sample from the flame onto the electron microscope grid. These factors create doubt as to whether the particles observed under the microscope are truly representative of the distribution in the flame in question. Optical techniques such as light-scattering and extinction methods are preferred specifically because they avoid these drawbacks. On the other hand, these methods are claimed to have the disadvantage of not differentiating between the effect of individual particles and those of agglomerates[56] a great deal of work has been done and is being carried out at present in an attempt to refine and increase the sensitivity of these methods for the purpose of measuring smaller particle size.

Wersborg et al[5] recently presented an interesting study. They demonstrated the advantages of optical techniques in measuring small particles, $d_p < .0015$ μm. This was inferred from the large difference between the soot volume concentration calculated along the flame from electron micrographs and that from flame absorption measurements. The comparison was made at several position along the flame height. They attributed the discrepancy to the contribution of heavy hydrocarbon molecules to the

light attenuation, undetected by the electron microscope. These molecules were assumed to have a maximum size limited by the particle-resolving power of the electron microscope, which was in Wersborg et al's case was d_p <0.0015 μm, which is equivalent to a mass number of 2130 amu.

In the work discussed above, agglomerates were only observed at a height of 60 mm above the flame height, after ~ 15m.sec. from the point where soot luminosity was first visible. This height also corresponded to the region where electron microscope and flame measurements were approximately the same; at this point concentration of absorbing hydrocarbon was negligible.

The presence of agglomerates in flames was demonstrated by Jones and Wong[62] using an extinction technique. They directed a laser beam into a propane-air flame buring on a Wolfhard and Parker burner (the beam was wide enough to encompass any sideways fluctuations by the flame.) The ratio of the fractional transmitted intensities at two perpendicular angles of polarisation decreased with increase in fuel flow rate. Jones and Wong's results indicate that agglomerates have a preferred direction of orientation in a heat flow.

Kunugi and Jinno[56] used a light-scattering technique to determine the particle size distribution along the axis of a diffusion flame. The fuel burned was composed of 91 per cent hydrocarbons containing four carbon atoms. The size remained constant, within 50 to 80 per cent of the flame height. The variation of the average diameter along the flame height was between 0.2 and 0.1 μm. In the case of the small non-smoky diffusion flame (height approximately 30 mm) the average diameter increased from 0,15 up to 0,2 μm. This particle range corresponds to about 95 per cent of the flame height. A different distribution .05 < d_p < 0.2 μm was determined by Kydd* for a premixed flame using a similar technique

*See comments at the end of reference (56).

Dalzell et al[63] set out to develop further aspects of light-scattering calculations in order to remove some of the doubts about the validity of the assumptions involved in determining the particle size and concentration of soot. The soot generated by burning a small propane diffusion flame. The measurements were taken at the chimney exit high above the flame in a region where particle agglomerates would be expected to have had sufficient time to form in large amounts. The experimental mass concentration was represented best by a model which assumed a bidistribution of small particles of dp = .035 μm, and agglomerates with a single equivalent diameter the ratio of single particle to cluster size, was about 50:1. However a cluster model best represented the experimental data on the theoretical and scattering patterns. It is appropriate to mention here the Erickson et al[64] had earlier undertaken research of a similar nature using a premixed laminar benzene-air flame. The results also indicate the bias of such techniques to the effect of one or more per cent of the mass of soot in the form of agglomerates.

Another interesting contribution in this field is Mori and Makino's[43] testing of the validity of using the Mie theory to measure the mean diameter of a cloud of particles having a size distribution. A light-scattering and an extinction technique (using three wavelengths in the visible) where chosen The study reported referred to observations on a small propane diffusion flame, although similar studies were carried out on city gas diffusion and on pre-mixed flames of unspecified fuel type. All measurements were taken between 60 and 80 per cent of the flame height where the average particle diameter was expected to remain nearly constant. The value of the effective diameter was around 0,14 μm regardless of the optical technique or type of flame used.

Agreement between the two techniques only occurred when a particle distribution was assumed to exist. However, the constantcy of the value of the effective diameter proposed by the authors for the case of propane and methane soots indicates that this diameter may be insensitive

to changes in primary particle size and extent of agglomeration. Finally, the effect of an increase in temperature which followed the addition of oxygen was corrected for by increasing the value of n and decreasing the value of K of the room temperature index.

Finally Dalessio et al[65] provided a number of curves which showed the increase of the average soot particle diameter with height above the burner and CH_4/O_2 ration(R). The minimum particle diameter at R = 0.45 increased from 0.005 μm near the reaction zone to .0150 μm at the maximum high measured (18mm). However at R = 1.27 the maximum size was about .1530 μm. The above trend was qualitatively confirmed by measuring the dissimmetry ratio at $Q_1 20/Q_1 160$ (where $Q_1(\theta)$ is the rate of energy scattered before attenuation). The particle size evaluated by the latter procedure was overestimated in some cases by about 60 per cent[65]. One should however note that the value of the equivalent particle from the dissymetry ratio depends on the particle shape i.e. whether it is elongated spherical etc.[66].

2) Conclusion:

The diameter of soot particles in flames varies with the type of fuel and with the speed at which the secondary chemical reactions are being completed. The value of the diameter as determined by light scattering techniques is somewhat doubtful, since up to the present time it depends on the value of the refractive index chosen and also on the type of particle distribution assumed. Both are unknown to some extent. Another drawback of light scattering techniques in general is their bias to relatively large agglomerates. It would appear that the size registered is more the average size of the agglomerates than that of a system composed of particles and agglomerates, which may exist side by side in flames, however un-

representative agglomerates may be of the total soot mass. This generalization is qualified in the cases in which particles in the range of .05 μm were detected using this optical technique.

Extinction methods have advantages in determining very small average particle diameters, <.0015 μm, in the region where the electron microscope fails. They also give better estimates of the average diameter than counts of particle per unit area made on electron micrographs up to .01 μm. However the electron microscope is a more useful tool for characterising the size, shape and internal structure of individual particles than optical techniques. Optical techniques on the other hand are preferred in some cases where physical probing is not possible or where the flow carrying the particles should not be disturbed. However it is advantageous when possible to make measurements using, for example, attenuation and to make similar measurements with electron microscope for comparison.

There is little doubt that particles may agglomerate in the form of chains at some position above the burner. What is yet unresolved is the position at which they are formed, their size, as well as their general orientation. These factors are important as they define the limit at which the effect of scattering on the attenuation coefficient can no longer be neglected. It does seem, however, that in some cases a knowledge of the particle diameter is not of great importance. This can be concluded from extinction measurements on small flames and on cooled plates.

2.4.4 Density of Soot Particles:

Various values for the density of soot have been quoted. Foster[67] used a value of 2×10^3 kg/m^3 to calculate the attenuation of radiation from a dispersed cloud of particles, whereas Newall determined the density of natural gas soots by an adsorption technique (known as BET) to be approxi-

mately 1.6 x 10^3 kg/m^3 (see ref. 30). The density of pure synthesized graphite is 2.1 x 10^3 kg/m^3, while the theoretical density of a single crystal of graphite is 2.26 x 10^3 kg/m^3, (ref. 68). The latter technique may give higher particle densities (considering the large surface area of soot) than, for example, electron-microscopy techniques; in this case the particle diameter is based on the surface area of a smooth solid particle. On the basis of such an argument, it has been suggested[30] that soot may have at some stage a density as low as: 1 x 10^3 kg/m^3.

Judging from the tarry appearance of "young soot" particles collected in the early stages of particle formation in a flame (using a molecular beam sampling system) Wersborg et al[5] proposed a range of densities (1.1 - 1.3) x 10^3 kg/m^3, characteristic of tarry materials, for the early stages of nucleation and growth. This was to replace the usual value of approximately: 2 x 10^3 kg/m^3m which is more representative of the fully grown soot particles (or clusters) formed at a later stage.

2.5 Absorption or Emission Coefficient (K):

The dependence of the absorption coefficient of a cloud of unit mass concentration, on wavelength may be presented from equation 2.10 as:

$$k_\lambda = B \bar{\lambda}^{g_\lambda} \quad (\frac{m^2}{kg})$$

This equation implies that k_λ is not dependent on the particle size parameters and is valid in the case of soot particles since $x < 0.3$[67]. Because other emitters are always present together with soot. This relation holds in general for small changes in λ, and in the region where the greater part of the emission is due to soot, i.e. banded or other radiation is weak[69]. There appears to be a fair degree of agreement between the values obtained experimentally for a small diffusion flame,[67,70]

as well as for an industrial flame[70], and those predicted from theory. However deviation of up to 300 per cent has been reported in the case of large flames and has been attributed to the measured emissivity used to calculate k_λ.[70].

As a result of analysing numerous data concerning radiation from luminous flames Gurvich et al[71] determined that in the infrared the specific attenuation coefficient may be represented as follows:

$$k_\lambda = B\ \lambda^{-(a + b\ \log\lambda)}$$

The value of the coefficients B and the constants a and b for a number of flames were defined in the visible and infrared and are shown in Table 3. The linear variation in the case of amylacetate soot observed in Table 2. was later corroborated by Siddall and McGrath[32]. It is interesting to mention in this context that Truelove[21] obtained the following correlation using the optical properties of soot determined experimentally by Foster and Howarth[41].

$$k_\lambda = 2.72 \times 10^3 \lambda^{-1.09}$$

The soots concerned were Sterling, Vulcan and Elf. It should be noted, however, that the value of B may vary by two-folds along a flame[69].

The monochromatic specific absorption coefficient may be represented from equation (2.15) as $B_o \bar{c}T$ where B_o stands for all the constants in the

The value of B_o was reviewed both theoretically and experimentally by Hein and Leuckel[24] and may be represented theoretically as:

$$B_o = \frac{10^3}{\rho}\left(\frac{m^3}{kg\ m\ K}\right) \qquad 2.20$$

Therefore within the density (ρ) range of full-grown soot particles, (1.6 - 2.0) x 10^3 kg/m^3, the theoretical limits of B_o are 0.625 to 0.473. It is interesting to note that Wall and Stewart[72] used a value of B_o = .730, which is between the upper limit of the theoretical values and the lower limit of the experimental values determined by Beer and

Claus[23] that is 0.835.

The local values of B_o seem to be related, at least in the case of gaseous fuels, to the local mixing conditions defined by a parameter M defined as the ratio of mass of oxygen to the mass of fuel at a point in the flame divided by the mass of oxygen to the mass of fuel for the stoichiometric mixture. The more developedthe mixing, the greater was the overall agreement across the flame, with theoretical values calculated for isothermal conditions.

The independent results of Millikan[31] and D'Alessio et al[6] (see section 2.2.2) lead us to conclude that K is practically independent of the soot temperature but dependent on the mass of emitting solid particles and pre-soot molecules in a flame. This agrees with Howarth, Hoster and Thring's[18] calculations, which indicate that the mean attenuation coefficient for the computed range 1 - 4 μm, varies by less than 10 per cent between 1000 = 2000 K. Therefore the attenuation coefficient under such conditions of T and range of λ, will not need correction if the optical path is non-isothermal[18]. A similar conclusion was reached experimentally by Hammond and Beer[69]. Finally, dividing k_m by the temperature T will only partly correct for the effect of black body shift but will not remove the effect of T on the absorption index [30].

CHAPTER THREE

SOOT IN FLAMES: A REVIEW

3.1 Discussion of Mechanisms of Soot Formation

Introduction:

This review is restricted to carbonaceous materials formed in the gas phase, generally referred to as soot. It is produced in various flames and related systems, e.g. during pyrolysis and in shock tubes during electrical discharges, etc. The word soot, rather than carbon, will be used here, although carbon has been used, albeit sometimes indiscriminately, in the field of combustion, to describe a great many different compounds formed under different conditions.

Soot in general has been a subject of great interest, even before Davey[73] related the luminosity in flames to incandescent soot particles. Since the study of Nef[74] on the production of large molecular hydrocarbons from smaller ones, as well as those of Berthelot[75] and Lewes[76] on the mechanism of soot formation, much progress has been achieved and much of the mystery has been resolved. Due to the complexity of the subject under review, it will be possible only to present a qualitative picture of the present state of knowledge on soot aspects such as the appearance, structure and mechanisms of formation. The effect of additives, is useful in this context, and will also be described in this chapter.

3.1.1 Some Aspects of Soot

a) Appearance:

Soot deposits vary in kind; they may be soft, fluffy, appear dry or sticky[40] the colour as well as the smell will depend on conditions of formation as well as the amount of flame products adsorbed during its collection. Other aspects of relevance are presented in section 2.4.3.

b) Microstructure:

A decade ago Heckman[16] summarised the current concept of the microstructure of soots. The aspects which are of direct interest are:

i) A primary particle is composed of a large number of layer planes. Each layer plane is a hexagonal network of carbon atoms chemically bonded. The dimensions of layer planes are much smaller in soot than in graphite. They are expected to have a larger proportion of hydrogen attached to carbons at the edges.

ii) These layer planes are piled up in stacks a few layers deep called parallel layer groups or crystallites, in which the layer planes are arranged roughly parallel and equidistant.

A few years ago Marsh et al[77] published a number of phase contrast electron photo-micrographs of several soots formed by different processes. Some of their findings may be summarised as follows:

i) Soots resulting from thermal decomposition of natural gas or from the vapours of cracked petroleum residues, produced what appeared to be one "growth centre" or nucleus around which carbon layers arranged themselved concentrically. Few primary particles were observed to have more than one nucleus.

ii) On the other hand soots produced by other processes such as impingement burning of natural gas flames (channel soot) or exothermic decomposition of acetylene (acetylene soot), appear to be built up around more than one nucleus. The carbon platelets build in circles around each individual growth centre as in the case of thermal soots. Towards the outer shell of the particle the layers orient themselves so as to produce the shape of the primary particle we are used to observing. In certain applications, for example the rubber industry, soots produced in (i) and (ii) were know as low structure and high structure soots respectively[78].

It is worth pointing out that the phase contrast electron micrograph of the non-graphitised region of a plasma soot, produced by Marsh et al[77] by subjecting ethylene to an arc at 10,273 K, has the internal morphology features of furnace soots, i.e. a "plurality" of growth centres. Each individual primary particle can easily be out-lined which is not the case in the micrographs of other furnace soots or soots produced from gas turbine emission, and the extent of primary particle fusion appears to be intermediate between furnace and thermal soots. Spheron 9, is another example of an intermediate stage between thermal soots on the one hand and furnace soots on the other. The particles in this type of channel soot tend to spheroidal, and common planes between particles are not extensive but few discrete particles are seen.[16] Finally the evidence presented above and elsewhere[80,81]; indicates that the basic structure of soot is not a parallel layer group, i.e. crystallite as had been inferred from early x-ray diffraction measurements, but that the alignment of a number of hexagonal layer planes in a given direction appears by chance. The basic structure, of this 'paracrystalline' material, being a hexagonal layer.[79]

c) Chemical Composition:

Elemental analysis of soot yields mostly carbon and hydrogen in various ratios depending on the method and conditions under which the soot was formed. Oxygen and oxygenated compounds have been detected and some of the oxygen is chemically bound. It may exist in the form of associated hydroxyl[38] and carbonyl (c=o)[38][40].

A detailed analysis of soot produced by diffusion flames of fuels belonging to different homologuous series, revealed that there was a "similarity" of the infrared and ultraviolet spectra[38] pertaining to the various fractions obtained by solvent extraction. This indicates that the composition of the extracts is independent of the type of fuel, which

finds corroboration elsewhere. This study also revealed the presence of groups of complex compounds. They were, however, unable to detect in general the presence of polycyclic aromatic hydrocarbons. The latter group of compounds was later discussed by Long and co-workers[33-38] as well as by others[39,40,82,6,65]. The effect of changing the shape of a flame by reducing the pressure or reversing the position of the fuel and oxygen produced a marked change in the nature of the soot deposits[40]. The volatile part of the soot in premixed and diffusion flames varied with height above the burner, and could acquire an asymptotic value after a certain height[39]. It was shown that the hydrogen in the polycyclic aromatic hydrocarbons may in some cases amount to about 1/3 of that which was initially present in the soot[6].

3.1.2. About the Mechanism of Soot Formation:

In the previous section the appearance and the microstructure of soot were discussed in some detail. Phase contrast electron microscopy indicates that the structure of soot produced by thermal reactors and flames, is similar except that soot particles produced by thermal processes generally have one growth centre only. The other difference is that conditions of temperature and residence time inside the flame favour the formation of individual primary particles, i.e. do not permit fusion of these particles into chain-lime agglomerates, as may occur in flame systems, though they may appear aggregated when observed by transmission microscopy. That soot with a structure intermediate to thermal soots on one hand and flame soots on the other, may be produced in different flame systems, indicates that the process of soot formation is qualitatively similar in both systems, excluding soot produced in shock-tubes or in cool-flames, since similar studies in these systems have not been found.

No attempt will be made to separate the work done in each system and the subject will be discussed as one, since the appearance and internal structure of soot formed in a given position during thermal processes and in flames, depends on the concentration of nuclei and their temperature of formation. Moreover, it depends on the time available for agglomeration and growth into a primary particle or, as in the case of some flame systems, into particle agglomerates. The mechanisms of soot formation have been discussed in several excellent reviews[25c)(83-90)] and therefore will not be reviewed in detail here.

It would be useful at this stage to say something about the systems in which soot is generally studied. A great number of experiments on soot formation have been done with either premixed or diffusion flames The process of combustion in both cases is essentially different. In the first, fuel and oxidant are intimately mixed prior to ignition, and an explosion wave travels against the fuel air stream. In the second case the fuel is first decomposed in the preheating zone, before its products of decomposition are oxidised in the reaction zone. It takes about 1 msec and 10 msec to convert a simple molecule of fuel into soot in a premixed and a diffusion flame respectively[91]. Standard burners were used in many cases and have been summarised by Place and Weinberg[99]. experiments have also been done in thermal reactors which may vary from a simple laboratory pyrolysis tube to a regenerator of industrial porportions.

It has been suggested[93-96] that ions have an important effect on the process of soot formation. However the results are complicated by the fact that in flames the reaction zone is generally thin (except at reduced pressures) and by the existence of large temperature and concentration gradients. Therefore changes in reactant concentration will reflect the effect of both chemical reaction and diffusion. A more homo-

geneous system, i.e. instantaneous temperature and homogeneous coreflow is provided by the shock tube[97]. Many experiments have, for these reasons, been made on such systems to obtain information on chemi-ionisation processes during the combustion of a hydro-carbon.

Basically all mechanisms of solid formation from a gas involve nucleation, coagulation and growth processes. These have been outlined by Palmer[84] for the case of a thermal system and will be represented with some minor modification as follows:

1st stage: Thermal decomposition of the gas and formation of unsaturated species. This is followed by condenstaion and polymerisation reactions.

2nd stage: Formation of polyacetylens, reactive polycyclic radicals and species of a similar nature. Reactions leading to the formation of solid growth centres.

3rd stage: Heterogeneous growth of these centres. Fuel gas decomposition on the particle surface. Formation of a primary particle.

4th stage: Agglomeration of the primary particles from stage three in the form of chains. Elimination of residual species.

The steps above are also valid under flame conditions, but the occurrence and duration with respect to the reaction zone will vary with type of fuel. All steps leading to soot formation are dependent on both the physical and chemical processes occurring in flames; evidence concerning each will be reviewed separately.

a) Chemical Mechanisms:

A review of the present state of the subject of reactions involving combustion of hydrocarbons points out that soot is mainly formed by a chain reaction propagated by a free radical mechanism. This can be the only explanation for the extremely low reaction times of a few milliseconds

or less[91] and the sudden change from a slightly luminous flame to a brightly luminous one[93]. At this stage conflicting evidence has been presented as to the nature of the free "radical nucleus"[98] or "key intermediate"[99] around which the building up process occurs as a result of of polymerisation[61] or dehydrogenation,[100] or both reactions occurring simultaneously[89]. Acetylene[75,76,89] and polyacetylenes[99,84-88] are perhaps the most popular proposals. Butadienne,[91,38] conjugated free radicals, (for example conjugated polyene radicals)[91], polycyclic aromatic hydrocarbons[101] and C_2 radicals[102] were among the many other suggestions, as well as droplet condensation from the gas phase followed by graphitisation[103-105][61].

It may be inferred from the outline above that a great many compounds are formed as a result of pyrolysis or during combustion. The problem which has not yet been resolved is the identity of the species responsible for the nucleation and growth processes. In the following paragraphs an attempt will be made to point out the various unifying factors as well as to discuss the relative importance of one group of compounds.

As a result of previous extensive studies which include optical, mass spectrometrical and weight analysis on flat, premixed hydrocarbon flames, mainly aliphatic and benzene, it was concluded that the following groups of hydrocarbons may be considered important[7]:

i) acetylene and polyacetylenes: mass range 26 to 146.

ii) polycyclic aromatic hydrocarbons: mass range 78 to 300.

iii) reactive polycyclic hydrocarbons, probably with side chains, containing more hydrogen than aromatics: mass range 150 to 550*

*This value corresponds to the limit of resolution of the mass spectrometer used.

It was maintained some time ago that "with the possible exception of aromatic molecules, the decomposition of any hydrocarbon leads eventually to the formation of acetylene and hydrogen"[89]. Results in diffi-diffusion flames indicated that an appreciable amount of acetylene was essential to produce reasonable amounts of soot.[107] Studies on the pyrolysis of various hydrocarbon vapour in a flow system showed that a minimum amount of acetylene had to be present in the diluted stream before soot was detected[58].

The importance of acetylene was also pointed out during the flash photolysis of ketene, (CH_2CO). Its peak concentration, at 20 mm Hg seemed to coincide with the onset of soot formation[108]. Dearden and Long[107] showed that there was a relationship between the sooting rates at the exit of a diffusion flame, burning either propane or ethylene, and the amount of acetylene ($\emptyset$). This symbol was called "the integral value" and has the dimensions of an area. It was defined as the amount of acetylene bounded by the fuel edge luminous zone on one side, and interface between the yellow (luminous) and blue reaction-zone up to a nominal height of 5mm, which defined the onset of soot formation.

Three points are of note:

i) Acetylene was the main stable species detected before soot was formed.

ii) It was possible to make a propane diffusion flame soot as much as an ethylene diffusion flame when acetylene was added to the former in sufficient amounts to keep the supply of input carbon in both cases constant.

iii) Addition of acetylene or oxygen to either ehtylene or propane increased in general the $\emptyset$ value of acetylene, as well as the sooting rate. The exception was the case of propane where the sooting decreased with addition of oxygen to the fuel.

Cole and Minkoff[109] studied diffusion flames of methane and ethylene on a Wolfhard and Parker flat plane burner similar to that which

was later used by Dearden and Long in the work cited above. Their study of the effect of several additives on the intensity of acetylene absorption and emission at 729 cm^{-1} failed to establish a correlation between acetylene concentration and the amount of soot formed. On this basis they decided that it was not an intermediate in soot formation. An influencing factor seems to have been the effect of addition one per cent acetylene to the immediate soot-forming zone of a methane flame. Although the amount of acetylene concentration was raised to a level similar to that in the ethylene flame, the amount of soot liberated in the atmosphere was not the same.

Two critical observations seem to be appropriate:

a) It is not clear if one per cent by volume of acetylene equalised the supply of carbon in the case of the methane flame and in that of the normal ethylene flame.

b) the amount of soot liberated and the intensity of the yellow luminosity appear to have been determined visually. Therefore a small increase in yield which Tesner et al[60] observed when C_2H_2 was added to a Ch_4 flame may have gone undetected. It is also possible that the flame temperature at which soot is formed should also be considered[110].

Shock tube studies of acetylene showed that C_4H_3, C_4H_2, C_6H_2 and C_8H_2 occur in that order, prior to the formation of a carbonaceous solid and hydrogen.[111] Analysis of the species in the oxidation zone of a flat premixed aliphatic fuel, revealed that when polyacetylenes were formed after the appearance of acetylene[99]. This substantiated previous shock tube studies discussed earlier, and indicates that the order of formation of these species has not been affected by much shorter duration of temperature, as well as the flatter temperature profile encountered in shock systems.

It does seem that the importance of acetylene is its role in the formation of polyacetylenes. Bonne, Homann and Wagner[99] suggested that the latter molecules could be soot precursors. However the proposition that nucleus build-up takes place solely via acetylene seemed improbable on the basis of both the physical and chemical structure of polyacetylenes, that is long chains of carbon atoms which are alternately connected by triple and single bonds. Their lack of reactivity, observed at some stage in the burnt gas region, is another factor to be considered.

Bonne, Homann and Wagner[99] favoured the following radical-based scheme to explain the nuclei formation via polyacetylenes, and the early stages of soot growth from aliphatic fuels.

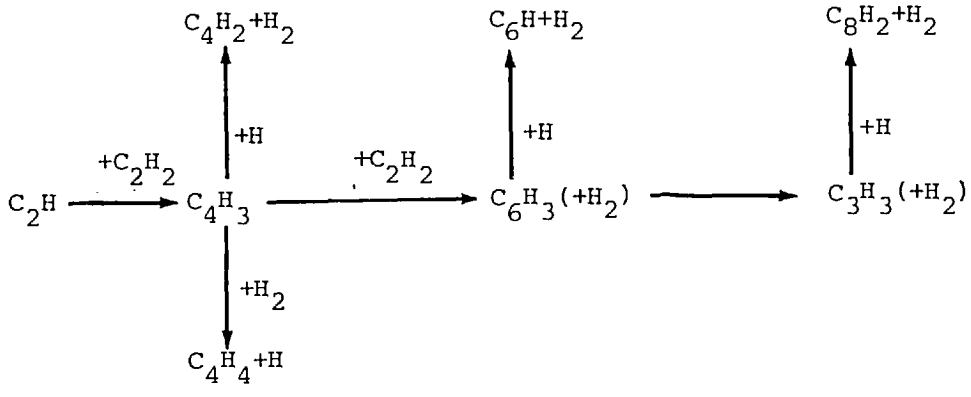

If the mixture of fuel oxidant was rich enough, higher polyacetylenes would be formed. Large radicals formed at some stage of the formation of large polyacetylene molecules, for example $C_{12}H_2$, would interact or combine with the large polyacetylenes, to form three-dimensional aggregates of carbon atoms which have a radical character and may contain ring closures. These aggregates would subsequently grow by both agglomeration and by addition of mostly larger polyacetylenes as well as polyacetylene radicals. It is expected that lower polyacetylenes react to form higher polyacetylenes, rather than add to the growing soot particle. The process would continue until primary particles were formed. A detailed schematic representation of this mechanism was later presented by Homann and Wagner[7].

Street and Thomas[90] made a study of bunsen flames burning various

fuels; two main points emerged:

i) In the case of acetylene, ethane and ehtylene flames, the blue-green reaction zone was completely surrounded by luminous radiation. The two zones were separated by a dark zone which appeared to be infinitisimal or non-existant at atmospheric pressure[99].

ii) Aromatic fuel and naphtalene derivatives show a yellow luminosity which appears to emerge from the tip of the blue-green reaction zone.

In benzene flames, unlike acetylene flames, soot is formed in a region where relatively large amounts of molecular oxygen exist. Mass spectrometric analysis in the case of flat premixed benzene flames indicates that reactive polycyclic hydrocarbons (100 to 600 mass units) are formed very rapidly, and that heavy hydrocarbons exist inside the oxidation zone. This may have been induced by the presence of large cyclic molecules in the initial feed, which explains the higher sooting capacity of a benzene flame compared to that of an acetylene flame of the same C/H[7], as well as their structure, above.

The concentration of polycyclic aromatic hydrocarbons produced in a similar flame for the same C/O ratio fed into the system was approximately a hundred times greater than the case of acetylene flames[82]. The maximum concentration follows the pattern of polyacetylenes in aliphatic flames, i.e the maximum leis within the reaction zone, and decreases at the end of the reaction zone, where most of the soot is formed. However, this was not the case for polyacetylenes formed in the reaction zone.

Polycyclic aromatic hydrocarbons, unlike polyacetylenes, have been detected in flat flames of aliphatic fuels, among substances evaporated from soot samples collected some distance from the oxidation zone[6] and in the gas phase by sampling with a molecular beam system[5]. This was sufficient indication that polycyclic aromatic hydrocarbons condense while the soot particles are being collected on cool probes or adsorbed on soot in the exhaust, where the relatively lower temperature favours their con-

denstion. It was therefore evident that these compounds could not be important and were by-products of certain reactions in aliphatic flames, a conclusion commonly reached. Long and co-workers[33-38] studied these compounds extensively in both diffusion flames and in a combustion engine. A great deal of their work had been done in an attempt to reduce their amount, mainly because of the hazardous effect certain groups of these compounds have on human health. Di Lorenzo and Masi[39] provided evidence that in a flat premixed-oxygen flame partial decomposition of some of the 'reactive'polycyclic aromatic hydrocarbons, for example 3,4 benzopyrene and benzoperylene, could account for some small percentage of the soot formed in the burnt gas.

Thermogravimetric analysis of soot collected close to the burner and that collected at a greater distance showed that the larger part of polycyclic aromatic hydrocarbons evaporates at 200-450°C. The total loss decreased with distance from the burner[39]. The analysis also indicated the influence of methane/oxygen feed ratio on the amount of polycyclic aromatic hydrocarbons of high boiling point. In a hotter flame, i.e. methane/oxygen = 1.1, relatively larger amounts of polycyclic aromatic hydrocarbons were boiled off between 450 and 1000°C than in a cooler one (mixture ratio = 1.27). This indicates that the 'reactive' polycyclic aromatic hydrocarbons polymerise and condense in the gaseous phase at high temperatures. Di Lorenzo and Masi's study provided evidence that the increase in C/H ratio of soot with height above the flame was due to the evolution of hydrogen i.e. a temperature effect and not a result of the loss of hydrocarbon, e.g. polycyclic aromatic hydrocarbons which have a high hydrogen content. It was proposed that the decrease in hydrogen content of soot may occur during the period of growth of soot aggregates of diminished free radical character, as a direct consequence of the addition of more reactive higher polyacetylenes[39].

One may therefore conclude that if 'reactive' polycyclic hydro-

carbons are important contributors in the formation and growth of a soot nucleus in aliphatic fuels then reactive cyclic hydrocarbons would be expected to play a similar role in aromatic fuels. It should be understood however, that compounds may be 'unreactive' in an experiment and become 'reactive' in another if conditions are favourable. As an illustration anthracene-phenanphrene, pyrene and fluoranthene were considered to be unreactive in the above study, although this was not the case in other experiments [35] [112].

It was suggested by Jessen and Gaydon that, in very hot flames, a radical nucleus (C_2 radical) may serve as a surface or nucleus on or around which "unsaturated" hydrocarbons could decompose; this was inferred from their observation of a rich C_2H_2-O_2 flame spectroscopically. They also proposed that "higher acetylenes" could be formed by a series of rapid reactions of this radical and acetylene.

Much has been written on both sides of the discussion of the importance of the role of C_2 radical in the process of soot formation [25c] [88] which need not be repeated here. Tesner [98] recently presented a very interesting article which dealt with the formation of soot particles in which he distinguished between the formation via a molecular nucleus, e.g. reactive polycyclic hydrocarbons and that via a radical nucleus, e.g. C_2. The scheme for the formation of a solid nucleus via acetylene can be represented as follows:

$$C_n + C_2H_2 \rightarrow C_{n+2} + H_2 , \qquad \text{(elementary act)}$$

$$C_2 \rightarrow C_4 \rightarrow C_6 - :.. \rightarrow C_n \qquad \text{(chain)}$$

radical nucleus nucleus (solid)

As a result of the structural similarity in industrial soots referred to by Tesner, and the lack of considerable amounts of volatiles collected with the soot, he inferred that a radical nucleus could be re-

sponsible for the formation of a solid nucleus as shown above. In industrial soots we may distinguish between thermal and furnace, according to certain features of their microstructure (section 3.1.1). Soots with intermediate features also exist. A comprehensive picture of the behaviour of volatiles, which are mostly polycyclic aromatic hydrocarbons may be obtained from the various works on diffusion and premixed flames. To summarise, the amount of polycyclic aromatic hydrocarbons adsorbed on the soot is influenced by factors such as type of flame, fuel, oxygen to fuel ratio, sampling technique or position, etc. Therefore the amount of volatile collected would appear to be insufficient evidence to ascribe the type of nucleus involved.

b) A physical mechanism: (the role of flame ions):

The work of Bartholomé and Sachse [113] was perhaps the initial spark which later aroused much interest and speculation as to the role of flame ions in the process of soot formation. The effect of electric fields on the various stages of soot formation in both seeded and unseeded flames was studied in great detail by Weinberg and coworkers [92,96,114]. They concluded that particles can be caused to acquire a desired charge (positive or negative) in the presence of a field, and can therefore be manipulated to the required size and the site at which it is deposited can be determined. However, it was affirmed that growth on charges contributes little to the mass of soot deposited. The "uncharged process" was responsible for the soot mass deposited in the presence of an appreciable field [115].

Howard [95] presented an attractive structural model. It attempts to explain how soot particles sampled from flames acquire their external appearance. The model assumes nucleation by flame ions of the type

$C_nH_m^+$, and that growth is influenced by the electrostatic force which exists between very small soot particles at their various stages of growth.

Until recently it was uncertain whether ions took part in the nucleation stage[116], although the influence of the electrostatic forces on particle clustering and formation of chains appears to have been resolved, and it was suggested that, because of these forces, a more compact arrangement of agglomerated particles was not possible[116,117]. A quite recent study on concentration and mass distribution of charged species in luminous C_2H_2-O_2 flat premixed flames, indicated that soot nuclei may be produced via reactions of positively charged, as well as uncharged heavy hydrocarbons[93].

$$R + R \rightarrow S \qquad (1)$$

$$R + R^+ \rightarrow S^+ \qquad (2)$$

$$R^+ + R^+ \rightarrow S^{++} \qquad (3)$$

Where R = heavy hydrocarbons and S = soot.

Accordingly, the quantity of soot produced will depend on the fraction of positively charged hydrocarbons that can serve as nuclei. If the total concentration of R^+ is abundant, under a particular set of circumstances, then effects such as increasing the temperature reducing fuel equivalence ratio or reducing the system pressure will reduce the amount of soot formed, as the fraction of higher hydrocarbons and soot particles which are positively charged will increase. Growth at the various stages will be governed by the extent of electrostatic repulsion. However, if R^+ is small, soot formation may be enhanced by its increase due to the favouring of reaction (2) as against (1) which is slower. Although this role attributed to positive flame ions had previously been suggested, the consensus is by no means general. A more comprehensive discussion on the role of flame ions is presented in section 3.2.4 which deals with metal compounds.

3.1.3 The Nucleus

The word nucleus, in connection to soot formation, has been used to mean a very small, or original, particle which is capable of growth. On the other hand reference has also been made to the existence of a radical nucleus[102] or one which would grow to a soot particle of minimum size, called a nucleus[98]. Parker and Wolfhard[61] showed that it was possible to convert liquid polymers produced during pyrolysis into soot particles by passing the stream into a flame. A related study by Johnson and Anderson[58] showed that it was not possible to convert polymer droplets formed during pyrolysis of acetylene into soot by passing the stream into a second furnace in series with the first. This led them to refute a nuclear mechanism built on droplet formation, since under such experimental conditions charring or carbonisation should otherwise have been possible.

The conflicting results reached by the two works discussed above may be aligned by considering the importance of oxygen in determining the yield of solids produced during the pyrolysis of relatively complex, highly condensed molecules[104]. However the fact that five ring compounds can be converted into a solid by pyrolysis[106], as well as other evidence[103][105] suggests that a droplet mechanism for soot formation is possible under certain conditions.

Conclusions:

Primary soot particles produced in a thermal system on the one hand and in flame systems on the other, are similar in appearance though not necessarily in size. When agglomerated, the former generally have a high structure and the latter a low one. The internal morphological details indicate that in flame systems, conditions favour the clustering of several growth centres (nuclei), in the process of formation of

a primary soot particle. Evidence from experiments on a flat premixed C_2H_2-O_2 flame indicates that these centres mainly grow via surface reaction to a volume mean diameter of the order 0.01 μm before coagulation contributes to their growth[93]. Further rounding up occurs by surface reactions at a rate which should account for the build up of the graphite layers towards the external surface of the particle. In the case of thermal soots the build-up is generally around one nucleus. Soot with internal morphological details intermediate to the two types above, also exists.

Conflicting evidence exists as to the role of oxygen in flame and thermal systems. There is no evidence that the nature of the soot deposit is dependent on the type of fuel. Aspects of the mechansim of soot formation have been discussed in some detail. As a result a schematic representation of how soot may be formed, has been outlined (Fig. 3). The general consensus concerning flame systems seems to be that solid growth centres are formed directly from the gas phase. Evidence obtained from thermal systems indicate that soot particles may be formed via the nucleation of liquid droplets. On the basis of known morphological features of the various soots, as well as the other aspects discussed, it is reasonable to conclude that the essential phases of soot formation are similar in the systems dealt with here, of which thermal systems and premixed flame systems are usually regarded as two extremes.

3.2. Effect of Additives

Introduction:

The objective of this chapter is to review work concerned with the addition of chemicals to hydrocarbon combustion systems. Work mainly related to diffusion flames will be stressed. The conclusions derived from this review will be useful as a guide in choosing the most suitable

additives for our purpose. An attempt will be made at the end to explain the various observations (physical or chemical) in the light of our present knowledge of the mechanism of soot formation.

Before starting the discussion on the effects of the various groups of additives, it is important to bear in mind that soot may be formed in premixed flames by a different mechanism than in diffusion flames. In the former type of flame the chemical species (e.g. positive ions or radicals) reponsible for the appearance of soot above the primary reaction zone originates within it. In diffusion flames soot is produced mainly as a result of a purely thermal process on the fuel side, see section 6.2.4. However, pyrolysis of the fuel has been reported in hot premixed flames burning in oxygen[118].

Discrepancies may arise, some of which may be attributable to the different types of flames used, large number of fuels, different burner geometries, fuel/oxidant ratio, positions, etc. studied in this review. Another variant to be considered is whether the effect is being studied on the amount of soot inside the flame or on the total soot in the exhaust gases (see Table 8). A point worth reiteration is that most of the flames reviewed are small laboratory flames burning at atomospheric pressure.

3.2.1 Gaseous additives (other than hydrocarbons and their derivatives):

The general effect of addition of CO_2 and N_2 in sufficient amounts, takes the form of a reduction in the flame luminosity or an increase in the amount of fuel required to make the flames smoke. Although very little additive is required to reduce luminosity, an impressively greater amount is required to suppress it completely. It is possible to work out from the curves presented in reference (40) that, for a methane rate of

335 c.c./min., a 75 per cent reduction in the flame luminosity was obtained using approximately 13 per cent CO_2 and 11 per cent N_2 of the amount required for its complete suppression.

It should be mentioned, however, that the gradual addition of CO_2 or N_2 to a number of liquid flames was found to produce at some stage, an increase in luminosity, which are preceded by an increase in the size and height of the flame. However when the critical concentration of an additive had been added, the flame had a tendency to lift from the wick and shrink in size. It eventually lost its luminosity and turned blue. The critical feed rate of CO_2 or N_2 required to suppress luminosity was found to be in most cases inversely proportional to the square of the molecular weight of the burnt fuel[119]. It is interesting to note that in a number of gas flames at the point where luminosity disappeared the flame lifted from the mouth of the burner and became elongated[76]. Arthur and Napier[40] determined that the rate of increase of the critical concentration of gaseous additives required to suppress luminosity in normal (or reversed) flames of methane, varied linearly with increase in fuel rate. The efficiency of the additives was in the following order: $SO_2 > CO_2 > N_2 > CO$. This indicates that the inhibiting efficiency is not simply related to the heat capacity of the additives. The greater effectiveness of CO_2 and N_2 reported above was reproduced in the case of a butane-air flame[120] and of basic gas[121] which is similar to town gas.

It has been suggested that under conditions where the flame height is only slightly altered by large amounts of additives (50 per cent N_2) the residence time of the fuel or decomposition products inside the flame is not altered[120]. There is evidence that addition of hydrogen and nitrogen to a small diffusion flame decreases the yield of soot and increases the number of smaller particles[60]. The latter effect had previously been observed by Szarvasy during the pyrolysis of natural gas[122]

However, Comferford[123] observed that when relatively small concentrations of N_2 were added to his propane flame, excessively large particles were formed which escaped destruction by reaction with air.

The greater soot inhibiting effect of H_2 than N_2 has been reported by Throp et al[124]. The latter is known to be effective in reducing the extent of formation of all hydrocarbon products as a result of upsetting the equilibrium between fuel and its decomposed products. A detailed experimental study concerning the effect of H_2 was undertaken by Bosse[125] and Herbst[121]. Finally, it is interesting to point out that addition of H_2 to a benzene flame made it acquire the sooting characteristics of an acetylene flame[7] previously defined by Street and Thomas[90].

Addition of O_2 to the air or to the fuel side of an ethylene diffusion flame increased the rate of soot collected. However a slight decrease was observed when oxygen was added to a propane flame on the fuel side[107]. Addition of oxygen increased the temperature in all cases and the maximum temperature was shifted towards the fuel side as the amount of oxygen was increased. In another report, Chakraborty and Long[35] studied the effect of oxygen added to the fuel stream in promoting the formation of polycyclic aromatic hydrocarbons and choloroform soluble materials. They noted that the concentration of the forementioned compounds reached a maximum when about 17.5 per cent of stoichiometric oxygen had been added. However the concentration became nil when the equivalent of 20 per cent stoichiometric oxygen was added.

A shock tube study of the effect of small amounts of oxygen on the pyrolysis of propylene, diluted in argon, (reaction time varied between 0.8 - 1 m.sec.), suggested that the role of oxygen is to promote the pyrolysis of the fuel by increasing the initiation reactions The latter determined the rate of reaction under such conditions of fuel dilutions and pyrolysis temperatures[126].

The amount of moisture in the fuel is very important, as it affects both the amount of soot produced from a flame and the heat released. Herbst[121] observed that the presence of a small percentage of moisture in the fuel reduced the amount of soot by 15 per cent by weight in some cases. The presence of moisture in the fuel greater than 30 per cent by vol in King's experiments[127] decreased the emissivity due to soot as well as the flame temperature. The emissivity within (4.2 to 5μm) from hot CO_2 seemed to be independent of the fuel moisture, however its relative importance with respect to other emitting species e.g. soot, increased with percentage of fuel moisture.

Muller-Dethlefs and Schlader[128] found that addition of steam to flat premixed ethyleneflames made the soot zones appear similar to that of propane flames, i.e. the zone which previouly surrounded the whole flame was reduced to a small cap on top of the flame. The observed shift of the carbon limit to higher C/O ratios with steam addition, was attributed to the role of OH radicals in reducing soot. Lastly it is possible, to reduced the amount of solid pollution, from fuel-oil combustion, by burning fuel-oil water emulsions[129].

Addition of SO_2 and H_2S to premixed flames has been found to reduce the soot luminosity while . on the other hand addition of small amounts of SO_3 (0.1 per cent by vol.) was noted to make a clear bunsen flame become luminous[130]. Parker and Wolfhard reported that they were unable to observe any effect on the luminosity of a diffusion flame by adding SO_2 and SO_3[61]. This is perhaps because the effectiveness of the forementioned compounds in flames is small and therefore may go undetected. This was pointed out by Cotton et al[131], who detected evidence of a small reduction in amount of soot formed when SO_2 and NO were added to a propane flame.

Conclusion:

The reduction in soot formation, or its suppression is assumed to be the result of the interplay of a number of factors of importance such as dilution, cooling and oxidation. From the discussion on gaseous additives, we can conclude that a very small amount of inert diluents, (e.g. N_2, CO_2) may increase the luminosity to a limited extent. However, a large amount of diluent produces a decrease in both temperature and the amount of soot which escapes at the top of the flame. The amount of moisture in the fuel is important due to its effect on the particle emissivity and temperature. Addition of oxygen to the fuel or air increases the flame temperature. It may also increase under certain experimental conditions the amount of soot and chloroform insoluble fraction.

3.2.2. Hydrocarbons and their derivatives:

Addition of halogenated additives to either the fuel or the air side increased the amount of soot formed, but the effect was stronger when the additives were added to the fuel side. Ibirrious and Gaydon[132] discussed in some detail the effect of halogenated additives on the OH, C_2 and CH emission from a parallel counterflow diffusion flame. They concluded that a soot increase may be brought about by the removal of oxidation centres and an increase in pyrolysis and polimerisation, which occur as a result of such additives. They had evidence that the reduction in OH emission was due to a genuine reduction in OH concentration as well as to a decrease in temperature.

Badakhshan[133] reported the effect of a number of halogen derivatives of methane on the rate of soot formation from a propagas diffusion flame. He postulated that there was no decrease in the rate of oxidation of the soot already formed but that the increase in soot was due to an in-

crease in the process of soot formation relative to the oxidation reactions. The curves for CO_2 and halogen-acid formation and oxygen consumption against additive concentration in the exit gases, indicated that CO_2 was constantly decreasing while O_2 and the different halogen-acids were increasing. The halogen-acid concentration appeared from the curves to level at a much earlier stage than CO_2. This is in agreement with early work on the combustion of carbon which shows that halogenated additives inhibit the oxidation of $CO \rightarrow CO_2$ and not oxidation by either dry air[134] or moist O_2[135]. However both works also demonstrate the importance of moisture in reducing the efficiency of halogenated additives.

The picture that emerges from the above discussion is that the increase in soot emission is accompanied by a reduction in OH concentration inside the flame, a decrease in CO_2 and halogen acid and an increase in O_2 concentration in the exhaust gases. This can be explained as follows: At flame temperatures the halogen molecules will react with atomic hydrogen, produced during the pyrolysis of the fuel, by a reaction in this form:

$$H + X = HX \qquad (1)$$

where X = $C\ell$, Br, etc. or give rise directly to $HC\ell$ e.g. $CH_2\ C\ell_2$.[134]

The halogen-acid may react with OH radical, thus destroying a propagation centre, as shown below:[136]

$$OH + HX = H_2O + X \qquad (2)$$

However, as a result of depletion of propagation centres such as H and OH, the rate of decomposition of the fuel will be decreased. The rate of formation of soot and subsequent particle growth will depend on the amount and the reactivity of the halogen additive. i.e. on the extent of reduction in temperature and OH radicals available for soot oxidation. The nature of the fuel is also important as these additives are know to react with unsaturated hydrocarbons, which may lead to a decrease in soot

formation.

If we consider that the following reactions account for the presence of the hydroxyl radical[135].

$CO + H_2O = CO_2 + H_2$	(3)	initiation
$H_2 + O_2 = 2OH$	(4)	
$OH + CO = CO_2 + H$	(5)	propagation
$H + O_2 = OH + O$	(6)	branching
$O + H_2 = OH + H$	(7)	branching

It is possible to attribute the increase in halogen-acid concentration obtained by Badakhshan[133] in the exhaust gas to a decrease in reaction (2). Since the concentration of oxygen also increased the reduction in OH concentration may have caused by a reduction in the rate of reaction (4) and (6).. The decrease in CO_2 concentration to the rate of reaction (5). This whole logic is built on the pre-assumption that hydroxyl radical concentration decreases. This was borne out by Ibiricu and Gaydon in their experiments.

It is difficult to determine the extent and flame position in which such a model is valid without sufficient data on the rate constants, concentration of carbon monoxide and H_2O vapour etc. Observation of the change in factors such as soot weight and temperature with flame height, provides relevant information.

This reasoning helps to explain the different observation discussed in the above reference. The form of the additve introduced is also important. For example the addition of CH_3Br on the air side was shown by Simmons and Wolfhard[137] to produce a secondary reaction zone and emission due to Br_2 bands. This emission was not produced when Br_2 was added to the air side. The induced reaction zone was formed due to reaction of methyl radical with oxygen in the air, so that:

$$CH_3Br \xrightarrow{heat} CH_3 + Br$$

The quenching of the flame is caused by a reduction in the amount of oxidant available to support combustion in the main reaction zone and consequently combustion CH_3Br. The extinguishing efficiency of CH_3Br was greater when it was added to the air than when it was added to the fuel.

However, CH_3Br behaved differently in the flat horizontal flame studied by Ibiricu and Gaydon[132]. Injection of even small amounts of CH_3Br to the fuel side reduced the flame emission in their ethylene-air flame. Addition to the air side showed a dependence on the rate of air supplied to their lean flames. A greater reduction in OH emission was also observed when CCl_4 was injected to the fuel side, than when it was injected to the air side. The lesser effectiveness of small amounts of additives when added to the air zone is probably a result of the lower rate of soot formation and therefore cooling of the flame by emission.

The extinction of the flame by addition of such inhibitors is dependent on several factors which may change the effectiveness of a given inhibitors in favour of another, as was demonstrated by Creitz[138] In his experiments, the halogenated inhibitors exhibited a lower efficiency when added to the air in agreement with Simmons and Wolfhard[137].

If it is accepted that inhibition is due to interference by halogen atoms with chain reactions involving hydrogen atoms, then the different efficiencies of CH_3Br reported in this section are due to the different-flame geometries used by the various authors. In the horizontal flat flame used by Ibiricu and Gaydon the flame was positioned between the flanges of the two opposed burners. The additive decomposition products will spread along the flat horizontal soot-forming zone more evenly than in the case of vertical flames used by Creitz and by Simmons and Wolfhard. The increase in sooting and hence extinction of a flame produced by opposed burners due to cooling would be expected to occur much more rapidly than in ordinary diffusion flames which are anchored to the burner by a premixed region.

The decrease of halogen efficiency with increase in oxygen in air,[138] which strengthens the premixed region, is in favour of this reasoning.

Finally, large amounts of carcinogenic materials are produced as a result of incomplete combustion of compounds containing carbon and hydrogen. Pretreating the fuel with, for example t-butyl hydroperoxide[37] or CH_3OH[112] reduced the soot and carbonaceous residues insoluble in chloroform. It is possible to increase the rate and extent of decomposition of a relatively stable hydrocarbon and increase its rate of particle formation by adding small amounts of another, less stable, hydrocarbon. However there is a limit after which the favourable effect on paricle formation is reversed[60].

Conclusion:

The effect of hydrocarbon additives is complex. As a general rule the amount of soot which escpaes at the top of the flame increases with decrease in hydorgen content of the main fuel or additive (fuel). When a hydrocarbon is halogenated, the amount of soot is increased, the extent depending on the degree of halogenation, e.g. $CH_3C\ell$ < CCl_4. The increase in soot collected depends on the type of halogen, as well as the side to which the halogenated hydrocarbon is added. This last remark also applies in the case of pure halogens. The inhibition efficiency of halogenated compounds seems to be related either to its tendency to produce a halogen ion, or to chemical bond strenth[163].

3.2.3 Metal Compounds (Mainly Alkali and Alkaline Earths)

There is evidence that soot particles are positively charged in the presence [115,92] as well as the absence of an electric field[94,93,113,95].

If soot nucleation and growth were only governed by an ionic

mechanism, then adding electrons to the soot-forming region of a premixed flame or a diffusion flame, would result in an successive decrease in both the positive ion concentration and the amount of soot. Evidence to this effect was presented by Salooja[139] using a tubular bunsen-type flame and a number of alkali and alkaline earths. The resultant soot reduction when a quartz probe coated with additive was positioned in the reaction zone was believed to be due to the neutralization of positive ions, some of which may be important in the process of soot formation (e.g. $C_3H_3^+$, CHO^+). The decrease in the amount of soot leaving the flame was related to the ionisation potential of the metal, i.e. $M \rightarrow M^+ + e$. The increase in the amount of soot produced in the secondary flame (diffusion) surrounding the main reaction zone of the premixed flame, was attributed to the neutralization of positive charges. This increased the rate of particle agglomeration and made it more difficult for them to be oxidised. An increase in particle size was also observed. Therefore the effect of an additive when added to the fuel will depend on the net effects in the different parts of a flame.

Cotton et al[131] postulated that metal salts suppress soot formation in diffusion flames by more than one mechanism. The role of alkali metal additives (M) is that of catalysing the rate of dissociation of H_2O and H_2 to form OH radicals, which may subsequently attack soot or its precursors by the reaction:

$$C_s + OH \rightarrow CO + \tfrac{1}{2}H_2$$

As OH radical concentration falls below the equilibrium value it is compensated by, for example, $H + H_2O \rightarrow OH + H_2$. The H radical mainly comes from a rapid sequence of homogeneous gas phase reactions:

$$H_2 + MO \rightarrow MOH + H$$

$$M(OH)_2 + (X) \rightarrow MO + H_2O + (X)$$

$$H_2O + MOH \rightarrow H + M(OH)_2$$

$$H + H_2O \rightarrow OH + H_2$$

where (X) is a third body, and M is an atom of metal additive.

However, under conditions where the concentration of free radicals, such as OH and H, exists above equilibrium, for instance in the post-reaction zone of laminar premixed flames of H_2/O_2, the effect of the additives is to enhance their recombination by the reverse of the above reactions.

The flame temperature was found to be very important in determining the efficiency of the various groups of additives. Except for alkaline earths and molybdenum, metals were only efficient in removing soot at high oxygen to fuel ratios. However when the saturated vapour pressure of a metal was exceeded in their flames due to the presence of a high temperature, solid oxides were formed. Other mechanism may have been involved.

Addecott and Nutt[140] determined that the soot-reducing efficiency of alkaline earths and alkalis in their counterflow diffusion flame indicated a dependence on the ionisation potential of the metals. The positive ion concentration, produced as a result of introducing the metals into an acetylene/air premixed flame, increased with decrease in ionisation potential or the metal and therefore the effectiveness was as follows:

$$Cs > K > Na \cdots\cdots Ba > Sr > Ca$$

The data of each group of metals fell on a separate line.

These as well as other observations indicated to the authors that the reduction of soot is associated with a degree of ionisation of the metal at flame temperature (1700°C), which in turn reduces the flame ion concentration of the type $C_nH_m^+$. This may occur by electron recombination or charge transfer to the metal or compound.

The effect of alkali metals and alkaline earths on the amount of soot produced in the burnt gas of a rich premixed C_3H_8/O_2 flame indicated that for each metal there may be an inhibiting as well as promoting effect. The dominant effect will depend on the type of additive and the experimental conditions. The lower the ionisation potential of the metal the greater is its promoting effect[141].

Feugier[141] proposed that the metal ion would promote soot formation by accelerating the nucleation process. This is supposed to occur when the ion concentration exceeds a critical value of M_c^+.

$$\text{concentration of soot} = f\left\{\frac{\text{soot formation rate (which is} \propto \text{no. of ions present}}{\text{soot formation rate + destruction of precursors by OH}}\right\}$$

However below this critical value, oxidation of soot will predominate due to the formation of OH radical at the end of the flame front by a mechanism similar to that proposed above by Cotton et al.

In the rich premixed flames used by Feugier[142] it was possible to observe at a given equivalence ratio (Φ = 2.73) for Cs first an inhibiting effect which was followed by a promoting effect as the total molar fraction of metal atom in the flame was increased. The dip in the curve increased at Φ = 2.81 which was equivalent to a decrease of temperature from (1780 - 1760) K. In the case of Li, Ba, Sr. Ca the author observed a net inhibiting effect except in the case of Ba where sooting was gradually promoted after minimum value of metal atom had been added.

Bowser and Weinberg[114] were in favour of a mechanism mainly based on the role of free electrons. They proposed to resolve whether chemical or electrical effects are more important by studying the effect of varying the electric potential across a fine uncooled, 2 mm in diameter, Ni-Cr wire and a similar wire coated with BaO, on the emission from a vertical flat diffusion flame. The results indicated that it is the

electrons which produce the effect characteristic of the additive. If, for example, the additive enhances the emission at a given height, an applied negative potential will increase soot formation. The absence of soot formation when a positive potential was applied across the wire led them to doubt the possible role of positive flame ions as nuclei.

Quite recently Bulewicz, Evans and Padley[143] studied the effect of a number of additives on the sooting rate of diffusion flames of propane/oxygen and acetylene/oxygen. They concluded that the anti-soot and pro-soot effects may be accounted for in terms of an ionic mechanism, supporting a previously-held view[139,114]. In order to explain the anti-soot effect of the larger concentrations of alkali halides in their experiments, they proposed that this arose from a reduction in the number of gaseous nuclei ($C_nH_m^+$), which are known to exist in flames[95,94] and were referred to by the authors concerned here[143] as R^+.

They believed that at least in the earlier stage of combustion this effect would occur by direct involvement of the metal, rather than by electrons produced by the additives, as suggested[114,139]. The following exothermic reactions would take place:

$$M + H_3O^+ \rightarrow M^+ + H_2O + H \qquad \text{(i)}$$

$$M + R^+ \rightarrow M^+ + R \qquad \text{(ii)}$$

The lack of available R^+ for nucleation and therefore production of charged particles S^+ would cause a reduction in the size and number of particles and therefore growth as a result of a reduction the rate of coagulation. The above reactions would be effective when equilibrium concentrations of $M^+ > H_3O^+ + R^+$.

In order to explain the pro-soot effect of the same metal additives at lower concentrations they proposed that M^+ may be formed above equilibrium levels. As its decay under these high concentrations occurs by

the following reaction: $M^+ + e^- + X \rightarrow M + X$, where (X) may be a neutral molecule. The level of R^+ may be then enhanced by charge exchange with neutral hydrocarbon precursors by the reverse of eqn. (ii). This step would provide new nucleus R^+ in a later stage to compensate for those destroyed, in the earlier stages of combustion, either directly by the electron recombinations to produce uncharged hydrocarbon fragments or indirectly by neutralisation of natural ions such as H_3O^+ which could provide ionisation of R. This would explain the increase in soot weight number observed in their experiments.

A similar reasoning to that above was used to explain the pro-soot effects of alkaline earth metals as well as other metals. However they believed that as alkaline earths exist mainly in molecular form e.g. MOH^+, the reverse of reaction (ii) would explain the anti-soot effect rather than a reduction in OH level which had been suggested by Cotton et al[131]. The promotion effect due to such ions has been suggested by Feugier[142] in the case of Ba and Sr for small ϕ values by the following reaction

$$M + OH \rightarrow MOH^+ + e^-$$

However, whether the process of ionisation occurs by this reaction or via MO is difficult to distinguish[25]d.

Discussion:

Before summing up the effect of metal additive we shall attempt to summarise some relevant aspects of soot formation and growth in their absence. One would be inclined to accept the view (section 3.1) that in hydrocarbon flames a solid nucleus is formed by sublimation of heavy hydrocarbon molecules (C_nH_m). This would be followed by a stepwise process of particle growth which involves the addition of hydrocarbons.

and via aggregation i.e. a reduction of the number of young particles. This is followed by surface growth, mainly by heterogeneous decomposition which is a slow process and accounts for the relatively spherical appearance of individual soot particles observed under the microscope.

The nature of these large molecules is still speculative in the case of flames. It has long been held that soot nucleation occurs via uncharged species mainly radicals by mechanisms which could involve polyacetylenes and polynuclear species.

That ionic nucleation is possible has been advanced by several workers during the last decade. An apparent problem is that the concentration of natural ions is relatively low when compared to the amount of unsaturated hydrocarbons and hydrocarbon radicals[87]. However evidence in a C_2H_2/O_2 flame indicated that the number of positive hydrocarbon ions (mainly heavy hydrocarbon species) were much greater than the soot particles collected[93] which incidently each carry one positive charge[93]. They were also found to be more than sufficient to provide for ionic nucleation[93]. There is, however evidence that a proportion of young particles may be formed without growing on ions as nuclei[115].

An interesting feature is that the level of soot reduction reported by Bulewicz et al[143] was not related to the ion concentration, unlike in the case studied by Addecott and Nutt[140]. This would agree with Howard et al's[93] results in which they found that a change from a weakly sooting flame to a rapidly sooting one in the absence of additive did not change the total concentration of large, positive hydrocarbon ions appreciably. One could take this evidence as an indication that the increase in positive ions concentration observed elsewhere with addition of $CC\ell_4$* is relatively unimportant, compared to the total positive ion con-

* See comment by Miller, ref. 96.

centration.

We must therefore accept at this stage the view that ions play a role in the process of soot formation. The extent of its importance is still difficult to determine. The importance of the chemical aspect cannot either be overlooked, considering that a young soot particle is highly reactive compared to a fully grown particle[87].

This relationship can be shown from the following reactions:[144]

$$CH + O \rightarrow CHO^+ + \bar{e} \qquad \text{(i)}$$

$$CHO^+ + H_2O \rightarrow CO + H_3O^+ \qquad \text{(ii)}$$

$$R + H_3O^+ \rightarrow R^+ + H_2O + H \qquad \text{(iii)}$$

$$CHO^+ + C_2H_2 \rightarrow C_2H_3^+ + CO \qquad \text{(iv)} \qquad \text{ref. 144}$$

The work reviewed here indicates that the soot inhibiting effect occurs by neutralization of chemi-ions and other useful ions to the process of soot formation by electrons from the metal[114,139,140] or their destruction by direct involvement of the metal[143]. On the other hand we find thereare those who are in favour of a role played by the metals[141,142], in the formation of OH radicals which results in a destruction of soot by oxidation. The promoting effect may occur if only electrons are added by enhancing soot agglomeration, this time by neutralizing positive charges on particles[114,139] or increase of R^+ due to the formation of M^+ above equilibrium[143]. Feugier[141,142] proposed that this would only occur if the M^+ was above a critcal amount.

Conclusion:

It is difficult to agree with all aspects of the mechanism advanced in the many publications discussed here. The conflicting results and the change in additive efficiency in different systems is another complicating factor. Many aspects would have been elucidated had their

effects on aspects such as chemical species and temperature flame structure been presented as well. No chemical analysis of the soot indicating the metal content has been reported in any of the work discussed. It is important when the metal is introduced into a system as this would under certain conditions enhance soot oxidation.

3.2.4 Solid Particles

As part of a study to increase flame radiation, Zalavadia and De Werth[145] seeded a natural gas flame with small particles. The particles added could be classified under two categories; those which can participate in the reaction, such as coke, charcoal and pulverised coal, and inerts such as cement, aluminium oxide, sodium nitrate, etc. which is due to the heat released during gasification of these particles and due to the increase in non-luminous radiation, which follows the increase in partial pressure of CO_2 and temperature of the flame.

Sato and Kunitomo[146] added a number of solids (mean diameter 5.8 - 10.5 μm) to a non-luminous town-gas flame. The furnace, unlike the previous case, was vertical and the solids were added to air flow supplied to the burner at the top of the water-cooled furnace so that the particles could be considered to be floating in the high temperature gas. The solids studied varied in substance, i.e. carbonaceous material, ferric oxide and a number of ashes were included. The reduction in temperature distribution across the flame was greater with the amount of additive, while the emissivity was highest when carbonaceous solids were added tothe flame. However, no conclusions were given with respect to radiation.

Thring[147] suggested that in general the introduction of inert materials to raise the flame emissivity is not worthwhile, as the gain is upset

by the subsequent reduction in temperature of the flame. However fly ash, and under certain conditions, dust from limestone-clay mixtures may produce useful effects, This is because the decrease in temperature which results when particles are added should be first compensated by an increase in the value of the emissivity before a useful effect is produced. He suggested that if particles are to be added then it is important that their size should be small, preferably $< 10\ \mu m$. However such small sizes require excessively fine grinding, also addition of particles will dilute the reaction products. An alternative is to produce sub-micron particles in a flame by delaying combustion at some stage. In this way it is possible to strike a balance between the value of emissivity, and temperature required to produce the required increase in emission.

Conclusion:

Seeding a non-luminous flame or hot gas with particles may produce an increase in radiation provided the gain in emissivity is not upset by a temperature decrease. Particles which can enter into chemical reaction such as coke, coal are more efficient than so-called inerts such as ferric oxide, lime, etc. The size and mass of the additive is critical as it determines the value of the emissivity and the extent to which the temperature will be reduced.

3.2.5 Addition of Heat:

The effect of preheating both the fuel and air streams, on the radiation from laminar and turbulent diffusion flames was undertaken by Guyomard [148]. He concluded that this was not the best way of increasing radiant energy from a town gas flame. The increase in radiation was disproportionate to the energy supplied. For example, preheating both the

air and fuel in the case of the turbulent flame to 700°C increased the radiation by only 50 per cent. This was negligible considering that under the same initial conditions addition of 9 per cent C_6H_6 produces over twice as much radiant energy. Another interesting conclusion from this work is that the effect of preheating is not always accompanied by a temperature increase. A minimum was observed at 500°C and 400°C in the case of the laminar and turbulent flames respectively.

A similar study was made by Guénebaut and Gaydon[149] using instead a laminar premixed flow of CH_4/air. An increase in radiation occurred only when the mixture had been preheated to above 500°C. In some cases a minimum was obtained at 400°C, which corresponds to the case of the turbulent flame above. When radiation was increased, due to the effect of preheating, a change in the flame shape was produced; it became thinner and longer, whereas the inner cone became shorter and wide at the apex. Guénebaut and Gaydon[149] found that although the change in radiation with flame height was different, the radiation from the total flame was nearly equal to that without preheating.

Another aspect of interest here is the effect of preheating the fuel on soot particle size. This is important as it may define the extent of particle pollution from a flame. Comerford[150] Tesner[59] and Johnson and Anderson[58] attempted to relate soot formation to residence time, and temperature of heating in tube furnace. As an extension to his pyrolysis study, Comerford investigated the process of burn-up of soot particles formed in a diffusion flame at one end of his pyrolysis tube. He determined that under certain conditions of low flow of the mixture of propane diluted with N_2, more soot escaped out of the flame[123]. This was attributed to a greater extent to fuel pyrolysis inside the flame as a result of preheating both the air and the fuel-nitrogen stream, which enhanced the formation of larger particles that were more resistant to oxidation.

In may industrial applications it is useful to recuperate part of the enthalpy leaving with the exhaust gases and in this way increase the efficiency of a given process. Under such conditions recycling the heat indirectly was found to be more beneficial in general than recycling part of the hot combustion gases. The adverse effects on the specific heat and temperature has been discussed in the case of a large combustion chamber by Barr and Mullin[151]. Finally it is relevant to mention that Lloyd and Weinberg have made a number of studies[152,153] in which they illustrated the uses of preheating to burn low-grade fuels and mixtures of fuel/air which are considered inflammable. However this will not be discussed here as their work is mainly concerned with the aspects of preheat related to the total efficiency rather than radiant efficiency.

Conclusion:

Flame radiation may either decrease or increase depending on the preheat temperature and experimental conditions.

Recommendations for future work:

It is fair to say that in most of the work reviewed in this chapter, the stress was on the effect on the amount of soot produced or escaping from a flame, that is from the point of view of pollution of the atmosphere and health hazards. There was no systematic work on the effect of additives on the factors which determine soot emissivity such as C/H ratio and mean particle size; although mention of these aspects is scattered in different reports. It is therefore difficult to come to any final conclusions as to the most useful additive to increase radiation at this stage; four types seem worth looking into:

1) Molecular oxygen.
2) Halogenated hydrocarbons or halogens.
3) Addition of heat.
4) Metal compounds

CHAPTER 4

EXPERIMENTAL DETERMINATION OF SOOT PARTICLE SIZE AND WEIGHT

Some Experimental Measurements concerned with Techniques of Particle Sizing and Collection

The influence of soot weight and particle size and shape on radiation from a flame has been discussed in some depth in Chapter 2. In section 4.1 of this chapter, two instruments used to sample soot for particle sizing were described in detail. A third method involving apparatus which was built incidentally and used first, is described. In this and the following section, the results obtained by the author are discussed and the appropriateness of the methods studied is demonstrated together with various other findings. The fourth and last section contains a brief discussion on measurements of temperature using a thermocouple and includes a number of suggestions.

4.1. Apparatus used for soot collection

4.1.1 a) The mechanical sampler:

It was possible by a suitable design to reciprocate from one to four rods, each carrying a glass strip cut from a slide. Details of one sampling unit are shown in Fig. (4). The trigger and line shaft assembly had to be swung clear before the sample holder could be loaded into the port The assembly was then returned to running position and the shaft run up to the desired sampling speed. The driver was a double-reduction, series-wound, variable speed motor, type SDISS (SD7), maximum speed five revolutions in sixty seconds, from Enicron Ltd. The sampling speed was varied by changing the input voltage using a variable transformer.

The friction sleeve was slipping normally until the trigger was released so that the rotation of the shaft carried the snail and eccentric

round and brought it to bear against the roller of the sample holder. The sample holder was held flat by a guide and fork on top, and followed the eccentric by means of a return spring made of fine stainless steel wire.

In order that each sample holder could be moved into or out of the 4 mm holes at the side of each calorimeter, it was necessary to release the coupling, loosen the two 5/16 inch nuts which controlled the movement of the frame carrying four triggers via two hinges, attached to the lowermost and fourth calorimeter, and pull it outwards towards the operator. This last step had to be carried out carefully or the rods carrying the samples would have suddenly be ejected by the springs, resulting in loss of the samples. The stainless steel guides are shown in Fig. (4).

An electron microscope grid was glued to each glass slide, using silver dag. The position of the grid was determined by the total length of the small metal holder and glass strip, and was adjusted so that approximately the centre of the grid was in the sampling region, which was generally at the axis of the combustion chamber. This construction made it possible to select the sampling position across the combustor.

Finally, the shaft carrying the snail and eccentric was coupled to a rod of similar thickness attached to the motor using a rubber disc 4mm in thickness. This allowed for a certain measure of flexibility useful for correcting imperfect alignment of the sampling section to the main apparatus. Moreover, it absorbed some of the shock at high sampling speeds and enabled the sampling section to be separated from the motor. The speed of rotation of the shaft connected to the motor, and hence the sampling speed, was controlled by the variable transformer which controlled the input current to the motor.

b) The oscillating thermal precipitator:

A picture of the instrument, which is made of brass, is shown in Fig. (6). One arm of a quartz probe Fig. (7b) was attached by a brass,coupling to the inlet (a) which was situated at the top of the instrument. The brass nut and nipple formed part of the probe. The sample was aspirated at $\leq 0.117 \times 10^{-6}$ m^3/sec down a channel (b) 0.508 mm wide, formed between the main brass body (c) and the reciprocating block (d), which was removed from the instrument in the picture. It had a motion of 2 mm amplitude and a period of five seconds. The velocity of motion was nearly equal in each direction. This arrangement gave, in the case of dust, a spread over an area of about 3 mm in width with a homogeneous region of slightly over 1 mm in width in the centre[154].

There are several ways of mounting a grid[154]. The simplest was chosen here and is illustrated in section in Fig. (8b). The plug carrying the grid is marked (e) in Fig. (6) and the location of the grid is marked (f). On the opposite side of the grid a glass slide, cut to size, was held vertically at an equal distance to a horizontal wire (g) by another block. The glass slide is positioned behind the wire in the photograph. The role of the electrically heated wire was to precipitate the soot particles on the electron microscope grid and the glass slide. The hot wire was made of Brightray Alloy C, 0.25 mm in diameter. It was held taut by a spring (h) situated outside the instrument. The heating current of the wire was varied from 1.5 to 4 amp. and was supplied by a 2 volt rechargeable battery.

From the above it should be clear that the two walls of the channel through which the sample was aspirated were composed of the oscillating block on one side of the wire and the brass-slide-brass wall on the other Fig. (8c) shows a schematic representation of the dust-free space when

the correct temperature difference exists between the heated wire and the cooler walls. The soot deposition occurs just above BB in Fig. (8c). The brass inner walls, as well as the facings of the sliding walls were machined with considerable precision to a high degree of fineness. The exit gas sample comes out at (j). Two metal srpings (k) at the top of the instrument were responsible for the return movement of the block carrying the electron microscope grid. The reciprocating movement of the block was achieved by a pin (ℓ) set in motion by a cam, which was driven by an Enicron geared motor, supplied by Enicron Ltd. The motor gave a maximum of 12 revolutions in 60 seconds. Details of operation of the precipitator, precautionary measures and techniques of adjusting the electron microscope grid to obtain the best distribution of the deposit may be found in references (155) and (156). A schematic representation of the thermal precipitator in the sampling circuit used is shown in Fig. (8).

4.2 Particle collection on an electron microscope grid

Sampling on grids was explored using a hand-operated device, which consisted of a rod carrying a glass on to which a grid was glued. The experimental set-up is schemetically illustrated in Fig. (9). It consists of a burner, which is, simply, a brass tube on to which was screwed a nozzle of 3 mm I.D. The nozzle is surrounded by a circular trough packed with glass beads 4-5mm diameter, to distribute the air flowing around it. The trough had about eight times the width of the nozzle.

A cylinder made of two layers of copper gauze was made to rest on top of the trough. A horizontal slit cut into it, allowed for the free movement of a glass slide carrying an electronmicroscope grid, as well as

the rod to which the latter was attached. The first fuel used was methane, which flowed at 33.3×10^{-6} m^3/sec at $20^{o}C$. The trough and gauze arrangement provided for a reasonably stable flame.

Before the grids could be glued with silver dag on to the glass slide, they had to be coated with a thin film of carbon, on which the soot particles collected during sampling. The techniques of grid preparation is described in most textbooks dealing with electron microscopey e.g. ref (157), and will not be discussed here. In this study copper grids of size 200 mesh were used, although these are manufactured of various metals, such as silver and gold, of various mesh sizes and shapes.

When a glass slide was scanned rapidly across the flame, the soot particles, when collected, were very small and barely visible at high magnification. The samples on the grid had to be shadowed with chromium in order to get better contrast. This is illustrated in Plate 2d, and refers to the case when the slide scanned rapidly five times across the flame at 40 per cent of the flame height. The scanning speed was varied so as to include much higher, and some lower, speeds. The speed refers here to the frequency with which the slide carrying the grid enters the flame per unit time.

The movement of the rod carrying the slide was controlled by the arm A. The sleeve to which the arm was attached was supported on a platform B, which could be fixed at any desired height by a screw at its lower section. The platform carried two short vertical plastic rods, one on each side of the arm A. These served to determine the maximum span of the arm and therefore the movement of the grid. This could be changed by first unscrewing the bolts holding the rods to the platform and then sliding each rod along its slot to the desired position. Section C served to prevent any accidential movement of the rod vertically and did not appear to hinder the movement of the rod in the horizontal direct-

ion. After examining the samples collected at different speeds, an increase in number and size was observed, with a decrease in scanning speed. It was deduced from a number of samples examined in this way that the very few particles agglomerated in a chain which occurred appeared to do so during sampling. In general, individual spherical particles were scattered all over the grid. When the scanning time was slightly prolonged, various shapes were observed under the microscope, some of which were rather decorative but which did not bear any relation to soot. This seemed to result from the curling or tearing away of the carbon coating on the grid.

When small amounts of propane were added to the methane stream, particles were usually easily observed at a magnification of 10,000 and were attributable to this additive. Further work on CH_4 seemed inadvisable since the effort involved was unjustifiable in the context of this study. It was therefore decided to concentrate on C_3H_8 flames, since the particles produced were easily observable with the electron microscope then available.

A propane diffusion flame was burnt at a flow of 10^{-5} m^3/sec at $20^{o}C$ in the same set-up previously described for methane. It was likewise scanned at about 40 per cent of the flame height. The results of five, fifteen, thirty and sixty passes are shown in Plate 1. Each grid was scanned, and then several squares on the grid (which contained about 200), were photographed and sometimes enlarged for comparison in order to choose the most representative. This procedure was followed throughout.

Plate 1a was magnified three times as much as the others during printing to show details that might not be clearly visible in the other photographs, which were magnified only to 10,500, in order to get as many particles as possible on one picture. Further reduction would have made it difficult to distinguish particles from agglomerates. The largest

Legend:

Propane flame sampled at 40 per cent of the flame height.

a) 5 passes across the flame.

b) 15 passes " " "

c) 30 " " " "

d) 60 " " " "

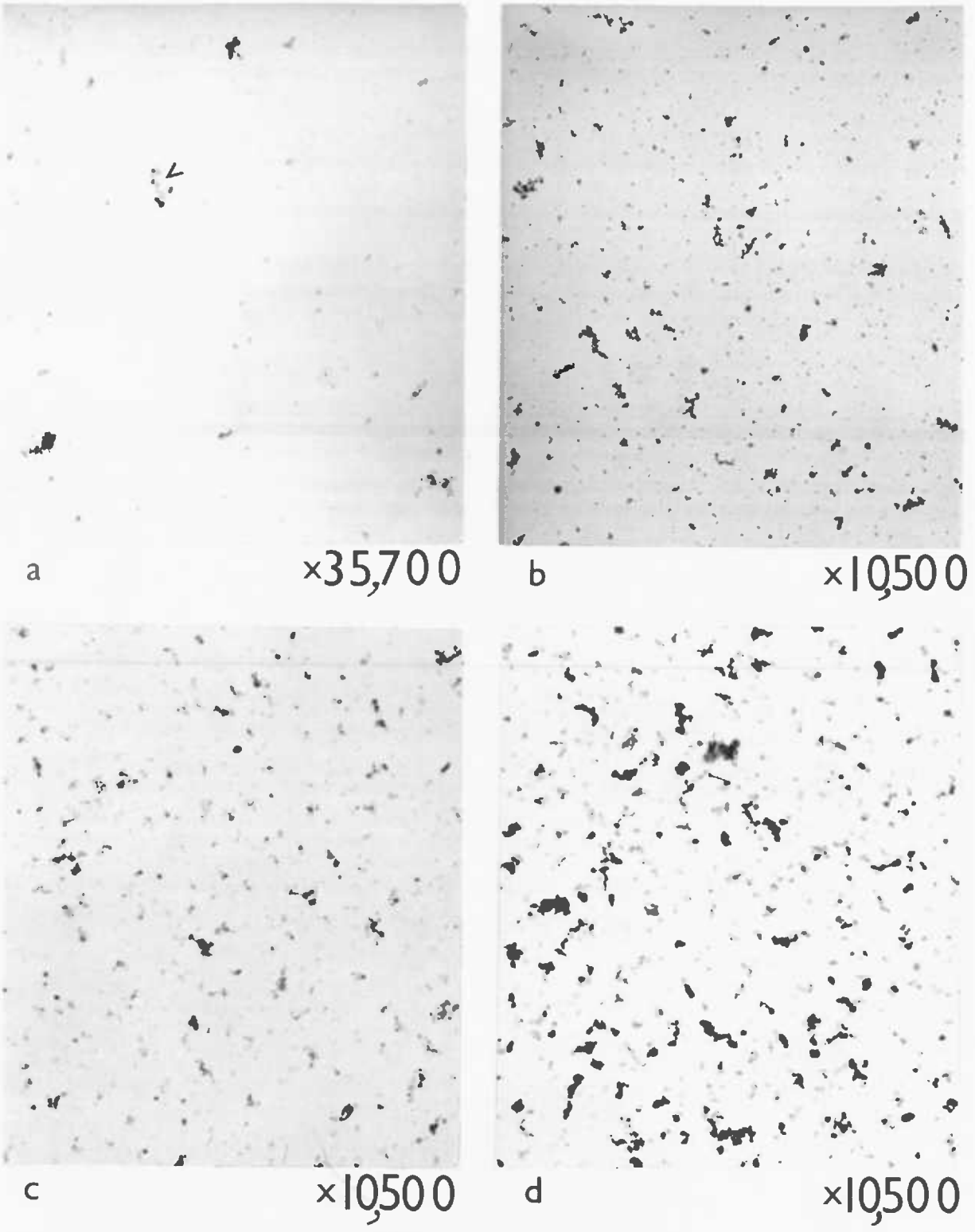

PLATE I

Legend:

Sampling position 40 per cent of flame height at flame axis.

C_3H_8 flame aspirated at 10^{-5} m^3/sec, flow in thermal precipitator = $.117 \times 10^{-6}$ m^3/sec for 30 seconds.

a) particles from within the center 1/3 of the grid.

b) " " " " " " " " :

c) " at the edge

CH_4 flame scanned 40 times.

d) illustration of the effect of shadowing at 35°.

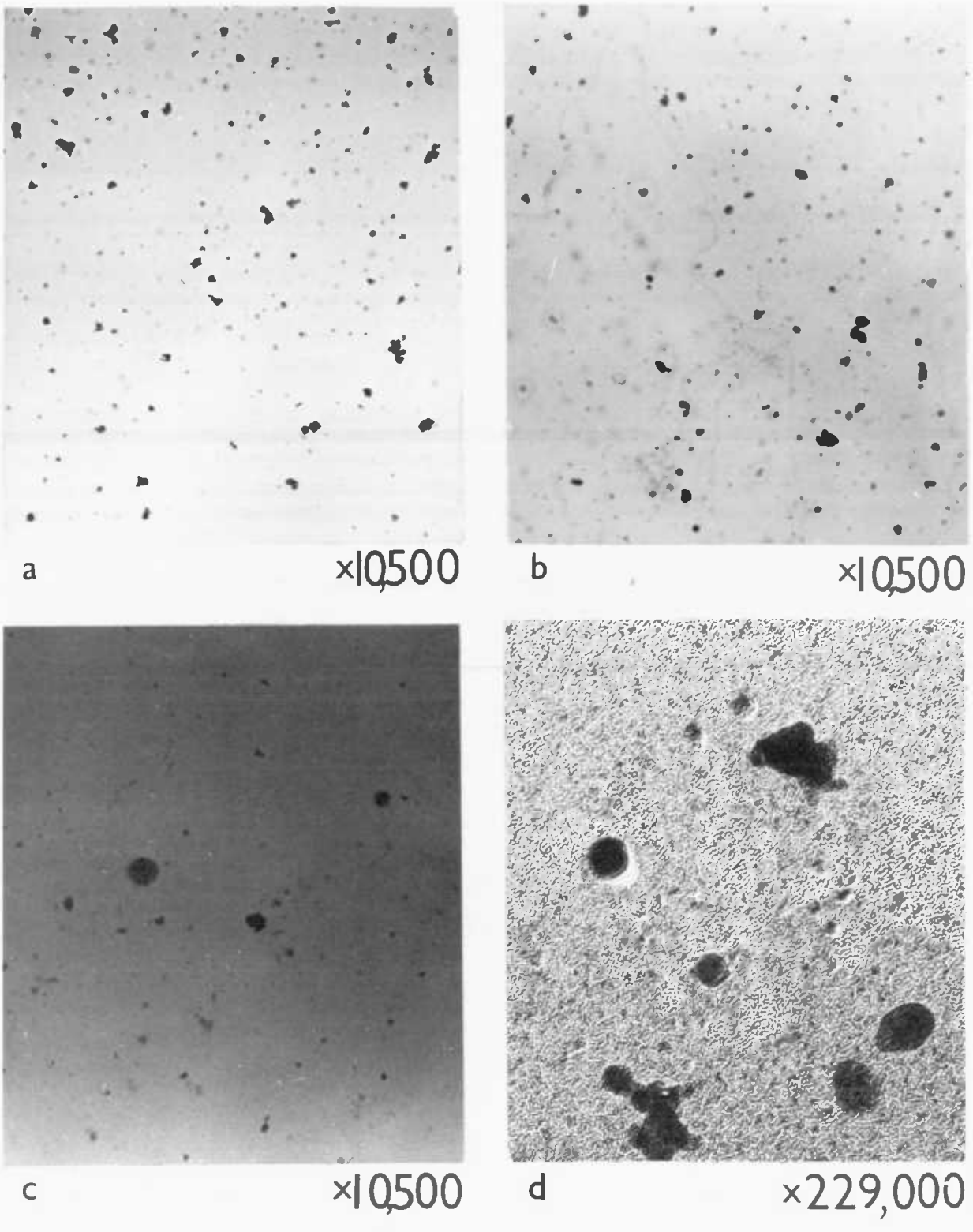

PLATE 2

particle agglomerate in Plate 1a is marked by a V. The increase in number and size of such agglomerates with the number of passes is clearly illustrated in a) to d). The same effect occurred when scanning speed was reduced. Having sampled soot on a flat surface and reached some preliminary conclusions the next logical step seemed to be to study the effect of sampling using a suction probe on the size and shape of the particles. This could provide substantiating evidence and will provide information on whether the average size of the primary particle is affected by the sampling method.

A quartz probe similar to that shown in Fig. (7a) was suitably attached to the inlet of the thermal precipitator described in section 4.1: this is a useful instrument by means of which very small particles may be sampled. The principle underlying it is that, when a solid-laden gas stream enters a region in which two bodies in close proximity are at two two different temperatures, the particles will move towards the cooler body, as a result of the thermal force acting on the, and deposit on it[155,156]. The probe connected to its inlet was heated by a Ni-Cr wire wound along its length up to 20 mm from its nozzle end. This was necessary in order to reduce the particle agglomeration that occurred along the probe during the condensation of water vapour in the gas sample.

Samples collected in this way were unevenly distributed along the electron microscope grid, unlike the case when a glass plate scanned the flame forwards and backwards. The density of particles and agglomerates in the former case seemed to be more or less even for only up to 1/3 of the grid from the centre (Plate 2a&b) and fewer particles were deposited at the edge (Plate 2c). This distribution seemed to result from the periodic motion of the grid[154]. Comparing (b) in Plates 1 and 2, it was immediately noticeable that, although the sampling height was the same, the apperance of the agglomerates was different, being somewhat

longer in the first case and rounder in the second.

These observations of sampling using two different techniques suggested that agglomeration might have been completely eliminated had correct sampling conditions been found. There was, however, some doubt as to the general applicability of such a conclusion. The propane flame in the main experiment was confined by water-cooled walls, unlike the case of a free-flowing flame. It was therefore possible that the above observations might not be entirely reproducible. It seemed that the simplest way of clearing this point and also of obtaining reproducible results was to pass in and out of the flame a glass slide carrying an electron microscope grid. The mechanical sampler described in section 4.1.1 was devised for this purpose. Details of one unit are shown in Fig. (4).

In actual practice, this was far from easy. Soot deposition on the water-cooled walls reduced the size of the opening through which the rods carrying the glass slide moved. This meant that lumps of soot were collected during sampling, a problem that grew worse with an increase in height and lapse in time. It was partly overcome by covering the holes, before the flame was lit, with a long, thin strip of stainless steel welded to a horizontal stainless steel ring, (Fig. 5). The ring was positioned between the fourth and fifth calorimeters and was rotated by moving the guide arm positioned between two of the eight pairs of bolts and screws used to hold the flanges together. It was therefore possible to cover and uncover the holes rapidly.

The deposition of a thin film of liquid hydrocarbon along the probe, as well as inside the 4 mm passage through which the probe moved, was another source of nuisance. Unless it was completely removed, the smooth motion of the probe was inhibited. This reduced the effective sampling speed at a given voltage (see section 4.1.1).

At low sampling speeds, agglomerates were always formed in great

numbers. At high sampling speeds the apparatus vibrated strongly, resulting in the loss of the sample, usually due to the breaking of the glass slide before the completion of its cycle or due to the grid tearing off.

It was therefore decided that as a result of the problems encountered it would not be possible, using the sampling units, to reach any conclusion regarding the actual state of the particles inside the flame. Such sampling units would however, have been ideal in the case of free-flowing flames. Their use in confined flames should be limited to cases where the walls are uncooled. Had the diameter of the furnace been twice as large (i.e. 102 mm) as in this case, it would have been possible to make the passage twice as large. It would then have been possible to make the sampling rod of two different sizes. This in itself would have been sufficient to reduce several problems mentioned above.

A probe similar to that shown in Fig.(7b) was used next. The thermal precipitator was attached to one of its ends. The probe body was made of brass except for a length of about 35 mm at the nozzle end which was not heated. In order to avoid disturbing the flame while introducing the probe, an extension tube with a P.T.F.E. gate similar to that shown in Fig. (15) was used which could accommodate on one side (when necessary) a Bakelite plug 20 mm in diameter. The plug filled the space between the probe and the opening of the section through which the probe now entered the combustion chamber.

Because of the number of probes used, more than one plug was made. Each had a hole drilled right through which corresponded to the size of the probe it had to accommodate. When a probe was in position, an O-ring which had previously been mounted on it was pushed towards the Bakelite plug and made to rest in a groove which was cut in it. This was expected to provide a seal, in order to prevent any air from being sucked into

Legend:

Sampling at window no. 2 at flame axis.

a) flame aspirated at 0.58×10^{-6} m^3/sec.

   flow in thermal precipitator: 0.117×10^{-6} m^3/sec for 60 seconds.

b) flame aspirated at $.08 \times 10^{-6}$ m^3/sec.

   flow in thermal precipitator: 0.08×10^{-6} m^3/sec for 10 seconds.

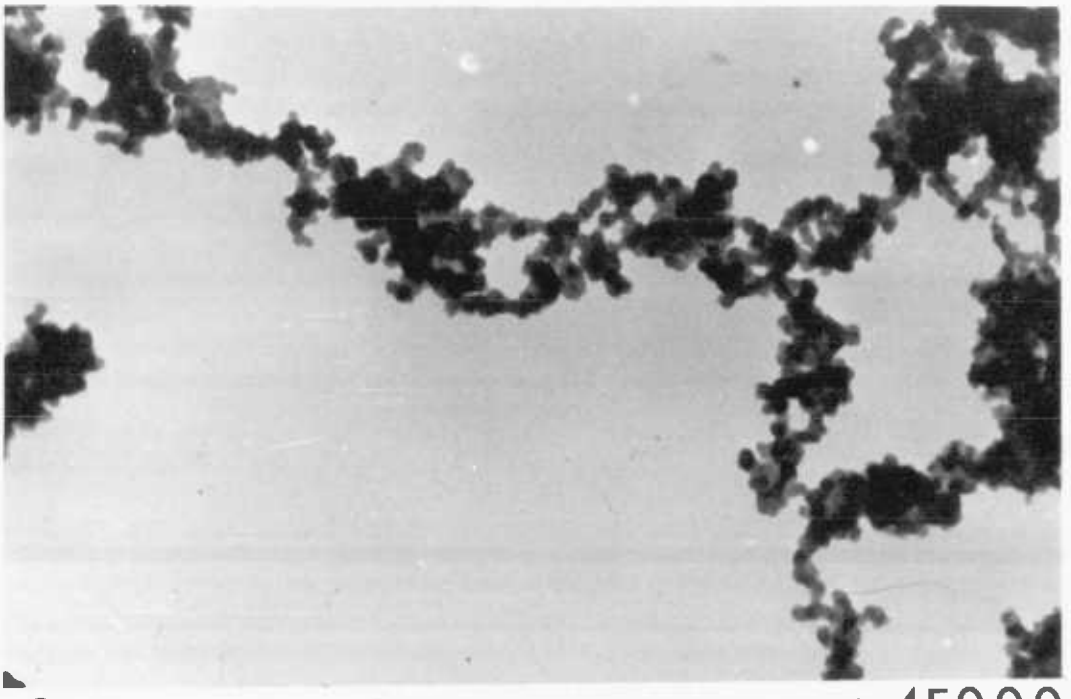

a ×45000

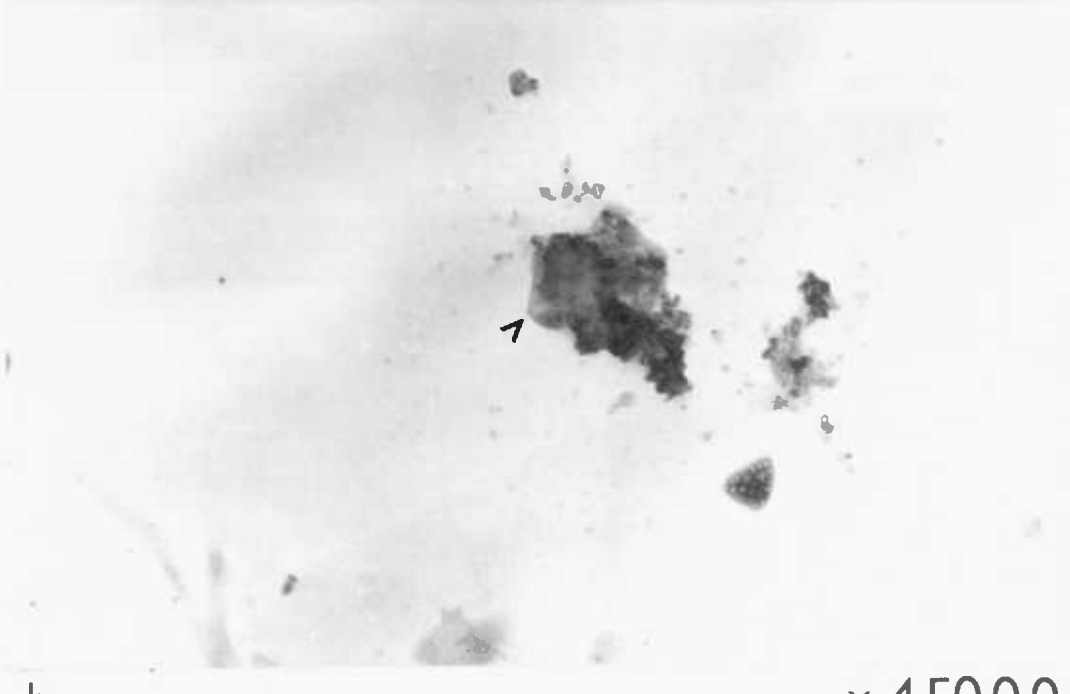

b ×45000

PLATE 3

the combuster. Plate 3 shows two photographs of samples which were drawn into the thermal precipitator at different sampling speeds and for different lengths of time. For the higher sampling speed and longer time, the particles were agglomerated into a huge matrix of particles (Plate 3a). This was expected to have been formed during the condensation of water vapour inside the thermal precipitator. When, however, the aspiration speed inside the precipitator, as well as the sampling time, were reduced, very little soot was collected. The photograph in Plate 3b shows all the soot deposited on the grid. The large lump marked with a V is probably carbonaceous material deposited on the probe and withdrawn during sampling.

4.3 A Discussion of Probes and Filters Investigated

Soot sampling may be achieved by using either suction probes or deposit surfaces. In comparison with others for example optical techniques they are at a disadvantage, due to their effect on the physical and chemical properties of the flame. The reliability of optical methods in determining soot weight as well as particle size and distribution is however, still doubtful at present, except when the weight is determined by extinction techniques*(see Chapter 2). In the following discussion, an attempt will be made to show to what extent it has been possible to overcome the problems which result from the physical presence of a probe. Suction probes may be classified under two types. In the first, a volume of soot-laden gas is aspirated through an orifice at sonic speed and the reaction is quenched by expansion inside the nozzle as the exit pressure is reduced. These are called sonic probes. In this class are microprobes, which are used for sampling in small laboratory-

*Indicate the weight of soot plus any heavy hydrocarbons.

type flames and are usually made of quartz or stainless steel. A comprehensive treatise which includes methods of construction has been presented by Friston and Westenberg[158]. Sonic probes have also been designd for the purpose of sampling in large flames of industrial scale[159]a.

A number of probes used in this study are shown in Fig. (7). Aspiration probes were generally made of quartz. The nozzles tapered to 20 to 40 degrees and the rotation asymmetry was kept to a minimum. One would expect that disturbances including the catalytic effect caused during sampling would be negligible because of the small ness of the capillary orifice, which was of the order of 800 μm. The flame was sampled at various sampling speeds not exceeding isokinetic flow velocity. This was done at right angles to the direction of flow and should not have affected the mass of soot collected, since soot particles follow gas stream lines, as may be deduced from the following equation derived by Badziock[160].

$$\frac{C_o}{C} = \alpha' \frac{V_o}{v} + (1 - \alpha')$$

where C_o/C is the ratio of the concentration of solids at the probe orifice to the true concentration, and v stands for the velocity. The inertia parameter α' is a function of the shape, size and density of the solid particles as well as of the factors which influence the shape of the stream. Because soot particles are very small, they have negligible inertia i.e. $\alpha' = 0$, and therefore $C_o = C$.

During sampling, hot gases are present together with the soot. It is therefore important to prevent any reaction since this will distort the results. In practice, quenching of the reaction is never completely achieved except with molecular beam sampling systems, where the quenching time in the probe is of the order of 1 μsec[94]. It is common practice, and sufficient for many purposes, to reduce the sample gas temperature to 300°C in about 3 msec[159]b. At this level, it is expected that re-

action of the initial mixture will be negligible within the given time lapse.

In order to ensure that the reaction was being quenched in a reasonable time, a sample calculation was perfomred for a probe orifice of 800 μm and a sampling flow rate of 7.9×10^{-6} m^3/sec, which is equal to the volumetric flow rate of unburnt propane used here. If we consider the case when the probe was positioned at the centre of the flame, we would expect the sampled gas temperature to be reduced to less than 150°C in about 1.7 msec. This assumes that, when the gas inside the probe reaches the boundaries of the cooled walls, its temperature does not exceed that recorded by the thermocouples at these positions (see fig. 30-33).

When sampling was carried out for the purpose of determining the size and distribution of particles, the probes had a side arm by which they were connected to the thermal precipitator (Fig. 7a). Sampling into the probe was done in two steps. First, the volume of gas flowing in the probe was partly aspirated into the rotameter. The flow into the water pump was regulated by a needle valve upstream of it. When the rotameter indicator reached the required level, the three-way glass valve at the bottom of the instrument was switched to position (B). In this way, the stream entered the thermal precipitator rather than the rotameter. The results obtained using this technique were discussed earlier in this chapter (section 2). A number of microprobes was also used for sampling soot for the purpose of weight and composition (soot) analysis. They were packed at their ends with quartz wool (see Fig. 7c), which seemed to provide a very efficient filter under these conditions. Most of the soot was collected in the region where the smaller and larger tubes met. Although this method was satisfactory for weight determination, the soot collected was insufficient in amount for chemical analysis. Two factors

were involved: the probe tended to block during sampling, and it was not possible to separate the soot from the filter material. The soot which was shaken off the quartz wool was never completely free of quartz and it was therefore difficult to estimate the amount of soot in volume being weighed for analysis. In most cases it was too little, and in some cases the water peak, which is an indication of the amount of hydrogen in the soot, did not even appear.

The possibility of using a different type of filter was investigated. The idea of using a simple filter paper disc resting on copper gauze seemed attractive at first, as it has the advantage of retaining fine particles. It lacks, however, strength and cannot be used when the soot is required for further analysis, which is the case here. Another alternative was to use sintered quartz or pyrex filters. These can easily be attached to probes and are manufactured in various grades. The major advantage of these latter filters is that they are robust enough to withstand handling,[159]b which however, was not a prerequisite in this work.

Soot,is produced within the blue reaction zone in a layer parallel to it. This presents another difficulty when the conetration profile of soot across the flame is required. Since the layer involved is of the order of 2 mm, it is not difficult to imagine that errors can occur. For these reasons, it was decided that it would be best to collect soot on a water-cooled surface.

A review of the literature showed that water-cooled probes made of duralumin[60], stainless steel, brass[6], quartz and porcelain[121] have been used. In these experiments, the cool horizontal surfaces obstructed the flame flow, and it was therefore expected that this would affect the amount of soot collected. Tesner[60] reported however, that, although in his experiments the cooled surface shifted the wake of the

flame towards the burner nozzle, the weight of soot collected did not seem to be affected. He came to this conclusion by comparing the weight of soot collected from a gas diffusion flame by a water-cooled cube formed of acpillaries which did not obstruct the flame, and that collected on a water-cooled flat plate made of duralumin. One could therefore infer that the soot collected using the small cylindrical probe shown in Fig. (7d), which was used here, corresponds to that present at the sampling position. Even if this is not absolutely true, it is not expected to affect the conclusions, since what is under investigation is the relative change in soot weight which occurs at each position(or window)is under investigation (see chapter 6).

As the probe diameter was much smaller than the opening at the side of each calorimeter, a special Bakelite adaptor about 3.3 mm in diameter was used to reduce the opening and to provide a guide for the probe. A plug also made of Bakelite, at the opposite side of the probe entrance kept it horizontal.

The flow of water into the probe was reduced until no condensation of water vapour in the soot occurred while the probe was in the flame. Sampling, which is another important factor, was generally kept at 30 seconds and in any case never exceeded 60 seconds. Although the amount of soot collected was found to be independent of time up to 300 seconds, it was necessary to keep this time short in order to reduce the thickness of the deposit, as a precaution against any possible dehydrogenation of the soot collected. A plot of composition against time did not provide any useful evidence. The deviation at one sampling time masked any genuine effect. This can be inferred from plots of temperature and soot composition in Figs (25 and 26), which refer to similar sampling times. The soot collected on the probe was scraped off with a metal scapula and collected into a container to be dried and

Legend:

Sampling at Window no. 2.

a) Flame scanned 10 times slowly, probe driven by mechanical sampler

b) Flame sampled at 0.58×10^{-6} m^3/sec , flow in thermal precipitator 0.117×10^{-6} m^3/sec for 3 minutes.

Note: Samples on grids were gold-coated prior to photography.

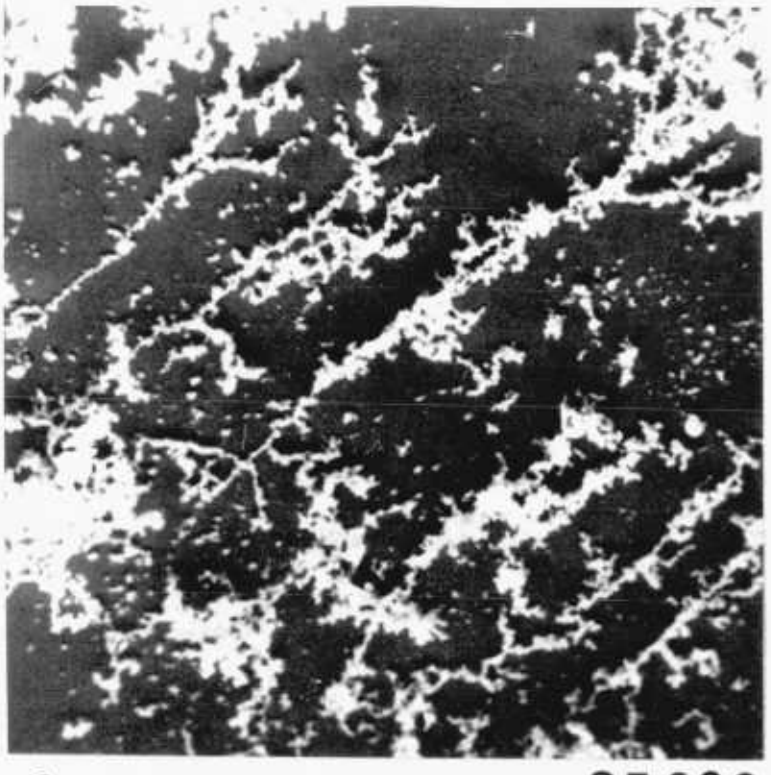

a ×25,000

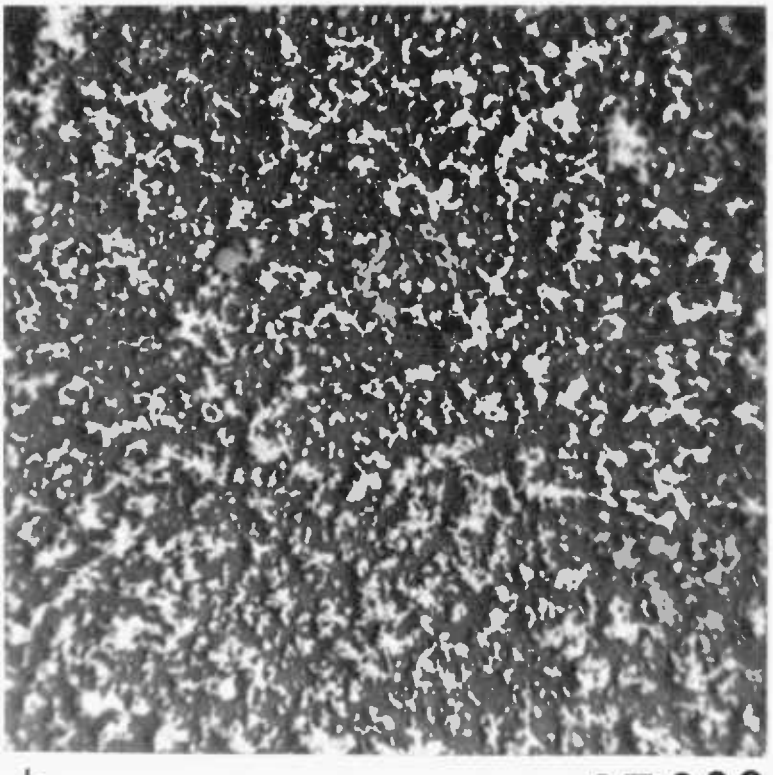

b ×27,000

PLATE 4

weighted. Part of the polymeric material that deposited on the probe during sampling appear to have done so before the soot particles and held strongly to the probe surface. This gummy deposit was easily removed by rubbing with a tissue paper moistened with carbon tetrachloride.

Discussion

Transmission electronmicroscopy, which in practice is one of the most useful methods of determining the size and shape of submicron particles, was used for particle characterisation of samples collected directly over a flat surface with a thermal precipitator. Particles collected using either technique showed a similar trend, i.e. the number of particle agglomerates or the size of agglomerate increased with exposure to the soot stream. There was, however, a difference in the way the soot deposited which was not unexpected considering the difference in techniques. This is shown in a three-dimensional picture obtained by use of a "Stereoscan" and is illustrated in Plate 4. It shows a preferred direction or plane of deposition. On the other hand, the soot collected on a flat plate (Plate 4a) shows a more even distribution all over the grid.

The mechanical sampler is, as has already been said, a modification of the manually operated scanning sampler described in Section 4.2 It is easy to handle and operate and offers a method of sampling at a predetermined speed. This can be achieved by calibrating the input current to the motor, which may be regulated by a variable transformer, with the speed of rotation of the motor. This can be read by attaching a special meter to it. A calibration curve was not obtained in this study, since the deposition inside the guiding cylinders attached to the main apparatus was polutted with polymer material, which would have made any calibration of little use. In fact, such an instrument should only be used under

conditions where the resistance offered to the probe movement is minimal.

Having reviewed certain points concerning the mechanical sampler, it would be proper to discuss next the thermal precipitator. There is little doubt that the former instrument is very efficient in collecting submicron particles which are relatively dry. When soot is sampled from a flame, it is surrounded inside the probe with an atmosphere of water vapour. Preheating the probe to the inlet of the thermal precipator may have overcome condensation along the probe, but there was nothing to prevent this from happening inside the instrument. Condensation of water vapour is not feared as such, but its effect on agglomeration introduced an extra factor to be considered when analysing micrographs.

Preheating the thermal precipitator was considered as a possible way of overcoming condensation of water vapour existing around the soot. This would, however, have meant that there would be no thermal gradient in the direction of the grid since the apparatus was made of brass which is a good conductor of heat, and separation of particles from gas due to the thermal forces would therefore not occur. This possibility was discarded for this reason.

There is perhaps one aspect which has been overlooked during the discussion, and that is the effect of sampling techniques on the average size of the primary particle. this was investigated as follows: forty particles were chosen at random from 2 electron microscope grids, sampled at the same position by each instrument: the size was around ($.04 \pm 10\%$)μm. The effect of additives on particle size was also studied using the mechanical sampler. The average particle size varied as ($.04 \pm 15\%$)μm. This suggests that additives did not, under these conditions, affect the average particle size to any important extent. The significance of this will become more apparent in chapters 6 and 7.

It is worth noting that the average particle size did not vary significantly in any position under any experimental condition. Finally, the various points relating to soot sampling for the purposes of weight and composition analysis have been discussed in detail, and there is no need to repeat them here.

Conclusions:

The evidence obtained in the case of the methane flame which is not illustrated here indicated that particle agglomerates were formed during sampling. Although it was not possible to eliminate agglomeration in the case of the propane flame, the evidence presented here would indicate a similar conclusion up to the height concerned. The average size of the primary particle does not appear to be affected by the different sampling techniques or by the additives used.

4.4 Measurement of temperature using thermocouples

Thermocouples are among the most widely used instruments for measuring temperature in industrial applications, as they are generally easy to make and highly sensitive. Whether the test junction comes to equilibrium with its surrounding medium depends on the particular case. When a thermocouple is inserted into a flame, the temperature of the junction depends mainly on the extent to which the heat loss by radiation is compensated for by the heat gained by convection.

Temperature measured by an uncoated thermocouple may read a higher value due to catalytic reaction of the wire. This may be reduced under certain conditions by coating the thermocouple with hexamethyl-disiloxane[162]

In flames containing soot particles, the measured temperature is below

the temperature of the gaseous medium by a factor ΔT due to radiation The deviation increases with prolonged exposure to the flame particles The magnitude of the factor ΔT may be calculated using the following equation:-

$$\Delta T = \frac{\varepsilon (T_g - T_s)^4}{h_c} \qquad (4.1)$$

where ε is the emissivity of the surface of the bead.

This equation may be obtained by equating convective heat to the net heat loss by radiation between the thermocouple and its surroundings at a temperature T_s. This holds provided factors such as conduction loss along the leads of a thermocouple, radiation from the surrounding gas and so on, are negligible.

The gas temperature profiles shown in Figs. 30-33 were obtained using a V-shaped thermocouple described in Chapter 5 which was coated with hexamehtyl-disiloxane. Had it been necessary to compensate the measured temperatures for radiation loss, ε in equation (4.1) would have taken three different values, depending on the location in the combustor. In the blue reaction zone, no soot was deposited: any soot previously deposited was burnt away. A value of $\varepsilon = 0.22$ as suggested by Kaskan[162] could therefore be used when a hexamethyl-disiloxane coating was used. Prolonged exposure to the hot atmosphere of this zone destroyed the protecture coating,which showed up as a sharp step-wise increase in the reading on the chart recorder.

When the thermocouple lead was positioned outside this zone, soot deposited only in very small amounts along the white coating on the thermocouple. Assuming that this may increase the emissivity, we would expect its value to be either equal to, or slightly greater than, the value $\varepsilon = 0.22$ given by the coating. It should however be mentioned that in this region the temperature values fluctuated violently. The

The values of the temperature used in plotting the profiles in Figs (30 to 33) corresponded to the arithmetic mean of a number of fluctuations. When the bead was positioned within the boundary of the blue reaction zone, the small fluctuations of the pen recorder indicated a regular response for a very short distance on the chart and then dropped steeply as excessive amounts of soot deposited on the probe and grew in the form of short filaments.

The steep, continuous drop in temperature occurred in the above case much more quickly during sampling in the soot layer. In this region readings had to be repeated more than once. Since the bead was completely covered in soot even in the region where the response was regular, it is expected that the recorded temperatures are somewhat underestimated, as a result of the cooling effect due to radiation loss. The emissivity in the region would be expected not to exceed the emissivity of soot 0.95 [25f] . Although we have been concerned here mostly with the regions where the reaction zone exists, the observations made are also applicable to the region where the reaction zone did not exist.

It may be inferred from the above that the emissivity poses somewhat of a problem, and its value is difficult to know for sure. Determining the heat transfer would prove to be problematic, since a knowledge of the size of the test junction is required, amongst other things. Even if this was determined after every reading using a high-powered microscope, there was no guarantee that the size measured would have corresponded to the value of the temperature recorded. Since the readings of the thermocouple were uncorrected for radiation, they were only useful as an estimate of the temperature. The next step was to determine the extent of reproducibility of the measurements since the magnitude of the error is not known. This was found to be satisfactory. Profiles

were duplicated in a number of cases and found to give an error of less than 7% in the value of the mean temperature across the reaction point-to-point measurements were in general easy to duplicate during the same experiment.

CHAPTER 5

DESCRIPTION OF APPARATUS AND PLAN OF EXPERIMENTS

5.1 Description of Apparatus

5.1.1 Main Apparatus

A general outline is shown in Fig. (10). There are two main parts: a) Burner assembly; a vertical section through the burner is shown in Fig. (11). This consisted of three sections:

i) The burner: was made of brass composed of three concentric tubes. The fuel and air flowed through the innermost and outermost tubes respectively. Oxygen was passed through the central tube to exit at the openings in the nozzle. The bottom flange was fixed to a large, 175 mm gasket made of Pierrite 60 which served as support and insulation. The gasket was supported by three vertical bars of aluminium, 25.4 mm thick, which were fixed to a metal plate at the bottom, each at the apex of an isosceles triangle of side ℓ = 140 mm.

The gasket was held in position by two 3/8 inch nuts, one below and one above each bar. The tripod system provided a means of levelling the combustion chamber, by manipulating the nuts corresponding to each bar.

ii) The nozzle: a vertical section through this is shown in Fig. (12) It was initially made of brass, but prolonged exposure to high temperatures at the higher oxygen content tended to thin down regions of the ring at the top of the nozzle on which the flame sat, which was only 1mm wide. This affected the stability of the flame and caused it to deflect by as much as 20 degrees from the vertical. A similar nozzle was made of stainless steel. It is interesting to note that the radiation profile did not seem to be affected by the change of material except when the higher levels of oxygen were added to the fuel. This indicates that the catalytic effect of copper in solid or vapour form was not important at the position cited.

The nozzle consisted of six equally spaced vertical holes. The holes

were first made using a one millimeter drill. They were later widened to their present size of 2 mm. This was convenient as it reduced the linear velocity of the oxygen coming out of each hole, thereby reducing the distortion of the flame due to shear flow. Unequal distribution of the flow may have resulted if the six holes were not identical, which is to be expected when very small holes are drilled in stainless steel, unless special precision tools are used.

iii) The air distributor: to achieve an even distribution of air at the cross-section at which combustion occurs, the air annulus was packed with 4 mm diameter glass beads, supported on a taut wire mesh of copper above the opening for the air inlet. After a number of trials it was clear that such an arrangement was not suitable. Condensation of water vapour at the colder walls, resulted in deposition of a water-soot mixture. With time this reduced the effective surface area of air flow. The extent of this effect on the distribution of air across the annulus was not known for certain. When $CC\ell_4$ was used the function of the distributor was greatly reduced or even nullified.

A new distributor was designed taking into consideration these difficulties, This was built of a number of brass tubes and is shown in Fig. 11. Its performance was adequate as a rule. Partial blocking of the tubes was noticeable in the experiments involving $CC\ell_4$.

b) Water-cooled Jacket: (or Calorimeters): Five vertical units placed one on top of the other, were used to recuperate and thus deduce the net heat flow to the walls. The first four were identical and similar to that shown in Fig. (13). Each was composed of two concentric brass tubes of 50.8 mm. and 60 mm I.D. respectively and 700 mm in length. There were four openings at right angles to each other. Three served as sighting ports and the fourth served to sample soot when the mechanical sampler described earlier in chapter 4 was used. It was otherwise closed. The sighting ports in each calorimeter were capped. A one-inch nut was modified to incorporate a glass

window 3mm thick, with a key-hole type cover which could be slid-off to observe the flame.

The fifth and uppermost unit was slightly different. It was made of two concentric cylinders with the same inner dimensions as the first four and had a length of 210 mm there was only one opening at the top and was unplugged when the exit gas temperature was to be measured. Each unit except the uppermost had tow end flanges. The five units, i.e. calorimeters were each separated by a 2mm gasket and their end flanges were bolted together. This extra height was neglected in the drawing of the plots and in the calculations in chapters 6 and 7.

The water for cooling was fed from an overhead tank with a capacity of about five times that of the five units. The water entered the lowermost unit and left through the uppermost via a water rotameter (maximum range 9.83×10^{-6} m^3/sec of S.T.P. A "flow watchman" was positioned before the rotameter to indicate whether the water was flowing normally. It consisted mainly of a circular hollow tube made of clear styrene in which a red ball moved freely. From the top stemmed an inlet and an outlet tube, the ends of which could be connected with a standard hose.

The first step taken to reduce the amount of air trapped inside the apparatus was to position the water outlet from each unit as close as was practically possible to the top flange. The exist tube through which the water left the system was extruded above the top of the fifth unit. The rubber tubing carrying the water was squeezed a number of times before and after the flame was lit until the flow watchman was free of air bubbles. The flow rate was kept nearly the same in all experiments. Two considerations influenced the choice of water flow rate. The first was that it should not be excessive and thus cause condensation or fogging of the sighting tubes. The second was that it should be sufficient to prevent steam formation.

5.1.2 Auxilliary Apparatus

a) Total radiation pyrometer: A land low temperature, radiation pyrometer, type ORF/10/6 was used. The calibration table for a black body temperature range 273-1273 K, provided by the manufacturers was used. The e.m.f. generated by the instrument was recorded on a chart released by a drum moving at a speed of 2 revolutions per minute. Temperatures quoted in this study correspond to the average output in 90 seconds. The pyrometer output was independent of the detector temperature, between 273 and 353 K. This was achieved inside the pyrometer by a shunt wound with nickel wire in parallel with the junction thermopile. The total resistance of the pyrometer was 20 ohms at 293 K. The measuring circuit had a resistance of more than 200 ohms and was therefore above the critical value at which the compensating circuit of the pyrometer would become ineffective[163].

The pyrometer was held by slipping it into a specially designed metal clamp in the form of a ring. This was tightened carefully around the pyrometer by a small screw at its neck so that it did not slip or twist. The ring was attached to the moving part of a cathetometer scale by a metal arm which formed part of the clamp, so that the pyrometer was at right angles to the vertical bar which formed part of the cathetometer body. This meant that the pyrometer could be held in a horizontal position by adjusting the screws at the bottom of the cathetometer.

The caps which ordinarily covered the sighting ports of the water cooled jackets, each incorporated a glass window and could not therefore be used to measured radiation 1 - 10 μm. Different caps, which incorporated ArS_3 windows Fig. (14), were hence used. During the preliminary experiments on the apparatus, fogging of the ArS_3 windows occurred during operation. This was more marked in windows 3 and 4 than in the lower windows. Passing a stream of nitrogen to screen the window is one way of overcoming this problem. However, an extension tube (Fig. 15) incorporating a sliding

P.T.F.E. gate was devised and screwed on to the side tube (facing the pyrometer) at any of the four positions. The cap which it replaced was screwed onto its free end. In this way it was possible to remove the cap in order to clean it or to replace it with one carrying an arsenic trisulphide window, without disturbing the flame as long as the gate blocked the line of sight. The ArS_3 window was held in place by two rubber (neoprene) rings.

Since the lens diameter was several times that of the sighting hole, it was necessary to have a device which would make it possible for the pyrometer to be correctly aligned every time. A pointer carrying a sharpened stainless steel rod was attached to the pyrometer casing. The axis of the pointer ran through the centre of the lens. The movement of the stainless steel rod was restricted by the length (20 mm) of a slot which was cut at the side of the sleeve inside which the rod moved. When the latter was in full extension its sharp end was 150 mm from the lens. The disc of four caps housing the glass windows (described above) were lightly marked in their centre with a metal puncher. The pyrometer was then brought to the correct position by means of the cathetometer slide and the pointer. The pointer was then retracted inside the sleeve; then the cap was removed and replaced by the cap (Fig. 14) enclosing at one end the arsenic trisulphide window. The pointer was carefully removed from the pyrometer. Readings could then be taken, after the P.T.F.E. gate was opened.

In this arrangement, the pyrometer was about 150 mm from the target. The size of the target focussed through the lens at the detector thermopile was about 23 mm at this sighting distance[163]. It consisted of an aperture of 12 mm in diameter through which the radiant energy of the flame left the sighting tube. The rest of the area was in the form of

an annulus which formed part of the flat face of the brass cap carrying the the A_rS_3 and was only a few degrees above room temperature.

b) Thermocouples

The flame temperature across the reactor was measured at various positions by a Pt/Pt-13% Rh thermocouple. In order to increase the accuracy of its hot junction it was built according to Kaskan[162] by fusing very fine wires, 0.127 mm in diameter. Each wire was fused to a thicker wire (.254 mm) of the same material, which acted as a support to the finer wire. The final shape of a thermocouple is shown in Fig.17a,i. Thermocouples made this way were too fragile and unsuitable for this type of work. They required a lot of trouble and time to make and broke very often, during an experiment or when the soot deposited on them was being burnt off before re-use, and then had to be rebuilt.

The thicker support wires being reasonably thin, it was decided that a thermocouple made of it would be stronger and hence more practical. The thermocouple and its holder used throughout the main experiments is shown in section in Fig.17a,ii. Each thermocouple was coated prior to use by hexamethyl disiloxane to minimise the catalytic effect which could otherwise be induced at its surface. The set-up is schematically drawn in Fig. 17b. When the flame was first lit, the three-way valve was in position (A) so that the stream of natural gas went straight into the A,Méker burner. By turning the three-way valve into position (B), the gas bubbled through the oily additive prior to entering the burner. A point worth noting is that the coating of the finer thermocouple discussed above was possible much more rapidly and thoroughly than in the case of the 0.254mm thermocouple used later. Prior to coating the thermocouple was made to scan the flame until the reading on the millivoltmeter connected to it was equivalent to 1853 K. Once this position was located the rod carrying the thermocouple support was clamped in position. This temperature

is above that required to evaporate the silica compound and just under that required to melt the thermocuple junction, 1973 K[162]. The latter flame was also used to remove the soot deposited on the thermocouple prior to coating with hexamethyl disiloxane.

The extension tube shown in Fig. 15 was also used when the temperature was being measured. It was transferred to the opposite side to complete the temperature profile. The temperature was measured slightly beyond the central axis on each side. The side facing the operator was designated the left-handside (L.H.S.) and that opposite the (R.H.S.). This was from the point of view of an observer looking through the third or middle window. This window as well as that facing the thermocouple was used to inspect the alignment of the thermocouple tip with respect to the axis of the flame, the extent of soot deposition, and the position of the tip inside the flame.

The chart recorder was made by Honeywell, and had a range of 0.1 to 1.0 mV. This was extended to 20 mV by a suitable shunt when the thermocouple readings were taken, which was removed from the circuit when radiation measurements had to be made.

A sudden pulse was sometimes recorded on the recording chart when the gate was opened and the probe pushed in too quickly. This was discarded. The next highest reading was used to calculate the local temperature. It then was necessary to make a number of random temperature measurements every time to check the accuracy of the results. These were made at intervals of 3 mm instead of the usual 1 mm.

Ten 1.5 mm copper-constantin thermocouples were used to measure the water temperature at the inlet and outlet of each calorimeter. Another thermocouple of the same material was positioned just above the air distributor and introduced from the side of the burner main body to measure

the temperature a few millimeters above the air distributor. Each of the ten Copper-constantin thermocouples as well as the Pt/Pt-13% Rh thermocouple used to measure the flame temperature had a separate cold junction. A selector switch type SPZ/P/MB with 24 positions supplied by Croydon Precision Instrument Co. was used to connect the output e.m.f. from the various positions to a Cambridge Junior Potentiometer. The mV read to three decimal points. Extension leads of copper wire were used to connect the outputs from the selector switch to the potentiometer and as extension leads for the Pt/Pt 13% Rh couple.

c) Method Addition of Halogen

The halogen was added by diverting part of the fuel flow into two glass bubblers kept at a constant temperature by a thermos flask and connected in series. Each glass bubbler was about 200 mm in length by 20 mm inside diameter. Glass beads about 4 mm in diameter, filled each bubbler half way. This was expected to increase their efficiency as the result of the increase in mass transfer area. In order to ensure a high degree of gas saturation at a particular temperature the water surrounding the bubbler in the second flask was $5^{o}C$ higher than the first.

d) Method of addition of heat

The air was preheated in a large stainless steel tube by two electric tube furnaces, each 0.50 m long and positioned in series. The preheating section was disconnected during other experiments, see Fig. (18).

5.2 Exploratory Studies Using the Apparatus

The interest in radiation from flames stems from the role it plays in total heat transfer. The energy flux from a unit volume of solid-laden gas is a function of both its physical and chemical properties. The solid mass concentration, size distribution and temperatures of solid and gaseous

media, fall under the first property. The composition of solid particles and gaseous medium fall under the second,

The following aspects were selected to quantify the effect of additives on the process of flame radiations:

1) The change of radiation and total heat transfer along the flame.
2) The temperature profile both along and across the flame.
3) The emissivity profile along the flame.
4) The change in soot weight and composition along the flame.
5) Radiation and thermal efficiencies.
6) Visible flame lengths and widths.

To assist selection of the operating parameters, (i.e. flow rate of C_3H_8 and air), a number of tests were undertaken. Initially, the effect of varying the fuel flow rate between 9 and 24 mg/sec on the radiation from the four windows was determined and is plotted in Fig. (19). The air flow rate was kept constant at 300 mg/sec. The value of 15.2 mg/sec was arbitrarily chosen for C_3H_8 because of its middle position among the curves. In order to avoid unnecessary errors, readings were taken only after the system had reached equilibrium. The time till equilibrium was determined by measuring the heat transferred to the calorimeters during a control run at small intervals of time. The heat flux was found to be constant in about 20 minutes. It was shown in chapter 3 that addition of O_2 to the fuel or air may increase the sooting rate as well as the temperature, of a flame. The effect on radiation of adding oxygen to the air was next studied. The fuel flow rate was kept constant at about 15.2 mg/sec., and the total air flow at 300 mg/sec. Addition of oxygen to the fuel seemed promising. As it was preferable that this should not be done through the fuel stream, it was introduced through a separate passage as shown in Fig. (11). The radiation profiles are shown in Fig. (20).

Addition of small amounts of oxygen to fuel produced a relatively larger increase in window one than when oxygen was added to the air. However

the increase in window two was more important when oxygen was added to the air. A minimum was observed at windows one and two when 8.9 mg/sec oxygen was added to the fuel, which was sometimes accompanied by a low sound. In the case of windows 3 and 4, the radiation was always reduced, although to a much greater extent when oxygen was added to the fuel. The total amount of soot produced in a flame is increased with addition of halogenated hydrocarbons (see chapter 3). Their efficiency depends on the amount and type of halogenated atoms attached to the hydrocarbon. Rather than study the effect of hydrocarbons containing different halogen atoms, it was decided to vary the chlorine atoms in one fuel and to study its effects on the total heat transfer, radiation, temperature at the centre of the flame and the mean temperature across the flame. Numerous additives (CH_2Cl_2,$CHCl_3$, CCl_4, etc.) were added by diverting part of the fuel flow into two galss bubblers in series, as was described in the previous section. The concentration of additive was determined using the method outlined in Appendix (I). Since CCl_4 on decomposition produces chlorine it would reflect to some extent the effect of addition of the pure halogen.

It is possible to observe in Fig. (21) the general decrease in temperature with additive. The variation of heat transfer and radiation with additive indicated a general shift of the maximum towards the burner. Total heat transfer from the four calorimeters and sum of the radiation from the four windows was highest with addition of CCl_4 by about 10 per cent more than the control run. In this set of experiments, the fifth unit was absent and the results were expected to be useful only in defining the order of effectiveness of the different additives.

On the basis of these observations it was decided to study the effect of adding two levels of concentration of CCl_4, namely .029 and .054 mole/hour. In both cases a slight increase in radiation was observed in window one and

and to a lesser extent in window two. It was therefore concluded that the lower concentration of CCl_4 should be used since the higher concentration produced only a negligibly higher emission in both windows. These results will not be shown here as they have been repeated in Fig. (22).

The cold wall temperature, less than 350 K, was a nuisance as it caused the by-products of halogenated additives to condense and pollute the air passage. In time the flame became very unstable. The drain at the bottom of the burner was quickly blocked by a greenish-blue viscous liquid. When extinguished, the flame was difficult or impossible to relight except when the system had been cleaned and thoroughly dried. The deposit was noxious and the process of cleaning it was repetitive and time-consuming The extinction was caused by saturation of air and fuel flow with condensate, (see for example Creitz[138]). The condensate in the fuel flow was collected in the glass T-shaped piece which acted as the fuel inlet, (Fig. 11). Having observed the separate effects of addition of CCl_4 and O_2. The effect of adding CCl_4 to the fuel and varying the oxygen to the air was next studied. The results obtained are plotted in Fig. 22. Comparing Figs. 20 and 22, it is possible to observe a slight increase in radiation at window 1. when small amounts of CCl_4 were added to the fuel. The change in radiation is linear rather than curved. Radiation at window 2. decreased with concentration of CCl_4. The change in radiation at windows 3 and 4 with addition of oxygen to the air was less steep in the presence of CCl_4. It is interesting that radiation at windows 3 and 4 increased when the higher concentration of additive was introduced. There was on the whole no overall beneficial effect, which indicated that addition of oxygen in the absence of additive was more useful.

The last set of experiments were intended to verify the extent to which the air preheat affected radiation and heat output in such a system. Before undertaking these experiments it was necessary to determine the most

suitable position for the thermocouple, which was connected to a temperature controller by which the air preheat temperature was kept at the desired level. It was initially expected that a few millimetres above theair distributor would be correct. A copper-Constantin thermocouple was used to measure the temperature at this position, at various intervals of time after the flame had been lit. The results were plotted in Fig. (23) and show that in 20 minutes the temperature was about 307 K but appeared to increase only to a small extent above this value. It was therefore decided that this was not a suitable position and that a better indication of preheat temperature could be obtained by placing the temperature indication at the bottom of the burner, i.e. the tip of the thermocouple was below the air inlet.

Radiation from window one was increased to a greater extent and reached a maximum value at 393 K as is shown in Fig. (24). However the general increase in radiation was not drastic. It appeared that due to the present flame geometry, preheating at temperatures greater than 423 K would not enhance radiation to an important degree, although it may upset the increase as was observed at window no. 4. One may therefore conclude that the general effect of additives is to increase the radiation at windows one and two to different extents, except in the case of air preheat where the increase persists up to window 4.

As a result of this exploratory study, the level of fuel and the total air input of the control run was fixed at 15.2 and 300 mg./sec respectively. Experimental conditions were varied as follows:

1) Control run, i.e. absence of additives.
2) Addition of two levels of oxygen to the air, namely 22.2 mg/sec and 44.4 mg/sec respectively.
3) Addition of four levels of oxygen to the fuel, 4.4, 8.9, 13.3 and

16.9 mg/sec. The total volume flow in (2) and (3) was kept constant by reducing the input volume flow of air.

4) One level of CCl_4 namely, .029 mole/h.

5) Preheating the air stream to 3 levels, namely 343, 393 and 443 K.

Finally, the symbols used in the diagrams to define these experimental conditions are shown in table 5.

CHAPTER 6

DISCUSSION OF RESULTS

6.1 Soot Composition

This section deals firstly with relevant work, discussed in previous chapters, which is presented here in empirical form where this has not been done by the authors. The purpose of this exercise is hopefully to provide a guide in correlating the author's own data, which will be dealt with in the later part of the section.

6.1.1 Formulation of relevant work

D'Alessio et al[6] collected soot from a flat premixed CH_4-O_2 flame at various heights from the burner on cooled and uncooled quartz plates. They had observed that a linear relationship represented the change of g_λ with C/H ratio. Table (6) shows within the range $1.95 < C/H < 3.61$, the values of temperature, and dispersion exponents g_λ at different heights, which were extracted from various curves provided by the authors. It was possible to obtain by the least square method up to a height of 17.5 mm the following correlations:

$$C/H = -.00785\ T + 15.12 \qquad 6.1$$

$$g_\lambda = \frac{2.42772}{C/H} + 0.75061 \qquad 6.2$$

The average per cent deviation, in both cases, is less than 2 per cent. Above this height g_λ remained relatively unaltered with decrease in hydrogen content of the mass of soot and absorbed material, collected on a cooled probe, although this content was still high.

Millikan[31] showed graphically that g_m for a number of soots was proportional to 1/(C/H) ratio in the range 0.33-1.0 μm. This data has been represented on page (18) of this thesis as:

$$g_m = \frac{2.45}{C/H} + 0.66 \qquad 2.18$$

The close agreement between equations 6.2 and 2.18 is interesting considering that the first equation represents a change of g_λ with C/H in one flame and in one wavelength in the visible, while the second equation represents the effect of soot composition this time using a number of deposits from different flames and over a wide range of wavelengths including part of the infrared. Each point in Millikan's graph from which the equation was deduced was obtained in two steps. A value of g_m for a deposit was first determined by using the extinction method outlined on page 25 for a change between $0.33 < \lambda < 1$ μm. This value was then plotted against the inverse of the corresponding C/H ratio.

A point requiring clarification is why the two different experimental procedure followed by Millikan and D'Alessio et al, on the basis of which equations 2-18 and 6.2 respectively were deduced here, give values of constants which are very close to each other, even though the approach followed by Millikan obscured the influence of volatiles on g_λ which was reported by D'Alessio et al. The volatiles concerned were polycyclic aromatic hydrocarbons which have a boiling point of less than 673 K. This point is important considering that g_λ was approximately constant, in D'Alessio et al's experiment while the flame material had a composition of $\geq C_{4.3}H$. Millikan's study of g_m included soot which varied in composition up to $C_{10}H$ It had previously been shown that there was no correlation between k_m and composition of samples of high carbon content of nearly 99.5 per cent[30]. This point will be taken up later in this section.

In chapter two the findings of Hottel and Broughton[51] amongst others were reviewed. These authors recommended a constant value of 1.39 for the dispersion exponent g_m in the visible and another ~1.0 for the infrared region of the spectrum. These values were obtained from the data of various investigators on transmissivity of soot layers from different sources

and flames against wavelength. The position of collection and composition of the sootswere not defined and the soot appears to have been collected on uncooled glass plates and therefore dehydrogenation of the flame material during collection cannot be ruled out. The authors also showed that g_m may vary for one type of fuel with position in the flame.

At this stage it would be proper to refer back to the work of Dalzell and Sarofim[42] discussed in Chapter 2, p. 44. These authors almost covered the range of the dispersion exponent (g_m) determined experimentally by only considering in theoretical models the change in the number of free (or conduction) electrons per unit volume F_c. This led them to conclude that the soot composition and to a lesser extent the molecular structure, were responsible for the different values of the refracture index and dispersion exponents of soot. Also an increase in F_c would lead to an increase in k_λ. This seems to be true up to a certain point. The spectral dispersion exponent g_λ was shown to acquire a constant value in some cases[6] [9] though the soot hydrogen content was still high $C_{4.3}H$[6]. The models[42] therefore do not appear to account for this stage. In this region and beyond it,

$$\not\equiv -\partial \ell n k_\lambda / \partial \ell n_\lambda$$

Since k_λ may only vary as soot dehydrogenates further. In the region where g_λ tends to be constant, its meaning is somewhat obscured, as it is no longer related to the compositions of the soot and the spectral absorption coefficient and refractive under are nearly totally dependent on soot structure. The different structures would be expected to give different values of k_λ as a result of the different conductivity of the soot deposits in question.

Unfortunately, we have to qualify the previous comments, which concern the region which $g_\lambda \simeq$ const., to the visible region of the spectrum.

No similar study of g_λ against height and compositions appears to have been made.One is therefore unable to predict for sure, if g_λ will eventually tend to a constant value, considering its known dependence on wavelength in this region (see chapter 2).

If we conclude from what has been said that g_λ is a measure of heavy hydrocarbon gas phase emitters, at least in the visible, then it is easy to understand why the emission coefficient of a number of soots which contained about 99.5 per cent carbon, did not correlate with composition. This would be equivalent to a composition of about $C_{8.3}H$ assuming that the rest of thecomposition was all hydrogen. It is perhaps easier to accept that at such high C/H ratios, the mean factor which determines the value of m is the way microstructure develops with temperature, than at lower values such as $C_{4.3}H$. It is unfortunate that the change of m and hence k_λ has not been studied in the regions where $g_\lambda \simeq$ const., as this would have provided indirect information on the extent of growth and ordering of the graphitic layers within a soot particle or agglomerate.

Finally referring once more to the work of Hottel and Broughton[51], it would appear that a constant dispersion exponent for the visible regions as was recommended by them, is representative of the region where g_λ remains approximately constant. Bonne and Wagner[9] and Dalessio et al[6] obtained assymptotic values of $g_\lambda \simeq 1.50$ and 1.42 respectively while collecting the soot on a cold plate. It is attractive to recommend a value of of g = 1.46, to represent approximately the visible, which bounded by the two extremes of gas stability i.e. acetylene and methene.

6.1.2 Chemical Analysis of Soot

In this work the composition of soot was determined by an elemental

analyser Model 1102, made by Carlo ERBA, Milan. The apparatus could analyse for C,H,N and O. Analysis of oxygen could be carried out through a separate channel. This meant that two samples were required to switch rapidly from one type of anlaysis to the other if the amount of oxygen had to be determined. In effect this was not required as the percentage of oxygen was negligible in this case.

The sample holder accommodated samples (0 - 20). The 0 hole was usually aligned above the free space on a base plate which was just below it and through which the sample dropped into a tubular vertical furnace. Two standard smaples of cyclohenxanone - 2.4 dinitrophenylhydrazone supplied by the manufactures were then placed in holes no. 1 and 2. The two following holes were left empty to ensure that sufficient time would have elapsed before the experimental samples were introduce and in this way avoid their being contaminated by the standards, which have a relatively high hydrogen content. The remaining holes (except the last) were used for the experimental samples. The last experimental sample was always followed by one standard sample of analar acido-benzoic acid. This served as a double check and to provide information on the effect of one sample on the other.

The flame material collected from windows 1 to 3 had, prior to analysis been extracted with chloroform and therefore the percentage by weight of the carbon in the soot was 90%. Under such conditions it was advisable to switch over the sensitivity of the CO_2 to that of H_2O and vice versa manually during analysis as an electronic integrator was not available. About ten minutes were required for each sample to be analysed, during which the sample holder rotated to align the next sample hole above the hole in the base disc. It is expected that under optimum conditions, i.e. homogeneity of samples, operating conditions, etc., the error would be less than $\pm$ 0.3%.

a) Quantitative Calculation of C, H

As no suitable integrator was available, sample peak areas were measured using a planimetre. The response factor for each element was calculated as follows:

$$K_e = \frac{\text{Percentage of element in theoretical standard} \times W_s}{A_s - A_b}$$

$$\text{Percentage e in sample} = \frac{K_e(A_s - A_b)}{W_e}$$

where e = element to be determined (i.e. C or H).

W_s = standard weight in mg.

W_e = sample weight in mg.

A_s = area of standard sq. mm

A_b = area of blank sq. mm

b) Evaluation of analytical procedure

In order to evaluate the analytical procedure seven samples of Cyclohexanone- 2.4 dinitrophenylhydrazone plus three standard samples of Acido-benzoicacid, also of analytical purity were analysed in one run. The response factor for the batch was calculated using the data of the second sample. This procedure was also followed when C/H ratio of the insoluble fraction had to be determined.

To test if the sample mean of 6 samples (the second was excluded) of cyclohexanone- 2.4 dinitrophenthydrazone was statistically equivalent to its standard value, μ determined from its chemical compositions the student analysis was used: t was calculated as:

$$t = (\mu - \bar{x}) \frac{S_x}{\sqrt{n}}$$

The results were of desired quality, at 99 per cent probability level, i.e $\mu = 0.868 \pm .003$, which indicated a high degree of precision, although the error on a single analysis was not small. This test was not repeated in the cases of acido-benzoic-acid on the basis that the number of samples were only three and since the deviation from the arithmetic mean, i.e. $\overline{X}-X/\overline{X}$ was slightly less than in the case of the first standard. However, it should be pointed out that this does not represent the accuracy of C/H ratio of the experimental samples.

c) Sample Preparation

The purpose of this section is to discuss the effect of the additives on the composition, i.e. C/H of the particles in the soot mass, and not the composition of the emitting mass, i.e. solids and high molecular weight compounds. Soot collected on a cold probe in some regions of the flame especially in the region of particle formation and growth, is coated with high-molecular-weight compounds. These have been known to contain large amounts of polycyclic aromatic hydrocarbons.

Ray and Long[37] treated soot collected from the exhaust of a number of flames with chloroform ($CHCl_3$) and n-pentane according to the scheme shown in Fig.(3). They found that polycylic aromatic hydrocarbons accounted for the major part of the n-pentane soluble material. These compounds may represent up to 2/3 of the chloroform soluble material, the amount, however, is shown to vary under different conditions[33,35,112]. It is, therefore, better to refer in general to heavy hydrocarbon emitters rather than to a specific group of compounds, unless they happen to be the only major species of importance in the spectral range being investigated.

Another point of interest is, that soot collected on a cold probe at the exhaust of a flame will have associated with it heavy hydrocarbon molecules. It is also possible that soot particles in the flame will also

have some associated compounds. If this be true, one would imagine that the amount will depend on their concentration neighbouring the particle, which may be governed by a sort of dynamic equilibrium situation. It is therefore reasonable to expect that the sample wihch is to be treated with $CHC\ell_3$ or even after treatment does not represent the nature of the soot in the flame. The extent of the deviation in each case may remain unknown until the nature of the soot in "situ" is known. An attempt will be made at the end of the following section to partly resove this point.

At this stage we may question the general use of the word soot to define material collected on cold probe or via a suction probe, for they will invariably contain, to various extents, polymeric materials which exist in the flame gas. In the region where polymeric materials do not exist in important concentrations, there is no controversy over the definition. The word soot, however, was used to name the flame material collected from all four windows. It should however, be noted that polymeric material deposited with the soot collected from windows 1 and 2 under all experimental conditions and in a number of cases from window 3. A possible suggestion is to define in such cases the flame material as soot (+p) where p stands for the polymeric materials. In this way soot would only be used when referring to the particles produced as a result of incomplete combustion of a hydrocarbon in the gas phase. Having discussed this somewhat important point in some detail, the experimental procedure will next be described.

After the soot had been collected in the present experiments, the high molecular weight compounds adsorbed were extracted with $CHCl_3$. This was achieved as follows:

Eight volumes of $CHCl_3$ were added to about one volume of soot in a standard V-shaped centrifugal tube. The insoluble fraction of soot was separated from the soluble in $CHCl_3$ by centrifugation. The liquid portion was poured out rapidly to prevent any loss of solid. These steps

were repeated a number of times, three times was sufficient in general, until the colour imparted by the soot to the $CHCl_3$ ceased to appear. When a number of such samples were ready the excess of $CHCl_3$ was boiled off in a water bath kept at around 373°K for a few minutes until the samples looked dry upon inspection. This was preferred to boiling off the excess at some distance above a flame, as there was the danger of losing the sample while the $CHCl_3$ was bubbling off. Another drawback was the possible dehydrogenation of the soot in the process of removing $CHCl_3$.

The tubes carrying the insoluble soot fraction which were practically free of $CHCl_3$ were then stood in a specially designed perspex holder and placed into a vacuum desicator containing silica gel in its base. The dessicator was evacuated for a few hours and the samples were left overnight under vacuum to ensure that they would contain minimum moisture when they are weighted. It is not known however, if this procedure would have removed any residual choloroform, which may have contained dissolved in it lower polycyclic aromatic hydrocarbons[164]. The soot was weighted in small special tin containers (4 x 4 mm.) in a 'Sartorius' electronic microbalance model 4125. The weight of the insoluble fraction prepared for analysis varied between 0.4 - 1mg. Each tin cup was folded, closed and flattened carefully, using a small spatula and a pair of tweezers. The sample was reweighted to ensure that soot was not lost during the process.

Each sample of soot in its tin container was introduced into a small dry and labelled glass tube,which had previously been cleaned with alcohol. The samples were dried once more under vacuum and kept in the dessicator. The vacuum was only released when the samples were to be introduced into the sample holder which was housed in the H,C,N analyser. It was hoped that if these laborious steps were followed for each batch of samples, and the different stages, e.g. centrifugation, weighing, etc., were performed within approximately equal times, the operator error during the preparation

of the sample would be reduced, therefore minimising one of the main sources of inaccuracy of the results.

It is worth noting that addition of oxygen diminished the intensity of the yellow colour imparted by the material extracted from soot collected from window no. 3 or made it disappear altogether. The soot extract from window 4 was found to be colourless in a number of experiments, and the composition of soot collected from window 4 is that of untreated soot. See table (4) the colours reported in the table are those visually observed when the V-shaped centrifugal tube was held against the sunlight. However when the extract was collected in a small beaker it had a dirty brown colour.

6.1.3 Dependence of the C/H ratio on the mean effective temperature

The experimetnal data of D'Alessio et al[6] presented in section 6.1.1 indicates that a linear relationship exists between temperature and C/H ratio. This is in agreement with results obtained in this thesis. The results corresponding to the insoluble fraction of soot collected in window (1), using apparatus described in chapter 5, are plotted in Fig. (25a) against the mean effective temperature of the soot, $\overline{T}_t$ (Appendix II). This represents the mean temperature across the flame of thickness (t) rather than across the combustor. The least square method was used to obtain the best straight line for the twenty five samples analysed in the case of window 1. This resulted in the following equation:

$$C/H = 0.01355\ \overline{T}_t - 9.6990 \qquad 6.3$$

which is expected to be only valid within the experimental range of T $\overline{T}_t$ and C/H studied. The above equation appears to represent the experimental data reasonably well giving a value of the correlation coefficient (r) = 0.57 and is significant at 5 per cent level. The straight line in the above figure was drawn using the predicted values of the C/H

ratios The number of readings at each experiment varied from 1 to 5. These correspond in Fig. (25a) to the points plotted vertically at each temperature.

The C/H ratio of the soot collected under various conditions in window no. 2 were also plotted in Fig. (25a). as circles and seem to be well represented by the above equation. This indicates that it is possible to represent the change in both regions by nearly the same constants, which is interesting considering that the sampling positions in windows (1) and (2) are 70 mm apart, involving a residence time in the range of 0.07 seconds (see Appendix II). The apparent lack of a residence time effect in this flame is further evidence of the direct effect of $\overline{T}_t$ on the rate of formation of soot.

In the case of window 4, it may be shown from Fig. (25b) that there is less interdependence between C/H ratio and T_{max}. This is indicated by the value of the correlation coefficient i.e. r'= -0.52. This is understandable considering that it corresponds to a zone in which the soot yield is in decline and in which the role of molecular oxygen may be important. The C/H ratio of the insoluble fraction of soot collected from window no. 3 was also plotted on the same graph for comparison. It is possible that the scatter in the results obtained above could be reduced had the residence time been considered together with the temperature.

A least square fit to the data at window 4 produced the following equation:

$$C/H = -0.01153T_{max} + 18.52 \qquad 6.4$$

It is interesting to point out that the ratio of the constants in this equation and those in equation 6.1 which represents D'Alessio et al's[6] data is close to 1.35. This value represents the sum average of the ratios . However, the significance of this common factor is unknown and may have emerged by chance.

The negative relationship obtained from D'Alessio et al's data (equation 6.1) represents a region above the reaction zone of a flat premixed flame in which the oxygen concentration was consumed and in which the stable gaseous produces which had been analysed were relatively constant. The only important variants were the particle number concentration (particles/cm^3sec), which increased steeply and the polycyclic and the aromatic hydrocarbons concentration which was in constant decrease. The former reached a maximum near the end of the region in which this equation is valid. However it must be noted that in D'Alessio et al's experiments some pyrolysis of the input fuel (CH_4) occurred up to a height of 10 mm, which accounts for part of the increase in soot weight or particle number concentration, the rest being accounted for by the contribution of polycyclic aromatic hydrocarbons as well as other hydrocarbons. Equation 6.4, however, represents a region where the concentration of large molecules is unimportant or probably non-existant.

6.1.4 Effect of additives

The curve representing the various additives are plotted in Fig. 26. The lines or curves are drawn through the arithmetic mean values. It is possible to observe in Fig. 26a a linear variation of composition when oxygen was added to the fuel. When the oxygen was added to the air the change took the form of a curve. The change observed here results from the increase in temperature produced by the additives. However at window 4 oxygen first produced an increase in C/H ratio followed by a decrease Fig. 26b. The change was more abrupt when the oxygen was added to the fuel. The effect of air preheat on the composition analysed, it is not possible to be conclusive about the actual trend. However, judging from scatter of the data in Fig. 26a and b there seems to be no important effect.

The same can be said of the effect of additives on the average particle size of the primary particles these ranged around .04μm (see chapter 4)

The relatively high molecular formula of soot observed here, in general $\geq C_7H$ and the apparent increase of soot C/H ratio with addition of oxygen in windows (1) and (2), together with the insignificant change in average particle size (see chapter 4), presented evidence that the effect of the additive may be relegated to a temperature effect. Attempting to explain the high C/H ratio in such regions where soot continues to form, suggests a role played by reactive hydrocarbons of relativey high C/H ratio, possibly polyacetylenes as was suggested[99]. However one cannot discount the possibility that polycyclic aromatic hydrocarbons may contribute to the surface growth of these particles. This was found to be of the order of 2 to 3 per cent in one case[65].

Much lower C/H ratios of soot have been reported elsewhere[65] for the case of a flat CH_4/O_2 atmospheric flame. After the polycyclic aromatic hydrocarbons had been removed by heating soot samples at 450°C, a value of 2.94 was recorded for the post-flame region ($\sim$7 mm above the burner mouth) and 4.17 (at about 20 mm) which corresponded to the height at which total solid material tended to become constant. The effective particle diameter (determined optically) increased from about .035 μm at 7 mm. to 0.16 μm at this height indicating the presence of particle agglomerates.

This is interesting when we compare these values with the C/H ratio of the flame material, which varied from 3.82 to 4.02 up to window (3) in the control experiment in this thesis. To explain the slow increase in C/H with height. D'Alessio et al[65] proposed that surface growth of primary particles was provided by compounds with a low C/H ratio such as 'reactive' polycyclic aromatic hydrocarbons, followed by rapid dehydrogenation. Other factors to which they attributed their low C/H ratio were the increasing rate of soot formation and the fact that the temperature

was relatively low at this fuel/oxygen ratio. Observation of particles formed in this CH_4/O_2 flame by transmission and direct electron microscopy would have provided a useful insight into the mechanism of formation.

A last point to be discussed is the relationship between the insoluble fraction in chloroform and soot particles in the flame. Referring to Figs. (26a-c) we may immediately observe that, there is a certain degree of scatter in the values of the C/H ratio under one experimental condition. This is generally less than ± 15 per cent of the average value. The scatter may be due to experimental error or to the inhomogenity of the sample realting to one position. There is also an obvious overlapping of the composition values, in windows 1 and 4 for the experiment. Considering the error referred to above, plus the fact that the soot at window 4 must have been formed within the blue reaction zone i.e. windows 1 and 2, would indicate, that these particles may be the same. This would inmean that the composition of the insoluble fraction changed only slightly as it travelled within the flame.

Conclusion

In the first part of this section we showed that the linear relatinship between g_λ and C/H ratio obtained from D'Alessio et al's[6] data was confirmed by Millikan's[31] results, which were obtained by a different approach. Another interesting aspect brought out here was that the composition of the insoluble fraction of soot was to some extent linearly dependent on the temperature ($\overline{T}_t$) in the region where their reaction zone existed. The correlation with T_{max} was negative in the region where the amount of soot was decreasing, that is in window 4 and was of the same order as that observed in window 1.

The effect of additives on composition is not in general considerable. This would indicate that the change in composition of soot particles (C/H ratio

$\geq$7) in the flame does not have an important effect on radiation. On the other hand, the concentration of emitting hydrocarbon molecules in the gas phase in the flame would be expected to influence radiation as a result of a change in composition. It is possible in this way to attribute the optical properties of soot particles in a flame mainly to the density and microstructural arrangement of the hexagonal platelets inside each particle. An exception is when the C/H ratio of the solid particles is unusually low as was observed in D'Alessio et al's[65] case. In the optical properties and hence the extinction coefficient are expected to vary with hydrogen content of the soot. Finally, it is possible that the composition of flame material which is insoluble in $CHCl_3$, is very close to that of the particles in the flame.

6.2 Soot yield

Figs. 27-29 represent the soot yield obtained from different levels along the height of the flame using a cooled quartz probe (see chapter 4). Each value is the average of ten samples and is bound on either sides by one standard deviation.. The average amount of soot up to window 4 is also represented in Fig. 29) so as to reflect the overall particle emission up to this stage. The latter was obtained by integration using the following expression:

$$\bar{c}_{av} = \frac{1}{z} \int_0^z \bar{c} dz \qquad 8.6$$

where z = height, which equals 245 mm up to the centre of the fourth window

6.2.1 Effects of Oxygen

The results obtained from the measurements show that addition of relatively small amounts of oxygen to the fuel produced comparatively greater

changes in soot yield and maximum temperature than when comparative amounts were added to the air side. This observation may be explained if it is taken into account that the yield of soot at a given height is the product of two competing reactions: i) soot formation and ii) soot oxidation. Soot is mainly formed in a diffusion flame in a relatively thin boundary that runs parallel to the blue-reaction zone, mainly as a result of the pure pyrolysis of the fuel, (see section 6.2.4). It is therefore to be expected that an increase in temperature across the pyrolysis zone would result in a greater soot yield.

This is due to an increase in the rate of build-up of a number of larger molecules via smaller molecules, hence of certain molecules responsible for the nucleation and growth of a soot particle. Addition of oxygen, even a small percentage of the stoichiometric requirements, to the fuel or air would be expected to form OH, O and other radicals. This would result in a higher rate of combustion and hence heat released in this way would increase the temperature in the blue reaction zone as well as across the pyrolysis zone. This is borne out by the temperature profiles in Figs. 30 and 31.

Due to the presence of these oxidising species (O_2,OH,O) the soot oxidation of large molecules of species of importance during the build-up, occurs more rapidly by reactions such as the following:

$$C_nH_m + OH \rightarrow H_2O + C_nH_{m-1}$$

However, the increase in temperature is expected to boost the rate of occurence of successive steps leading to the formation of the soot precursors.

The amount of hydrogen formed during the process of formation and growth of a soot particle and of carbon monoxide might also encourage the destruction of OH radical by reactions such as:

$$H_2 + OH \rightarrow H_2O + H$$

$$CO + OH \rightarrow CO_2 + H$$

These reactions have been reported to occur in the cooler part of the oxidation zone of a premixed C_2H_2/O_2 flame[87]. Such reactions would be expected to stop the penetration of OH inside the carbon-forming zone of a diffusion flame and provide for H_2O and CO_2 which are believed to be the soot-oxidising agents[165,132,166]. The effectiveness of OH and O radical has been discussed elsewhere[167].

A minimum was observed in window 1 when oxygen was added to the fuel Fig. 27a. This may have been caused by diffusion of sufficient oxygen into the soot-forming zone before the increase in temperature was effective At higher oxygen concentrations the pyrolysis effect predominated over the oxidation effect until a maximum was reached and the dominance was once more reversed. At window 2 there was no minimum however the curve went through what appeared as an inflection point Fig. 27a. This indicated the general domiance of pyrolysis over oxidation.

At windows 3 and 4, a minimum was once more produced at small oxygen concentrations and was probably caused by the amount of oxygen diffusing into the soot zone Fig. 27b and c. However the dip was more obvious than in window 1. At window 4 the curve appeared to become horizontal with increase in oxygen added to the fuel, this indicated that the oxidation process at this level was slowing down even though the amount of oxygen might have been sufficient Fig. 27d. This phenomenon was caused by a reduction in temperature at window 4 with addition of oxygen, which is borne out by Figs. 33a and b. The decrease in temperature is also an indication of the flame shortening. Finally, similar reasoning may be used to account for the affect of oxygen added to the air on yield of soot, except for the factor of oxygen presence inside the soot-forming region which is not involved.

It is also observed that as the flame shrinks, with addition of oxygen, the outside diameter of the flame decreases while its hollow centre

shrinks, i.e. the thickness of soot cylinder increases. The maximum temperatures in Figs. (30) and (31), correspond to that of the reaction zone It should be noted that it is appropriate to picture the soot-forming region as a hollow cylinder only as regards narrow strips of the flame.

It may be deduced from these figures that the extent to which the flame shrinks, indicated by the distance between the two maxima, is greater when oxygen is added to the fuel than when an equal amount is added to the air. This is understandable considering that in the former case an additional factor comes into play, namely the physical presence of molecular oxygen and its products of decomposition. This increases reaction rate as a result of fuel degradation.

The effect of the size of the soot-free volume inside the flame on the velocity of the unburnt fuel inside the hollow may also be of some importance. However in this context the fuel may be considered to be any small gaseous intermediate product that is convertible to soot. The height inside the flame at which C_3H_8 almost completely disappears has not been determined

6.2.2 Effects of Preheating the Air

This is best understood by referring to Fig. 28a. A decrease in soot yield occurs as the air is preheated, but this trend was reversed at temperatures above 350 K. The progressively greater increase with height (position of window) as the temperature was increased above 350 K seemed to follow the increase in temperature profile (Figs. 32) and (33). This was true except for the yield at window no. 2. When the air was preheated to 373 K, a sudden jump in the yield occurred. The magnitude of the deviation indicates that there is a high probability that this trend is real. The sharp increase with temperature of air preheat can once more be explained on the basis of the predominant action of the pyrolysis re-

actions as against those of oxidation. However the closeness of the temperature profiles in Fig. 31c suggests that aerodynamic factors rather than thermal were responsible, that is the time during which cracking occurred before mixing was prolonged.

There seemed to be no direct explanation for the decrease of soot with air preheat up to 330 K except as a consequence of the increase in velocity of air and fuel which reduced the time for cracking before mixing set in. The slower increase of soot which occurred when the air was heated to higher temperatures resulted from the change in the aerodynamics (mixing) pattern which influences the extent of soot oxidation. However the observed increase in temperature at windows 3 and 4 indicated its influence on the soot formation process. The effect of air temperature on the soot formed up to window no. 4 is represented in Fig. 29b for comparison.

6.2.3 Effects of CCl_4

Halogenated hydrocarbons have been studied in a number of publications which are reviewed in Chapter 3 in some detail. The experimental results are plotted in Fig. (28b) together with the control experiment (no. 1). Although the amount added was very small, it resulted in an obvious increase in yield up to window no. 3. The decrease that occurred after that was also related to the decrease in temperature profile. Addition of CCl_4 is expected to reduce the rate of soot oxidation and therefore result in more solid particle pollution. The mechanism by which CCl_4 is expected to act during combustion has been detailed in Chapter 3 and will therefore not be repeated here.

Miller* reported that in a low pressure C_2H_2/O_2 diffusion flame,

*See comment ref. 96.

addition of up to 0.5 per cent by vol. CCl_4 made a non-sooty flame turn sooty. The concentration of positive ions such as $C_3H_3^+$, $C_4H_3^+$ and $C_{12}H_5^+$ were greatly increased. A similar effect was obtained by increasing fuel richness elsewhere[93]. There is therefore no doubt that both occur simultaneously. The reverse can be brought about by electron or metal seeding, as detailed in Chapter 3. Before translating the effect of the additive in terms of an ionic mechanism we should consider two conflicting points of view related to chemical inhibitors by halogenated organic compounds.

It was suggested[138] that gases which capture electrons such as H_2O, N_2 and halogenated organic compounds, have a strong influence on the process of combustion. Only those which have a strong negative electron affinity can act as inhibitors, e.g OH^-, O^- and negative halogen ions. Recent evidence indicated that inhibition is mainly neutral rather than ionic. This could occur by removal of H, O, OH, etc.[168]. This would be a more likely explanation and would explain the soot-promoting efficiency of these additives when added in very small amounts on the basis of the type of halogen. The relationship between the soot inhibiting effect of hydrogen and the concentration profile of charged heavy hydrocarbons would, however, be interesting to know.

One would be inclined here to favour the dominance of chemical effect over the ionic. However until further evidence emerges from new work it is not possible to elaborate any further. Finally, it is interesting that addition of small amounts of CCl_4 produces as much soot as in the case of preheating the air to 420 K, (see Fig. 29b).

6.2.4 Relationship between soot weight and temperature

A plot of the soot weight against temperature showed that the following relationships stood for window 1 and 2 respectively:

$$\bar{c} = .1126\ \bar{T}_t - 123.7$$

$$\bar{c} = .2355\ \bar{T}_t - 256.4$$

These were obtained using the least square method and are highly significant at 95 per cent level, see Figs. 34a and b. At windows 3 and 4 there was very low correlation between soot weight and temperature, see Fig. 34c and d. The decrease of correlation with flame height within the bluee reaction zone is possibly connected with the relative decrease in amount of heavy hydrocarbons collected with the soot. Upon inspection of those two equations it became apparent that the rate of flame material collected at window 2 was about twice that at window 1. The net rate of particle formation, at any position in the flame, is dependent on the temperature and residence time of the different species which contribute to soot formation, as well as the extent of attack by H_2O and CO_2 (see discussion to follow).

A linear least square fit of the data in the form

$$\overline{c} = f(\text{residence time} \times \overline{T}_t)$$

produced a lower correlation than when the residence time was not considered. This may have resulted due to the fact, that the residence time calculated according to Appendix II, fails to take into account, the decrease in flame thickness that follows the addition of example oxygen. The reduction in such cases may reach up to 38 per cent of that in the control run.

One should consider, however, that the flame material which was collected at windows 1 and 2 is composed of soot plus polimeric material. The quantity used to correct the residence time in Appendix II should therefore give more weight to the effective flame temperature $\overline{T}_t$, since the zone formation of soot or precursors is somewhat removed from the blue reaction zone. One would therefore recommend the use of $\overline{T}_t + T_{max}/2$ rather than T_{max} in the correction factor. Finally, one would at this stage prefer to refrain from further contemplation of various possibilities due to the lack of necessary data and considering that it is likely that some other important

factor has been missed out.

Discussion

It is appropriate at this stage to analysis the various points of view concerning the oxidant of soot particles in diffusion flames. A review of the literature shows that there is some objection to considering the flame reaction inside the fuel zone of a diffusion flame as a purely thermal process. Traces of oxygen were detected at the lower part of a methane/air diffusion flame. The disappearance of methane at temperatures several hundred degrees below that at which methane decomposes was evidence that oxygen enhanced the pyrolysis process in that region[169]. The appearance of C_2 and CH bands on the fuel side of the main reaction zone where OH is minimal,[170] would indicate that decomposition is not purely thermal.

Further evidence, such as the presence of chemically-bound oxygen in the form of hydroxide and carbonyl groups in material extracted from soot by solvents, indicates that soot oxidation does not necessarily depend on diffusion of molecular oxygen into the soot zone, but that diffusion of O and OH radical is a reasonable substitute[40]. This would be in partial agreement with Bradley[171] who suggested that OH may diffuse into the fuel zone and contribute to its pyrolysis.

Experimental evidence has been presented by Tsybulevskii and Tesner Tesner[165,166] to the effect that no molecular oxygen exists inside the flame as long as a flame front exists. Spectroscopic observations in a flat C_2H_4/O_2 diffusion flame indicate that molecular oxygen, OH does not penetrate the soot boundary[25]e. Ibirricu and Gaydon[132] pointed out that some premixing may occur close to the burner edge in the region where C_2 and CH bands occur; their intensity will decrease with pressure. The occasional presence of molecular oxygen is also caused by the presence of a similar premixed region close to the cool edge of the flame.

The presence of chemically bound oxygen in soot extracts in not a precondition for the presence of species such as O_2, OH or O within the boundary of the soot zone. Since in the reports in question[40] soot was sampled at the exit of the flame, it is reasonable to expect that chemisorption of oxidising species would most likely occur at the top of the flame, in the region where the combustion front ceases to exist. There seems to be little to corroborate that OH or even molecular oxygen is involved to a great extent in hydrocarbon pyrolysis or soot oxidation, except in Region(2) where the flames front does not exist or under conditions of parasitic diffusion in the cold boundary surrounding the fuel port. The question that has yet to be resolved is, which species are then responsible for the oxidation of soot inside the blue reaction zone which will be called Region (1). It has been suggested that soot burn-up occurs at the soot surface or within the soot zone, by reaction with H_2O vapour and CO_2 which diffuse from the main reaction zone[165,132,166]. H_2 and CO formed will diffuse back to be reoxidised close to the oxygen side of the reaction zone. This will be the situation as long as the concentration of fuel or decomposition products can support the hypothetical wedge of combustion products, separating the two distinct zones. Molecular oxygen may only penetrate in the region where the blue reaction zone does not exist[165,166]. This is believed to occur when the CO concentration at the edge of the flame falls below a minimum value[165].

Lastly the role of oxygen and that of air according to Feugier[172] and Comerford[123] respectively would be compatible with both Ibirricu and Gaydon's[132] and Tsybulevskii and Tesner's[165,166] hypothesis only if we assume that their results apply to what has been referred to as Region (2). That this is the case can be deduced from a careful analysis of their discussions. The work of Lee, Thring and Beer[173] as well as Fennimore and Jones[174,175] also falls in this region.

Conclusion

It is reasonable to conclude that soot is mainly oxidised in the region where the flame front exists, by CO_2 and H_2O. However OH may be also effective at theinterface between soot and burned gases. On the other hand, in the Region (2) where oxygen penetrates and is present in sufficient amounts, hydroxyl radical formation is possible and may enhance the rate of oxidation of soot. The relatively high correlation of the hydrocarbon flame material with temperature, obtained by the author within the blue reaction, together with the evidence presented in this section, favour the hypothesis that the decomposition inside the fuel zone of a diffusion is mainly a thermal process.

6.3 Temperature

The method of obtaining the temperature profiles drawn in Figs. 30 to 33 and their reliability have been discussed in chapter 4. With each figure the corresponding control run (i.e. experiment one) was redrawn to provide reference for comparison.

6.3.1 Effects of oxygen

Addition of oxygen to fuel or air produced in windows one and two the same effect, namely i) an increase in maximum temperatures of the blue reaction zone, ii) these drew closer to the axis, which was an indication that the flame was getting thinner and iii) an increase in the value of the minimum around the axis. These effects occurred to varying extents depending on whether the oxygen was added to the fuel or air.

Comparing for example Figs. 30 and 31, it is possible to observe that addition of 16.9 mg/sec oxygen to the fuel increased the maximum flame

temperature by 250°C as against 135°C when 22.2 mg/sec oxygen was added to the air. The thinning of the flame as well as the rise in temperature at its axis occurred to a greater extent when oxygen was added to the fuel. These observations are also applicable to window number 2, see Figs. 31(a and b).

Temperatures at window number 3, Figs.32 (a and b) were more uniform and showed only one maximum. This corresponded to the region where oxygen diffused into the flame from the surrounding air and the reaction was distributed more evenly across the flame. At this level as well as at window number 4, Figs. 33(a and b) the temperature decreased with additive, which suggested that flame heights were reduced. At window number 4 the temperature profiles were flatter as they followed the rate of reaction.

6.3.2 Effects of Preheating

This did not have a marked effect on the temperatures at windows number 1 and 2 except for a small increase in the maximum temperatures, see Figs. 30c and 31c. However, the temperature increased progressively in windows 3 and 4 as may be seen in Figs. 32c and 33c. It is possible that pre-heating increased the rate of reaction at these levels by providing oxygen at a slightly higher temperature. It was however difficult to say if the flame was lengthened under these conditions. An attempt was made to measure the flame heights in all the flames studied in this thesis by attaching a transparent glass unit in place of the fifth calorimeter. This however failed due to rapid fogging of the glass due to soot deposition.

6.3.3 Effects of CCl_4

The profiles shown in Figs. 30d to 33d were in accord with the ex-

pected behaviour of this additive. The decrease in heat released reduced the mean temperature ($\overline{T}_t$) across the combustor by less than 10 per cent at window number 1. There was no obvious deposition of additive or its decomposition products on the thermocouple as was observed when higher concentrations were used during the preliminary investigations referred to in Chapter 5. It is therefore unlikely that the observed temperature reduction in window 1 has been influenced by this effect.

6.4 Flame Radiation

The experimetnal results shown in Figs. (20,22 and 24) were determined using the total radiation pyrometer described in a previous chapter, and represent the radiation of soot particles and emitting species distributed in a given volume of gas. The spectral range of measurements, that is 1-10μm, includes strong bands in which triatomic gases emit. Their importance for the total gas emission will be discussed in a later section.

6.4.1 Effects of Oxygen

By referring to Fig. 20 it is possible to grasp the effect of oxygen on total radiation when it is added either to fuel or air. A better overall effect was obtained when the oxygen was added to the air. A steeper increase in the value of radiation was obtained in window (1) when oxygen was added to the fuel. A maximum, rapidly followed by a minimum accurred in windows 1 and 2 when small amounts of oxygen were added to the fuel. This indicated that in this region the competition between pyrolysis and oxidation was very close. Whether this effect would have been reproduced had similarly small amounts of oxygen been added to the air has unfortunately not been tested.

At oxygen concentrations greater than 75 mg/sec* the increase in radiation at windows 1 and 2 of Fig. 2o may be traced to the increase in soot mass Fig. 27a. Although the overall temperature of the flame increased as is illustrated in the temperature profiles (Figs. 30 and 31), the effective radiation temperature generally decreased with oxygen addition due to the decrease of flame width which defines the size of the emitting envelope or emissivity. The effect of oxygen is illustrated in Fig. 35a for the case of the bulk temperature $\overline{T}$.

Decrease in radiation at windows number 3 and 4 appears from the evidence in Figs. 27b, 32 and 33 to have been caused mainly by a decrease in temperature and in some cases of soot mass. One may infer from Fig. 26b that the soot composition contributes in some cases to the decrease in radiation, however, the curves may be misleading (see section 6.1.4). To conclude, although addition of oxygen caused a decrease in mean temperature of the flame (across the combustion chamber), the increase in radiation may be due to the increase in soot formation which occurs at these conditions.

6.4.2 Effects of Air Preheat

The effect of preheating the air on infrared radiation from the diffusion flame is presented in Fig. (24). All the results show that under the given experimental conditions total radiation increased with preheating temperature. The increase in radiation at a preheat temperature less than 350K was mainly due to an increase in temperature sufficient to overcome the effect of decrease in soot on emissivity. At temperatures greater than 350 K both temperature Figs.(30 to 33)c and soot weight Fig. 28 contributed to increase in radiation. The highest increase in radiation occurred at window number 4. However at about 400 K this trend was reversed. Finally,

*Oxygen in air = 66.70 mg/sec.

although the change in flame shape and therefore its effect on flame emissivity could not be determined, the temperature increase which occurred in all cases was an influential factor.

6.4.3 Effects of CCl_4

This is shown in Fig. (22) and indicates that there is a slight increase at windows one and two when either 0.029 or .054 mole/hr CCl_4 was added to the fuel. At windows three and four a decrease of at least 10%. The relative increase in soot weight, (Fig. 28,b), did not compensate for the effect of the decrease in temperature at these positions, Figs (31 and 32)c.

CHAPTER 7

RADIATION CONVECTION AND TOTAL HEAT TRANSFER

This chapter is, in a sense, an extension of the previous one as it discusses the experimental results. The first three sections are mainly concerned with aspects of radiation such as the sources of radiation reaching the pyrometer and the emissivity. In section 7.4 a simplified model is presented which is tested with experimental data and discussed in the following section. Sections 7.6 and 7.7 deal with the effect of the additives on the convective and total heat transfer which will provide, with the radiation profile, a complete picture of the effects of these additives.

7.1 On the Radiation Reaching the Pyrometer

The measured flux of radiation corresponds to that coming from a surface diametrically opposite the pyrometer lens. A schematic representation of the pyrometer and window which transmits the flame radiant energy is shown in Fig. 16.

A point worth elaboration is the source of the radiation reaching the pyrometer. The surface (i.e. target) at 15 mm is composed of a brass annulus approximately 38 mm in diameter and a window 12 mm in diameter, which is the inner diameter of the brass annulus. Though the cylinder of radiation from the flame exists through a cross section 12 mm in diameter, the unobstructed path of radiation is in effect reduced by approximately 1 mm all round. During the design of the cap the protrusion (as a result of tightening the cap) of the 5/16 inch O.D. O-ring between the extension tube and cap was not fully taken into account, Fig.(14) This effect is, however, small and will be neglected. The radiation reaching the detector may therefore be represented as:

$$\text{Flux} = \frac{\pi}{4} d_1^2 E_b + \frac{\pi}{4}(d_2^2 - d_1^2)E_2 + Q_s$$

radiation from flame | radiation from brass annulus | stray radiation

where d_1 and d_2 are the inner and outer diameters of the annulus respectively. and E is its emissive power.

When the flame was alight, the calorimeters were only slightly warm. The heat lost to the atmosphere was greatly reduced by lagging the calorimeters with a half-inch layer of asbestos rope. The latter was completely covered by a blue tape, which served to keep it in position. The response of the pyrometer was negligibly small. One may therefore, with some degree of confidence, assume that all energy radiated by the target to the pyrometer is solely due to the flame; that is,

$$\text{Flux} = \frac{\pi}{4} d_1^2 E_b$$

7.2 Mean Total Emissivity

The emissivity of a luminous flame may be calculated from the ratio of the black body temperature T_b and the mean furnace temperature:

$$\varepsilon_T = \frac{T_b^4}{T^4} \qquad (7.1)$$

It has been shown in the previous section that the rate of energy received by the pyrometer is proportional to the equivalent black body temperature of the flame T_b. This means that values of T_b calculated from the calibration curves of the pyrometer provided by the manufacturers could be used without modification.

The temperature distribution across the water-cooled tube was not uniform, as may be observed from the profiles in Figs. 30 to 33. In measuring the effective mean furnace temperature which was used to calcu-

late the emissivity in equation 7.1, the mean of the local temperatures, each raised to the power of four, was used as shown below, rather than the mean temperature raised to the power of four $(\overline{T})^4$.

$$\overline{T^4} = \frac{1}{\pi R^2} \int_0^{\pi} \int_{r=0}^{r=R} \left[r\{g_1(r) + g_2(r)\} \right] dr d\theta$$

r and θ are cylindrical polar coordinates (see section 7.4) and g(r) represents T^4 in this case, where

$$g_1(r,\theta) = g_1(r) \qquad 0 < \theta < \pi$$

$$g_2(r,\theta) = g_2(r) \qquad \pi < \theta < 2\pi$$

Had $(\overline{T})^4$ been used, the total emissivity calculated by equation 7.1 would have been over-estimated. This was found, in the control experiment for the lowermost window, to be of the order of 10.

T_b^4 as measured by the pyrometer, however, includes both the flame emissionand the contribution from the furnace walls. In the work presented in this thesis, the walls were water-cooled and a thin layer of soot of variable thickness was deposited along most of its surface. The water-cooled walls may be considered black for practical purposes, i.e R = O. The absorption of the volume of warm gas along the sighting tube carrying the ArS_3 cap, and the absorption due to the small volume on the opposite side of the window being sighted, are believed to be negligible under these conditions, and ε_T may be assumed to be due only to the flame.

7.3 An Effective Gas Emissivity

As shown in chapter 2, the emissivity may be represented as follows:

$$\varepsilon_T = 1 - (1 + B\overline{c}\ L\ T/C_2)^{-4} \qquad 2.16$$

The error involved in the case of soot is discussed in Appendix V. As no gas analysis was carried out, an estimate of the magnitude of the gas emmissivity equation had to be obtained. This was achieved by first writing equation 2.16 in the following linear form:

$$(1 - \varepsilon_T)^{-.25} - 1 = k_m \bar{c} L + (1 - \varepsilon_g)^{-.25} - 1 \qquad 7.2$$

and then fitting a least-square equation to the experimental data. k_m equals BT/c_2 in equation 2.16. An empirical value of the specific absorption coefficient k_m was obtained in each case from the slopes of the lines, while average gas emissivity ε_g was determined from the intercept with the ordinate. The values of k_m and ε_g corresponding to each window are summarised in Table (7) and the experimental points are plotted in Figs. 37.

In the case of windows 1 and 2, the flame thickness (t) rather than the tube diameter (D) was used as the mean beam length (L) in equation 7.2. This was because the soot in this region was confined within the boundary of the blue reaction zone. At windows 3 and 4, however, the tube diameter was used instead, since the particles were free to move in the horizontal direction. The values of the effective gas emissivity and specific absorption coefficient, defined as k'_m, were once more determined this time using the logarithmic form of emissivity, equation 2.15 or 2.17 in order to gauge the extent of deviation of the results, when the least-square method was used to determine the constants in both cases.

The ratio of the absorption coefficients k_m/k'_m determined by the two respective methods shows an increase as the value of k_m decreases (Table 7). Although the trend is by no means drastic, this point is worth noting when comparison is called for between the two. A point worth mentioning here is that the value of the gas emissivity was only negligibly altered.

k_m is a function of the refractive index of soot, which is itself dependent on soot composition. The value of $B/c_2 (\equiv k_m/T)$ is plotted in Fig. (36) against the average value of the C/H ratio in windows 1 and 4.

The first impression gained from looking at Figs. 36(a and b) is that a trend exists in the first case which is not visible in the second. In Fig. 36a, which corresponds to the data of window 1, B/C_2 increases with a decrease in mean C/H ratio, except in the case when the air was preheated to 443 K. This would appear to contradict what has been said in chapter 6 concerning the lack of correlation of k_m on soot composition when the C/H ratio is high.

Comparing Figs. 36(a and b), we can easily see that the average values of C/H ratios for the same experiment in most cases are very similar. The trend observed in Fig. 36a may thus have appeared by accident, thus indicating that there is no contradiction. Figs. 26 and 36 are quite similar, although the ordinates are different. In the first case, the composition is represented as a function of the amount of additive, whereas in the second, it is presented as a function of B/c_2. The difference is in fact artifical, since the effect of the additive may be considered in a terms of a temperature effect. Finally, the extent of of variation is shown in column 7 of Table 7. The variation in the value of B in windows 3 and 4 is small, which indicates that one value of B could, in effect, be used. A factor of about 2 is involved in the case of windows 1 and 2. This should be noted if a tentative value is to be recommended for general use.

7.4 Theoretical Model for the Emission from a Cloud of Soot Particles

It is possible in Fig. (a) to integrate over θ directly as emission

is considered independent of direction

Thus flux in is $Q = 2\pi rzE_\lambda$

and flux out is $Q + dQ = 2\pi\ (r + dr)\ z(E_\lambda\ + dE_\lambda)$

$$\simeq 2\pi z(rE_\lambda + E_\lambda\ dr + rdE_\lambda)$$

$$\therefore \quad dQ = 2\pi\ z\ d(rE_\lambda)$$

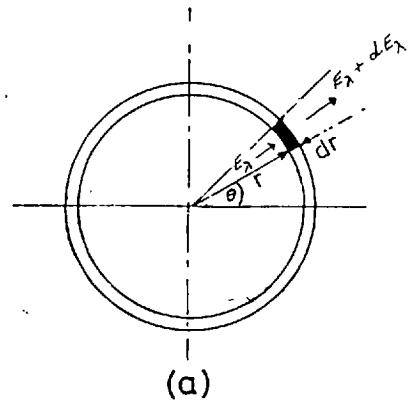

(a)

where z is the height of the slab.

$dQ = (\ -\ fKE_\lambda + 2KE_{b,\lambda})\ 2\pi rdrz$

where the f is a geometrical factor. The f and the 2 before $E_{b,\lambda}$ disappear in the optically thin limit and in division as in equation 7.10. They will therefore be neglected in what follows.

whence $$\frac{1}{r}\ \frac{d}{dr}(rE) = K(E_{b,\lambda} - E_\lambda) \qquad (7.3)$$

where $K = NC_{ab,\lambda}$

For small particles the monochromatic absorption coefficient may be represented, using equations 2-9 and 2-10, as:

$$K_{ab,\lambda} = -\frac{6\pi\overline{c}}{\lambda\rho} \cdot Im\left(\frac{m^2-1}{m^2+2}\right) = B\ \overline{c}/\lambda^{g_\lambda}$$

where B = const., and $g_\lambda \sim 1$ in the infrared.

If all the radiation at the wavelength concerned is due to soot, i.e. banded absorption is negligible, we may rewrite equation (7.3) as:

$$\frac{1}{r}\frac{d}{dr}(r.E_\lambda) = \frac{B\,\overline{c}}{\lambda}(E_{b,\lambda} - E_\lambda) \qquad (7.4)$$

Also:

$$\int_0^\infty \frac{1}{\lambda}\ E_{b,\lambda}\,d\lambda = T^5 \int_0^\infty \frac{c_1(\lambda T)^{-6}d(\lambda T)}{\exp(c_2/\lambda\ T)-1} = \gamma T^5 \qquad (7.5)$$

where γ is a constant o its value was found by numerical integrations to equal 15.1×10^{-9} KW/m^3K^5. (see Appendix VI).

Integrating equation (7.4) over all wavelengths and considering the result in equation (7.5) we get:

$$\frac{1}{r}\int_0^\infty \frac{d}{dr}(rE_\lambda)\ d\lambda = B\ \overline{c}\,\gamma\,T^5 - \int_0^\infty \frac{B\,\overline{c}}{\lambda}\ E_\lambda\,d\lambda$$

Self-absorption of the cloud tends to zero, as $KL \to 0$. The above equation therefore reduces to:

$$\frac{1}{r}\int_0^{\infty}\frac{d}{dr}(rE_\lambda)\, d\lambda = B\bar{c}\gamma T^5$$

and

$$\frac{1}{r}\frac{d}{dr}(rE) = B\bar{c}\gamma T^5$$

$$\int_0^{RE} d(rE) = B\bar{c}\gamma \int_{r=0}^{r=R} rT^5 dr \;;$$

and therefore:

$$E_p = \frac{B\bar{c}\gamma}{R}\int_{r=0}^{r=R} rT^5 dr = \varepsilon_p \sigma T^4 \qquad (7.6)$$

or, in General,

$$E_p = \frac{B\bar{c}\gamma}{2\pi R}\int_0^{2\pi}\int_{r=0}^{r=R} rf(r,\theta)\, dr\, d\theta \qquad (7.7)$$

If, however, T = constant, it may be shown that $\varepsilon_p = \frac{1}{2}KR$

Under practical conditions, the temperature profile is assymetric and integration is carried out in each half separately giving:

$$E_p = \frac{B\bar{c}\gamma}{\pi R}\int_0^{\pi}\int_0^{R} r\left[f_1(r) + f_2(r)\right] dr\, d\theta \qquad (7.8)$$

where $f_1(r,\theta) = f_1(r) \qquad 0 < \theta < \pi$

and $f_2(r,\theta) = f_2(r) \qquad \pi < \theta < 2\pi$

7.5 To test model against experimental results

The emissivity calculated according to section 7.3 is, in fact, due to soot as well as banded radiation, i.e.

$$\varepsilon_\lambda = 1 - \exp - (K_g + K_p)L \ ,$$

for a small absorption strength, which is the case under study here. It may be represented approximately as:

$$\varepsilon_T \simeq (K_p + K_g)L$$

i.e. $$\varepsilon_T \simeq \varepsilon_p + \varepsilon_g$$

The soot emissive power is therefore equal to the total radiation flux, which is in this case the value σT_b^4, detected by the pyrometer, minus the flux due to banded radiation, i.e.

$$\frac{B\bar{c}\gamma}{\pi R}\int_0^{\pi}\int_{r=R}^{r=R} r\left[f_1(r) + f_2(r)\right] dr d\theta = \sigma T_b^4$$

$$- \frac{\sigma\varepsilon_g}{R^2}\int_0^{\pi}\int_{r=o}^{r=R} r\left[g_1(r) + g_2(r)\right] dr\, d\theta \qquad (7.9)$$

where ε_g is the mean gas emissivity, as given in Table (7) and f(r) and g(r) represent T^5 and T^4 respectively. It should, however, be noted that the effective soot path length was calculated at windows 1&2 as t rather than D. Integration of the quantity on the left-hand side of equation 7.9 was therefore from r=0 to r=t/2. Had the above equation been used without modification, the error in equation 7.10, below, would be small. This was found in a number of cases to be less than 5 per cent. It is expected that the emission of non-luminous gases will fill the whole tube diameter.

The following equation represents the ratio E_{pn}/E_{pl}:

$$\frac{B_n \bar{c}_n \overline{T^5_n}}{B_1 \bar{c}_1 \overline{T^5_1}} = \frac{T_{bn}^4 - \varepsilon_g \overline{T^4_n}}{T_{b1}^4 - \varepsilon_g \overline{T^4_1}} \qquad (7.10)$$

The subscripts refer to conditions 1 and n, where n for each window could take values from 2 to 11. The percentage deviation of the ratio of the emissive power from the left-hand side of the equation to that on the right-hand side is plotted in Figs. (38 to 40). The individual values of the constant A' could not be obtained from the information in this work, and there appears to be no alternative but to assume that $A'_n \simeq A'_1$ in testing the model against the experimental data.

In Figs. 38 to 40, the quantities compared are defined as X and Y, where

$$X = \frac{\bar{c}_n \overline{T^5_n}}{\bar{c}_1 \overline{T^5_1}} - \frac{T_{bn}^4 - \varepsilon_g \overline{T^4_n}}{T_{b1}^5 - \varepsilon_g \overline{T^4}} \Big/ \frac{T_{bn}^4 - \varepsilon_g \overline{T^4_n}}{T_{b1}^4 - \varepsilon_g \overline{T^4_1}} \quad \times 100 \qquad (7.11)$$

and Y is the above quantity when $\varepsilon_g = 0$.

We are therefore comparing the radiation ratio from model $(\bar{c}_n \overline{T^5_n} / \bar{c}_1 \overline{T^5_1})$ to that measured by the pyrometer with (X) and without (Y) correction for gas emissivity. The gas emissivity ε_g is the mean value determined as described in section 7.3.

There seems generally to be very good agreement between X and Y in window 2 (Fig. 38b). A reasonably good agreement is illustrated in Figs. (38 and 39)a and large deviations are apparent in Figs. (38 and 39)c. The different appear to take intermeidate positions in other cases. This somewhat complicated picture may partly be resolved if we consider the number of approximations made and that mean gas emissivities were used. The flux ratio derived from the theoretical formula, the first quantity inside the large brackets of equation 7.11, should in fact be multiplied by B_n/B_1, as shown in section 7.4.

It is not possible to evaluate this fraction under the present

experimental conditions, and thus to estimate its contribution to the error. The effect of the gas emissivity can be estimated. This was done for a number of cases in window 3, which showed excessively large deviations (see Figs. (38 -40)c. The ratio was once more calculated for this window using a value of $\varepsilon_g = 0.028$, which is close to that determined for windows 1 and 4, rather than the value $\varepsilon_g = .0453$ determined using equation (7.2). There values are plotted as hexagons and very close to the corresponding value of (Y). This indicates the actual gas emissivity is overestimated, the magnitude and direction of the error depends on the parameters in the ratio.

In these experiments, the soot emissivity was of similar magnitude to the gas emissivity determined by the least-square method, unlike the case of a number of oil flames [23]. Such evidence discourages the use of the extrapolation method to determine an average value of ε_g, when the value of the total emissivity is small or of the same magnitude.

The flux due to radiation is known to be a function of a number of parameters, such as particle shape and composition. These have been neglected in the model. It is however, doubtful if their contribution to the error would be of major importance under the present conditions, considering that in a number of cases the deviation was less than 10 Per cent, which is quite small. The value of (Y) was ≤ 30 per cent in 60 per cent of the cases. This is quite good, considering that we are comparing differences in the ratio of fluxes obtained using different methods. The values of (X) will not be considered at this stage of the discussion, since when the radiation was corrected for ε_g, a larger error was generally produced. One may therefore conclude that the flux may be represented as a $f(\bar{c},T)$ only. Finally, as a result of close agreement between X and Y in window 2, the value of B was calculated from equation 7. Using the least-square method, and was found to equal $0.28 \times 10^3 . \frac{sec}{kg}$.

7.6 Convective Heat Transfer

The effect of additives on the various aspects of radiant transfer has been discussed in the previous sections. The experimental conditions chosen in this thesis resulted in convective heat transfer being the dominant mode of heat transmission to the water-cooled walls. It is widespread knowledge that the heat transfer rates from hydrocarbon flames can be increased by replacing some of the air with oxygen[176]. This relatively cheap method has often been used to improve heat transfer in industrial applications. The equivalent amount of air was reduced in order to keep constant the total volume inflow constant. The effect of preheating the air has also been known to increase the heat transfer coefficient by improving the driving force ΔT. The only factor that does not appear to have been studied with respect to convective transfer is the addition of CCl_4.

7.6.1 Local Heat Transfer Coefficient

To evaluate the effect of the additives on the local heat transfer coefficient between gas and surface, the latter was defined at the steady state as:

$$h = \frac{Q_c/A_i}{\overline{T}-T_s} \quad ,$$

where Q_c is the rate of heat transfer by convection and A_i is the area of the heating surface. It was calculated as the total flux (Q_c) received by a calorimeter minus radiative flux Q_r from an area of flame noted as A_f.

$$\text{i.e. } Q_c = wc_p\Delta T - \sigma T_b^4 A_f$$

where wc_p and Δt represent the heat capacity and temperature rise of the water flowing in a calorimeter. This seems justifiable, considering that

the terminal difference between the temperatures of the ingoing and outgoing water generally fell between 4 - 10°C, with the exception of a few cases of 15°C.

The results for the first four calorimeters are shown in Fig. 42 as a function of height. When oxygen was added to the fuel, it was possible nearly to double h. When, however, the percentage of oxygen in the air was raised, there was an overall increase in the value of the coefficient h, though there was no obvious peak. The change of h with height when oxygen is added is due to the increase in the product enthalpy and decrease in the mass flow rate when the input heat is constant[176].

Preheating the air shifted the maximum towards the nozzle, the input heat in this case is not constant. It appears that the position (i.e. height) at which the driving force ΔT and hence maximum heat release is somehow a function of the linear velocity and Reynolds number of air, which increases and decreases respectively with temperature. The only overall decrease occurred when CCl_4 was added to the fuel. This is as a direct result of the decrease in total heat release rate and is therefore Q_c.

7.6.2 Average Convective Heat Transfer Coefficient: $\bar{h}_c$

In most industrial applications, the heat transfer coefficient averaged with respect to the length of the furnace is more useful. Such values were calculated in this thesis according to the procedure in Appendix IV, using the following equation:

$$\frac{1}{\bar{h}} = \frac{1}{n} \sum_{1}^{n} \frac{1}{h_n}$$

where n stands for the number of calorimeters.

The average coefficient determined by the above equation incorpor-

ates the effect of soot which is deposited along most of the inner wall of the calorimeter. An estimate of soot resistance, $(1/h_d)$, was obtained by assuming that a layer of soot 1 mm thick was deposited along the length of the tube. When the thermal conductivity of lamp black[177a] was used, this gave a value of $h_d = 65.82$ watts/m^2K. The values of the mean convective heat transfer coefficient $\bar{h}_c$ to be used later were determined from the following relationship:

$$\frac{1}{\bar{h}_c} = \frac{1}{\bar{h}} - \frac{1}{h_d} \qquad (7.12)$$

It is, however, assumed that convective heat transfer coefficients $\bar{h}_c$ will be unaffected by the presence of soot particles[176].

7.6.3 Empirical Equations and Correlation of Heat Transfer by Convection

It was deduced from Figs. (8-11), in reference[178], that the flow was laminar-free convection. This was based on the values of the Reynolds and Grashof numbers, both evaluated at the mean film temperature T_f:

$$T_f = \frac{\bar{T}_z + T_{sz}}{2}$$

using the physical properties of air[177a]. The mean Nusselt number $\bar{Nu}$ was then evaluated using the following recommended equation in McAdams[177c] for laminar flow in pipes:

$$\bar{Nu} = .59(Gr\ Pr)^{.25} \qquad (7.13)$$

The convective heat transfer coefficient $\bar{h}_c$ evaluated by the above equation was less by up to a factor of 2 than that obtained experimentally using equation 7.12. When the factor $\frac{\bar{T}_z}{T_{sz}}$ was introduced on the left-hand side of equation (7.13) the following equation, obtained by

the least-quare method, was found to be more representative of the average and local heat transfer coefficients:

$$\bar{Nu} = .209\ (GrPr)^{.25}\ \frac{\bar{T}_z}{T_{sz}}$$

Better agreement with an individual deviation of less than six per cent was, however, obtained using the following equation:

$$\bar{Nu} = 2.388\ (Gr\ Pr)^{3.28}$$

This indicates that, when somewhat large temperature differences exist between bulk and surface temperatures, the existing correlations for laminar flow by free convection (equation 7.13) does not represent the data satisfactorily. This conclusion was later corroborated by finding supporting conclusion in an early study on heat transfer in a packed bed[179].

7.7. Total flux to the calorimeter

The results are plotted in Fig. (41). The general effect of most additives was to increase total flux, with the exception of the addition of 16.9 mg/sec. of oxygen to the fuel and the addition of CCl_4, where a decrease occurred. In the case of oxygen, this resulted from a decrease in convection which was no compensated for by the increase in radiation. It should also be noted that addition of O_2 to the air also decreased Q_c though Q_T was increased. In the case of CCl_4, a slight decrease in both convection and radiation was attributable to the decrease in reaction rate caused by this addition, i.e. less fuel was burned. The shape of the curves indicate that the levels of additive were sufficiently wide-ranging to include the regions of optimum heat transfer. The effect of preheating increased the total heat transfer by a greater extent than addition of oxygen. It is interesting that addition of 4.4 gm/sec oxygen to the fuel increased the total efficiency to a similar degree produced by preheating the air to 343K.

CHAPTER 8

CONCLUSION AND RECOMMENDATIONS FOR FUTURE WORK

It was stated in Chapter 2 that the flux Q is a function of soot weight, temperature, composition, size of flame and particles. The somewhat extensive study on soot composition in chapter 6 indicated that it was the change in composition of the gas-phase hydrocarbons, adsorbed on the soot, rather than that of soot particles which was important and that the microsturcture of soot was the major factor which determines the optical parameters of a soot in gaseous flames in chapter 7. It seemed reasonable to infer that this applied equally to oil flames. Various points were also clarified. The dispersion exponent g_λ was related to soot composition and it appeared that, in the visible the lack of dependence on composition occurred at a height where it was constant. It would be interesting from the theoretical point of view to define the limit where g_λ is not a function of composition in the infrared. The study of the relationship between the net rate of soot formation and temperature showed a good correlation in the region bounded by the blue reaction zone. This decreased with height and was very low where it ceased to exist. The correlation seemed to depend as well on the concentrations of heavy hydrocarbon molecules present in the flame.

The amount of soot plus polymeric material collected at either windows 1 and 2 was found to depend mainly on the temperature. This indicates that their formation within the blue reaction zone is mainly by pyrolysis and chemical species such as oxygen, OH radicals or O atoms therefore are not expected to penetrate within this zone, with the possible exception of the cooler region near the burner, where some premixing may occur. These findings suggest that the region where the blue reaction zone exists should be treated separately from that where it ceases to exist, due to the penetration, in the latter case of oxygen present in the air.

The reasonable agreement between the measured flux and that calculated

from experimental data indicated the lack of dependence in particular size distribution. This, together with the evidence in Chapter 4, suggested either that agglomerates did not exist in the regions of the flame studied here, or that, if they did, their shape is such that they did not affect flame absorptivity to any important extent.

The effect of composition is expected to be quite small. A linear correlation was obtained between the average C/H ratio of the insoluble fraction of soot and B/c_2 Fig. (36). The trend is believed to be artificial as a result of point-to-point comparison with data at window 4; and the magnitude of the change falls within the variance in composition at each position. This would be in agreement with theoretical findings, which suggest that there is no obvious correlation between k_m and composition for soots with C/H ratio > 8.

The beneficial effects of adding oxygen on radiation only reached window (2) although one would expect it to reach up to the end of the blue reaction zone; whereas when heat was added, they reached up to window (4). These results indicate the importance of the size of the reaction zone except in the preheating experiments. This is because the effect of oxygen is believed to be mainly a temperature effect. A better radiation efficiency would be expected to occur, as the length of reaction zone to flame height and to flame width increases and decreases respectively. Finally, radiation represented less that 30 per cent of total heat released in this flame, while convective heat transfer was the dominant mode. The total heat output increased in almost all cases, which was in some cases due to an increase in convective heat transfer. In the case of CCl_4, both convection and radiation decreased.

APPENDIX I

Method of Calculation of the Amount of Halogen Additive Required to Saturate a Known Volume of Fuel at a Given Temperature

For a mixture composed of n_f moles of dry fuel and n_a moles of additive vapour we get, according to Dalton's Law[180] the following:

$$\frac{p}{P} = \frac{n_a}{n_a+n_f} \qquad (1)$$

where p and P stand for partial pressure of fuel and additive respectively.

Assuming the gas law holds true for propane gas at atmospheric pressure, therefore:

$$P = n_f RT/V_f \qquad (2)$$

where V_f is the volume of n_f moles of dry propane entering the saturator at an atmospheric pressure P, and R is the gas constant.

Hence, from (1) and (2),

$$n_a = \frac{V_f}{RT} \cdot \frac{Pp}{P-p} \qquad (3)$$

p in this case is equal to the vapour pressure which was determined using the following expression:

$$\log p = -\frac{A}{T} + C$$

where A and C are constants corresponding to type of additive and were determined from ref. 181.

APPENDIX II

Calculation of Soot Residence Time

For steady motion, $\dot{m}$ = constant:

then $$\tau = \frac{R^2 z \bar{\rho}}{\dot{m}}$$

If $$\bar{\rho} = \frac{2}{R^2} \int_{r=o}^{r=R'} \rho \, r dr$$

$$\tau = \frac{2\pi 2}{\dot{m}} \rho_o T_o \int_{r=o}^{r=R} \frac{r}{R} \, dr$$

In obtaining equation (1), it is assumed that the equation of state for an ideal gas relates to the state properties of a unit flow volume. This is allowed for, provided that the gas molecules are extremely small, i.e. have negligible inertia of their own, and negligible attractive forces. Although soot particles are positively charged, it will be assumed that their behaviour may still be expressed by that of an ideal gas. This implies that they would move with the same linear velocity of the gas stream. It should be noted that the total mass was slightly varied when the oxygen and CCl_4 were the additives. This is not however, expected to be of much significance here.

In a diffusion flame, soot forms in a thin boundary parallel to the blue reaction zone. The temperature at a given cross-section of the flame varies considerably in the case of windows 1 and 2, in the radial direction, and to a lesser extent at windows 3 and 4. A mean effective soot residence time was therefore defined as:

$$\tau \times \frac{\bar{T}}{T_{max}}$$

where T_{max} is the arithmetic average of the two maxima in windows 1 and

2 or the maximum in window 3 and 4.

This was felt to give a more realistic estimate of the soot residence time. Since the maximum temperatures was used, this effective soot residence time will be slightly on the low side. It may, however, be that it will be close to the true average residence time, considering that the temperatures used to calculate (τ) in equation(1) are somewhat below their true values (see chapter 4).

APPENDIX III

Mean Stream Temperature $\overline{T}$:

Some controversy exists over the definition of the mean temperature of a stream of fluid for the purpose of evaluating the physical properties of the fluid concerned It is usually preferable to use the temperature attained by completely mixing the fluid passing a given section, i.e. bulk temperature, than, e.g. the axial temperature (T_a) [182].

It should be noted that when a hot fluid moves in a relatively colder cylinder, the bulk of the hotter fluid will move faster than the cooler layers of the fluid near the tube wall. If the temperature at the axis is highest, the true mean fluid temperature should be higher than that calculated by the integral equation used to evaluate the mean temperature, i.e.

$$\overline{T} = \frac{1}{\pi R^2} \int_0^{\pi} \int_{r=0}^{r=R} r \left[h_1(r) + h_2(r) \right] dr d\theta \qquad (1)$$

r and θ are cylindrial polar coordinates and h(r) represents (T) in this case where,

$$h_1(r,\theta) = h_1(r) \qquad 0 < \theta < \pi$$

$$h_2(r,\theta) = h_2(r) \qquad \pi < \theta < 2\pi$$

The differences between the temperature calculated using the integral form above and that which takes into account only the distribution up to the laminar boundary layer near the wall (T_m) has been expressed as: [183]

$$T_m - \overline{T} = \frac{1}{1.82 \times 72} (T_a - T_s) \qquad (2)$$

$$\text{where } T_m = \frac{8T_a + T_s}{1.8 \times 9} - \frac{273}{1.8} \qquad (3)$$

The fractions in equations (2) and (3) have been allowed to stand

so as not to lose the initial form in which the equations have been presented. Equation (2) was used to calculate the error introduced in the true mean temperature for a temperature difference of 1500 K between the axis and the surface. It was found to be less than 15^{o}C which is very small. It is worth mentioning at this stage that, in calculating $\overline{T}$, the temperature at r = R was at least 30^{o}C higher than that at the cooled wall. This may be observed from the temperature contours in Figs. (30 to 33). A point worth reiterating here is that $\overline{T}$ will be slightly underestimated due to the effect of soot particles, (see chapter 4).

APPENDIX IV

Method of calculation of the average heat transfer coefficient (hot side)

All measurements were performed only after steady state had been achieved, (see chapter 5). This made is possible to calculate the average heat transfer coefficient for the first four calorimeters by means of the following equation:

$$Q_c = \frac{\bar{h}\, A_i (\Delta T_{hi} - \Delta T_{ho})}{\ell n (\Delta T_{hi} / \Delta T_{ho})} \qquad (1)$$

where ΔT represents the terminal temperature differences between gas and wall surface, and subscripts hi and ho stand for hot side, inner and outer respectively.

The wall and bulk temperatures at the common plane between any two consecutive calorimeters was calculated as the arithmetic man of the temperatures at their respective centres; this assumes that $\frac{dT}{dx}$ between the two points concerned is constant.

However the inlet temperature to the lowermost calorimeter and exit temperature to the fourth were unknown. The surface temperature to the first calorimeter T_s was assumed to be 293 K in each case. But when the temperature was used for the input gas temperature, the value of $\bar{h}$ was grossly overestimated. Equating the coefficient calculated from the area (Fig. 42) and that from equation (1), the temperature was found to be in experimental one approximately 533 K. A sufficiently close temperature about 4 per cent less, was obtained in this case by intersecting the extended line, joining the value of $\bar{T}$ at windows one and two,,with the Y axis (Fig. 35).

The bulk gas temperature $\bar{T}$ at the exit of the fourth calorimeter, which is also the inlet to the fifth calorimeter, was determined graphi-

radiation and soot deposition on the wall, and $\frac{1}{h''}$ stands for the sum of the individual resistances due to the wall thickness, scale deposition and convection on the water side.

The average coefficient h" was calculated for calorimeters numbers 3 and 4 and found to be of the order of 1100 watts/m^2K. This value was used to calculate h' for calorimeter number five in every case as a variation in h" of 50 per cent did not change the value of h' to a significant extent.

Considering that the contribution of the heat transfer by radiation at window no. 4 varied between 3-6 per cent of the total heat received by the cooling water, the assumption that h' derived from equation (b) is proportional to the average heat transfer coefficient $\bar{h}$, due to combined effect of convection and soot deposition, is not very farfetched. At this stage the average heat transfer coefficient along the length of that tube was calculated as follows:

$$\frac{1}{\bar{h}_o} = \frac{1}{n} \sum_{1}^{n} \bar{h}_n \quad \ldots \qquad (4)$$

where n is the number of calorimeters.

cally from the same figure, showing a plot of $\overline{T}$ versus height (z). The wall temperature T_s was determined by assuming that $\overline{T} = 2.1\ T_s$, a value which represented the average ratio at the centre of window four. The ratio of $\overline{T}/\overline{T}_s$ fluctuated around 2 at the other positions.

The average heat transfer coefficient for the first four calorimeters was calculated from the area under the curve in Fig. (42a) for experiments 1, 4 and 5. The difference between the area measurements and the method detailed above was less than 5 per cent. As the deviation was in no specific direction and since the area measurements were much quicker to do, it was used to calculate the average coefficient of heat transfer of the first four calorimeters.

The fifth calorimeter was only added in order to recuperate part of the enthalpy of the exit gases. Only the mean temperature $\overline{T}$ close to the exit was known. The average heat transfer coefficient was determined as follows:

The first step was to calculate the overall heat transfer coefficient using the following form of Fourier's statement:

$$Q_T = \frac{U\ A_i (\Delta T_i - \Delta T_o)}{\ell n(\Delta T_i / \Delta T_o)} \qquad (2)$$

where ΔT represents the terminal temperature differences between gas and water and the suffices, i.e O stand for inlet and outlet respectively.

Since the thickness of the wall was small in comparison with the tube diameter, the equation for series flow through a plane wall was used, as the error is not referring each coefficient to its corresponding area of heat flow will be negligible[177]c. If the total resistance is represented as:

$$\frac{1}{U} = \frac{1}{h'} + \frac{1}{h''} \qquad (3)$$

where $\frac{1}{h'}$ stands for the sum of the individual resistances due to convection,

APPENDIX V

Error in Using Wein Function rather than the Planck Function

If frequency is used to define the intensity rather than wavelength in (eqn. 2.1) the total hemispherical flux of a black body (E_b) may be represented as:

$$E_b = \int_0^\infty E_{b,}\, d\nu = T^4 \int_0^\infty \frac{(\nu/Tc)^3\, d(\nu/Tc)}{\exp(c_2\, \nu/Tc)-1}$$

Letting $x = c_2\nu/Tc$,

$$E_b = \frac{6.494 c_1 T^4}{c_2^4} \qquad \text{ref. (17) f.}$$

If Wien's function $c_1(\nu/c)^5 \exp(-c_2\nu/Tc)$ is integrated throughout the frequency spectrum we get

$$E_b' = 6.0 \frac{c_1}{c_2^4} T^4$$

Therefore the error in using Wien's function rather than the Planck function to calculate the total flux from a black body is 7.6 per cent. Soot particles because of their size emit preferentially at shorter wavelengths and therefore the actual error is expected to be smaller and less than one per cent when $\lambda T < .3 \times 10^{-2}$ mK.

APPENDIX VI

Calculation of the constant γ

From equation 7.5:

$$\gamma = \int_0^\infty \frac{c_1 (\lambda T)^{-6} \, d(\lambda T)}{\exp(c_2/\lambda T) - 1}$$

Writing the above equation as a $f(\nu/T)$ gives

$$\gamma = c_1 \int_0^\infty \frac{(\nu/Tc)^4 \, d(\nu/Tc)}{\exp(c_2 \nu/Tc) - 1}$$

$$= \frac{c_1}{c_2^5} \int_0^\infty \frac{x^4 dx}{\exp(x) - 1} \qquad \text{where } x = c_2 \nu/Tc$$

$$= \frac{c_1}{c_2^5} \Gamma 5 \left[\frac{1}{1^5} + \frac{1}{2^5} + \frac{1}{3^5} + \ldots\ldots \right]$$

$$= \frac{c_1}{c_2^5} \, 24.888$$

and therefore:

$$\gamma = 151 \times 10^{-10} \text{ KW m}^{-3} \text{ K}^{-5}$$

REFERENCES

1. JONES, A.R. and SCHWAR, M.J.R.

Light scattering by particles in flames (A review)

High temp., - High press. 1, 369 (1969).

2. JONES, A.R.

Emissivity of agglomerated soot.

Combustion Institute European Symposium, (FJ. Weinberg, Ed.)

Academic Press London (1973), p. 376.

3. JONES, A.R.

Scattering and emission of radiation by clouds of elongated particles.

J. Phys. D: Appl. Phys., 5, L1, (1972).

4. BÉER, J.M.

Radiation from flames in furnaces.

Combustion Technology: Some modern developments.

(ed., by H.M. PALMER and J.M. BEER) Academic press, London, 1974, p.213.

5. WERSBORG, B.L., FOX, L.K. and HOWARD, J.B.

Soot concentration and absorption coefficient in a low-pressure flame.

Combust. and Flame, 24, 1, (1975).

6. D'ALESSIO, A., DI LORENZO, T., BERETTA, F., and VENITOZZI, C.

Optical and chemical investigations on fuel-rich methane-oxygen premixed flames at atmospheric pressure.

Fourteenth Symposium (International) on Combustion, p. 941,

The Combustion Institute, 1973.

7. HOMANN, K.H., and WAGNER, H. Gg.,

Some new aspects of the mechanism of carbon formation in premixed flames.

Eleventh Symposium (International) on combustion, p. 371,

The Combustion Institute, 1967.

8. LAUD, B.B. and GAYDON, A.G.

Absorption spectra of ethylene diffusion flames.

Combust. Flame, 16, 55 (1971).

9. BONNE, Von U., and WAGNER, H. Gg.
Investigation of the completion of a reaction in oily hydrocarbon-oxygen flames III Optical investigation of sooty flames.
Ber. Busenges. Physik. Chem., 69, 35 1965).

10. ECHIGO, R. and NISHIWAKI, N. and HIRATA, M.
A study on the radiation of luminous flames.
Eleventh symposium (International) on Combustion, p. 381,
The Combustion Institute, 1967.

11. WEEKS, D.J. and SAUNDERS, O.A.
Some studies of radiating flames in a small gas turbine type combustion chamber.
J. Inst. Fuel, 31, 247, (1958).

12. HEAP, M.P. and LOWES, T.M.
Methods available for the calculation of luminous flame attenuation coefficients.
I.F.R.F., Ijmuiden, 1970, Doc. nr.D 07/a/42.

13. WARREN, B.E.
X-Ray diffraction in random layer lattices.
Phys. Rev. 59, 693, (1941).

14. BALL, R.T. and HOWARD, J.B.
Electric charge of carbon particles in flames.
Thirteenth Symposium (International) on Combustion, p. 353, The Combustion Institute, 1971.

15. MEDALIA, A.I. and HECKMAN, F.A.
Morthology of aggregates II. Shape and bulkiness factors of carbon black aggregates from electron microscopy.
Private Communication.

16. HECKMAN, F.A.
Microstructure of carbon black.
Rubb. Chem. Technol. 37, 1245 (1964).

17. HOTTEL, H.C. and SAROFIM, A.F.

Radiative Transfer

McGraw-Hill Co., New York (1967), Page no. a) 13 b) 392 and 409 c) 247 d) 244 e) 397 f) 19.

18. HOWARTH, C.R., FOSTER, P.J. and THRING, M.W.

The effect of temperature on the extinction of radiation by soot particles.

Proceedings, of the third International, Heat transfer Conference, 5, 122, (1966).

19. TAYLOR, P.B.

The evaluation and measurements of radiative emission from luminous and non-luminous flames using mathematical modelling and rapid scanning spectrometry.

Ph.D. Thesis, Sheffield University, April (1974)

20. LUDWIG, C.W. et al

Study on exhaust plume radiation predictions.
General dynamics/convair, reports numbers:
(i) GD/C-DBE-66-001; GD/C-DBE-66-011a (1966) (reports on CO_2)
(ii) GD/C-DBE-66-017 (1966); NASA-CR-61233 (1968). (reports on H_2O vap.)

21. TRUELOVE, J.S.

Mathematical modelling of radiant heat transfer in furnaces.

AERE-R 7817 (1974).

22. SPARROW, E.M. and CESS, R.D.

Radiation heat transfer

Brooks/Cole, Belmont, California, (1966), p. 193-194.

23. BEER, J.M. and CLAUS, Ir. J.

The "traversing" method of radiation measurement in luminous flames.

J. Inst. Fuel, 35, 437 (1971).

24. HEIN, K. and LEUCKEL, W.

The formation, combustion and radiation of soot in luminous oil- and-gas diffusion flames.

I.F.R.F, Ijmuiden, 1970, Doc, nr, Tg K 20/a/46.

25. GAYDON, A.G. and WOLFHARD, H.G.

Flames: Their structure radiation and temperature.

Chapman and Hall Ltd., London, (1970) page numbers a) 263 b) 191 c) 175 d) 320 e) 143.

26. HOTTEL, H.C.

Private Communication (1975).

27. HAWKSLEY, P.G.W.

The physics of particle size measurement (Review) Part II: Optical methods and light scattering.

B.C.U.R.A. Month Bulletin, 16, 117 (1952) and 16, 181 (1952).

28. McCARTHY, J.T. and ERGUN, S.

Optical properties of graphite and coal.

Fuel, 37, 272, (1958).

29. SATO, T. and KUNITOMO, T.

Experimental study on luminous flames.

Mem. Fac. Engng. Kyoto Univ., 31, 47 (1969).

30. LOWES, T.M. and HEAP MP.

Emission/attenuation coefficients of luminous radiation.

I.F.R.F. Ijmuiden, (1971), Doc. nr. K 20/a/62.

31. MILLIKAN, R.C.

Sizes, Optical properties, and temperatures of soot particles.

Temperature/its measurements and control in science and industry.

Vol. III, part 2, p. 497, Reinhold: New York, 1962.

32. SIDDALL, R.G. and McGRATH, I.A.

The emissivity of luminous flames.

Ninth Symposium (International) on combustion, p. 102, The Combustion Institute (1963).

33. CHAKRABORTY, B.B. and LONG, R.
The formation of soot and polycyclic aromatic hydrocarbons in diffusion flames. Part one.
Combust. Flame, 12, 226, (1968).

34. CHAKRABORTY, B.B. and LONG, R.
The formation of soot and polycyclic aromatic hydrocarbons in diffusion flames Part two.
Combust. Flame, 12, 237, (1968).

35. CHAKRABORTY, B.B. and LONG, R.
The formation of soot and polycyclic aromatic hydrocarbons in diffusio-flames - Part three: Effect of additions of oxygen to ethylene and ethane respectively as fuels.
Combust. Flame, 12, 469, (1968).

36. TOMPKINS, E.E. and LONG, R.
The flux of polycyclic aromatic hydrocarbons and insoluble material in premixed acetylene-oxygen flames.
Twelfth Symposium (International) on combustion, p. 625. The Combustion Institite, 1969.

37. RAY, S.K. and LONG, R.
Polycyclic aromatic hydrocarbons from diffusion flames and diesel engine combustion.
Combust. Flame, 8, 139 (1964).

38. THORP, N., LONG, R. and GARNER, F.H.
Carbon formation in hydrocarbon diffusion flames.
Fuel, 34, S1 (1955).

39. DILORENZO, A. and MASI, S.
Formation and evolution of polycyclic aromatic hydrocarbons in soot-forming flames.
Second European Symposium on Combustion, (Orlean 1975). The Combustion Institute, 1975, p. 368.

40. ARTHUR, J.R. and NAPIER, D.M.

Formation of carbon and related materials in diffusion flames, Fifth Symposium (International) on combustion, p. 303. The Combustion Institute 1955.

41. FOSTER, P.J. and HOWARTH, C.R.

Optical constants of carbons and coals in the infrared.

6, 719 (1968).

42. DALZELL, W.H. and SAROFIM, A.F.

Optical constants of soot and their application to heat-flux calculations.

Trans. Am. Soc. Mech. Engrs. (J. Heat Trans.) 91, 100, (1969).

43. MORI, Y. and MAKINO, K.

A study on radiation from a luminous flame.

Bull. J. Soc. Mech. Engrs. 12, 1448, (1969).

44. LOWES, T.M. and NEWALL, A.J.

The emissivities of flame soot dispersions.

Combust. FLame, 16, 191 (1971).

45. WATERS, P.L.

Semiconducting properties of carbonized coal.

Proceedings Fifth Conference on Carbon, vol. 2, p. 131, Pergammon Press, 1963.

46. GRENIS, A.F. and LEVITT, A.P.

The spectral emissivity and total normal emissivity of commercial graphites at elevated temperatures.

Proceedings Fifth Conference on Carbon, vol. 2, p. 639, Pergammon Press, (1963).

47. STULL, V.R. and PLASS, G.N.

Emissivity of dispersed carbon particles.

J. Opt. Soc. Am. 50, 121. (1960).

48. BENNETT, H.E. and PORTEUS, J.O.

Relation between surface roughness and specular reflection at normal

incidence.

J. Opt. Soc. Am. 51, 123, (1961).

49. DITCHBURN, R.W.

LIGHT

Interscience Publishers, New York, (1954), p. 454.

50. BOYNTON, F.P., LUDWIG, C.B. and THOMPSON, A.

Spectral emissivity of carbon particle clouds in rocket exhausts.

AIAA Jnl. 6, 365 (1968).

51. HOTTEL, H.C. and BROUGHTON, F.P.

Determination of true temperature and total radiation from luminous gas flames (Use of special two-colour optical pyrometer).

Ind. Eng. Chem., Anal. Ed., 4, 166, (1932).

52. WILLIS, C.

The complex refractive index of particles in a flame.

J. Phys. D: Appl. Phys. 3, 1944 (1970).

53. BEER, J.M. and HOWARTH, C.R.

Radiation from flames in furnaces.

Twelfth Symposium (International) on Combustion, p. 1205. The Combustion Institute, 1969.

54. ROSSLER, F.

Determination of the absorption coefficients of soot particles of various flames.

Optik, 6, 145, (1950).

55. BECKER, Von, A.

Radiation and temperature of the Hefner lamp.

Ann. Physik, 28, 1017 (1909).

56. KUNUGI, M. and JINNO, H.

Determination of size and concentration of soot particles in diffusion flames by light-scattering techniques.

Eleventh Symposium (International) on Combustion p. 257, The Combustion Institute, 1967.

57. MEDALIA, A.I.
Morphology of aggregates: 1. Calculation of shape and bulkiness factors; application to computer-simulated random flocs. J. Coll. Interf. Sc. 24, 393 (1967).

58. JOHNSON, G.L. and ANDERSON, R.C.
An electron microscope study of carbon formation in the pyrolysis of hydrocarbons.
Proceedings of the fifth conference on carbon, vol. 1, p. 395, Pergammon Press, 1962.

59. TESNER, P.A.
Formation of dispersed carbon by thermal decomposition of hydrocarbons.
Seventh Symposium (International) on Combustion, p. 546. The Combustion Institute, 1960.

60. TESNER, P.A. ROBINOVITCH, H.J. and RAFALKES, I.S.
The formation of dispersed carbon in hydrocarbon diffusion flames.
Eighth Symposium (International) on combustion, p. 801. The Combustion Institute, 1962.

61. PARKER, W.G. and WOLFHARD, H.G.
Carbon Formation in Flames.
J. Chem. Soc. (1950) p. 2038.

62. JONES, A.R. and WONG, W.
Direct optical evidence for the presence of sooty agglomerates in flames.
Combust. Flame, 24, 139 (1975).

63. DALZELL, W.H., WILLIAMS, G.C. and HOTTEL, H.C.
A light-scattering method for soot concentration measurements.
Combust. Flame 14; 161, (1970).

64. ERICKSON, W.D., WILLIAMS, G.C. and HOTTEL, H.C.
Light scattering measurements on soot in a benzene-flame.
Combust. Flame 8, 127 (1964).

65. D'ALESSIO, A., DI LORENZO, A., SAROFIM, A.F., BERETTA, F., MASI, S., and VENITOZZI, C.
Soot formation in methane-oxygen flames.
Fifteenth Symposium (International) on Combustion, p. 1427.
The Combstion Institute, 1975.

66. KERKER, M.
The scattering of light and other electromagnetic radiations.
Academic Press, 1969, p. 432.

67. FOSTER, P.J.
Calculation of the optical properties of dispersed phases.
Combust. Flame, 7, 277, (1963).

68. ROSNER, D.E. and ALLENDORF, H.D.
Comparative studies of the attack of pyrolytic and isotropic graphite by atomic and molecular oxygen at high temperatures.
AIAA Jnl. 6, 650, (1968).

69. HAMMOND, E.G. and BEER, J.M.
Spatial distribution of spectral radiant energy in a pressure jet oil flame.
Trogir Heat Transfer Conference, Yugoslavia, 1973.

70. THRING, M.W., FOSTER, P.J. McGRATH, I.A. and ASHTON, J.S.
Prediction of emissivity of hydrocarbon flames.
International Heat Transfer Conference, University of Colarado and London, 1961-62, American Society of Mechanical Engineers, p. 796, 1963.

71. GURVICH, A.M., MITOR, U.V. and TERENTEV, V.D.
The radiation of the luminous flame.
Teploenergetika 7, 35 (1956).

72. WALL, T.F. and STEWART, M.C.

The measurement and prediction of solids - and soot - absorption coefficients in the flame region of an industrial P.F. chamber.

Fourteenth Symposium (International) on Combusiton, p. 689.

The Combustion Institute, 1973.

73. DAVEY, H.

See Bonne, W.A. and Townend, D.T.A., Flame and Combustion in Gases, Longmans, Green, and Co.,1927.

74. NEF, J.U.

On the fundamental conceptions underlying the chemistry of the element carbon.

J. Am. Chem. Soc. 26, 1549 (1904).

75. BERTHELOT, M.

Effect of an electric spark on marsh gas.

C.r, hebd. Séanc. Acad. Sci. Paris, 67, 1188 (1868).

76. LEWES, V.B.

The luminosity of coal-gas flames.

Trans. Chem. Soc., 69, 322 (1892).

77. MARSH, P.A., VOET, A., MULLENS, T.J. and PRICE, L.D.

Quantitative micrography of carbon black microstructure.

Carbon, 9, 797 (1971).

78. FORD, F.P. and HESS, W.M.

Microscopy of pigment-elastomer system.

Rubb. Chem. Technol. 36, 1175, (1963).

79. SCHIRMER, R.M.

Effect of fuel composition on particulate emissions from gas turbine engines.

Emissions from Continuous Combustion Systems; Ed. W. Cornelius and W.G. Agnew. Plenum Press, N.Y., 1972, p. 189.

80. BAN, L.L. and HESS, W.M.
Orientation of graphite layers in standard and heat-treated carbon blacks.
Abstract: Ninth Biennial Carbon Conference, Boston College, June 16-20, 1969.

81. BAN, L.L.
Direct study of structural imperfections by high resolution electron microscopy
Surface and defect properties of solids. Vol. 1, (Special periodical report.) (Ed. M.W. Roberts and J.M. Thomas).
The Chemical Society, London, 1972, p. 54.

82. HOMANN, K.H., MORGENEYER, W. and WAGNER, H. Gg.
Optical measurements of carbon forming benzene-oxygen flames.
Combustion Institute European Symposium (Sheffield, 1973), Academic Press, 1973, p. 394.

83. FEUGIER, A.
Soot in flames.
Extrait de la revue de l'institut francais du petrole et annales des combustible liquides, 24, 1374, (1969).

84. PALMER, H.B.
Carbon formation during the pyrolysis of a hydrocarbon.
Journal de Chimie Physique et de Physico-Chimie Biologique, numero special,Avril, p. 87, 1969.

85. HOMANN, K.H.
Soot formation in premixed hydrocarbon flames.
Angewandte Chemie, 7, 414, (1969).

86. HOMANN, K.H. and WAGNER, H.G.
Chemistry of carbon formation in flames.
Proc. Roy. Soc. A 307, 141, (1968).

87. HOMANN,K.H.

Carbon formation in premixed flames.

Combustion and Flame, 11, 264, (1967).

88. PALMER, H.B. and CULLIS, C.F.

The formation of carbon from gases.

Chemistry and Physics of Carbon, (Ed. P.L. Walker), Vol. 1, p. 265. Edward Arnold Ltd. 1965.

89. PORTER, G.

The mechanism of carbon formation.

AGARDOGRAPH-9, Combustion Researches and Reviews, Butterworth Scientific Publication, London, 1955, p. 108.

90. STREET, J.C. and THOMAS, A.

Carbon formation in premixed flames.

Fuel, 34, 4, (1955).

91. THOMAS, A.

Carbon formation in flames

Combust. Flame, 6, 46, (1962).

92. LAWTON, J. and WEINBERG, F.J.

Electrical aspects of combustion.

Clarendon Press, Oxford, 1969.

93. WERSBORG, B.L., YEUNG, A.C. and HOWARD, J.B.

Concentration and mass distribution of charged species in sooting flames.

Fifteenth Symposium (International) on Combustion, p. 1439, The Combustion Institute, 1975.

94. MILLER, W.J.

Ions in Flames: Evaluation and prognosis.

Fourteenth Symposium (International) on Combustion, p. 307. The Combustion Institute, 1973.

95. HOWARD, J.B.

On the mechanism of carbon formation in flames.

Twelfth Symposium (International) on Combustion, p. 877. The Combustion Institute, 1969.

96. PLACE, E.R. and WEINBERG, F.J.

The nucleation of flame carbon by ions and the effect of electric fields.

Eleventh Symposium (International) on Combustion, p. 245. The Combustion Institute, 1967.

97. LESTER, T.W., ZALLEN, D.M. and WHITTIG, S.L.K.

Shock-tube studies of chemi-ionisation processes in hydrocarbon combustion systems.

Recent developments in shock tube research, (Ed., by Bershader, D. Griffith, W.). Standard University Press, 1973, p. 700.

98. TESNER, P.A.

Formation of soot particles.

Symposia of the Faraday Society, "Fogs and Smokes", no. 7, p. 104. The Faraday Division, Chemical Society, London, 1973.

99. BONNE, V., HOMANN, K.H. and WAGNER, H. Gg.

Carbon formation in premixed flames.

Tenth Symposium (International) on Combustion, p. 503, The Combustion Institute, (1965).

100. SMITH, E.C.W.

The emission spectrum of hydrocarbon flames.

Proc. Roy. Soc. 174, A, 110, (1940).

101. RUMMEL, K. and VEH, P.O.

The radiation of luminous flames.

Archiv. fur das Eisenhuttenwesen, 14, 489, (1941).

102. JESSEN, P.F. and GAYDON, A.G.
Estimation of carbon radical concentration in fuel-rich acetylene-oxygen flame by absorption spectroscopy.
Twlefth symposium (International) on Combustion, p. 481.
The Combustion Institute of Combustion, 1969.

103. LAHAYE, J., PRADO, G. and DONNET, J.B.
Nucleation and growth of carbon black particles during thermal decomposition of benzene.
Carbon, 12, 27 (1974).

104. GIBSON, J. HOLOHAN, M. and RILEY, H.
"Amorphous Carbon".
J. Chem. Soc., 456, (1946).

105. GRISDALE, R.O.
The formation of black carbon.
J. Appl. Phys. 24, 1082, (1953).

106. CULLIS, C.F. and NORRIS, A.C.
The pyrolysis of organic compounds under conditions of carbon formation.
Carbon 10, 525, (1972).

107. DEARDEN, P. and LONG, R.
Soot formation in ethylene and propane diffusion flames.
J. Appl. Chem., 18, 243 (1968).

108. KNOX, K., NORRISH, R.G.W. and PORTER, G.
The photochemical decomposition of ketene by means of light of a very high density.
J. Chem. Soc. 1477, (1952).

109. COLE, J.D. and MINKOFF,
Carbon formation in diffusion flames and the role of acetylene.

Proc. Roy. Soc. 239.A, 28, (1957).

110. MILLIKAN, R.C.
Non-equilibrium soot formation in premixed flames.
J. Phys. Chem. 66, 794 (1962).

111. GAY, I.D. KISTIAKOWSKY, G.B., MICHAEL, J.V. and NIKI, H.
Thermal decomposition of acetylene in shock-waves.
J. Chem. Phys., 43, 1720 (1965).

112. CHAKRABORTY, B.B., and LONG, R.
The formation of soot and polycyclic aromatic hydrocarbon in ethylene diffusion flames with methanol as an additive.
Combust. Flame 12, 168 (1968).

113. BARTHOLOMÉ, E. and SACHSE, H.
Catalytic phenomena in aerosols.
Z. Electrochem., 53 326 (1949).

114. BOWSER, R.J. and WEINBERG, F.J.
Electrons and the emission of soot from flames.
Nature, 249, 339 (1974).

115. MAYO, P.G. and WEINBERG, F.J.
On the size, charge and number-rate of formation of carbon particles in flames subject to electric field.
Proc. Roy. Soc. 319 A, 351, (1970).

116. HOWARD, J.B., WERSBORG, B.L. and WILLIAMS, G.C.
Coagulation of carbon particles in premixed flames.
Faraday Symposium of the Chemical Society, No. 7, p.109, 1973.

117. WERSBORG, B.L. HOWARD, J.B. and WILLIAMS, G.C.
Physical mechanisms in carbon formation in flames.
Fourteenth Symposium (International) on Combustion, p. 929.
The Combustion Institute, 1973.

118. AMBROSIO, M., D'ALESSIO, A. DI LORENZO, A. and ROSSO, G.

Incomplete combustion of methane for the production of intermediate compounds for the chemical industry.

Italian Flame day San Remo, April 1975.

119. IYENGAR, M.S., VAIDYESWARAN, R. and DATAR, D.S.

Studies on carbon deposit formation in flames: Part I: Suppression of carbon deposit formation in flames of some organic compounds by carbon dioxide and nitrogen.

J. Scient. ind. Res. 11B. 455 (1952).

120. VAERMAN, J.

Quelques caracteristiques des flammes de diffusion laminaire.

Private communication, (1973).

121. HERBST, G.

Carbon black formation from hydrocarbons.

Brennstoff-Chem. 44, 1 (1963).

122. SZARVASY, E.

Process for the production of fine soot suitable for the manufacture of pigments.

U,S, Patent no. 1, 383,374, (1921).

123. COMERFORD, F.M.

Combustion of carbon particles in luminous flames.

Fuel 35, 333 (1956).

124. THORP, N., LONG, R. and GARNER, F.H.

Carbon formation in benzene-oxygen diffusion flames.

Fuel, 30, 266, (1951).

125. BOSSE, K.O.

The influence of the type of hydrocarbon in town gas and natural gas on the combustion process in gas appliances.

Die Forshungsberichte des Landes Nord Rhein Westfalen, Nr. 924.

126. BRADLEY, J.N. and DURDEN, D.A.
The role of pyrolysis reactions in hydrocarbon oxidation,
Combust. Flame, 19, 452 (1972).

127. KING, N.K.
The influence of water vapour on the emission spectra of flames.
Comb. Sci. Technol. 6, 247 (1973).

128. MÜLLER-DETHLEFS, K. and SCHLADER, A.F.
Effect of steam on flame temperature, burning velocity, and carbon formation in hydrocarbon flames.
To be published in Combust. Flame, (1976)

129. SCHERER, G. and TRANIE, L.A.
Pollution reduction by combustion of fuel oil water emulsions.
Private communication (1973).

130. GAYDON, A.G. and WHITTINGHAM, G.
The spectra of flames containing oxides of sulphur.
Proc. Roy. Soc. A, 189, 313 (1947).

131. COTTON, D.H., FRISWELL, N.J. and JENKINS, D.R.
The suppression of soot emission from flames by metal additives.
Combust. Flame 17, 99 (1971).

132. IBIRICU, M.M. and GAYDON, A.G.
Spectroscopic studies of the effect of inhibitors on counterflow diffusion flames.
Combust. Flame, 8,51 (1964).

133. BADAKHSHAN, A.
The formation of carbon in diffusion flames.
Ph.D. Thesis, Birmingham University, 1957.

134. ARTHUR, J.R., BANGHAM, D.H. and BOWRING, J.R.
Kinetic aspects of the combustion of solid fuels.
Third Symposium on Combustion and Flame and Explosion Phenomena, p. 466.

The Williams and Wilkins Co. 1949.

135. MERTENS, E. and HELLINCKX, L.
Mechanisms of carbon combustion.
Third Symposium on Combustion and Flame Explosion Phenomena, p. 474. Williams, Wilkins and Co., 1949.

136. ROSSER, W.A., WISE, H. and MILLER, J.
Mechanism of Combustion inhibition by compounds containing halogen.
Seventh Symposium (International) on Combustion, p. 175, The Combustion Institute, 1959.

137. SIMMONS, R.F. and WOLFHARD, H.G.
Critical concentration of methyl bromide.
Trans. Faraday Soc. 52, 53 (1956).

138. CREITZ, E.C.
Inhibition of diffusion flames by methyl bromide and trifluoromethyl bromide applied to the fuel and oxygen side of the reaction zone.
J. Res. Nat. Bur. Stand.,- A: Phys. Chem. 65A, 389 (1961).

139. SALOOJA, K.C.
Carbon formation in flames: control by novel catalytic means.
Combustion Institute European Symposium 1973, (Ed. F.J. Weinberg), Academic Press, London, 1973, p. 400.

140. ADDECOTT, K.S.B. and NUTT, C.W.
Mechanism of smoke reduction by metal compounds.
Am. Chem. Soc. Div. Pet. Chem., 14, A. 69 (Sept. 1969).

141. FEUGIER, A.
The effect of metal additives on the amount of soot emitted by premixed hydrocarbon flames.
Combustion Institute European Symposium 1973. (Ed. F.J. WEINBERG) Academic Press, London, 1973, p. 406.

142. FEUGIER, A.

Effect of metal additives on the amount of soot emitted by premixed hydrocarbon flames.

Private communication, 1975.

143. BULEWJCZ, E.H., EVANS, D.G. and PADLEY, P.J.

Effect of metallic additives on soot formation processes in flames.

Fifteenth Symposium (International) on Combustion, p. 1461,

The Combustion Institute, 1975.

144. PEETERS, J. and VINCKIER, C.

Reduction of chemi-ions and formation of CH and CH_2 radicals in methane- oxygen and ethylene-oxygen flames.

Fifteeth Symposium (International) on Combustion. p. 969, The Combustion Institute, 1975.

145. ZALAVADIA, J.V. and DEWERTH, D.W.

Effects of particle injection on natural gas flame radiation.

J. Engr. Power, 88, 111, (1960).

146. SATO, T. and KUNITOMO, T.

Radiation from fine particle clouds in high-temperature combustion gases.

mem. Fac. Engrg. Kyoto Univ., 27, 1, (1965).

147. THRING, M.W.

Luminous radiation from flames.

Chem. Proc. Engrg., 46, 544 (1965).

148. GUYOMARD, F.

Experimental study of radiation from luminous diffusion flames.

C.r. hebd. Seanc. Acad. Sci. Paris, 233, 237, (1951).

149. GUENEBAUT, H. and GAYDON, A.G.

The effect of preheating on flame radiation and flame shape.

Sixth Symposium (International) on Combustion, p. 292.

The combustion Institute, 1957.

150. COMERFORD, F.M.

Carbon particle formation in a gaseous fuel.

Fuel, 32, 67 (1953).

151. BARR, J. and MULLINS, B.P.

Combustion in vitiated atmospheres, I-Combustion process in vitiated air.

Fuel, 28, 181, (1949).

152. LLOYD, S.A. and WEINBERG, F.J.

Limits to energy release and utilisation from chemical fuels.

Nature, 257, 367, (1975).

153. LLOYD, S.A. and WEINBERG, F.J.

A burner for mixtures of very low heat content.

Nature, 251, 48, (1974).

154. WALTON, W.H. et al

See: Symposium on particle size analysis, London.

(supplement to transaction of the Institute of chemical Engineers) 25, 45 (1947).

155. WATSON, H.H.

The dust-free space surrounding hot bodies.

Farad. Soc. Trans., 32, 1073, (1936).

156. WATSON, H.H.

Instructions for using the thermal precipitator dust-sampling apparatus.

Trans. Instn. Min. Metall. 46, 176, (1936).

157. KAY, D.H.

Techniques for electron microscopy (second edition).

Blackwell Scientif. Publication Oxford, 1965.

158. FRISTROM, R.E. and WESTENBERG, A.

Flame structure.

McGraw Hill, New York, (1965).

159. CHEDAILLE, J. and BRIVAD, Y.

Industrial flames.

Vol. 1, Measurement in flames,

(Ed., Beer, J.M. and Thring, M.W.) Edward Arnold, 1973 (a) p. 94

(b) p. 105.

160. BADZIOCH, S.

Collection of gas-borne dust particles by means of an aspirated sampling nozzle.

Brit. J. Appl. Phys. 10, 26 (1959).

161. BADZIOCH, S.

Correction for anisokinetic sampling of gas-borne dust particles.

J. Inst. Fuel 33, 106 (1960).

162. KASKAN, W.E.

The dependence of flame temperature on mass burning velocity.

Sixth Symposium (International) on Combustion p. 134,

The Combustion Institute, 1957.

163. Operating Instructions for radiation pyrometer type ORF 35/10/6.

Land Pyrometers. Ltd.

164. CHAKRABORTY, B.B. and LONG, R.

Gas chromatographic analysis of polycyclic aromatic hydrocarbons in soot samples.

Envir. Sci. Technol. 1, 828 (1967).

165. TSYBULEVSKII, A.M. and TESNER, P.A.

Gasification of dispersed carbon in hydrocarbon diffusion flames (i) acetylene nitrogen flames.

Comb. Explos. Shock Waves, 2, 38 (1966).

166. TESNER, P.A. and TSYBULEVSKII, A.M.

Gasification of dispersed carbon in hydrocarbon diffusion flames (iii) Flames of acetylene-hydrogen and acetylene-water vapour mixtures.

Comb. Explos. Shock Waves 3, 163 (1967).

167. WRIGHT, F.J.

The oxidation of soot by O atoms.

Fifteenth Symposium (International) on Combustion, p. 1449.

The Combustion Institute, 1975.

168. SPENCE, D. and McHALE, E.T.

The role of negative ions in hydrocarbon flame inhibition.

Combust. Flame 24, 211 (1975).

169. SMITH, S.R., and GORDON, A.S.

A study of diffusion flames. I - The methane diffusion flame.

J. Phys. Chem. 60, 759 (1956).

170. WOLFHARD, H.G. and PARKER, W.G.

A spectrocopic investigation into the structure of diffusion flames.

Proc. Phys. Soc. (A), 36, 2 (1952).

171. BRADLEY, J.N.

Flame and combustion phenomena.

Methuen and Co. Ltd. p. 52 (1969).

172. FEUGIER, A.

Soot oxidation in laminar hydrocarbon flames.

Combust. Flame 19. 249 (1972).

173. LEE. K.B.. THRING. M.W. and BEER. J.M.

On the rate of combustion of soot in a laminar soot flame.

Combust. Flame 6, 137 (1962).

174. FENNIMORE, C.P. and JONES, G.W.

Oxidation of soot by hydroxyl radicals.

J. Phys. Chem. 71, 593 (1967).

175. FENNIMORE, C.P. and JONES, G.W.

Coagulation of soot to smoke in hydrocarbon flames.

Combust. FLame 13, 303 (1969).

176. CHEN, D.C.C. and McGRATH, I.A.

Convective heat transfer in chemically reacting systems.

J. Inst. Fuel. 12, 12 (1969).

177. McADAMS, W.H.

Heat transmission, (Third Edition).

McGraw Hill Book Co., Inc., 1954, a) p. 443 b) p. 172

c) p. 187.

178. ECKERT, R.G. and DIAGUILA

Convective heat transfer for mixed free and forced flow through tubes.

Trans. Am.Soc. Mech. Engrs. 76, 497, 1954.

179. CHURCHILL, S.W. and BRIER, J.C.

Convective heat transfer from a gas stream at high temperature to a circular cylinder normal to the flow.

Heat transfer - Chem. Eng. Prog. ser. 51 57 (1955).

180. GLADSTONE. S. and LEWIS, D.

Elements of physical chemistry, (second Edition).

MacMillan and Co. Ltd., 1964.

181. CRC Handbook of Chemistry and Physics, (53rd Edition)

The Chemical Rubber Co., 1972-1973.

182. SPALDING, D.B.

Some fundamentals of combustion.

Butterworth Scientific Publications, 1955.

183. SCHACK, A.

Industrial heat transfer.

John Wiley and Sons, Inc. 1933, p. 114.

TABLE 1*

Emissivity	B'
0.000	4.000 B
0.149	3.9207 B
0.300	3.8300 B
0.648	3.5010 B

*From Reference 26.

TABLE 2*

	Type of flame	Average particle diam. μm	k_o	visible		infrared	
				a	b	a	b
1	Acetylene	2.0	11.7	0.8	0	0.83	0.25
2	Stearene/Paraffin	12.5	9.9	1.20	0	1.12	0.45
3	Amyl Acetate	25.0	8.6	1.35	0	1.20	0.55

*From Reference 71.

TABLE 3*

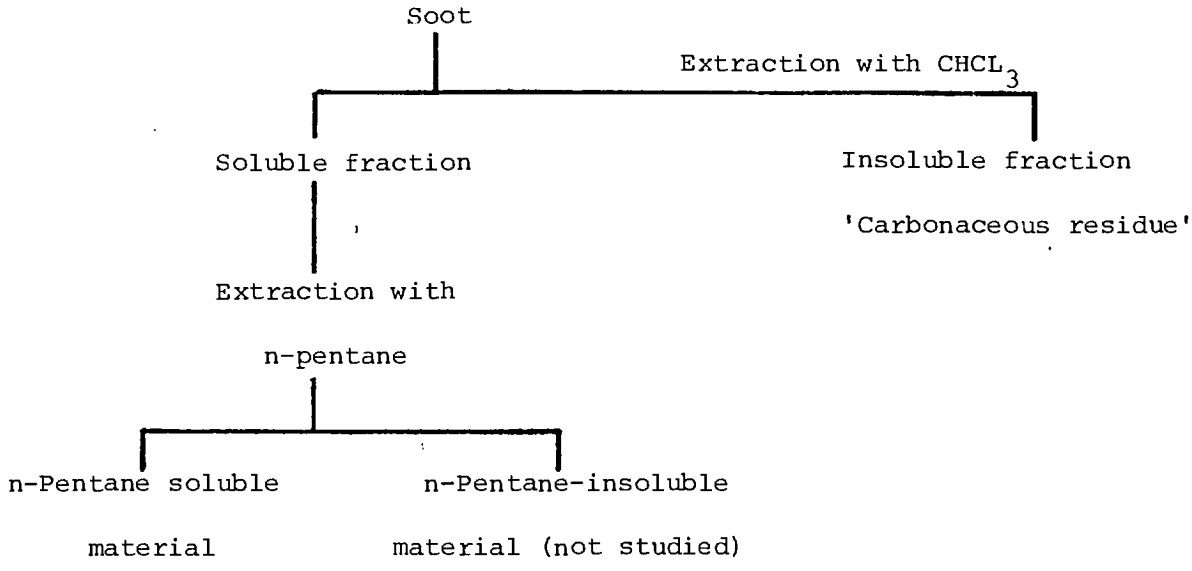

*from ref. 37

TABLE 4

Experimental conditions	window 1	window 2	window 3	window 4
Control	deep yellow-ish green colour	yellow colour	pale or straw yellow	colourless
22.2 mg/sec oxygen.added to fuel.	"	plane or straw colour	colourless	colourless
44.4 mg/sec oxygen to fuel	"	very faint yellow colour	colourless	colourless

*Colour is an indication of the extent of adsorbed hydrocarbons.

TABLE 5

List of symbols used to define the experimental conditions.

Expt.	Symbol	Additive and position of addition	Level
1	•	Control(None)	None
2	○	Oxygen to the fuel	4.4 mg/sec
3	□	" " " "	8.9 " "
4	△	" " " "	13.3 " "
5	◇	" " " "	16.9 " "
6	●	Oxygen to the fuel	22.0 " "
7	■	" " " "	44.0 " "
8	×	Heat to the air by raising its temperature to	323 K
9	▽	Heat to the air by raising its temperature to	373 K
10	▼	Heat to the air by raising its temperature to	423 K
11	▲	$CC\ell_4$ to the fuel	0.029 mole/h

Note: Symbols a to d inside figures 252, 260, 263, & 264 also denote window numbers i.e. 1 to 4 respectively.

⬢ Represents values calculated using ε_g = .028 (see p. 172)

W = window.

TABLE 6

z(mm)	T	C/H ratio	λ
7.5	1680	1.95	2.03
10.0	1640	2.20	1.79
12.5	1570	2.80	1.62
15.0	1530	3.21	1.50
17.5	1460	3.61	1.45
20.0	1415	4.02	1.42
22.5	1360	4.33	1.42

TABLE 7

Window No.	$\varepsilon_T = 1-(1+k_m\bar{c}L)^{-4}$		$\varepsilon'_T = 1-\exp(-k'_m\bar{c}L)$		k'_m/k_m	$B/c_2 \times 10^4$
	k_m	ε_g	k'_m	ε'_g		
1	.01991	.028	.07746	.028	3.89051	.167 - .140
2	.03415	.009	.13291	.009	3.89195	.322 - .213
3	.00028	.045	.00112	.045	4.0000	.003 - .002
4	.00268	.027	.01122	.026	4.18660	.036 - .025

Ref. No.	Source	Flame type	type of burner	FUEL		OXIDANT		Method(s) of Analysis	Position (s) studied	Comments
				type	Additives	Type	Additives			
119	IYENGAR et al (1952)	diffusion	a wick in a modified spirit lamp	Liquid hydrocarbons, alcohols, ketones & ethers.	N_2 & CO_2	air		Visual(?)	flame	Reduction of luminosity $(\frac{1}{\text{molec.wt.fuel}})^2$
40	ARTHUR & NAPIER (1955)	diffusion	tubular	CH_4	CO_2, H_2 CO_2 & SO_2	air		Photocell	flame	•Efficieny of additive to reduce luminosity $SO_2 > CO_2 > N_2 > CO$ •Inhibiting efficiency is not proportional to heat capacity.
76	LEWES (1892)	premixed	a bunsen burner	coal gas oil gas	N_2, CO_2	air	N_2, CO_2	Visual (?)	flame	•Effect of dilution is decreased by temperature increase. •Formation of C_2H_2 is retarded by dilution. CO_2 more effective than N_2 in making flames non-luminous.
120	VAERMAN	confined diffusion	tubular	C_3H_8 C_4H_{10}	CO_2, N_2 Ar, H_e	air	-	smoke point visual(?)	flame tip	•Efficiency of additives in increasing the amount of hydrocarbon before the flame smoked. $CO_2 > N_2 > Ar > H_e$.

Note ? When it had not been specified by the author(s).

TABLE 8

Ref. No.	Source	Flame type	type of burner	FUEL type	FUEL Additives	OXIDANT Type	OXIDANT Additives	Method(s) of Analysis	Position(s) studied	Comments
122	SZARVASY (1921)	pyrolysis tube	tubular	CH_4	N_2,H_2 & CO_2	-	-	Electron microscopy(?)	tube exist	•Dilution reduced particle size.
124	THORP et al (1951)	pyrolysis tube	tubular	C_6H_6	N_2 and H_2 as carrier gas	-	-	Weighting or visual(?)	tube exit	•Replacement of N_2 by H_2 reduced solid deposition to a greater extent.
125	BOSSE (1961)	confined diffusion	tubular	A number of hydrocarbons		-	-	weighing (cold surface)	flame tip or near end	•Soot formation increased with total C/H ratio of fuel and additive combusted.
121	HERBST (1963)	confined diffusion	tubular	cookery gas	H_2,N_2,CO, CO_2,O_2 & air. H_2O 3% C_2H_6	air	-	photocell and weighing(cold surface)	at one position in flame	•Moisture content of fuel is critical. Soot reducing efficiency O_2> CO_2> air >N_2> CO > H_2, upon addition of 3% C_2H_6 to the basic gas, the effectiveness of CO_2 and air were reversed as well as N_2 and CO. •The decrease in soot yield is > than due to dilution only, indicating the effect on combustion.

TABLE 8 (cont'd)

Note ? When it had not been specified by the author(s).

Ref. No.	Source	Flame type	type of burner	FUEL		OXIDANT		Method(s) of Analysis	Position (s) studied	Comments
				type	Additives	Type	Additives			
107	DEARDEN & LONG(1968)	flat diffusion	Wolfhard & Parker	C_3H_8, C_2H_4	O_2,H_2 H_2,C_2H_2	air	oxygen	weighing (filtration)	exhaust	• O_2 increased the sooting rate, except when added to the fuel side of C_3H_8 flame
35	CHAKRABORTY & LONG(1968)	"	"	C_2H_4 C_2H_6	oxygen	air	-	"	exhaust	• Oxygen decreased the amount of polimeric material deposited with soot.
126	BRADLEY & DEARDEN (1972)	Pyrolysis tube		C_3H_6	Ar,Ne, O_2	-	-	chemical analysis	tube-exit	• Oxygen slightly promotes initial reaction
127	KING(1973)	Enclosed diffusion	T-piece on which a no. of small flames burned.	Pure H_2 CO,CH_4 C_2H_6, C_2H_2, C_2H_4	H_2O	air	-	spectral & thermocouple	flame	• Moisture in the fuel 20% by vol. decreased both soot emission as well as flame temperature.
128	MULLER-DETHLEFS &SCHLADER (1976)	Premixed	bunsen-type	C_3H_8, C_2H_4	-	air	H_2O vap	Photography & other.		• H_2O vap. inhibited soot formation and increased heat released. This partly made up for its cooling effect. • Evidence of the role of OH radical in inhibiting soot formed.

TABLE 8 (cont'd)

Ref. No.	Source	Type of flame	Type of burner	FUEL		OXIDANT		Method(s) of analysis	Position(s) studied	Comments
				Type	Additive	Type	Additive			
130	GAYDON & WHITTING-HAM(1947)	premixed	Quartz jet bunsen burner	CO, H_2, CH_4, C_2H_4, CH_3OH & coal-gas	SO_2 H_2S	air	-	spectral, chemical analysis	flame	• SO_2 & H_2S decrease soot formation. • SO_3 increases soot formation, however, this effect is relatively much greater than the decrease above.
61	PARKER & WOLFHARD (1950)	diffusion	Wolfhard& Parker	?	?	?	-	?	?	• SO_2 & SO_3 had no effect on luminosity observed.
129	SCHERER & TRANIE (1973)	domestic oil boilers		fuel-oil emulsion	water	air	-	weighing(?)		• Reduction of fuel drop is achieved which reduced flame pollution
132	IBIRICU & GAYDON (1964)	diffusion	parallel counter-flow	C_2H_4, CH_4 and H_2	CH_3Br, Br_2, CCl_4 Cl_2, $PoCl_3$	air	CH_3Br, Br_2 CCl_4, Cl_2 $PoCl_3$	emission spectra, temperature measurements chemical analysis	flame	• An increase in soot luminosity occurred in general which was accompanied by a reduction in temperature. • Flame extinction is due to a temperature effect. • $PoCl_3$ most effective inhibitor. • Generally strongest inhibiting effect when additives were introduced on the fuel side.

Ref. No.	Source	Type of flame	Type of burner	FUEL Type	FUEL Additives	OXIDANT Type	OXIDANT Additives	Method(s) of analysis	Position(s) studied	Comments
133	BADAKH-SHAN (1957)	enclosed diffusion	tubular	Butagas Kerosine N-heptane methyl-cyclohexane	CH_2Cl_2 $CH\ Cl_3$ Ccl_4 CH_2ClB_r $C_2H_4Br_2$	air	CH_2Cl_2, $CHCl_3$ Ccl_4, CH_2ClBr $C_2H_4Br_2$	Weight analysis (filtration)	exhaust	• Rate of soot formation increased with carbon content, C/H ratio and type of halogen in fuel (i.e. Br > Cl).
137	SIMMONS & WOLFHARD (1956)	diffusion	Wolfhard & Parker	CH_4, C_2H_6, C_2H_4, C_2H_2	CH_3Br Br_2	air	CH_3Br, Br_2	spectroscopic	flame	• Soot formation increase • Structure of flame is altered. • When CH_3Br was added to the air side, an induced reaction was formed.
134	ARTHUR et al (1949)	pyrolysis - tube		carbon		dry air	$POCl_3$, Cl_2, PCl_3, Ccl_4, $CHCl_3$, HCl, $SnCl_4$, CH_2Cl_2, I_2, H_2SO_3, H_2O	chemical analysis	tube exit	• Additives increase concentration in exit gas of CO & O_2 at the expense of CO_2. • Addition of H_2O or H_2 greatly reduced the extent of inhibition.
135	MERTENS & HELLINCKX (1949)	pyrolysis - tube		carbon		moist oxygen	-	"	"	• Additives reduced conversion of $CO \rightarrow CO_2$

TABLE 8 (cont'd)

Ref. No.	Source	Type of flame	Type of burner	FUEL		OXIDANT		Method(s) of analysis	Position(s) studied	Comments
				Type	Additives	Type	Additives			
37	RAY & LONG (1964)	enclosed diffusion	tubular	"Bottogas" propane	i) CH_2Cl_2 ii) nitro paraffins alkyl-nitrates. iii) butylhydro-peroxide	air	-	weight (filtration)	exhaust	i) increased both soot & carbonaceous residue insoluble in chloroform. ii) decreased amount of polycyclic aromatic hydrocarbons. iii) decreased both soot and carbonaceous residue insoluble in chloroform. The latter did not vary in diesel engine experiments.
112	CHAKRABORTY & LONG (1968)	flat diffusion	Wolfhard &Parker	C_2H_4	CH_3OH	Oxygen or air	-	weight (filtration)	exhaust	•decreased both soot and polycyclic aromatic hydrocarbons.
60	TESNER (1960)	diffusion	tubular	CH_4	N_2, H_2 C_2H_2, C_6H_6 $C_{10}H_8$	air	-	weight	various positions along the flame	•The soot yield decreased with addition of N_2 or H_2. •The specific surface area was on the other hand increased. •Addition of hydrocarbons increased the yield and decreased the specific surface area of soot.

TABLE 8 (cont'd)

Ref. No.	Source	Type of flame	Type of burner	FUEL Type	FUEL Additive	OXIDANT Type	OXIDANT Additive	Method(s) of analysis	Position(s) studied	Comments
131	COTTON et al(1971)	enclosed diffusion	tubular	C_3H_8	N_2,H_2O, salts of alkaline earths and other metals (atomiser)	O_2	-	weight analysis	exhaust	•Soot reduction occurs by at least two mechanisms. •Type of cation in metal is important. •A combination of additives is more effective inhibitor. •Reduction of soot by NO & SO_2 is very small Anti smoke effecting e.g. Ba > Cs
113	BARTHOLOMÉ & SACHSSE (1949)	reaction furnace of synthesis gas process		Ni in various forms was added to catalyst bed and to gaseous space between gas and catalyst. Many compounds, e.g. alkalis and alkaline-earths.				visual & weight analysis	catalyst bed, soot-laden gas exhaust.	•Ni reduced soot on surface of catalyst and at exit. •Alkaline and alkaline-earths suppress soot formation completely. •Inhibition is electrostatical. •Phenomenon explained on basis of competition between coagulation and abrasion.
140	ADDECOTT & NUTT (1969)	i) flat diffusion ii) reversed premixed.	parallel counter flow	C_2H_4+ 10% C_6H_6+ N_2	alkali & alkaline earths (atomiser)	O_2	-	weighing (filtrations) mass spectrometer.	exhaust flame	• Effectiveness proportional to destruction of soot nuclei those which are effective in reducing soot reduce natural ion concentration - each metal group to be compared separately.

TABLE 8 (cont'd)

Ref. No.	Source	Type of flame	Type of burner	FUEL		OXIDANT		Method(s) of analysis	Position(s) studied	Comments
				Type	Additives	Type	Additives			
138	CREITZ (1961)	enclosed diffusion	tubular	C_2H_6, H_2, C_3H_8, C_4H_{10} CO, natural gas	CH_3Br, CF_3Br, N_2	various mixtures of O_2 & N_2	CH_3Br, CF_3Br	visual	flame	• O_2+N_2 mixture affects efficiency of inhibitors especially at O_2/N_2 concentrations less than in air. • Halogenated additives were more effective inhibitors when added to oxygen side of reaction zone.
96	PLACE & WEINBERG (1966)	flat horizontal diffusion	parallel counter-flow	$C_2H_4+N_2$	CsCl	O_2+N_2	–	weighting & electron microscope	along the flame & exhaust	• Positive ions, either flame ions or from thermal ionisation of CsCl may act as a nucleus. • Manipulation of nucleation growth and rate of deposition using electric field.
139	SALOOJA (1973)	premixed bunsen type	tubular	ethylene, propane, isobutane butene-1, isobutene	quartz fibre coated in alkalis & alkaline earths	air	see under fuel	Smoke point	along flame & exhaust	• Additives decreased soot formation in premixed regions and increased it in diffusion flame (surrounding premixed flame). • Mixtures of additive produced higher effect than combined individual effect • Catalytic activities correlate with ionisation tendencies of atoms.

TABLE 8 (cont'd)

Ref. No.	Source	Type of flame	Type of burner	FUEL		OXIDANT		Method(s) of analysis	Position(s) studied	Comments
				Type	Additive(s)	Type	Additive(s)			
114	BOWSER & WEINBERG (1973)	flat diffusion	fish-tail nozzle	C_3H_8 + Ar	Ni wire coated with BaO	air	see fuel	Photography Effect of electric field	flame	• Pro & anti soot effects of ionising metals can be described in terms of electrons they produce. • Metal is not expected to melt at flame temp.
143	BULEWICK et al (1974)	Premixed flat enclosed (position of fuel & oxidant reversed in some cases)	tubular	C_2H_2, C_3H_8 + N_2 (diluent)	mainly alkalie & Alkaline earths (atomiser)	O_2		weighing (filtration) electron microscopy measurement of ion concentration	exhaust flame	• Anti-soot effect due to neutralization of ions by M^+ • Pro-soot effect based on a sudden increase in M^+ • Soot particle size collected decreased in either cases. • Anti smoke effect e.g. Ba > Cs.
141	FEUGIER (1973)	enclosed premixed	tubular	C_2H_4	see under oxidant	Oxygen + nitrogen mixture	alkalie metals (atomiser)	optical (extinction)	burnt gas	• A metal may have dual effect. • Promoting effect was proportional to metal ionisation potential; occurred when metal ion was greater than a critical amount. • Inhibition due to formation of OH radical.

TABLE 8 (cont'd)

Ref. No.	Source	Type of flame	Type of burner	FUEL Type	FUEL Additives	OXIDANT Type	OXIDANT Additives	Method(s) of analysis	Position(s) studied	Comments
142	FEUGIER (1975)	enclosed premixed	tubular	C_2H_4	see under oxidant	O_2+N_2 mixture	alkalie metal, alkaline earth metals	optical	burnt gas	• At small ϕ^*, Cs, K, N soot increased with concentration of metal • Li, Ba, Sr, & Ca produced in general a net inhibiting effect except Ba wh which had a promoting effect.
145	ZALAVADIA & DEWERTH (1966)	turbulent	commercial nozzle-mixing dual fuel burner	natural gas & air additives: i) coke, charcoal, coal & gas. ii) lime, silica iii) injection of fuel perpendicular to flame flow.				optical (total red pyrometer)	4 positions along flame	• Group (i) much more effective than (ii) in increasing radiation. • (i) increased total heat & CO_2 emission. • (ii) useful when added to flames which heat material like glass. • (iii) caused small increase in radiation.
146	SATO & KUNITOMO (1965)	non-luminous turbulent	nozzle-mixing facing down	town gas/oxygen(non-luminous), carbon ferric oxide, converter ash, diatomaceous earth and boiler ash.				optical, thermo-couple & weight analysis.	flame & exhaust	• Flame temperature decreased with additive concentration • In the case of boiler ash ε increases with decrease in temperature unlike in the case of carbon

*Φ = stoichiometric air/actual air

TABLE 8 (cont'd)

Ref. No.	Source	Type of flame	Type of burner	FUEL		OXIDANT		Method(s) of analysis	Position(s) studied	Comments
				Type	Additive(s)	Type	Additive(s)			
148	GUYOMARD (1951)	laminar & turbulent diffusion	tubular	town gas, H_2	preheating C_6H_6 (to fuel or air?)	air	preheating	using various pyrometers	flame	•Addition of around 7% benzene to either flame was much more effective than preheating air of fuel or both above 500°C
149	GUENEBAUT & GAYDON (1954)	premixed	tubular	CH_4	heat	air	heat	pyrometer and Schlieren photography	various positions along flame	•Preheating lengthened & thinned flame. Inner cone shortened. •Average radiation change was negligible

TABLE 8 (cont'd)

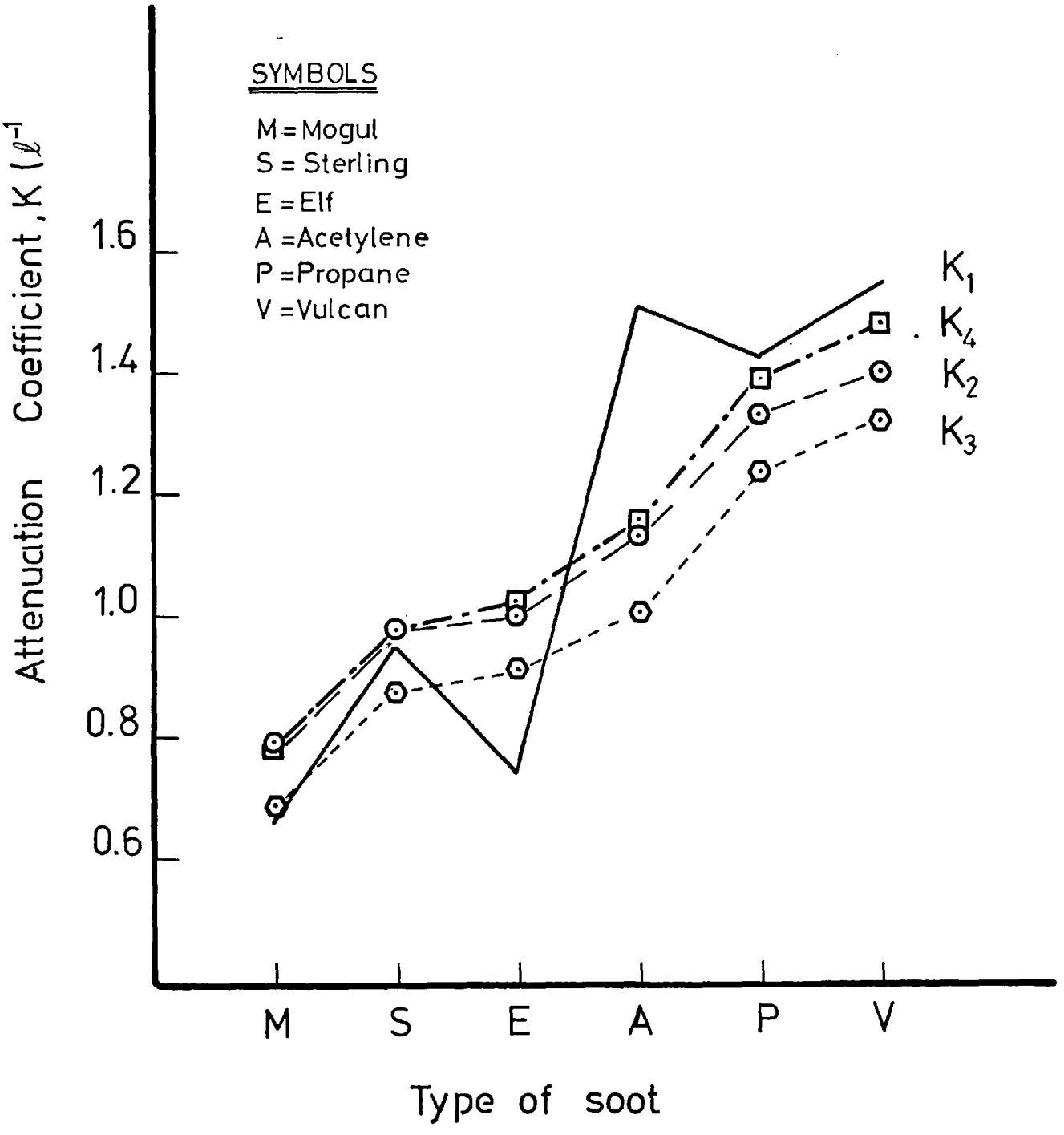

Fig (1) Attenuation coefficients of some soots.

(Data from ref. 12.)

[a] L = 0.2 m
[b] L = 0.5 m
[c] L = 1.0 m

} T = 1600 K

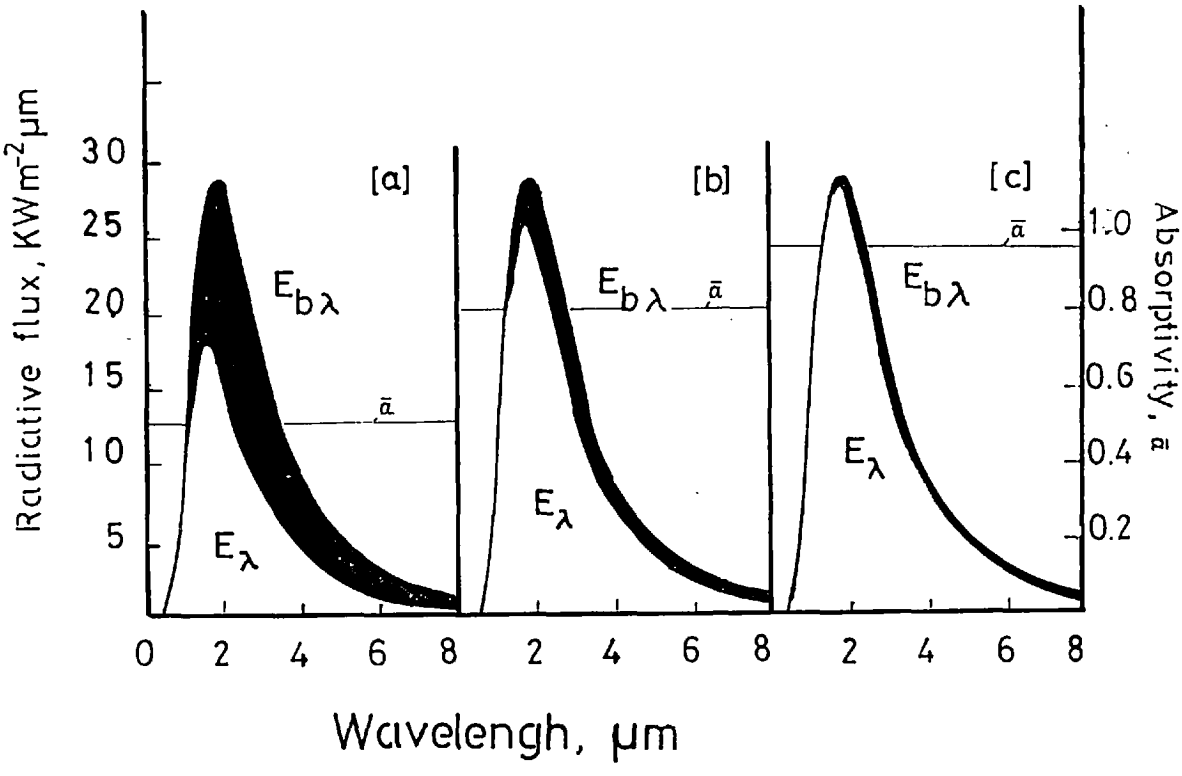

Fig(2) Effect of cloud thickness on radiation.

(From ref. 71.)

FIGURE 3

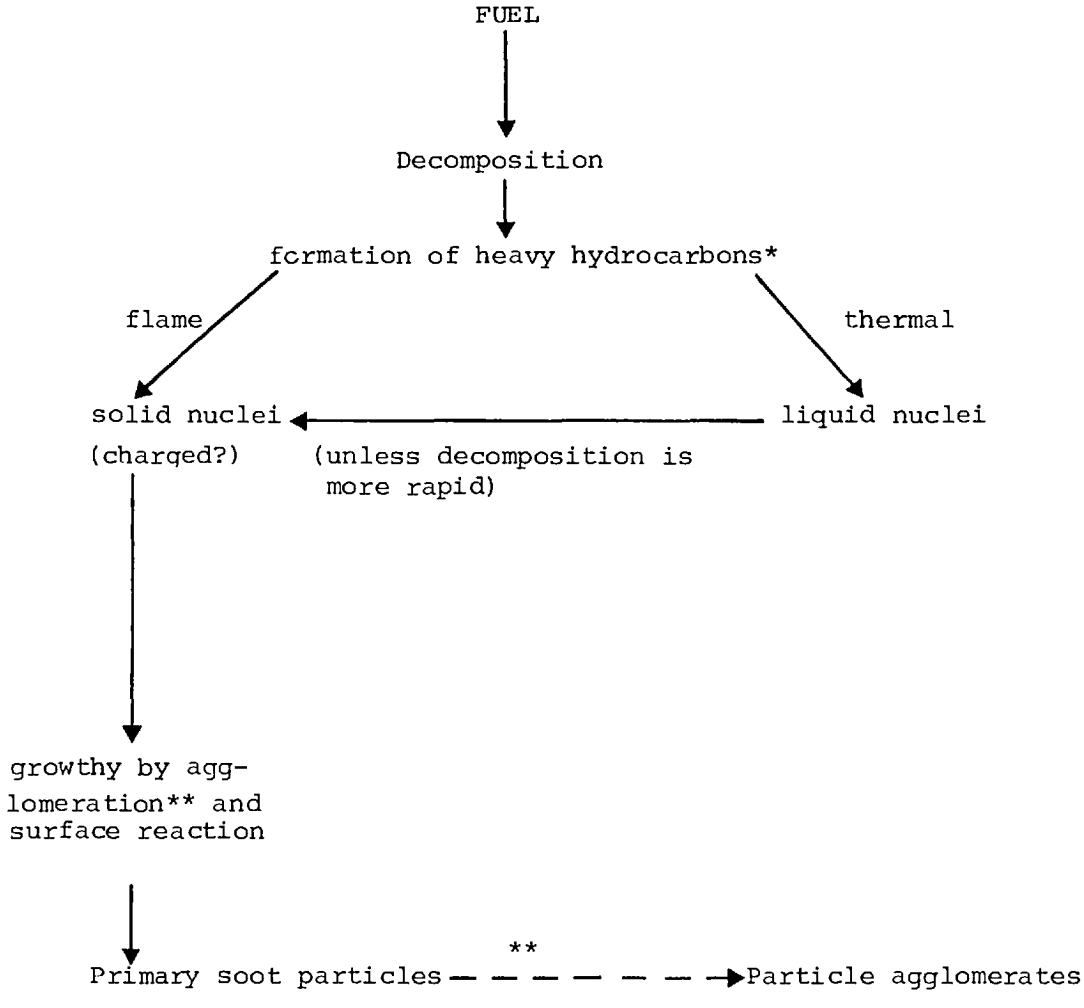

* precursors of soot nuclei influenced by type of fuel, i.e. aliphatic or aromatic

** influenced by charge on particles.

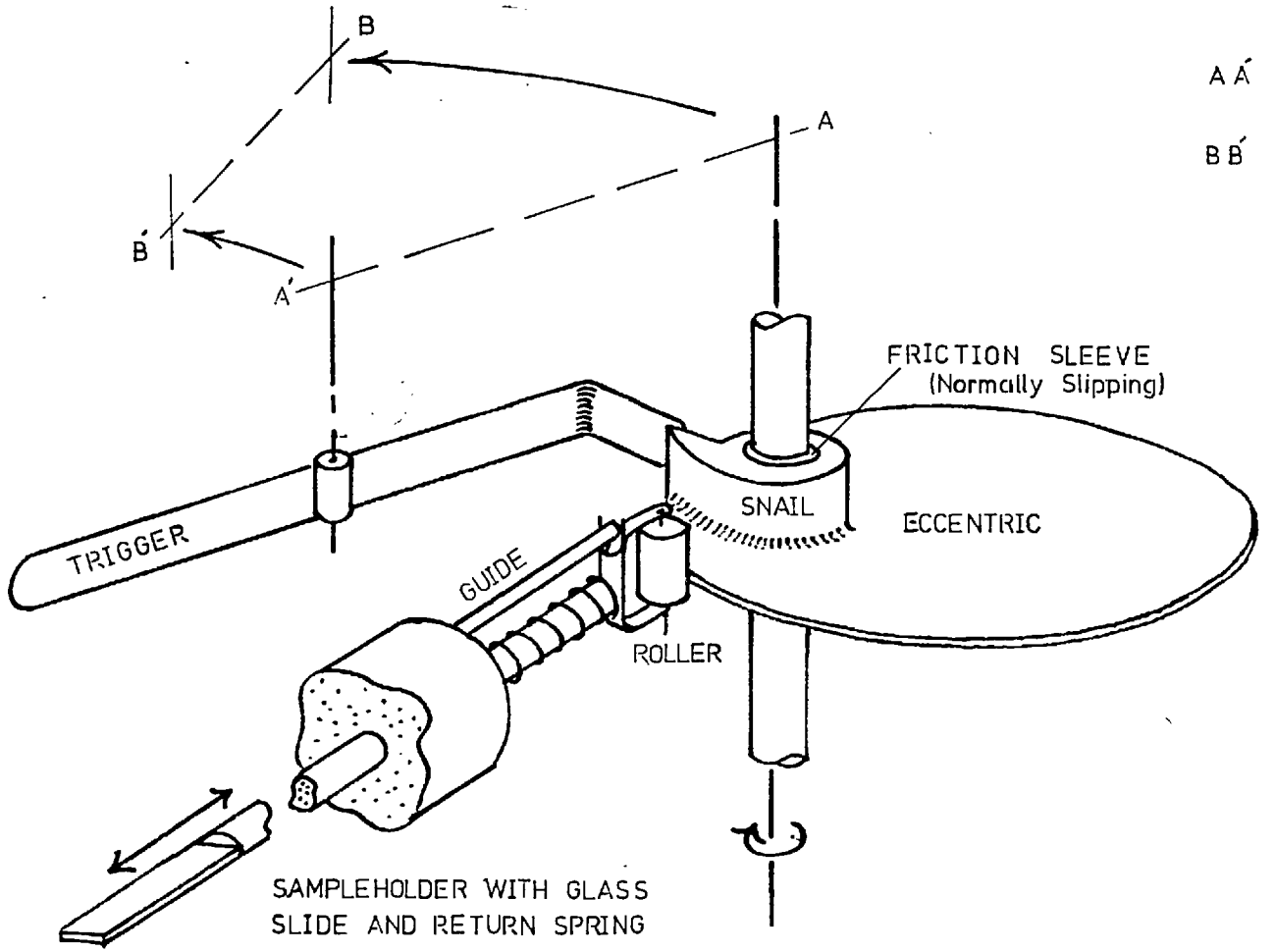

Fig(4) Details of a unit of the mechanical sampler.

A A' RUNNING POSITION FOR TRIGGER AND SHAFT

B B' LOADING POSITION

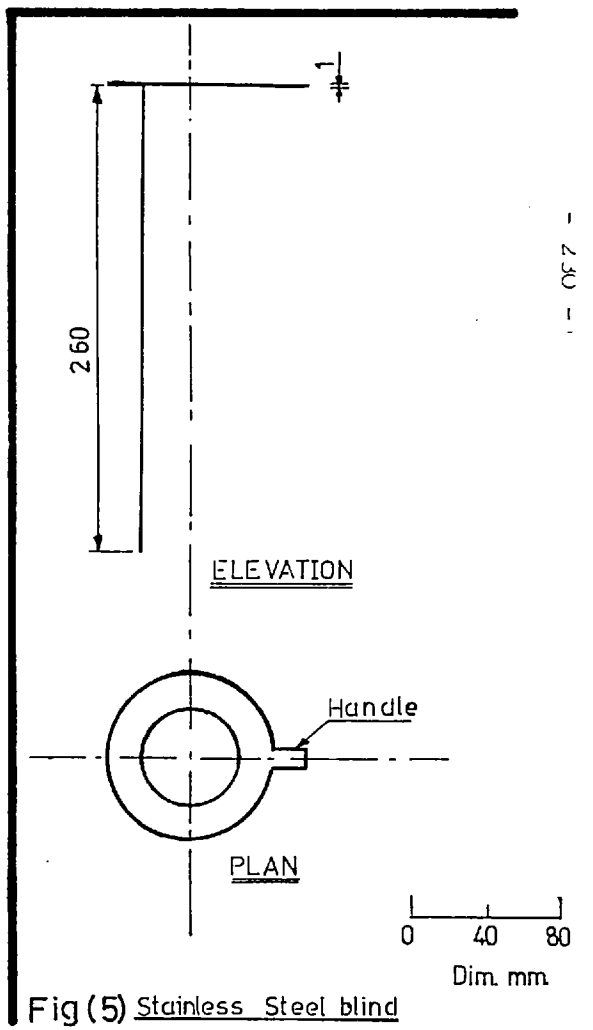

Fig (5) Stainless Steel blind

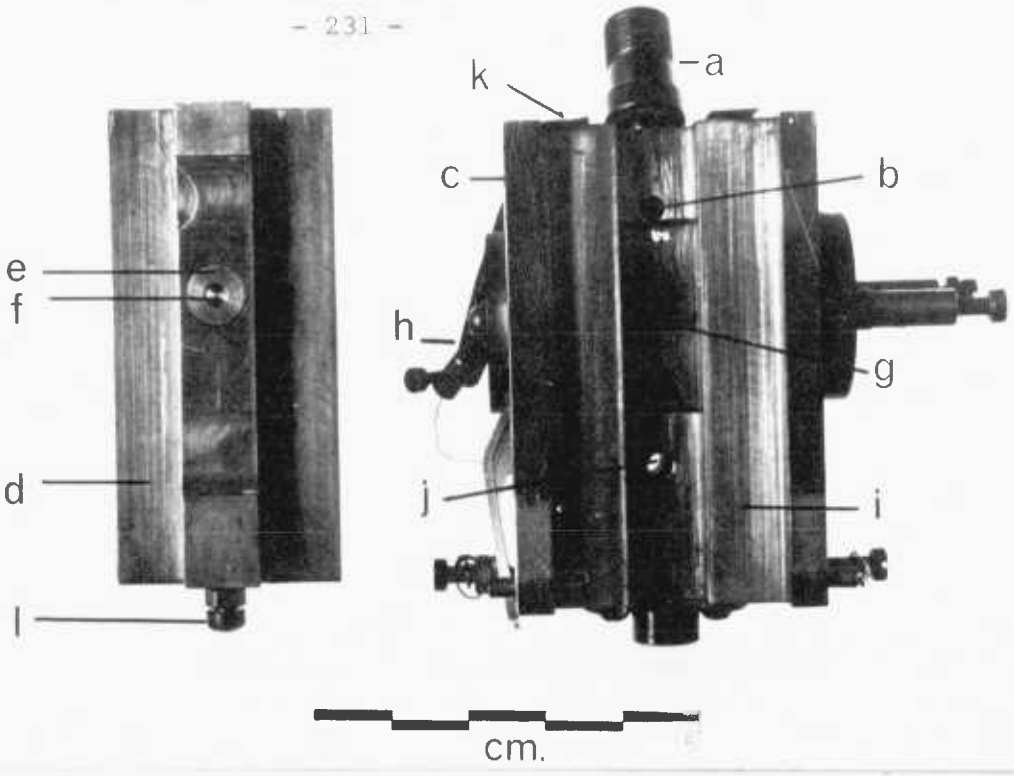

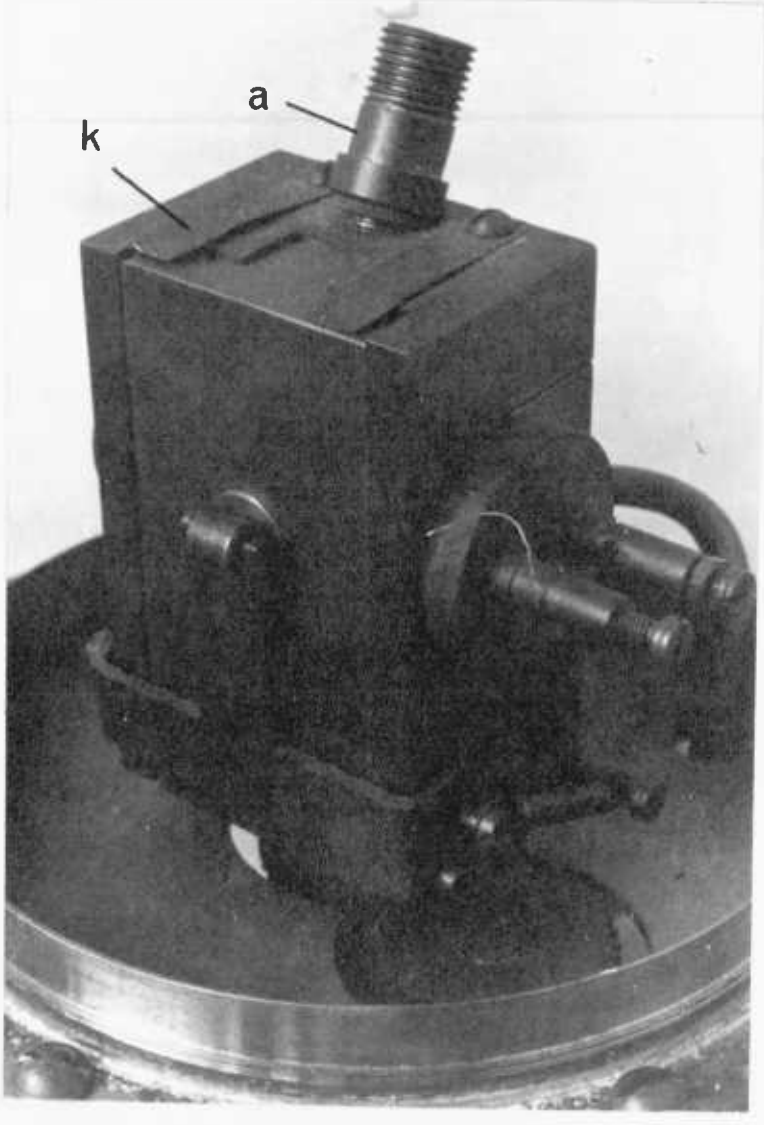

Fig(6) Oscillating thermal precipitator.

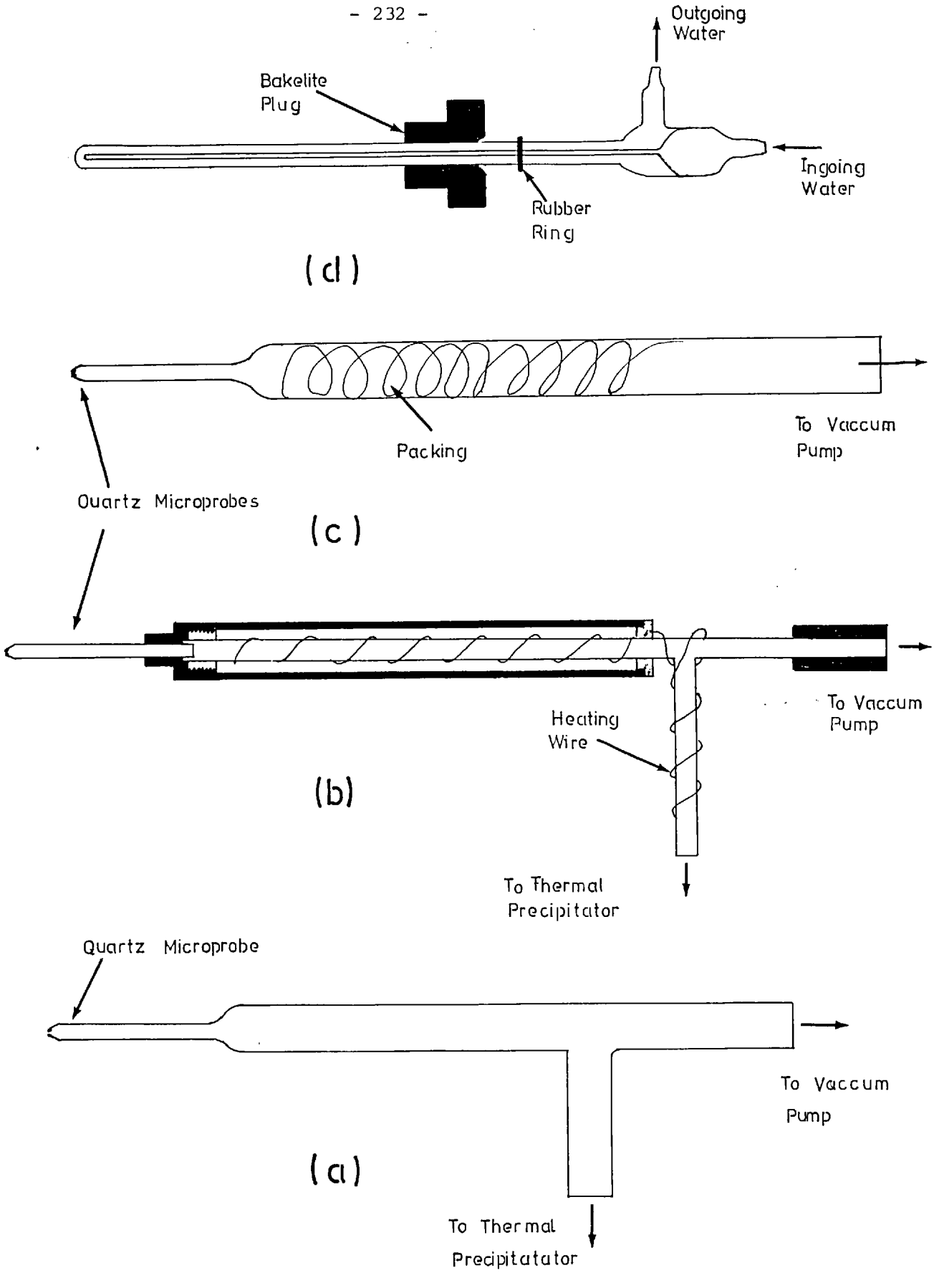

Fig(7) Sampling probes.

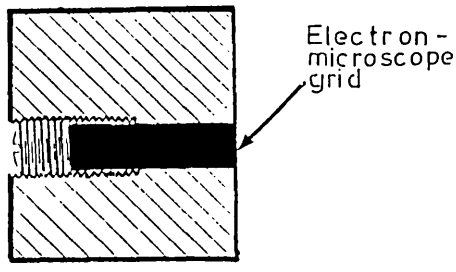

b) Grid holder in thermal precipitator.

ref (154)

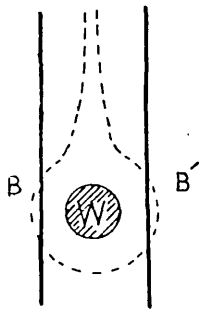

c) Schematic representation of the dust-free space.

(W = wire.) ref (155)

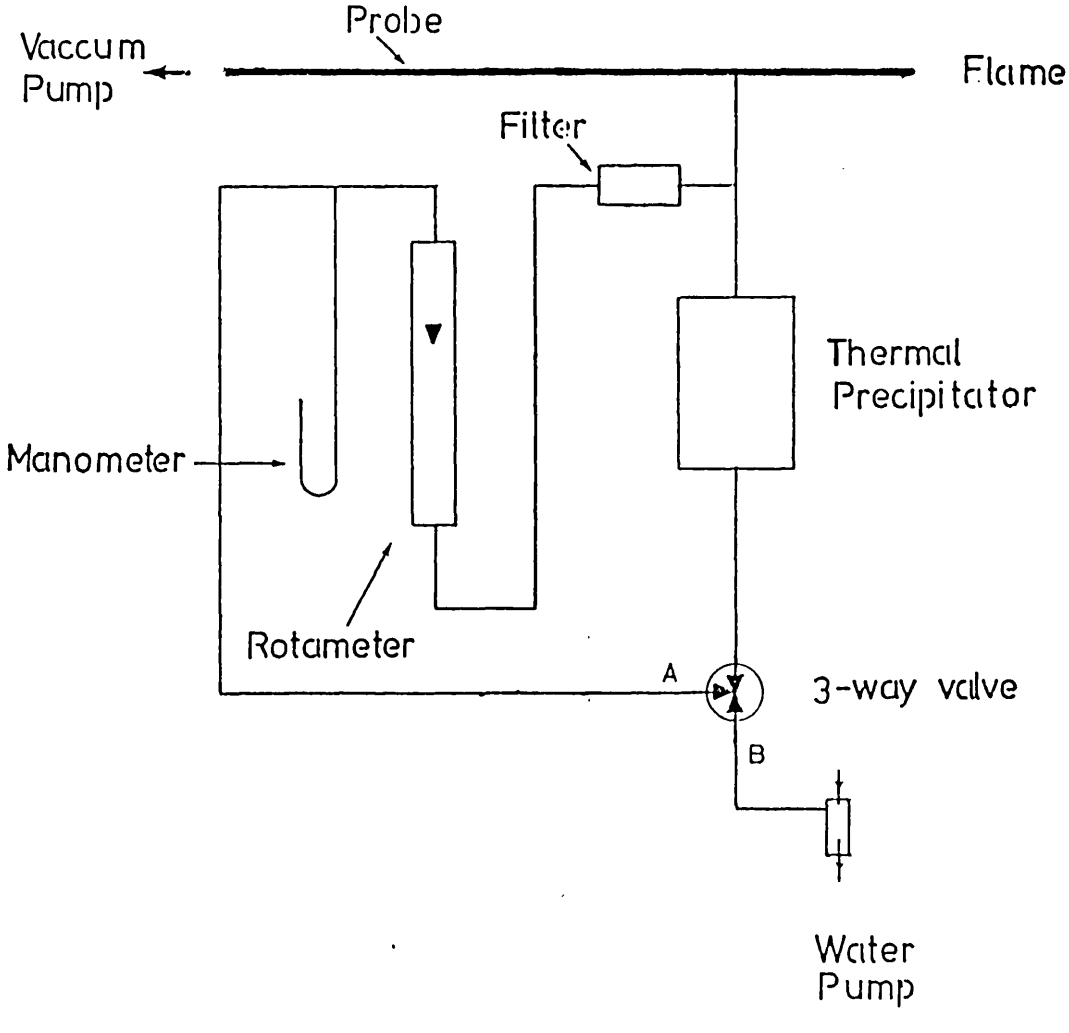

(a) Schematic representation probe and oscillating thermal precipitator.

Fig (8)

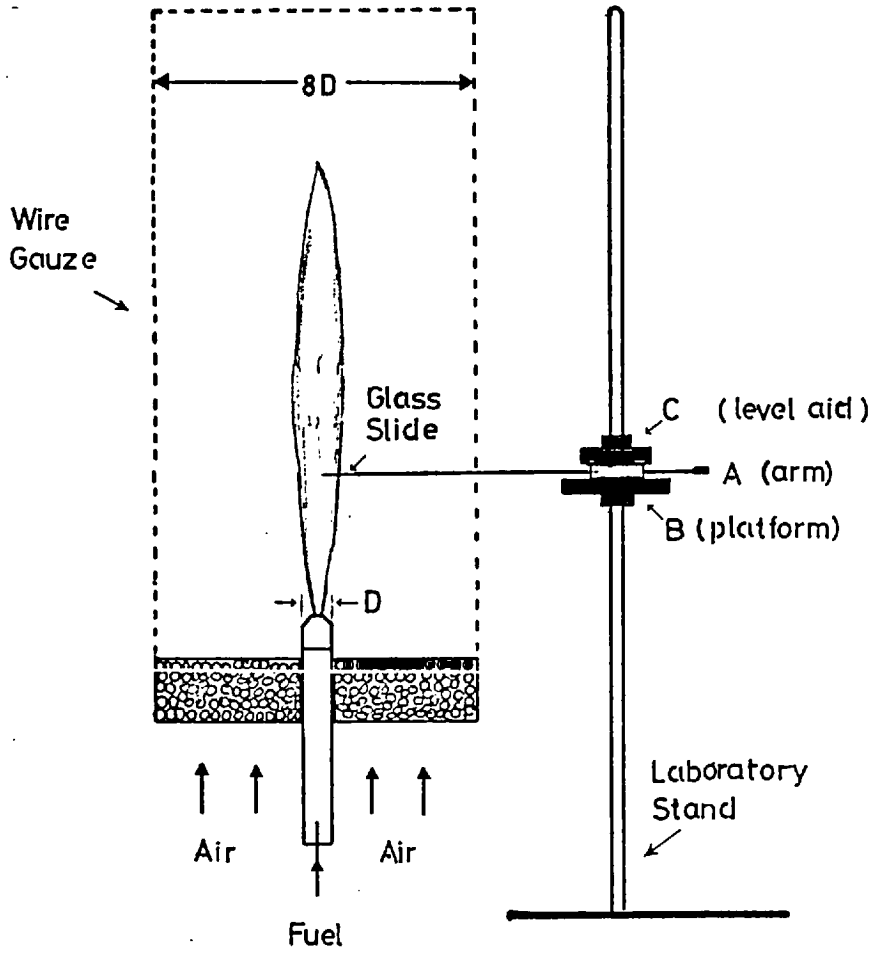

Fig(9) Schematic representation of sampling from a free-flowing diffusion flame.

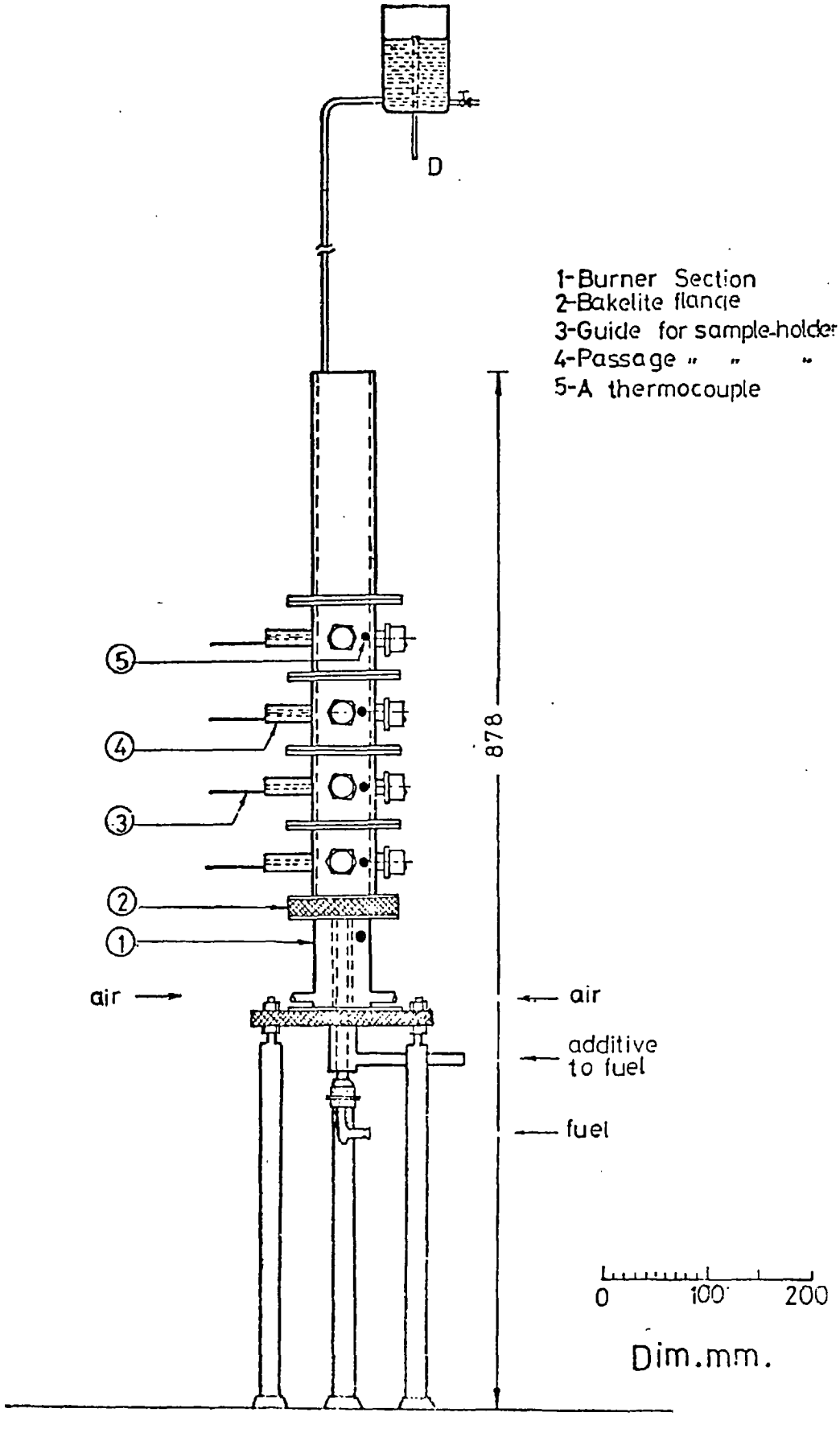

Fig (10) A general outline of the apparatus.

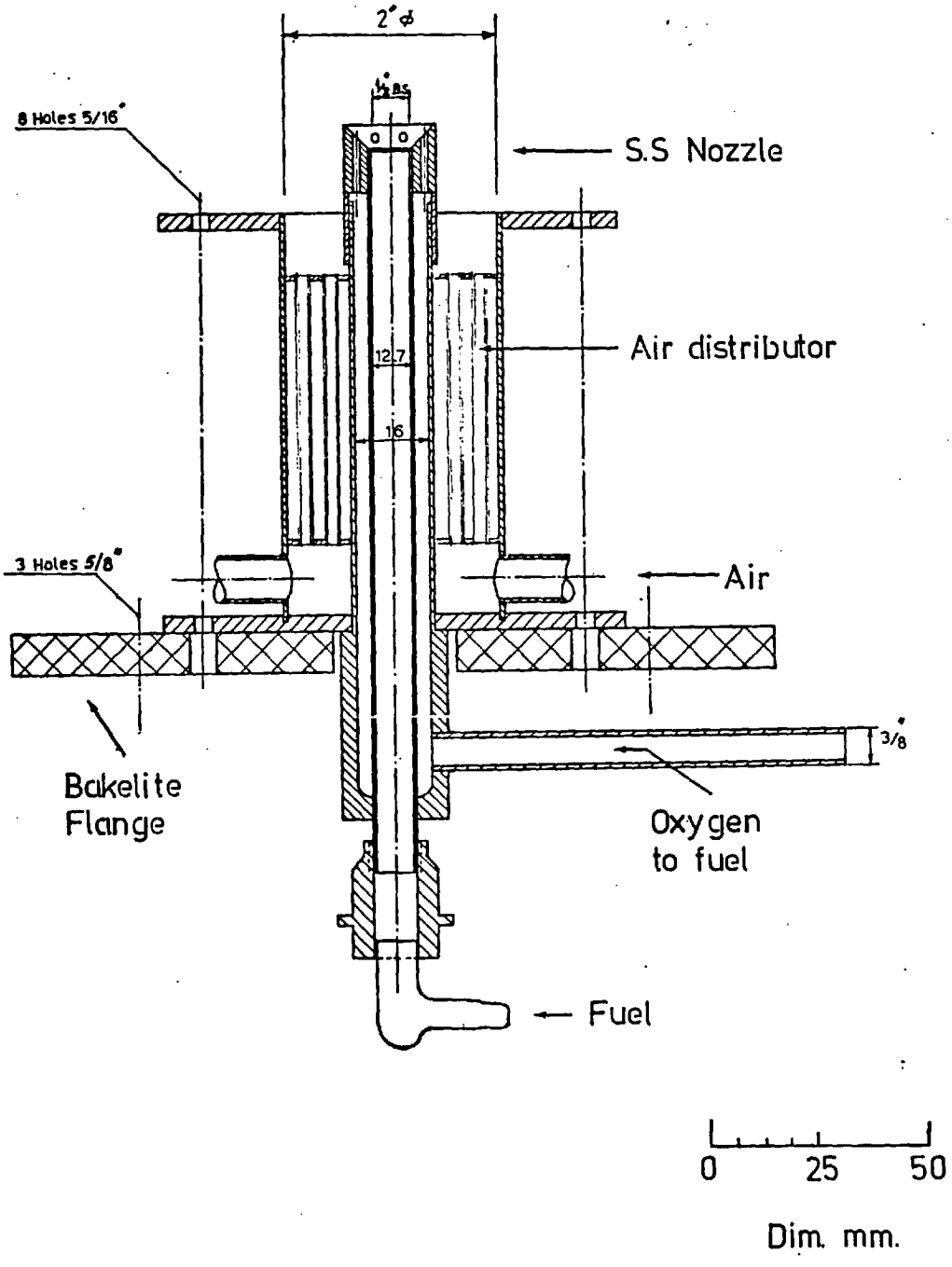

Fig(11) A vertical section through the burner.

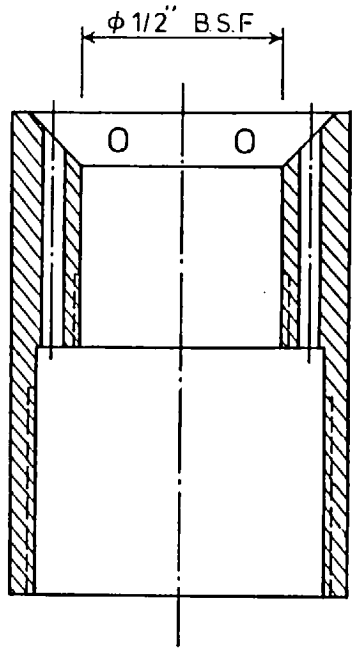

Section Elevation

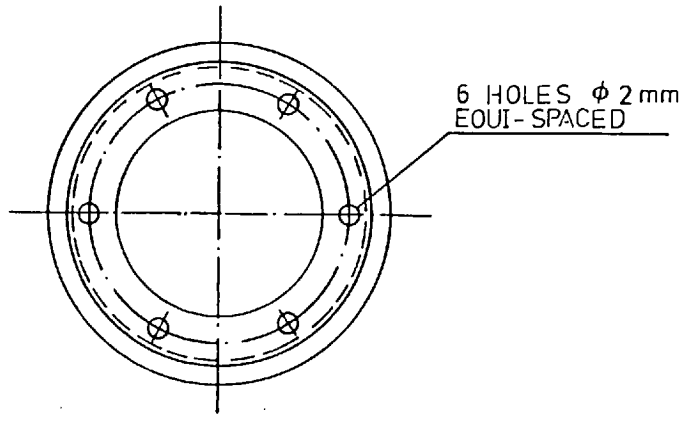

Plan

Scale 2:1
Dim. mm.

Fig (12) Details of the nozzle.

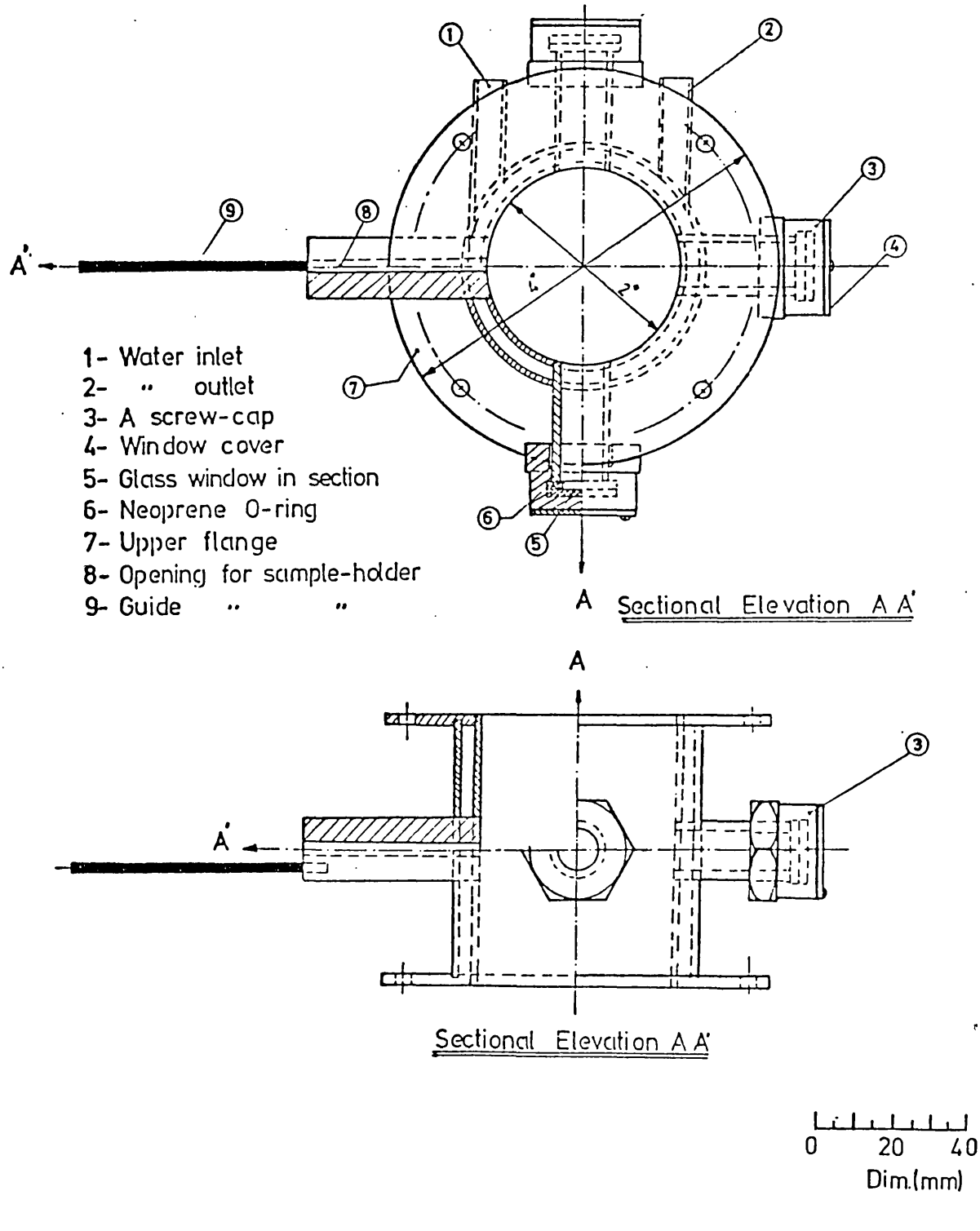

Fig (13) Details of a water calorimeter.

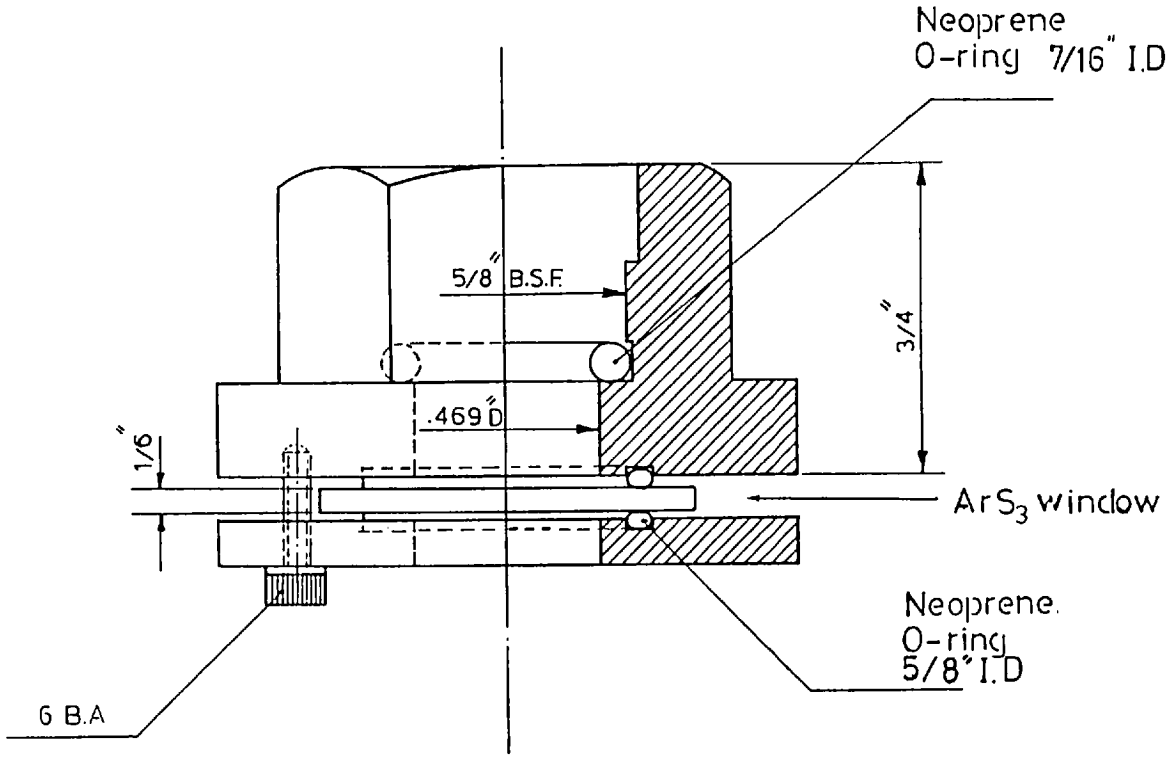

Half Section Elevation

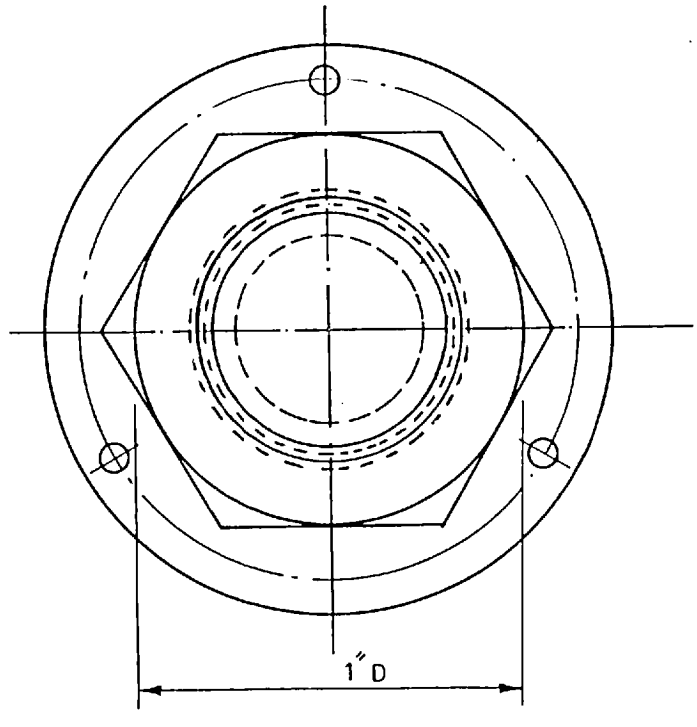

Plan

Scale 2:1
Dim. Inch.

Fig (14) Details of cap holding ArS_3 window.

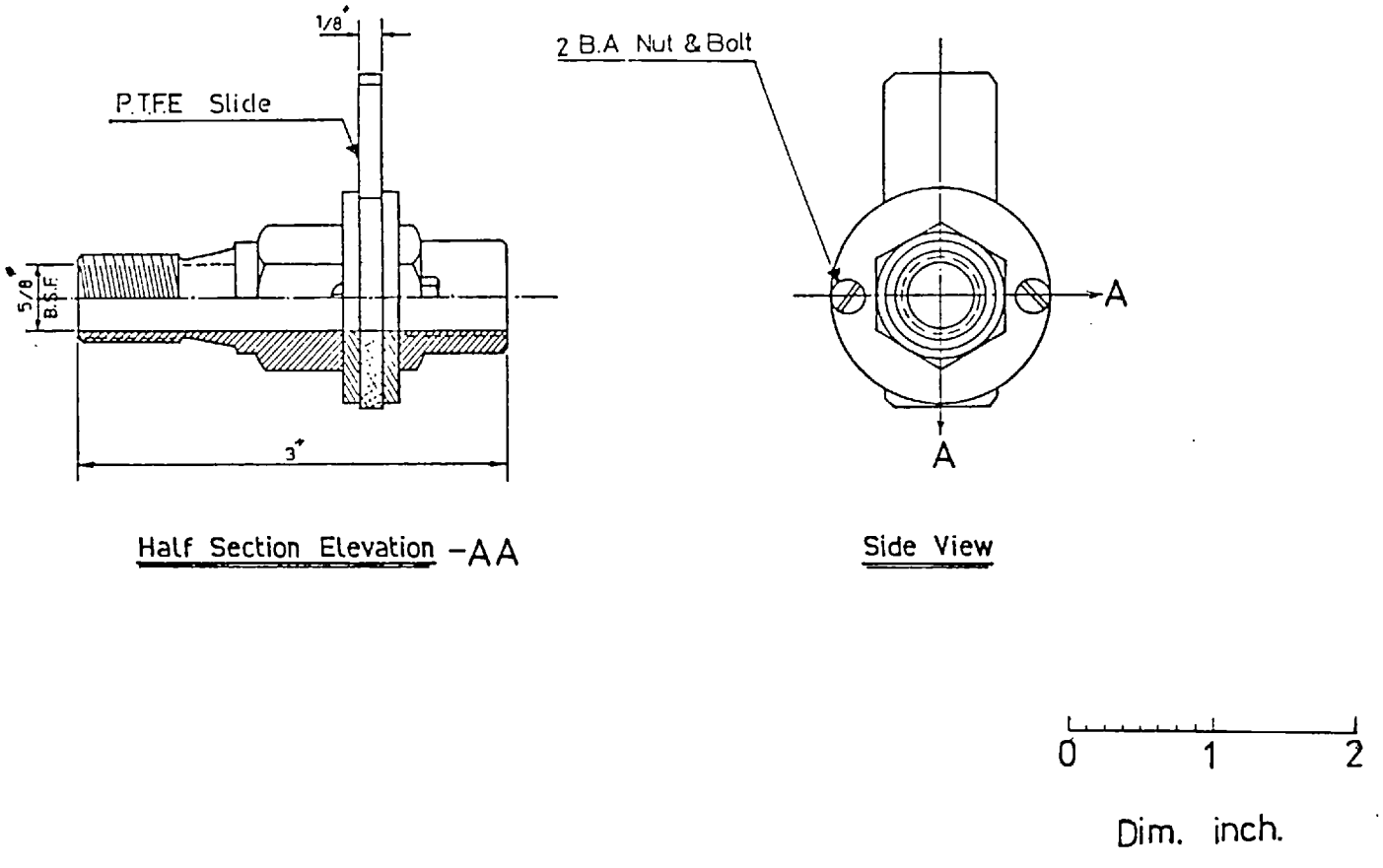

Fig(15) Details of extension tube.

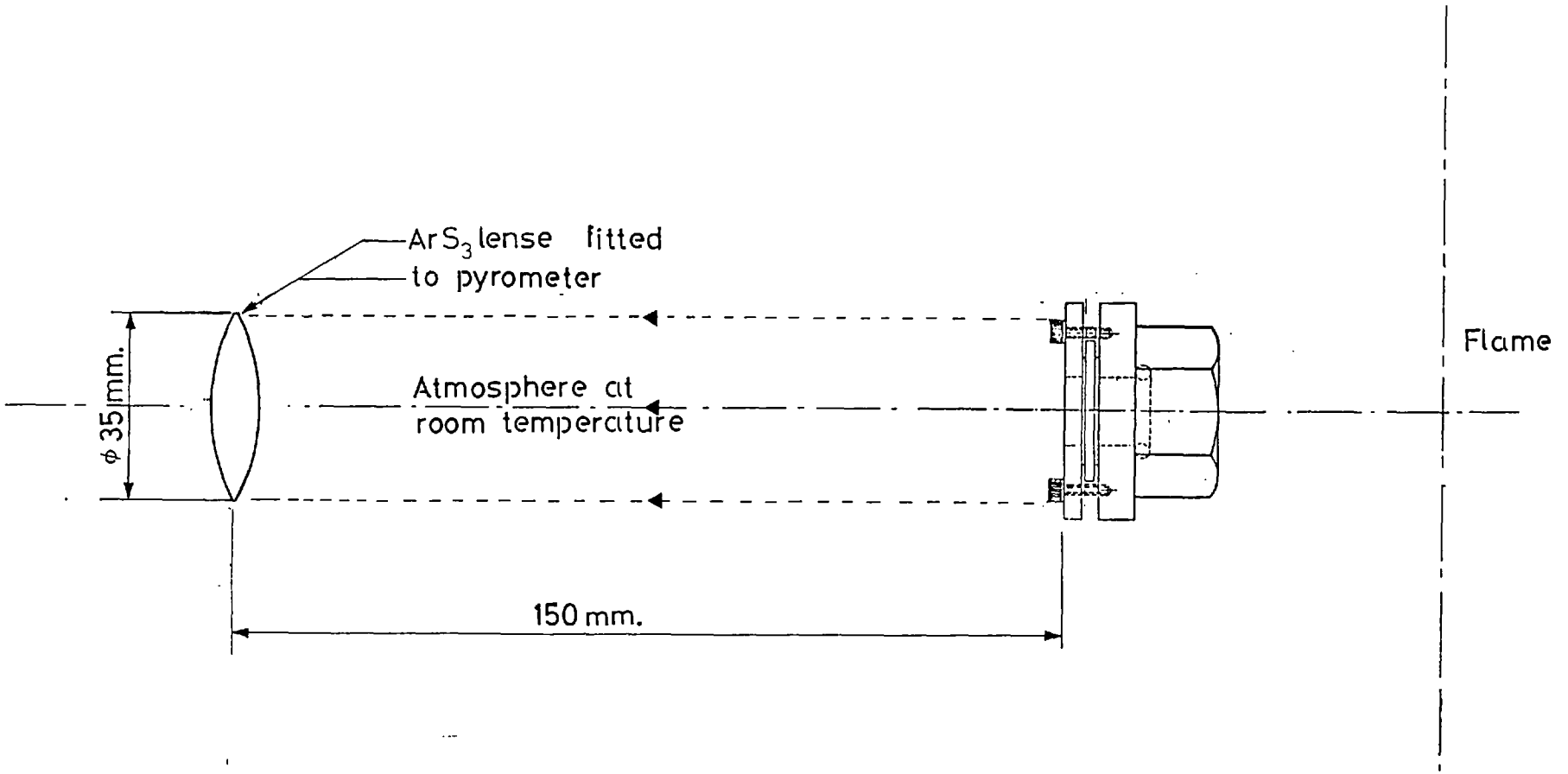

Fig(16) Schematic representation of the pyrometer focused on ArS_3 window.

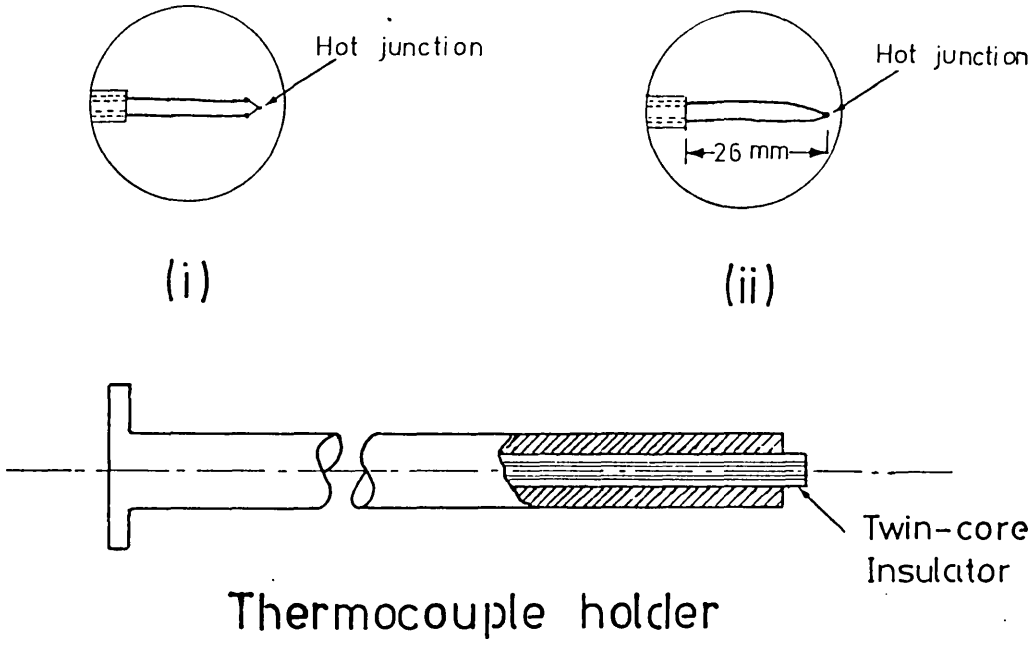

Fig(17a) The thermocouples.

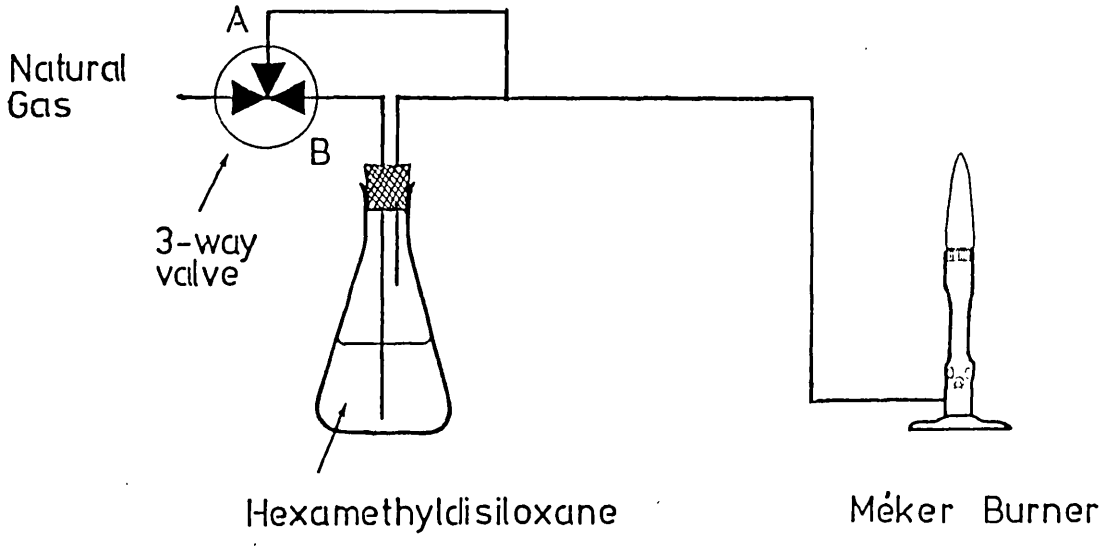

Fig(17b) Schematic representation of the thermocouple coating unit.

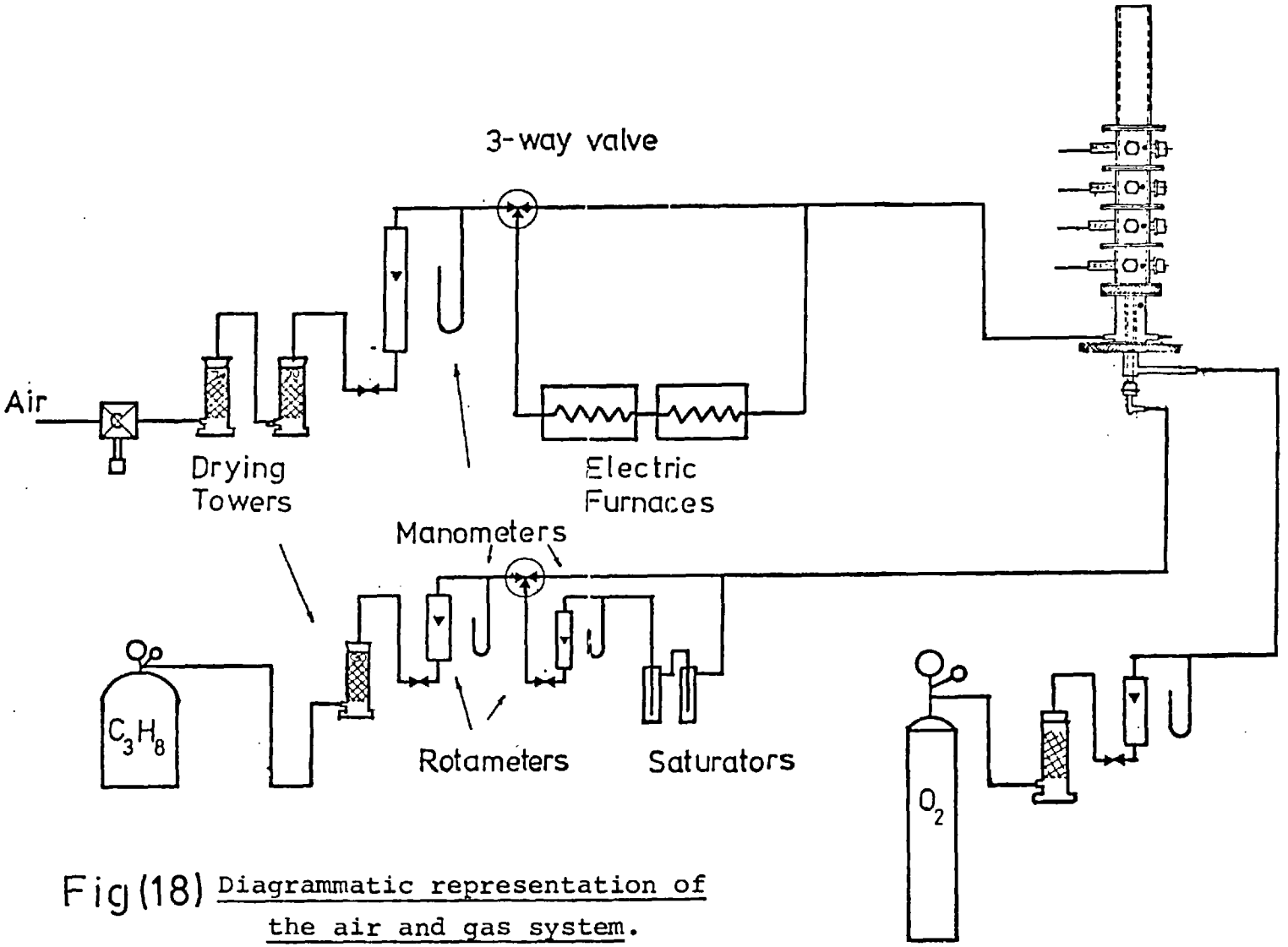

Fig (18) Diagrammatic representation of the air and gas system.

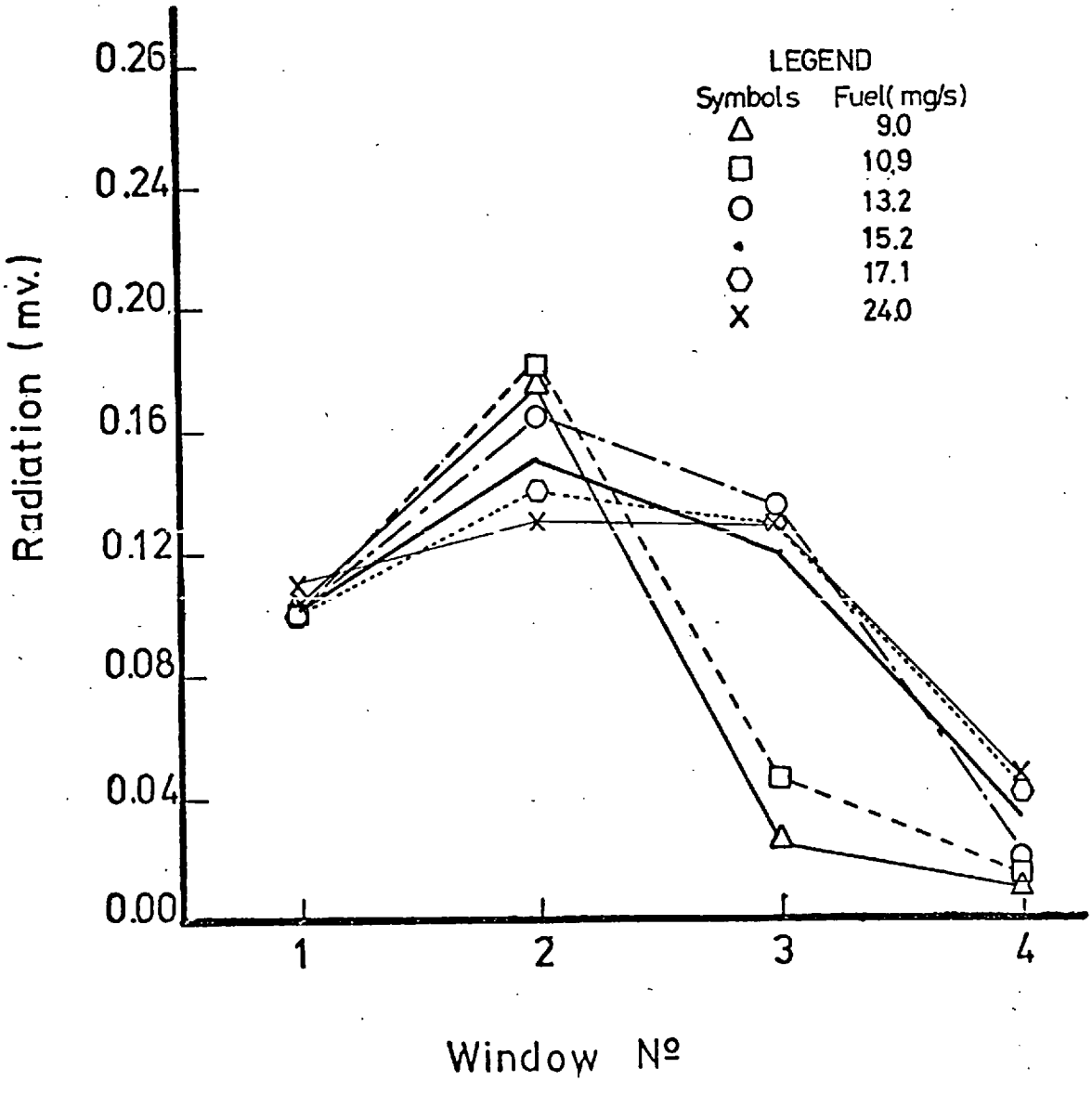

Fig (19) Effects of varying the fuel flow rate on radiation (air flow = 300 mg/sec.).

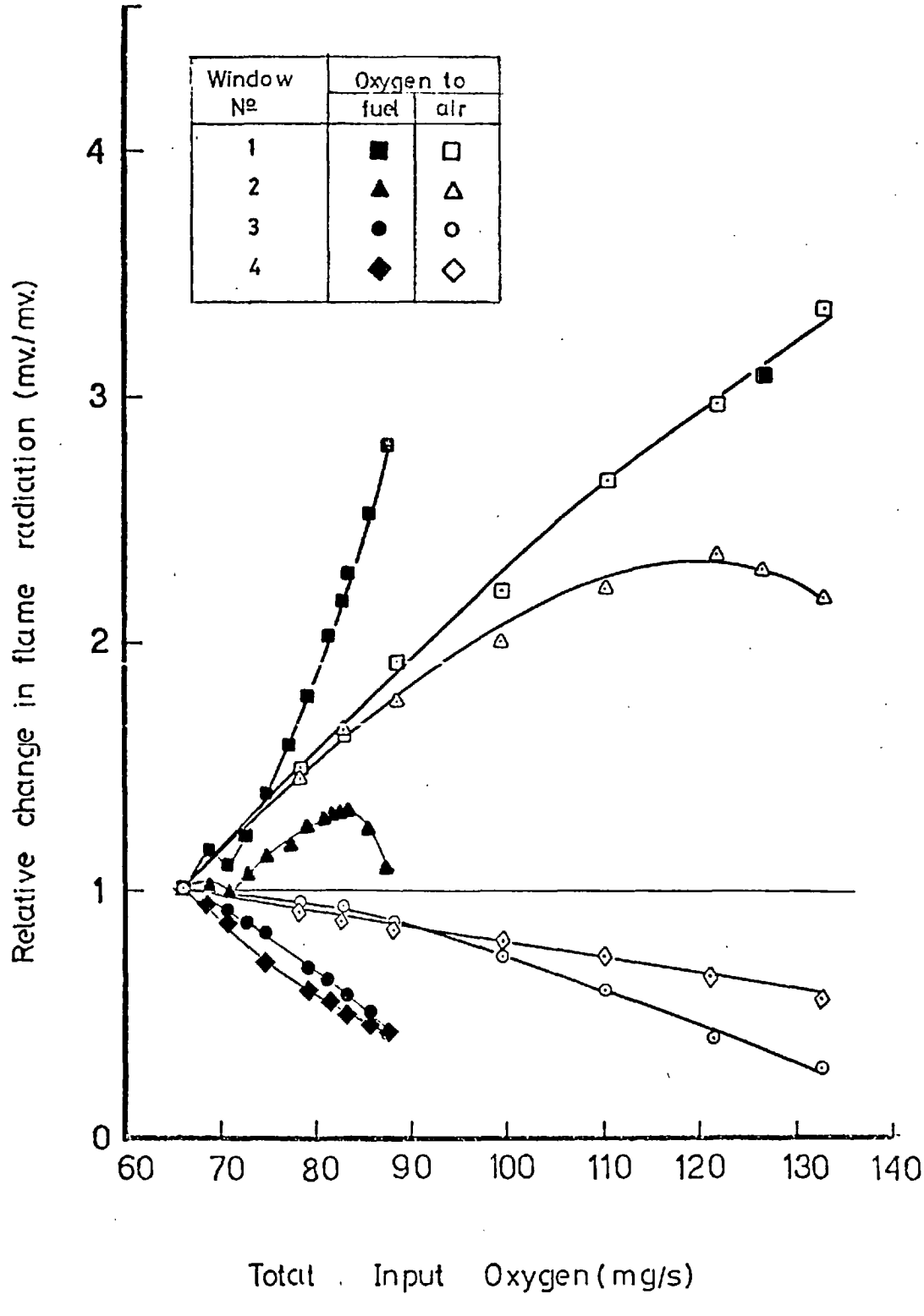

Fig(20) Effects of oxygen on flame radiation.

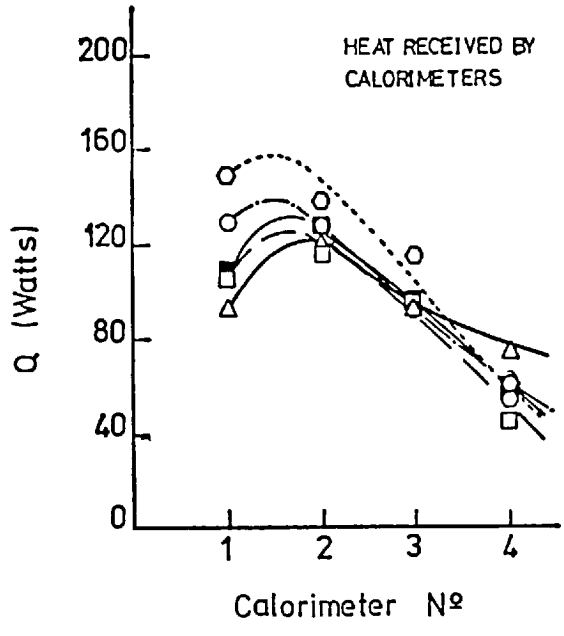

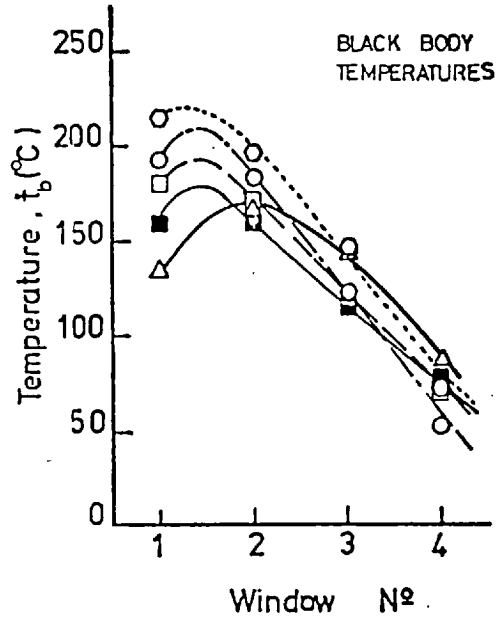

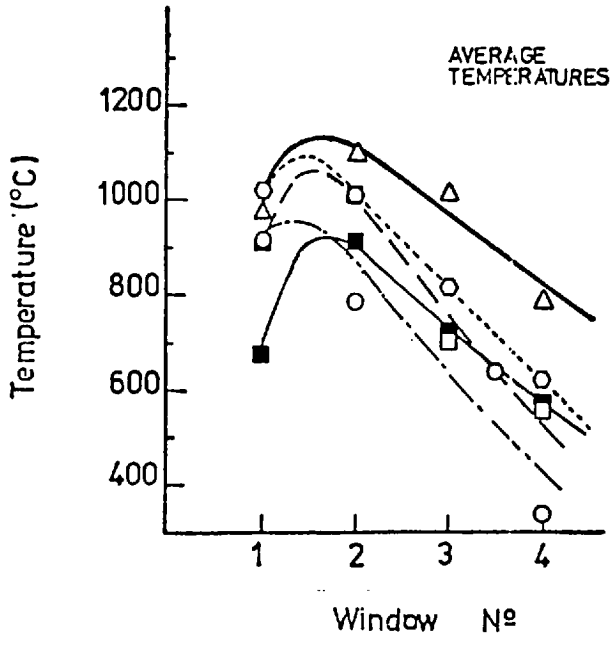

LEGEND

Symbols	Additives	Atoms of Cl_2
△	NONE	NONE
■	$CHCl_3$	0.270
□	"	0.470
○	CH_2Cl_2	0.560
○	CCl_4	0.520

Fig(21)

Effects of chlorine atoms on the total heat transfer, radiation and temperature.

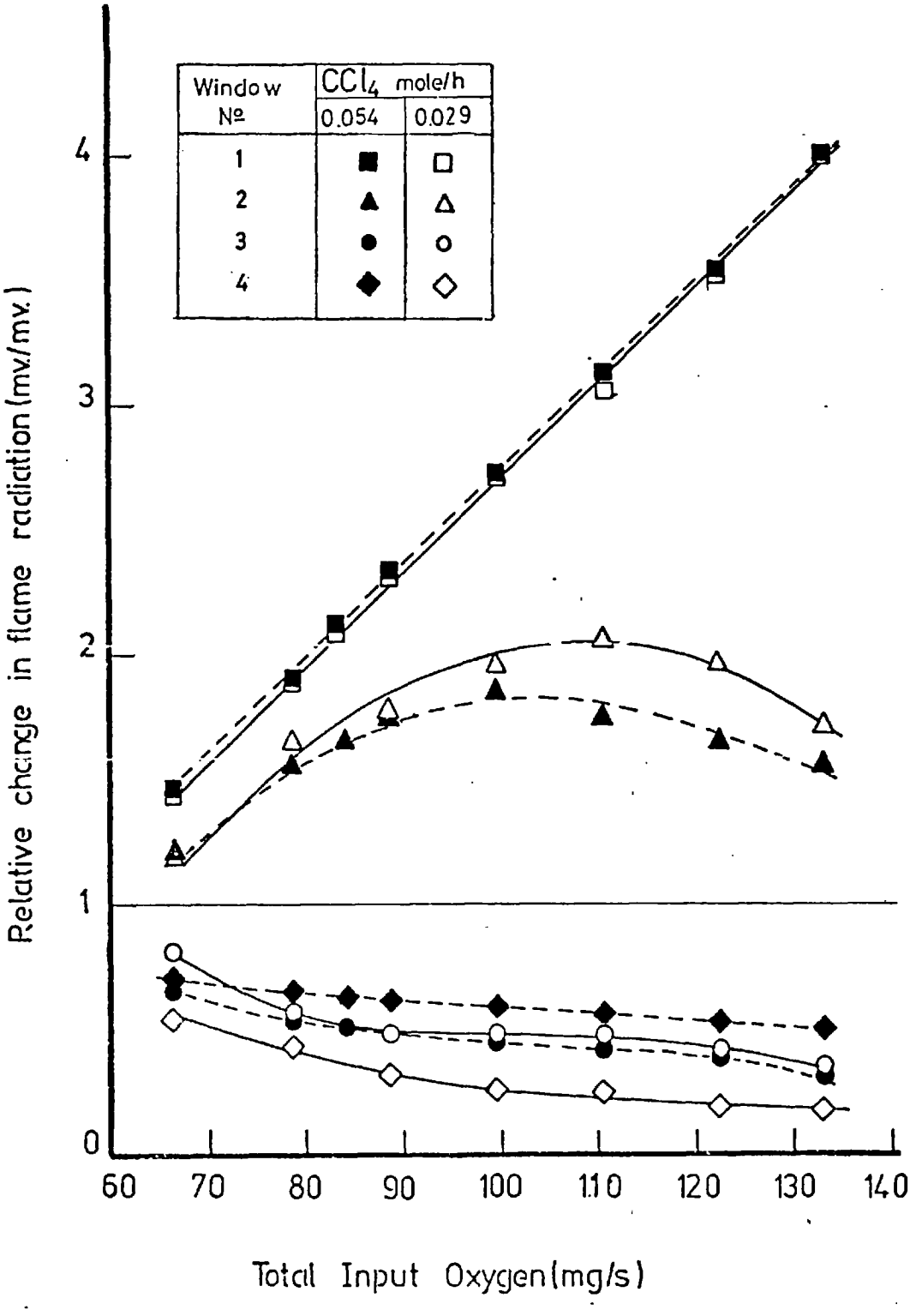

Effects of replacing the air with oxygen on flame radiation when 0.029 and 0.054 mole/hr. CCl_4 respectively were added to the fuel.

Fig (22)

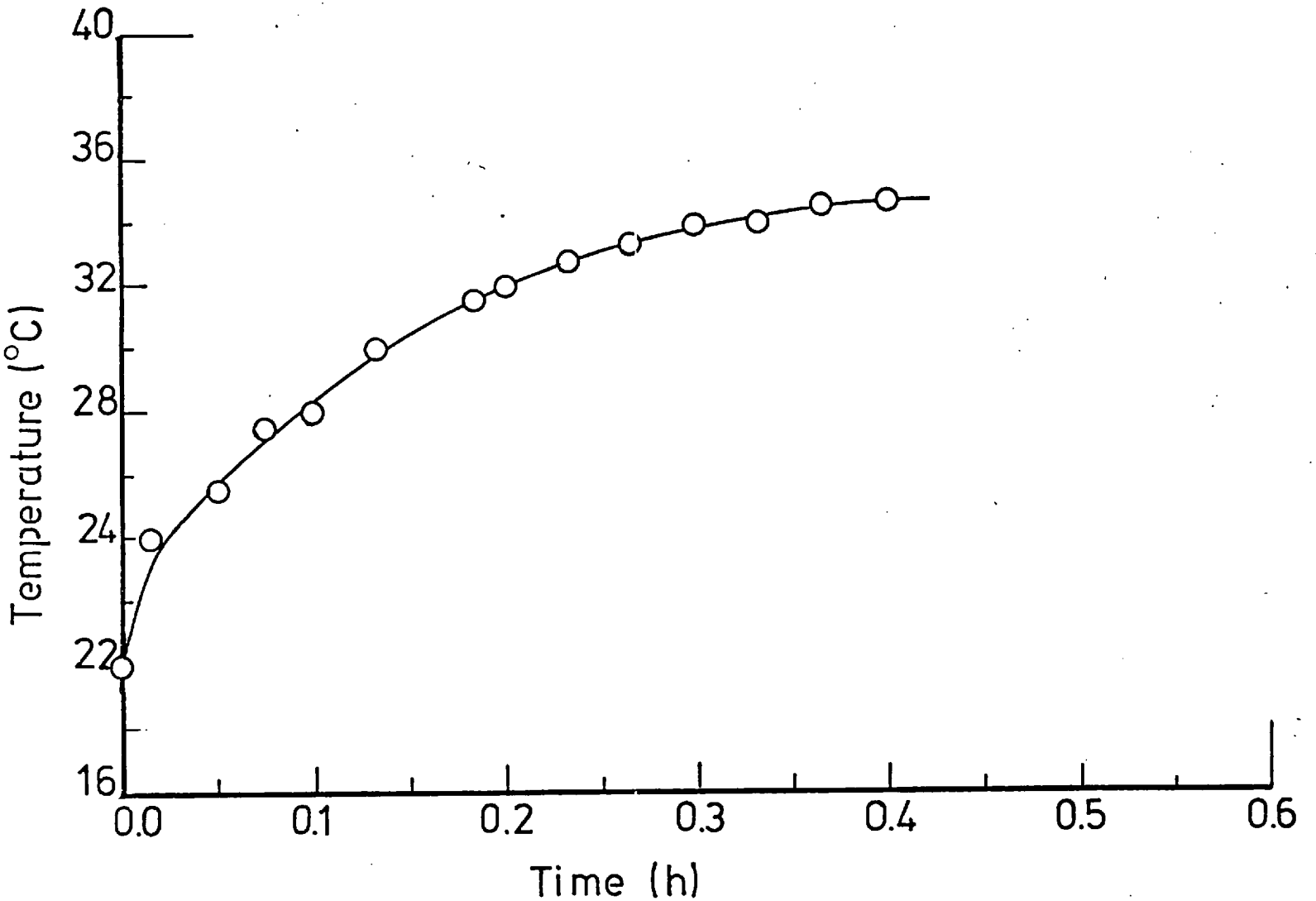

Fig (23) Change of temperature above the air distributor with time.

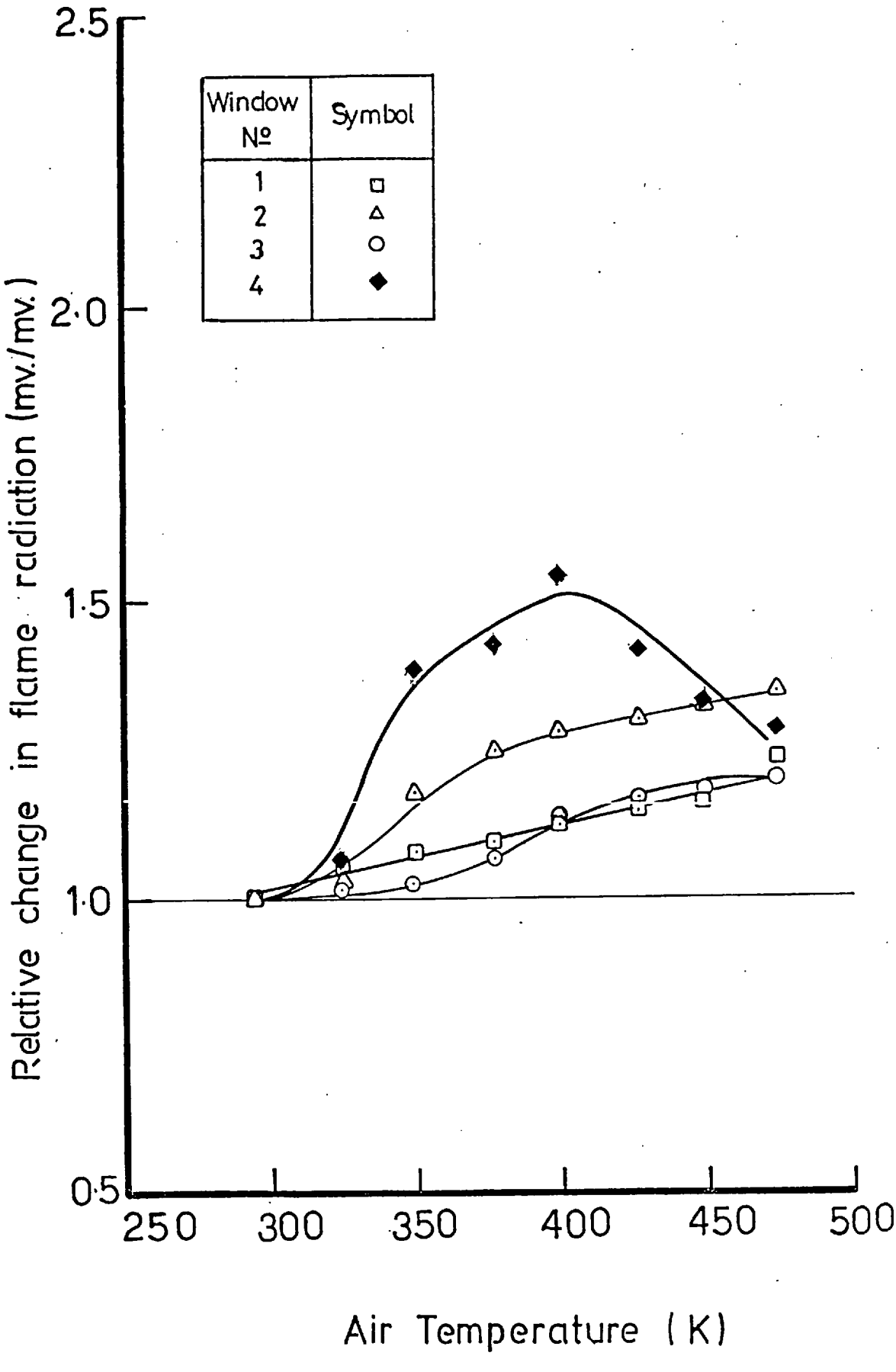

Fig(24) Effects of air pre-heat on flame radiation.

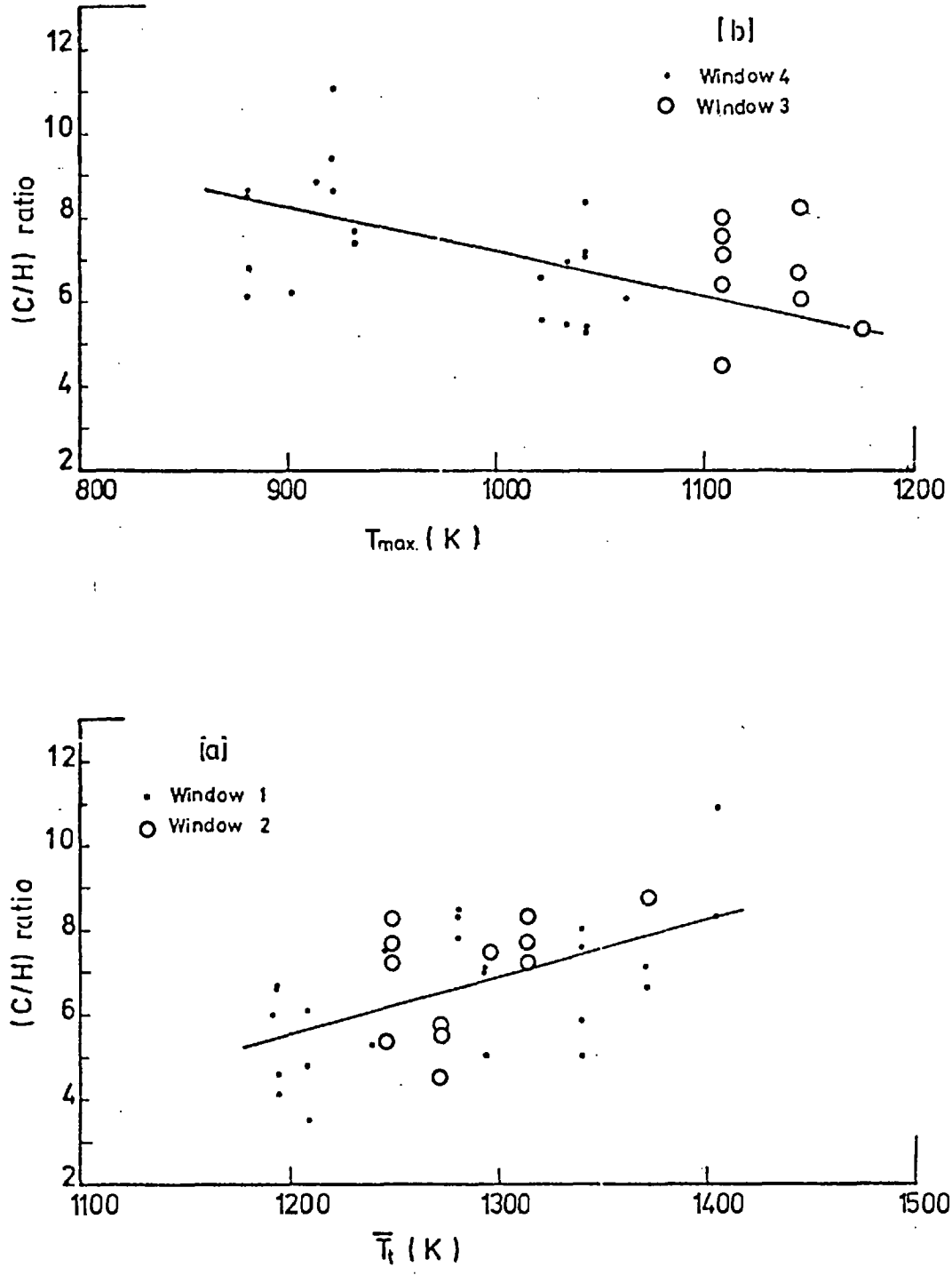

Fig(25) Correlation of the composition of soot and carbonaceous residues with temperature.

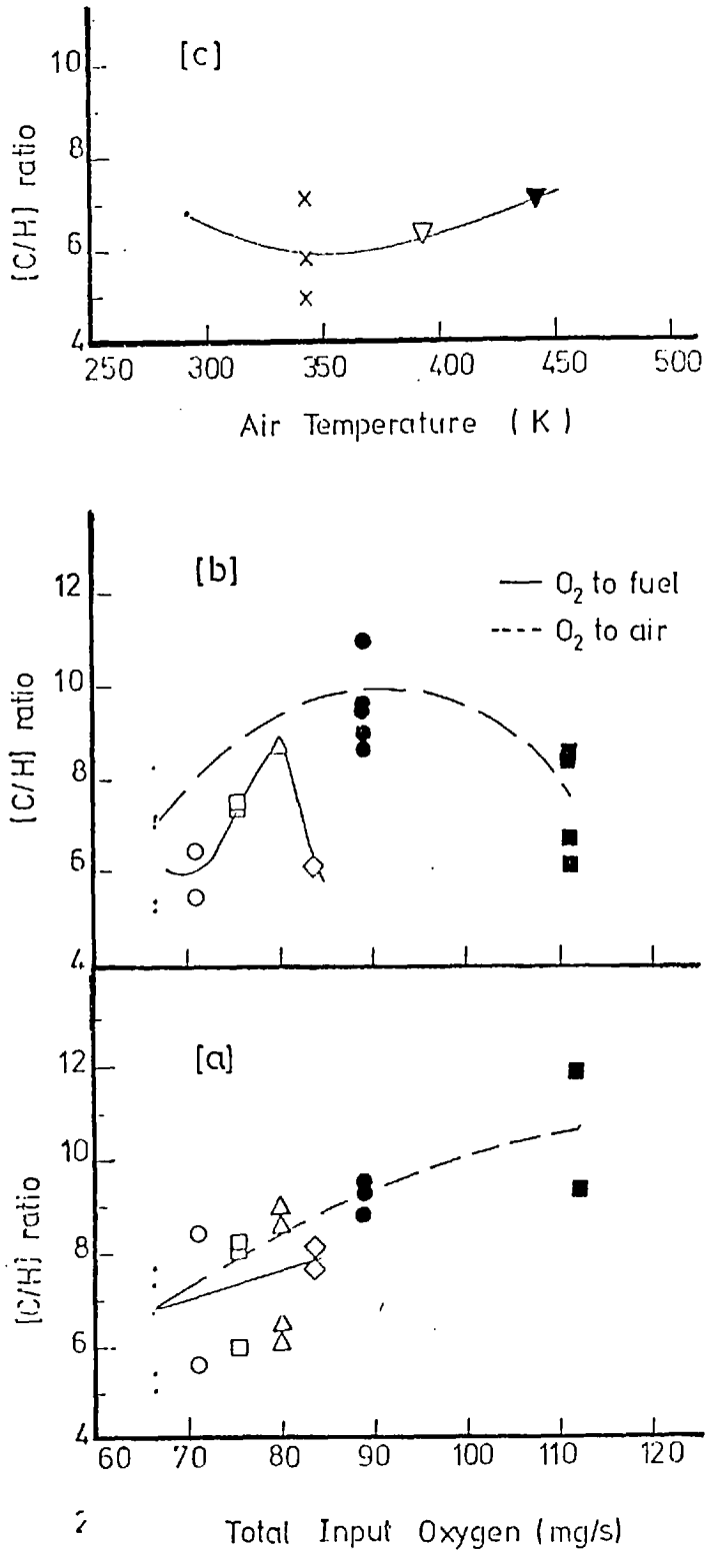

(a) Dependence of the C/H ratio of the insoluble fraction of soot on distribution and amount of input oxygen at Window 1.

(b) Dependence of the C/H ratio of soot on distribution and amount of input oxygen at Window 4.

(c) Dependence of C/H ratio of the insoluble fraction of soot on air temperature at Window 1.

Fig(26)

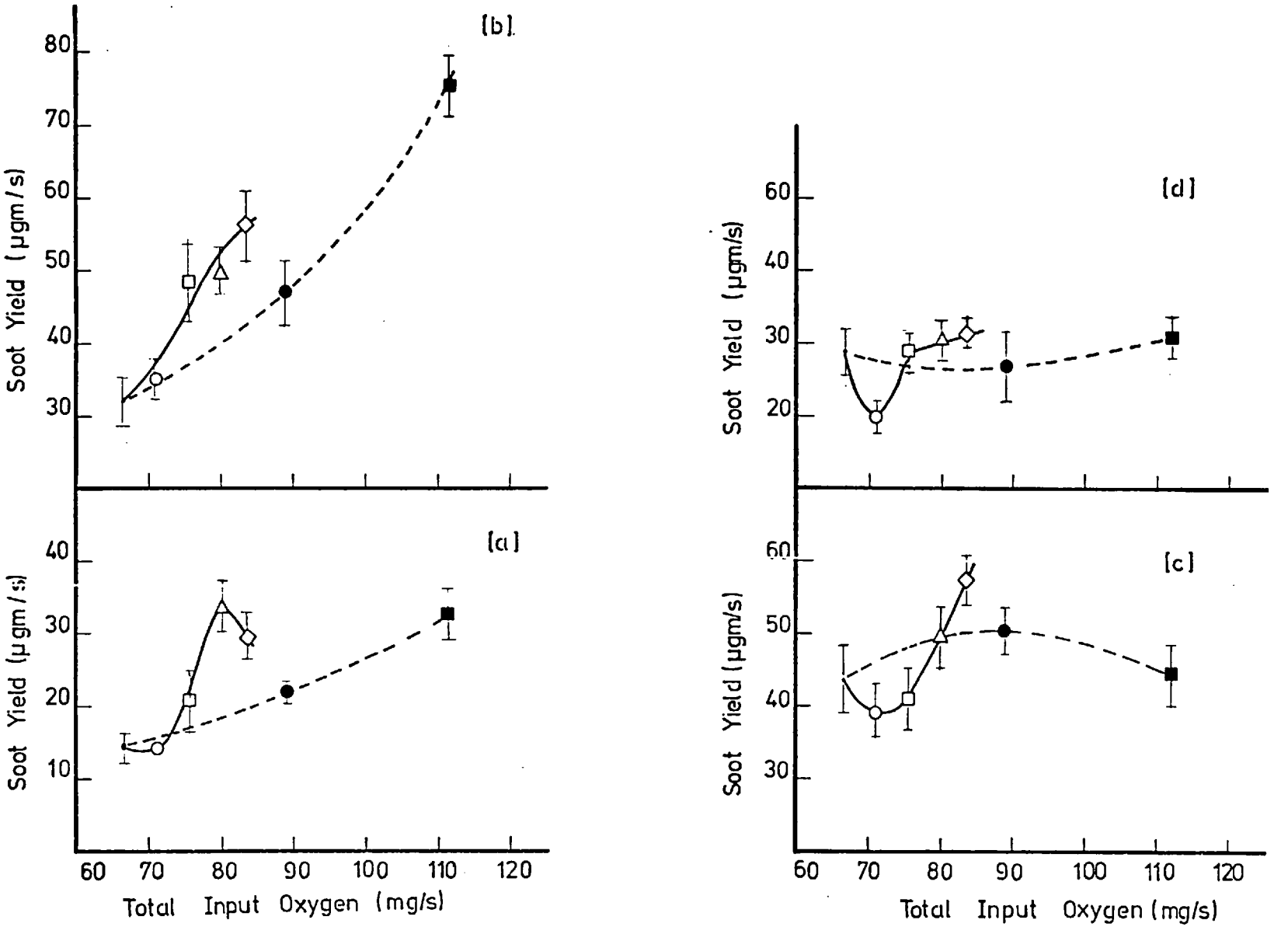

Fig (27) Effects of oxygen on yield of soot
(see Table 5 for symbols.)

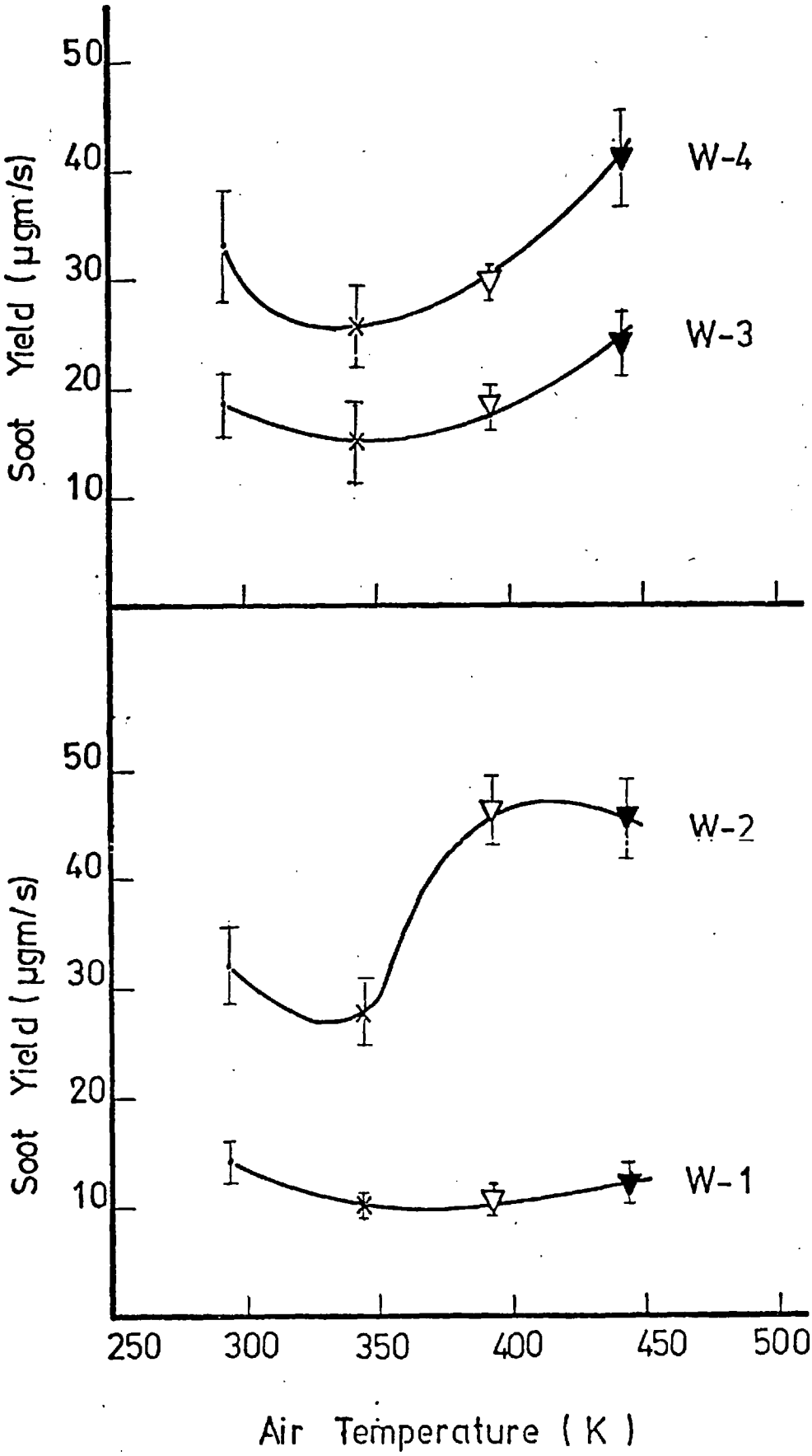

Fig(28 a) Effects of air pre-heat on the yield of soot.

(See Table 5 for symbols.)

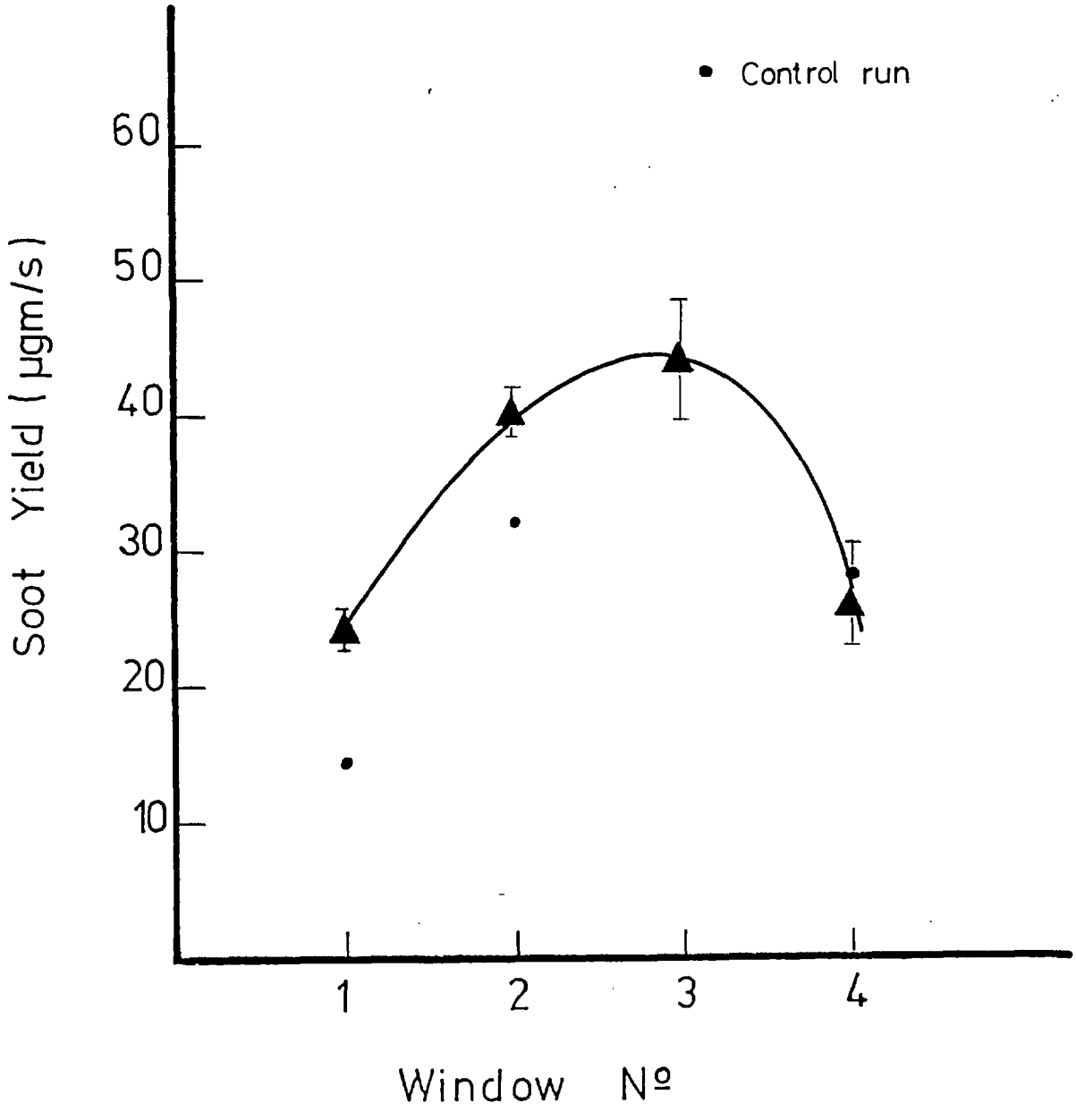

Fig(28 b) Effect of CCl_4 on the yield of soot

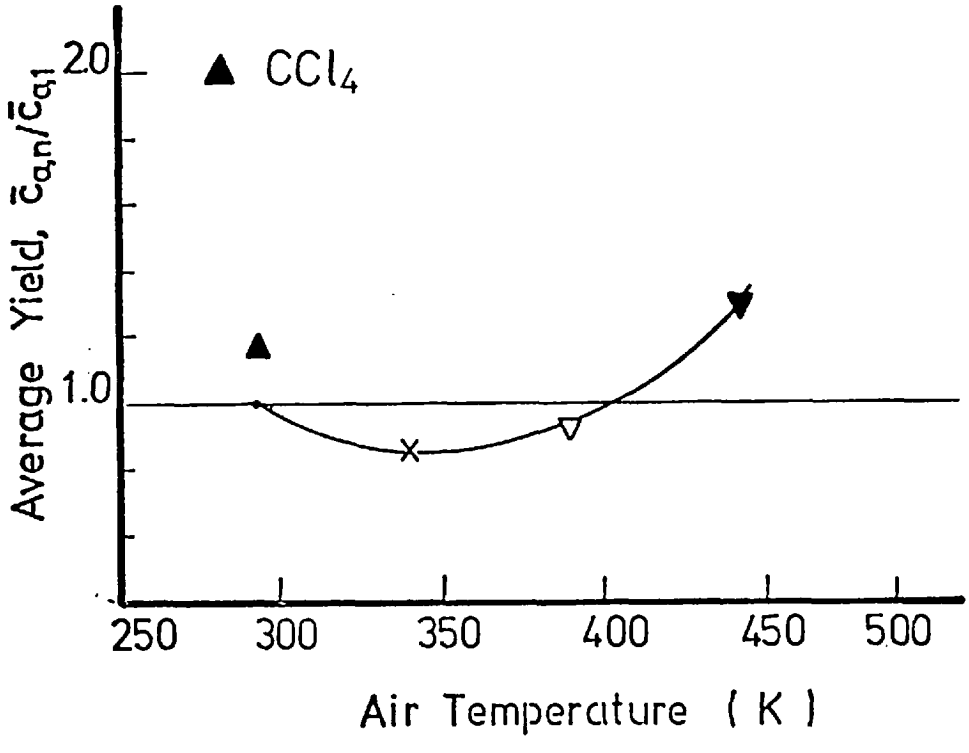

(b) Effects of pre-heating the air and addition of CCl_4 on average yield of soot up to Window 4.

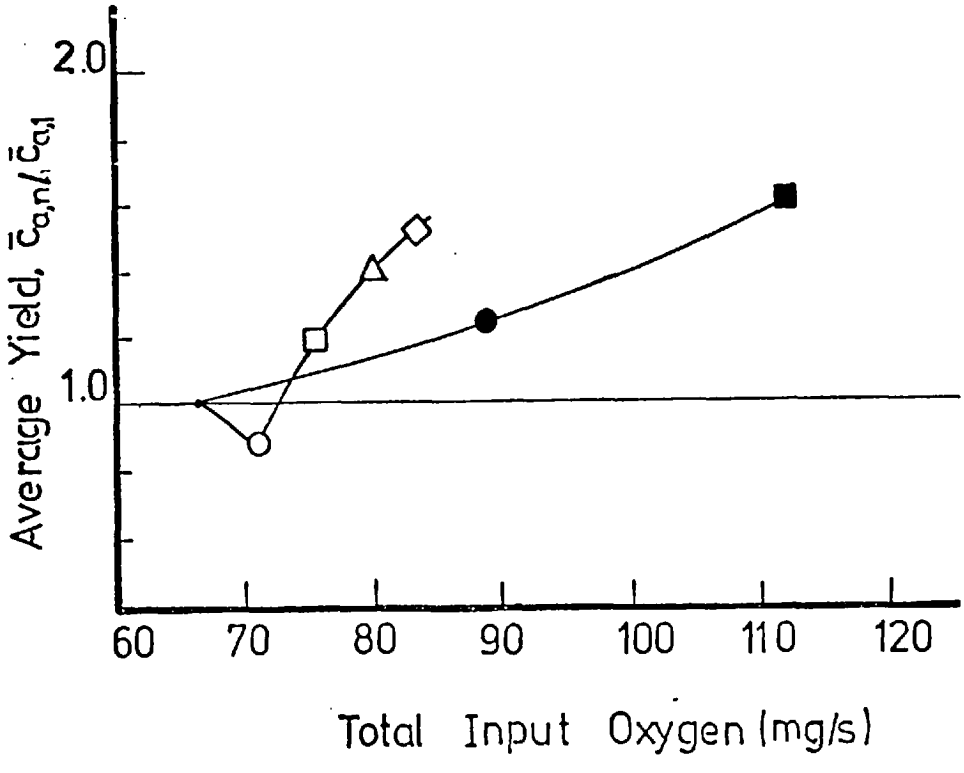

(a) *Effects of oxygen on the average yield of soot (Window 4).

*See Table 5 for symbols.

Fig(29)

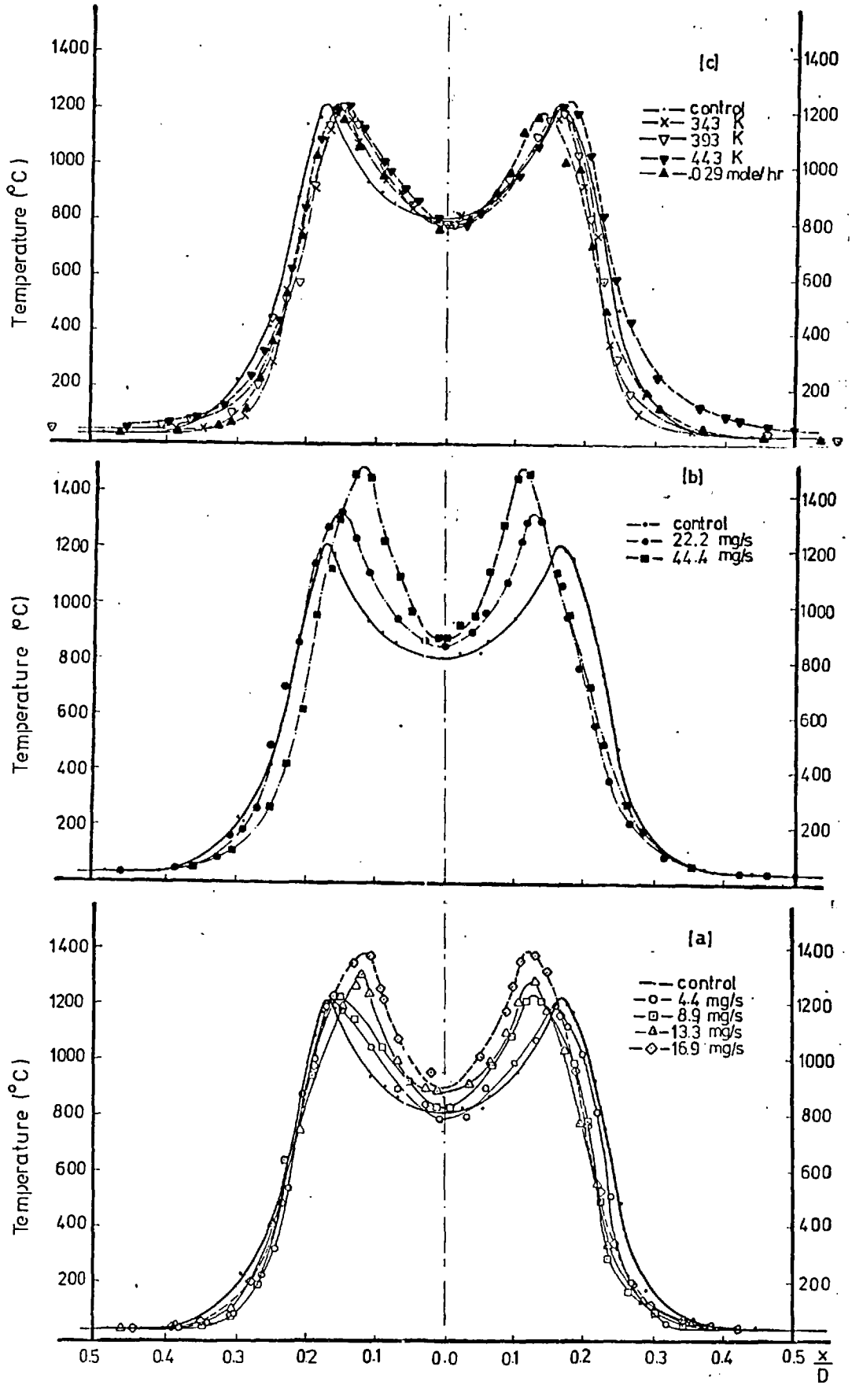

Fig(30) Effects of additives on temperature at Window 1.

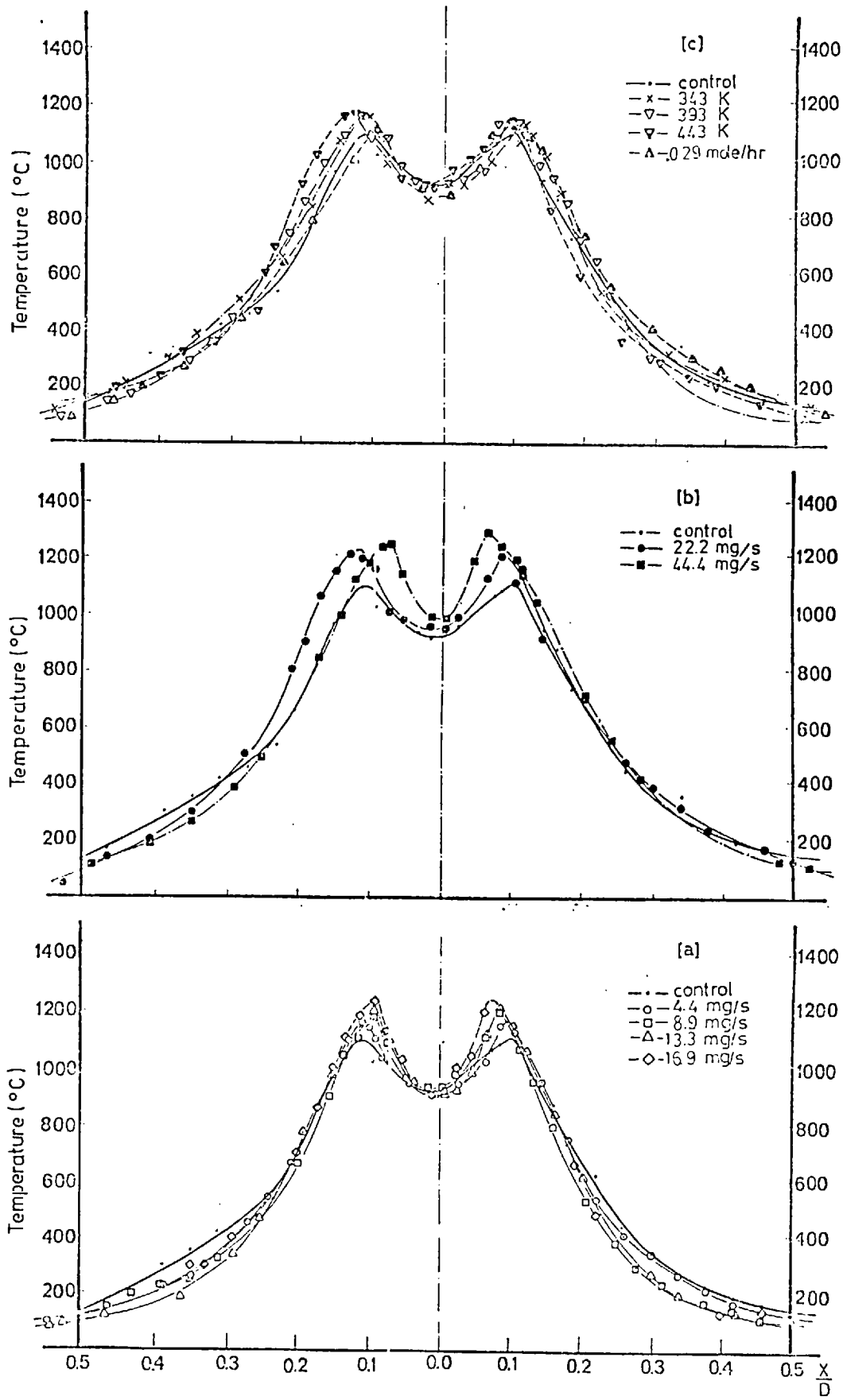

Fig(31) Effects of additives on temperature at Window 2.

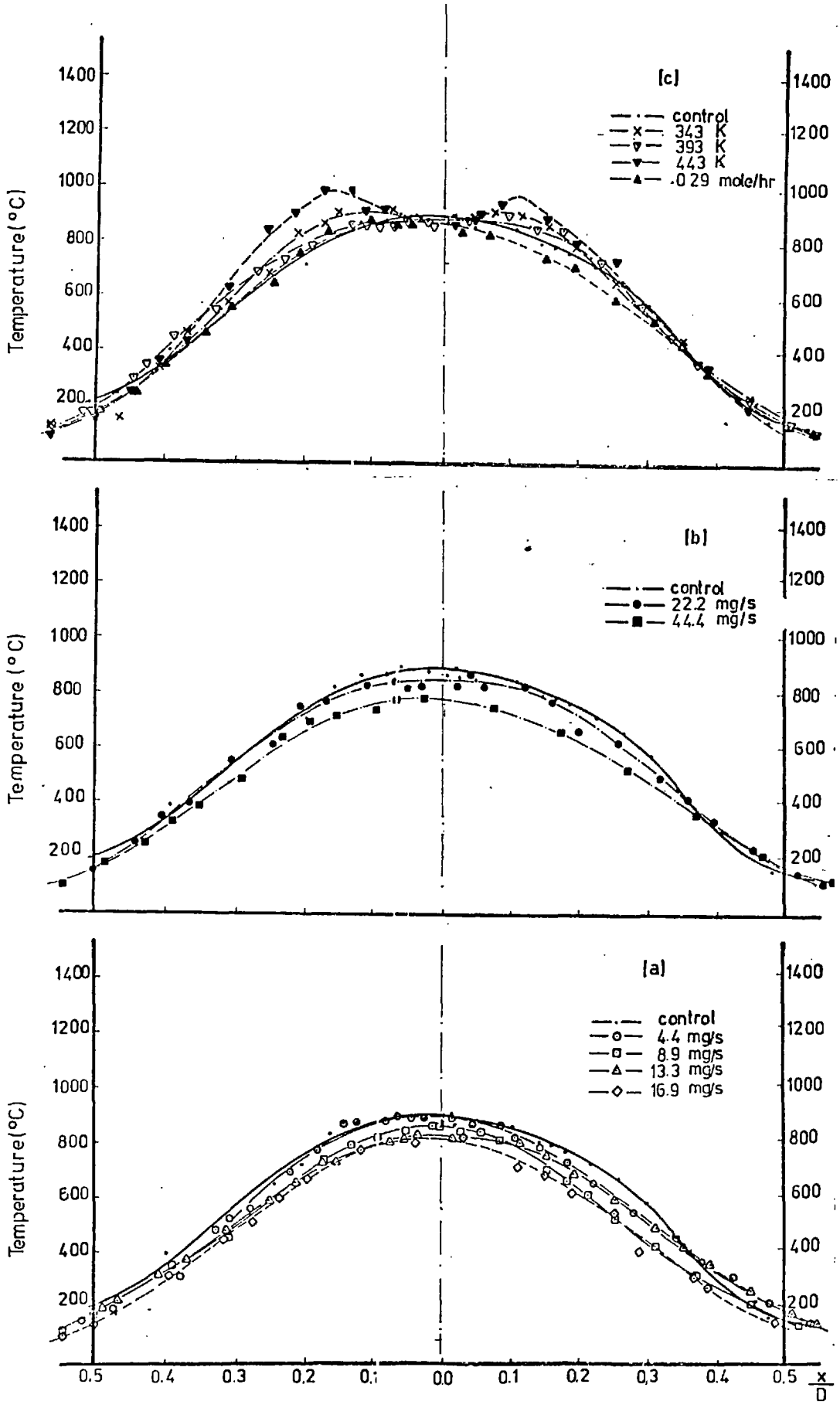

Fig(32) Effects of additives on temperature at Window 3.

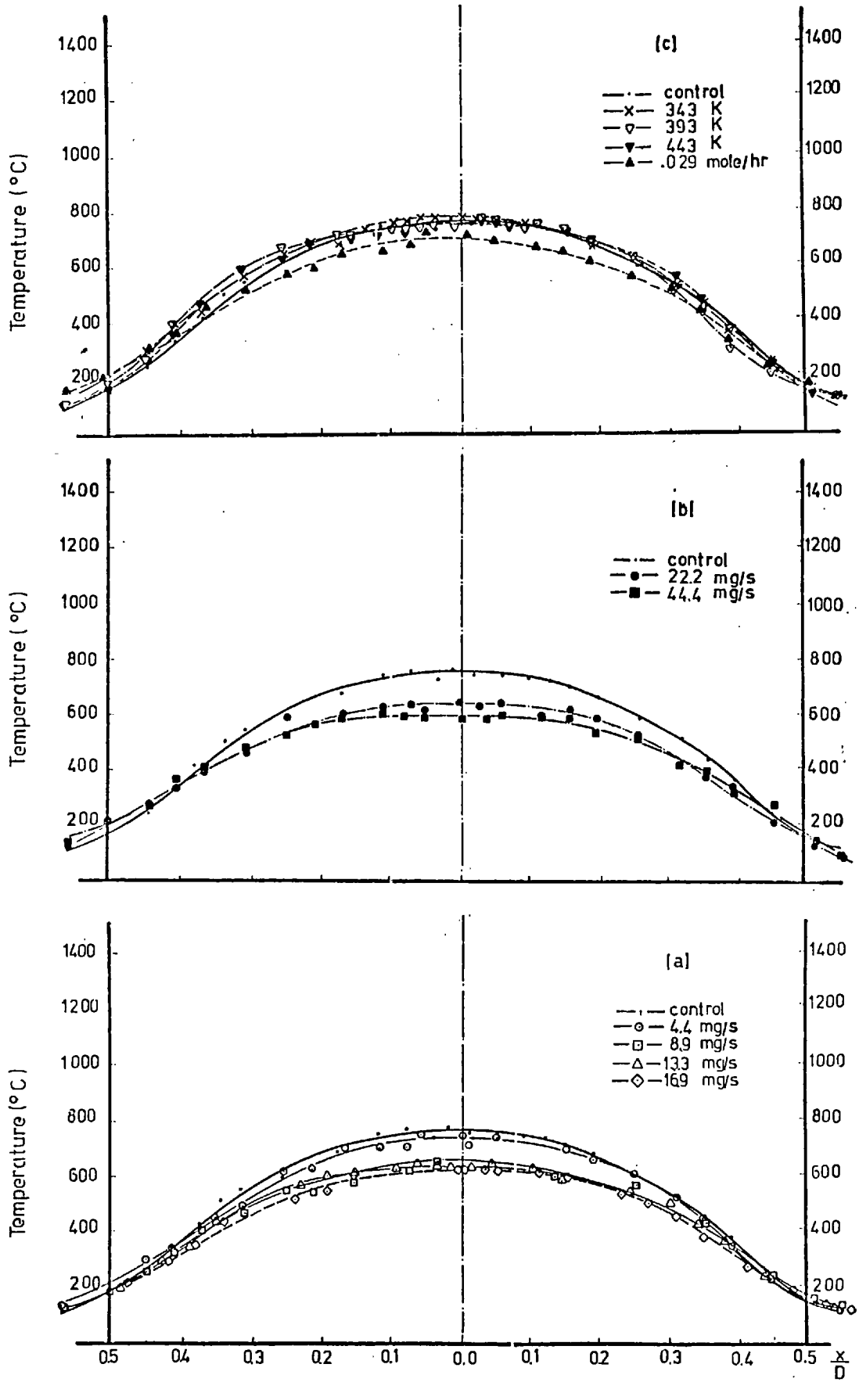

Fig(33) Effects of additives on temperature at Window 4.

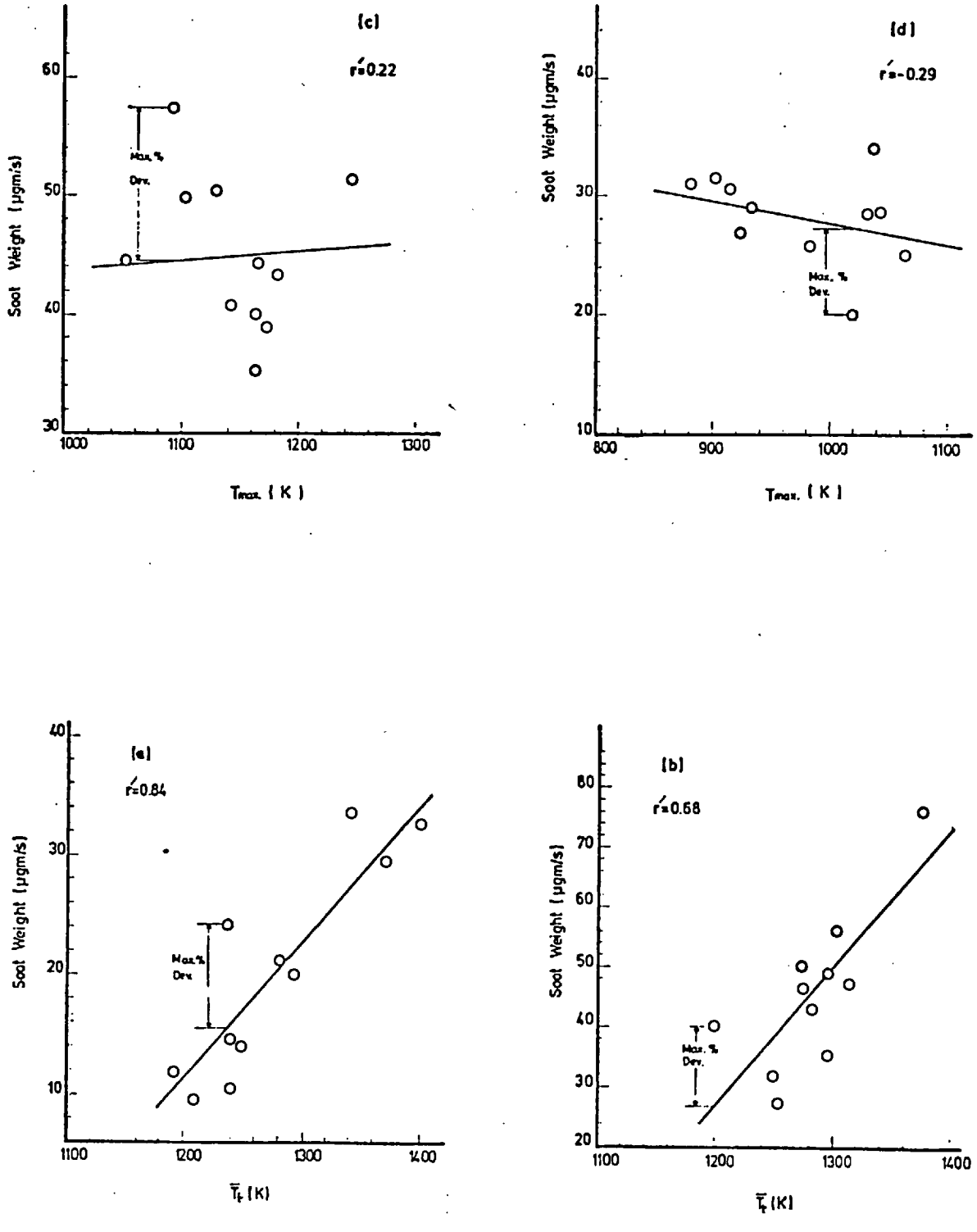

Fig(34) Relationship between sooting rate and temperature.

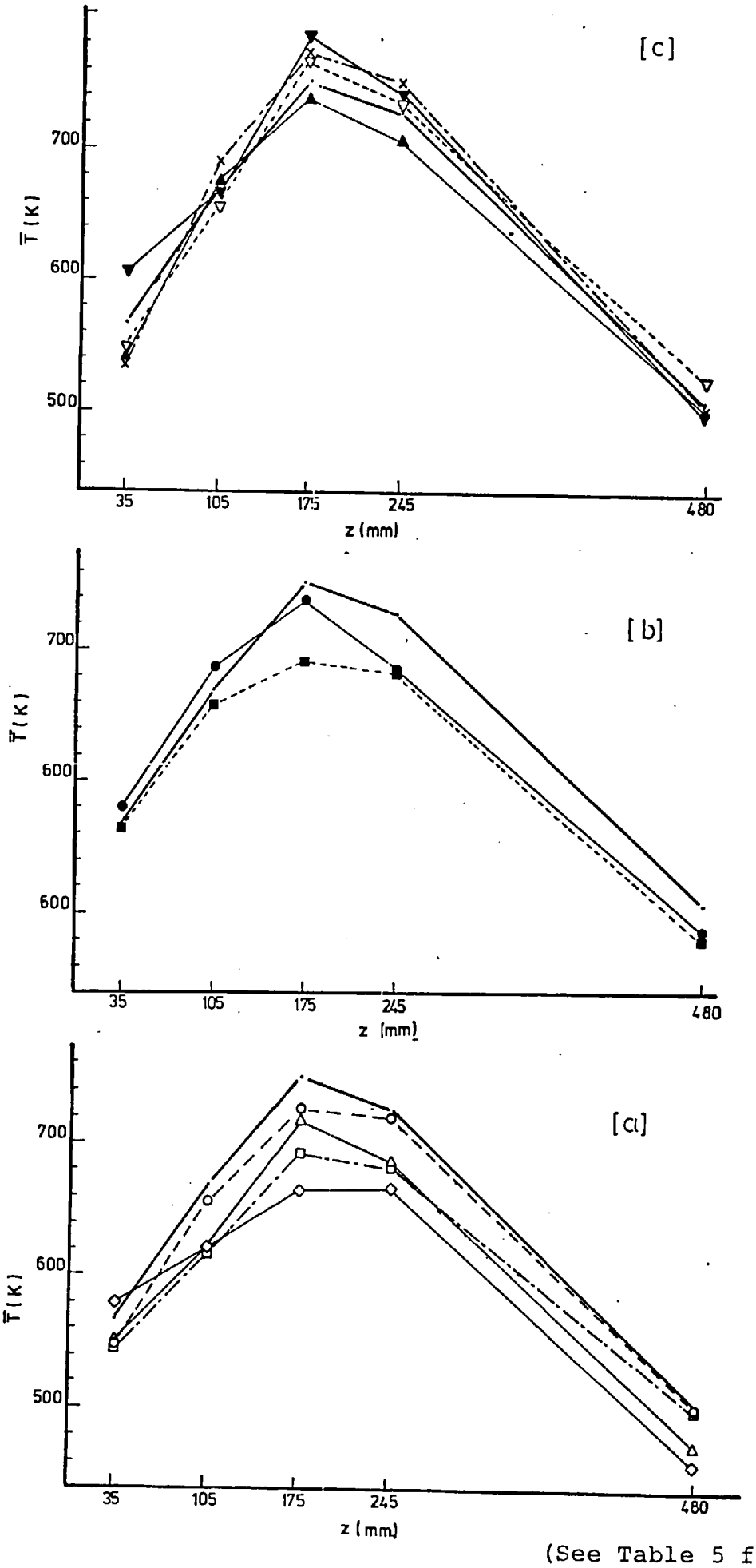

(See Table 5 for symbols.)

Fig(35) The change of bulk temperature along flame length.

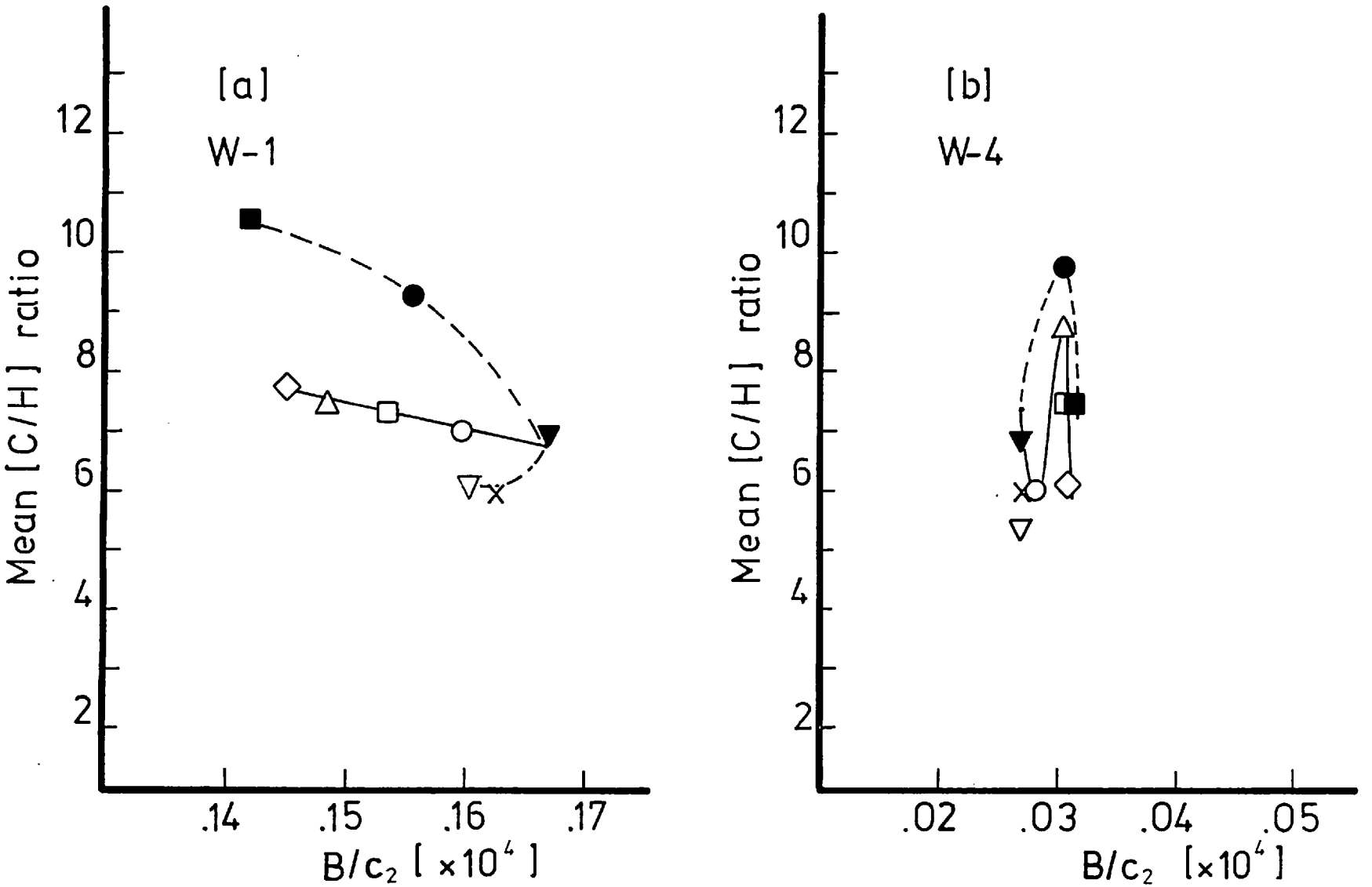

Fig(36) Relationship between B/c_2 and average composition of solid particles.

(See Table 5 for symbols.)

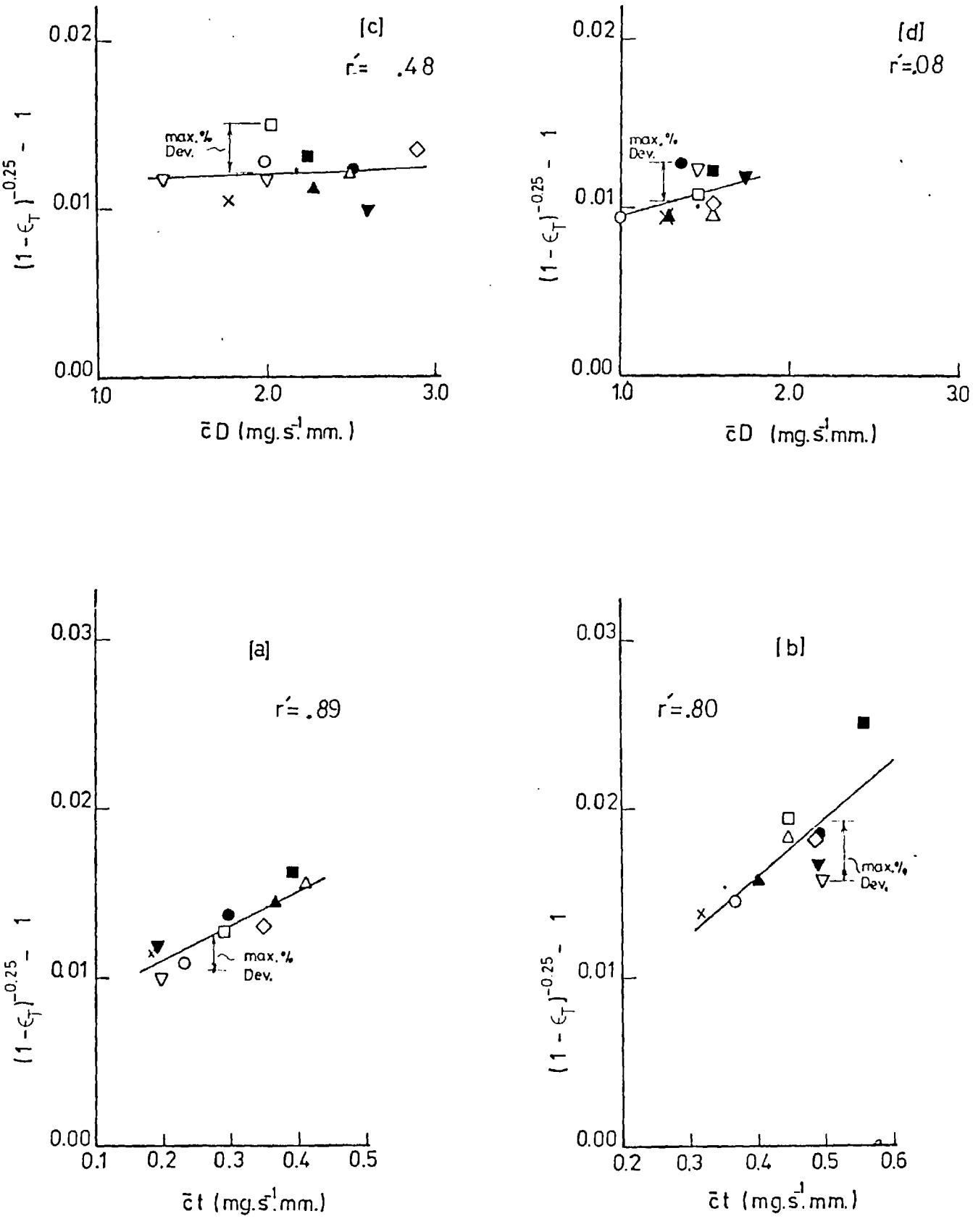

Fig(37) The total emissivity as a function of soot concentration and flame thickness.

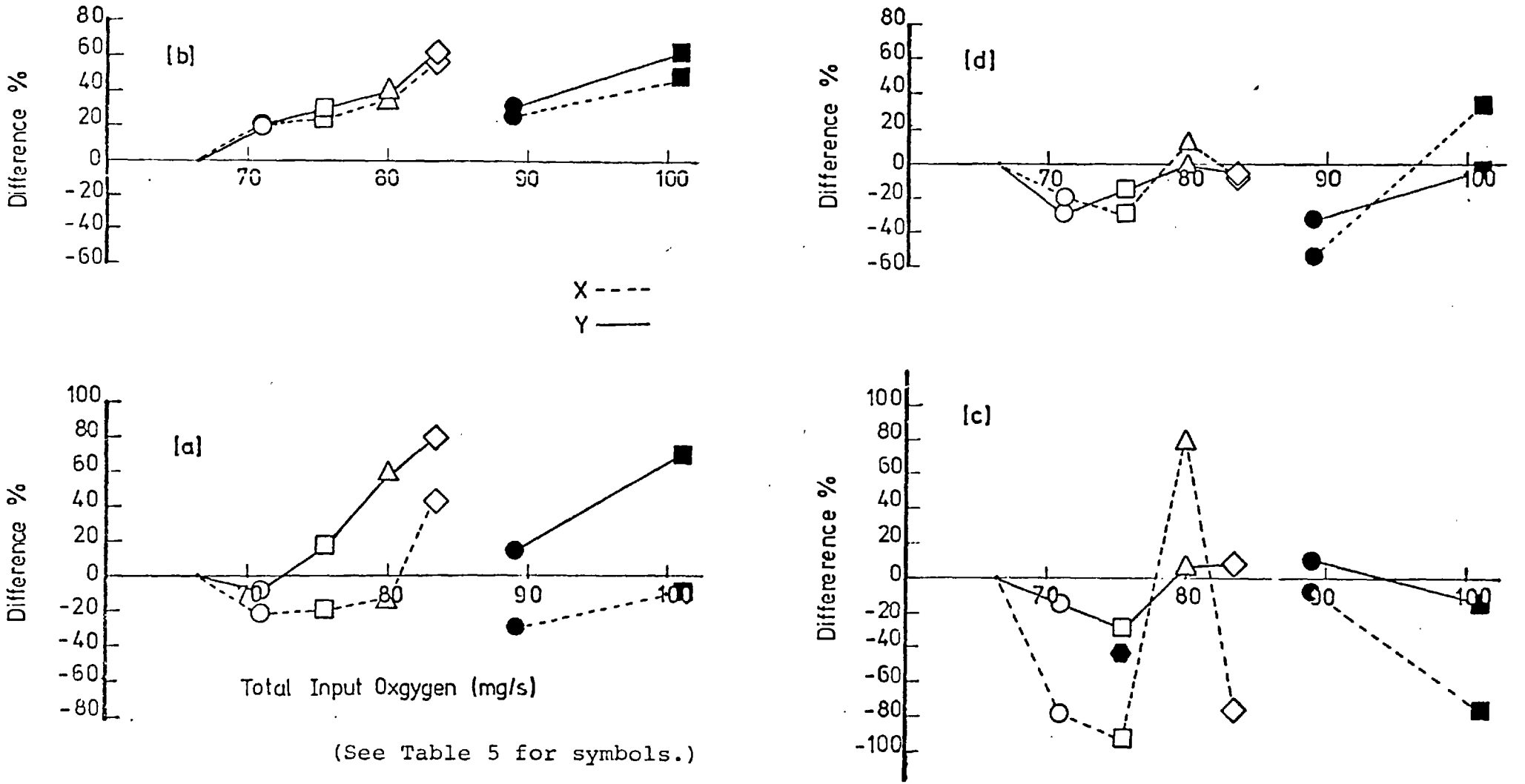

Fig(38) Difference between radiation (ratios) calculated from model and measured with (X) and without (Y) correction for gas emissivity (addition of oxygen).

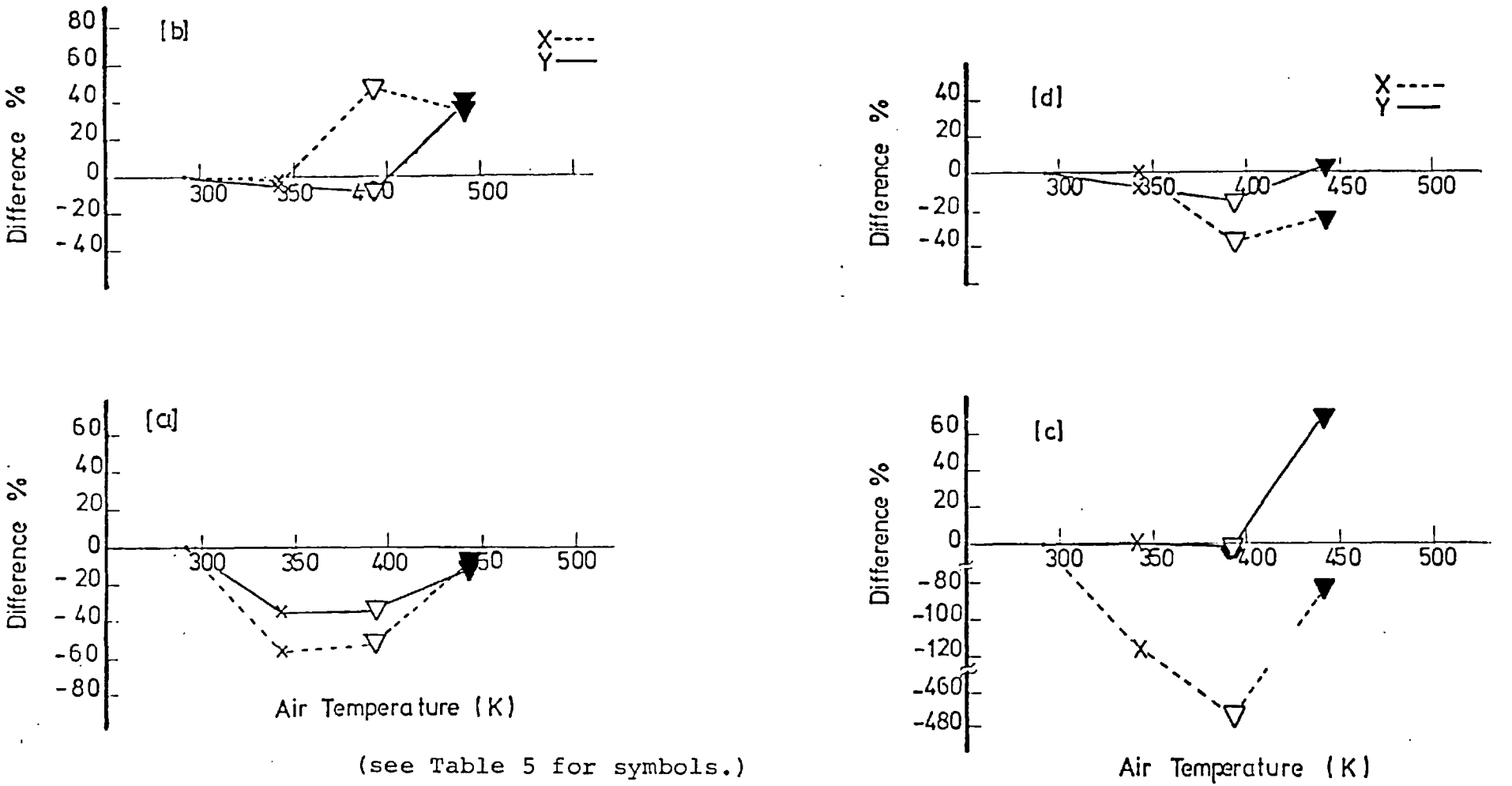

(see Table 5 for symbols.)

Fig(39) Difference between radiation (ratios) calculated from model and measured with (X) and without (Y) correction for gas emissivity (pre-heating the air).

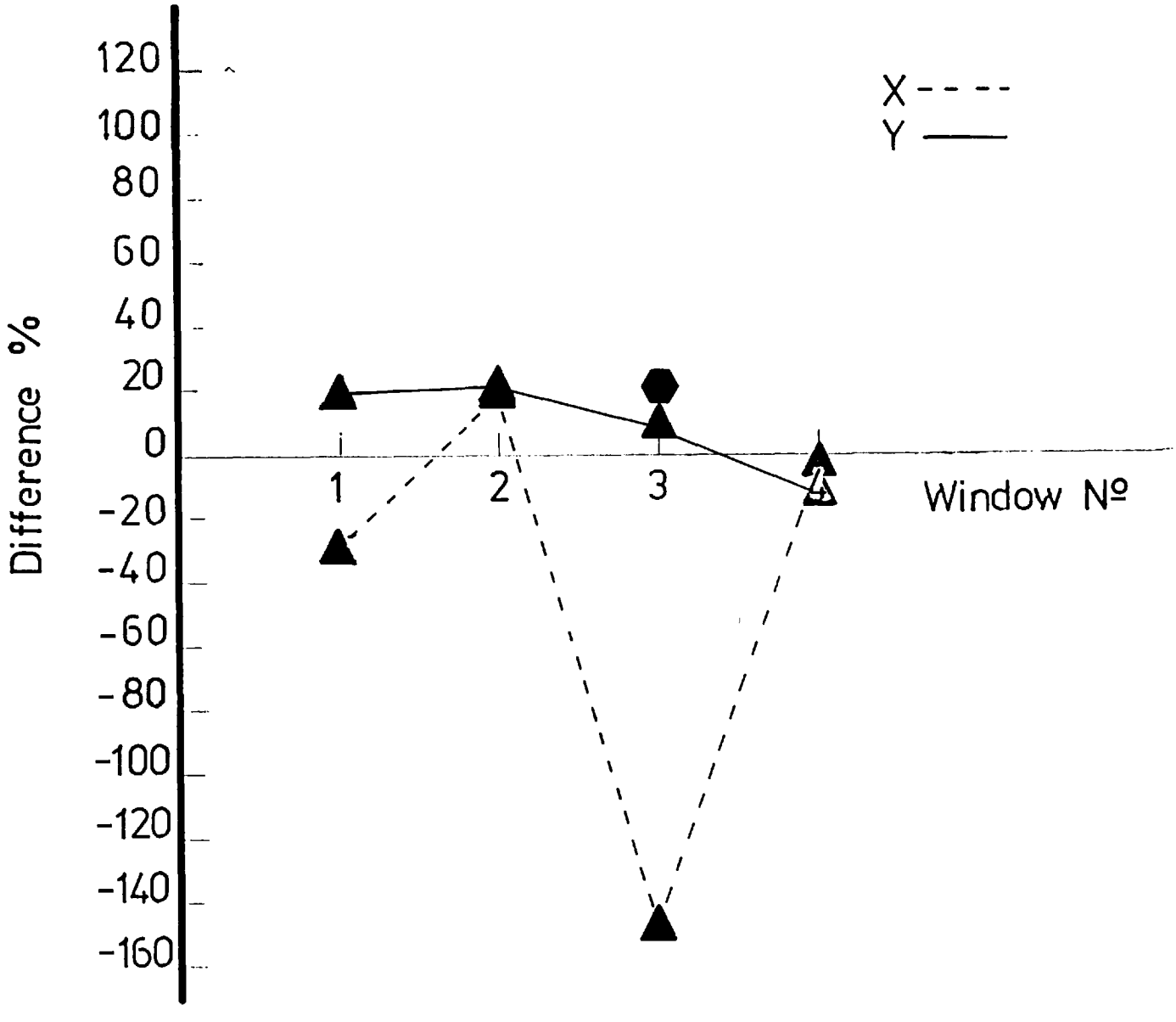

(See Table 5 for symbols.)

Difference between radiation (ratios) calculated from model and measured with (X) and without (Y) correction for gas emissivity (addition of 0.029 mole/hr. CCl_4 to the fuel.

Fig(40)

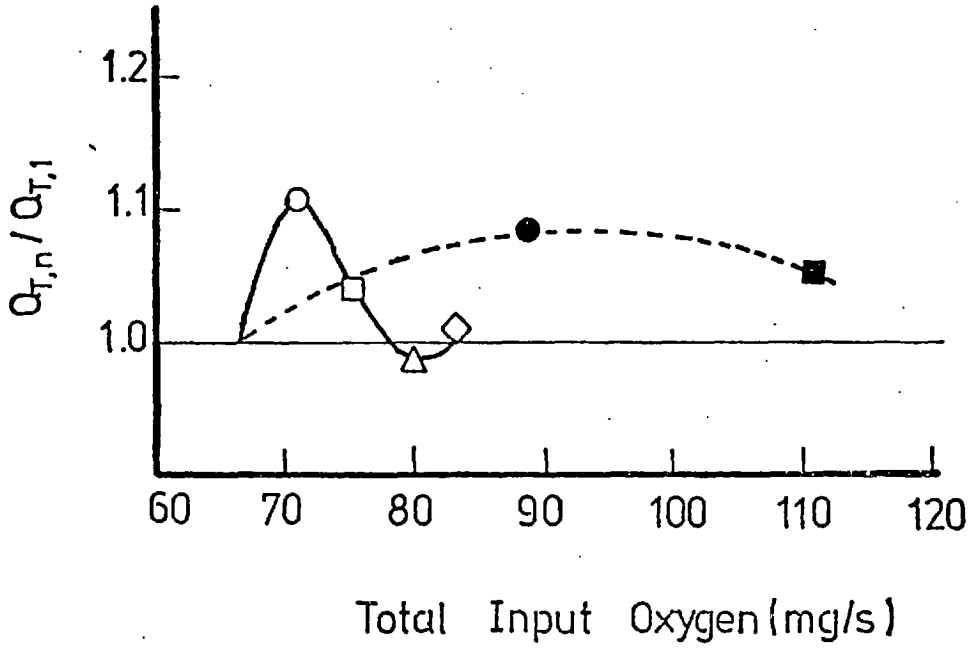

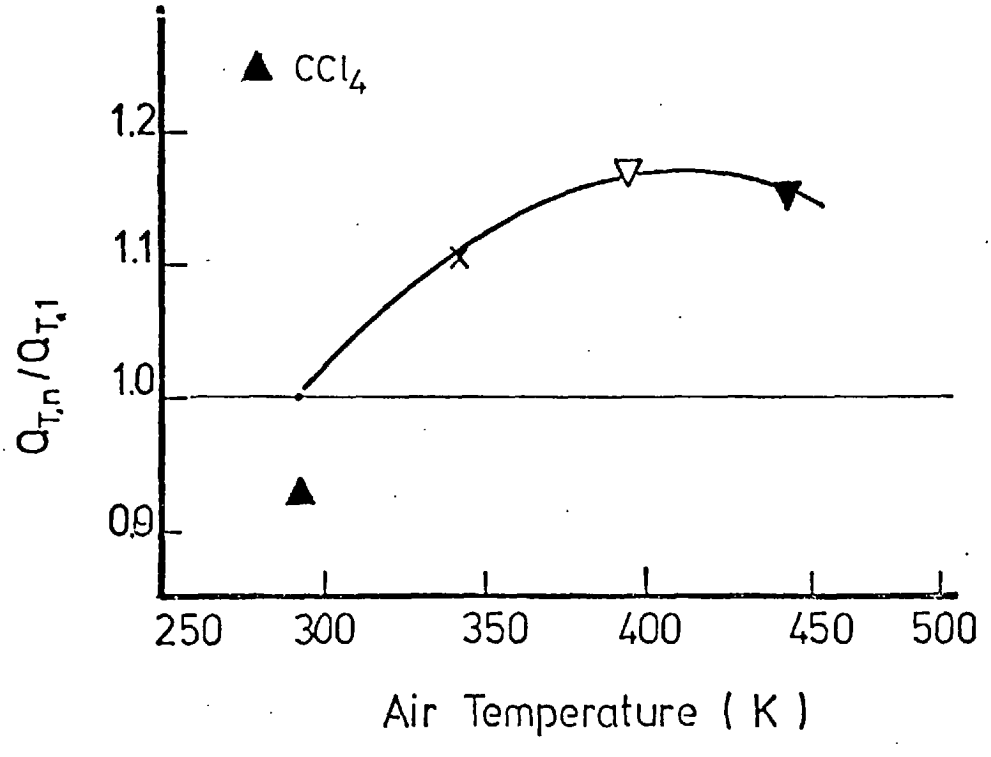

Fig (41) Effects of additives on the total heat transfer.

(See Table 5 for symbols.)

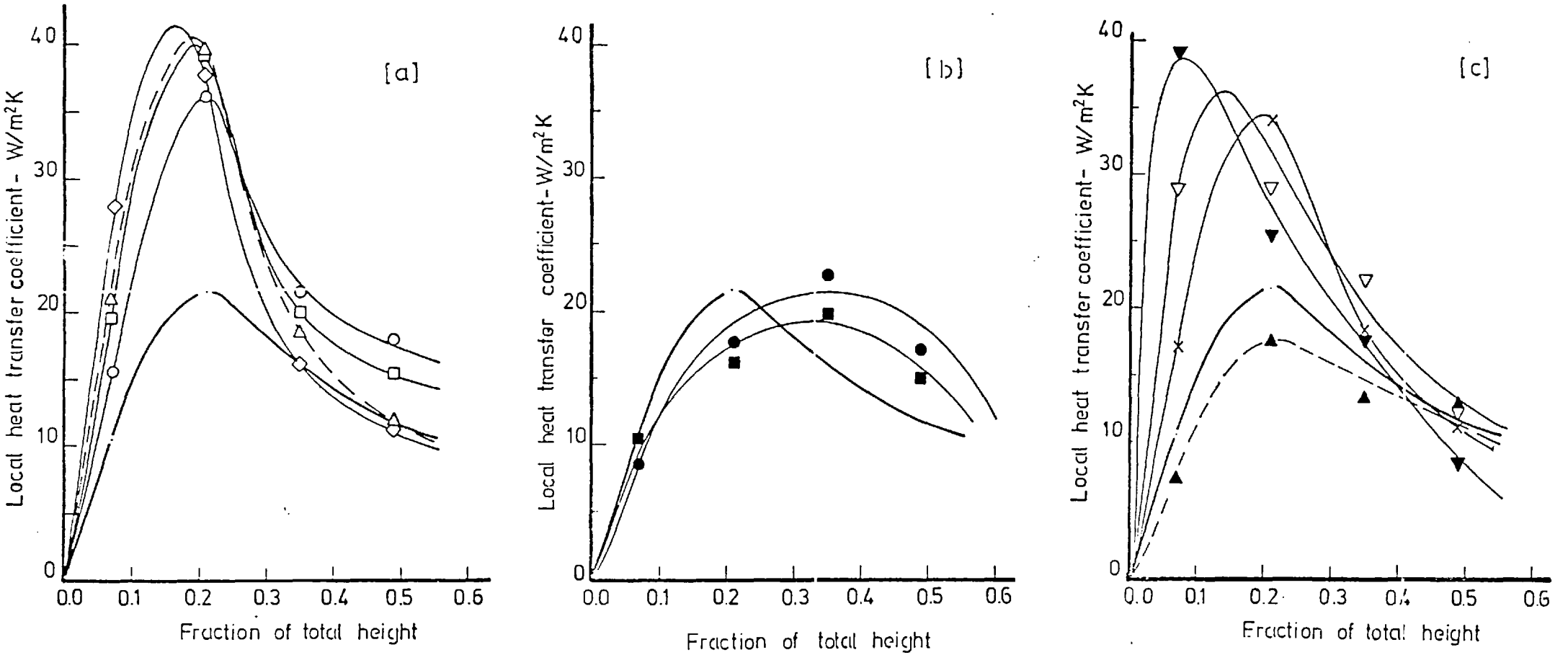

Fig(42) Variation of the local heat transfer coefficient along the flame.